THE UNIVERSITY *of* EDINBURGH

Reactivity of electropositive f-block metal N-heterocyclic carbene complexes

Anne I. Germeroth

University of Edinburgh

Submitted for the degree of Doctor of Philosophy

October 2012

Declaration

Except where specific reference has been made to other sources, the work presented in this thesis is the original work of the author. It has not been submitted, in whole or in part, for any other degree.

Signature: Date:

Abstract

The combination of Lewis acidic f-block metals and a labile nucleophilic carbene can be an excellent means to activate small molecules such as silanes, CO_2 and other traditionally inert substrates. Furthermore, bidentate alkoxy-NHC ligands have shown promise in the support of unusual high oxidation state organometallic complexes, including examples of Ce^{IV}, Pd^{IV} and U^{VI}. In this thesis the synthesis and reactivity of a series of f-block metal NHC complexes is described.

Chapter One introduces N-heterocyclic carbenes and their f-block metal complexes, in particular of cerium, praseodymium and uranium. Furthermore, it will give an overview of small molecule activation by NHCs, lanthanides and specifically [Ce(L^{Ar})N''], (L = $OC(CH_3)_2CH_2(CNCH_2CH_2NMes)$ the magnetic properties and use of lanthanides e.g. as single molecule magnets and oxo-functionalisation of the uranyl moiety.

Chapter Two describes the addition-elimination reaction chemistry of Ce^{III} and U^{IV} NHC complexes in which polar reagents add in a heterocyclic fashion across the M-NHC bond. It also describes the synthesis of the lithium salt of the alkoxycarbene proligand $[LiL^{Ar}]_4$ and its reactivity towards f-element halide and aryloxide salts. A series of reactions to target the formation of metal-metal bonds is described.

Chapter Three focuses on the synthesis of novel cerium and praseodymium complexes [Pr(L^{Ar})N''$_2$], [Pr(L^{Ar})$_2$N''], [Pr($OAr^{2,6\text{-}tBu}$)$_3$] and [Ce($OAr^{2,6\text{-}tBu}$)$_3$] and their reactivity towards oxidants. A series of alkoxide bridged lanthanide dimers [(Cl)Ce(μ-L^{Ar})$_2$Ce(Cl)$_2$], [N''(L^{Ar})Ce(μ-$OAr^{2,6\text{-}tBu}$)$OAr^{2,6\text{-}}$ $_2$Ce(L^{Ar})N''] and [N''(Cl)Pr(μ L^{Ar})$_2$Pr(Cl)N''] have been made and characterised including by SQUID variable temperature magnetometry.

Chapter Four evaluates the synthesis and reactivity of uranyl complexes [UO_2(L^{Ar})$_2$], [UO_2N''$_2$(py)$_2$] and [UO_2($OAr^{2,6\text{-}tBu}$)$_2$(py)$_2$], specifically their reactivity towards haloboranes in different solvents. Additionally, the oxo-functionalisation of uranyl compounds with haloboranes is discussed.

Chapter Five draws conclusions and provides a summary of the work presented.

Chapter Six comprises the experimental details and analytical data.

Acknowledgements

I would like to thank my supervisor Professor Polly Arnold for her constant support and encouragement throughout my PhD.

My thanks also go to the postdocs in our group Dr. Sergey Zlatogorsky, Dr. Stephen Mansell, Dr. Lorena Postigo-Gallindo and Dr. Emmalina Hollis.

Thank you to everyone in the Arnold and Love group past and present and all the "honorary" group members that have made my PhD such an enjoyable time. From running events to sink fires, cakes, attempted hat-tricks, bad jokes and Friday nights I enjoyed it all.

I would also like to thank all the people that helped my research with their knowledge and expertise: Juraj Bella, Dr. Marika de Cremoux and Dr. Lorna Murray for NMR, Prof. Simon Parsons, Dr. Gary Nichol, Dr Fraser White and the Parsons and Moggach group members for helping me whenever I was out of depth solving a crystalstructure, Alan Taylor for mass spectrometry, Stephen Boyer for elemental analyses and the people from the stores, workshops and office.

I owe a big thank you to my family for supporting me throughout this PhD. I really appreciated so many of you coming here to visit and taking an interest into what I was doing during this time. Vielen Dank!

Finally, thank you Stewart for always being there for me.

Abbreviations

°	degrees
°C	degrees Celsius
Å	Angstrom
Ar	generic aryl group
9-BBN	9-borabicyclo[3.3.1]nonane
^{t}Bu	*tert*-butyl
CAN	ceric ammonium nitrate $(NH_4)_2[Ce(NO_3)_6]$
COT	cyclooctatetraene
DCM	dichloromethane
NHC	N-heterocyclic carbene
L^{M}	$OC(CH_3)_2CH_2(CNCH_2CH_2NMes)$
N"	bis(trimethylsilyl)amide
Cp	cyclopentadienyl
Cp*	pentamethyl cyclopentadienyl
Cy	cyclohexyl
d	day(s)
Dipp	2,6-diisopropylphenyl
DME	dimethoxyethane
DFT	Density Functional Theory
g	gram(s)
h	hour(s)
IR	infrared
K	Kelvin
Me	methyl
Mes	mesityl
mL	millilitre(s)
mmol	millimole(s)
μmol	micromole(s)
Ph	phenyl

^{i}Pr	*iso*-propyl
py	pyridine
rt	room temperature
R	generic alkyl group
s	seconds
THF	tetrahydrofuran
TIP	temperature independent paramagnetism
TMP	2,2,6,6-tetramethylpiperidine
TMEDA	tetramethylethylene diamine

Nuclear Magnetic Resonance Spectroscopic Data

$^{13}C\{^{1}H\}$	proton decoupled ^{13}C NMR experiment
$^{1}H\{^{1}H\}$	proton decoupled ^{1}H NMR experiment
br	broad
δ	chemical shift in ppm
d	doublet
^{x}J	coupling constant over x bonds
Hz	Hertz
m	multiplet
MHz	Megahertz
NMR	Nuclear Magnetic Resonance
ppm	parts per million
s	singlet

Magnetism Data

χ_M	molar magnetic susceptibility
μ_{eff}	effective magnetic moment
SQUID	superconducting quantum interference device
T_N	Néel temperature

Table of Contents

Chapter 1 Introduction and Background

F-block complexes are known to be effective at activating small molecules including alkanes, as has been shown by Watson in 1983.[1] She showed that the lutetium complex [(η^5-C_5Me_5)$_2$Lu(CH_3)] **A** can react with $^{13}CH_4$ in an exchange reaction, Eq. (1).

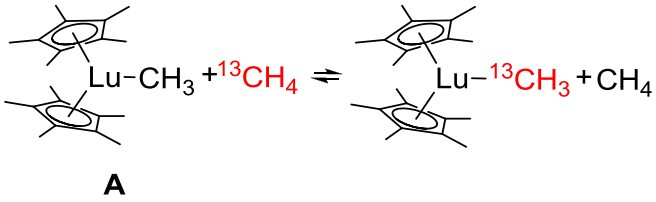

(1)

Subsequent functionalisation of these compounds is difficult; therefore it is beneficial to have a ligand system that can bring in a second substrate. The ligand system used in this thesis is an N-heterocyclic carbene (NHC).

1.1 N-heterocyclic carbenes

1.1.1 Carbenes

Carbenes were introduced to organometallic chemistry by Fischer in 1964 after Doering introduced them into organic chemistry in the 1950's.[2,3] Carbene chemistry itself has been well recognised for its potential and has been researched since the 1980's.[4,5]

Carbenes are neutral compounds of a divalent carbon where the carbon atom has six electrons in its valence shell. Depending on whether the free electrons have the same or an opposing spin it is possible to distinguish between triplet and singlet carbenes. Carbenes are highly active because of their electron deficiency.

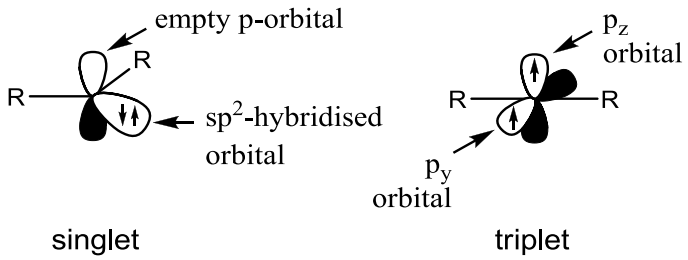

Figure 1 Electronic configuration of the singlet and triplet carbene state

The carbene carbon atom can exist in one of two geometries, either linear or bent, depending on the degree of hybridization. Because of one orbital being filled and the other being vacant, singlet carbenes have an ambiphilic character. The spins are opposing and paired. The bent shape originates in the nearly sp^2 geometry. Triplet carbenes are often described as diradicals and have a linear sp-geometry. They follow Hund´s rule and have an occupied p_y and p_z orbital with parallel spins. The singlet ground state is stabilised by push-pull effects of donor and acceptor substituents. Singlet carbenes can be stabilized by the mesomeric effect of π-electron withdrawing and π-electron donating groups. Further, σ-electron withdrawing substituents accommodate the singlet state.

1.1.2 N-heterocyclic carbenes

Dimeric N-heterocyclic carbenes (NHCs) were first introduced by Wanzlick in the 1960's.[6] The carbene in these NHC complexes is stabilised by the π-electron donating nitrogen atoms.

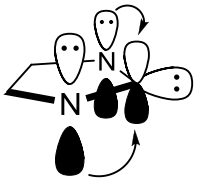

Figure 2 Electronic configuration of an NHC

In 1991 Arduengo et al. managed to synthesise a stable crystalline NHC.[6] The Arduengo carbene, which was obtained by treating the chloride salt of a 1,3-di-1-adamantylimidazolium with potassium hydride in the catalytic presence of dimethyl sulfoxide or potassium-*tert*-butoxide, Eq. (2).

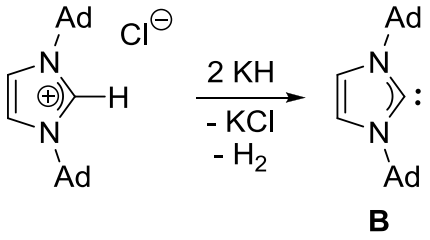

B (2)

It was commonly believed that the stability of the Arduengo carbene **B** was based on the electronic factors, the bulky adamantyl groups and the Hueckel aromaticity

of the unsaturated backbone. Both latter assumptions have since been disproved. The steric bulk helps to stabilize the carbene but is not essential, as was shown by Arduengo *et al.* when they replaced the adamantyl groups by the much smaller methyl groups **C**.[7]

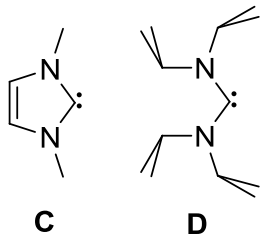

Figure 3 Arduengo carbene **C** and Alder carbene **D**

Alder showed in 1996 that the aromaticity is not vital by synthesising an acyclic persistent carbene **D**.[8] A study by Apeloig and co-workers and one by Frenking and Boehme in 1996 showed that the aromaticity is not the major stabilising effect in cyclic carbenes but that the interaction of the carbene centre with π-donating and σ-attracting amino substituents is more important.[9,10]

The different resonance structures of aminocarbenes are shown in Figure 4.

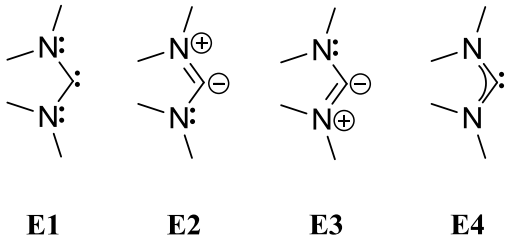

Figure 4 Resonance structures of aminocarbenes

These resonance structures illustrate the π-donor characteristics of the nitrogen carbon bond. A result of this is that the CN bonds have some multiple bond character as shown in resonance structure **E2** and **E3**. Diaminocarbenes can therefore be summarised by structure **E4**.

NHCs can be characterised by NMR spectroscopy. The cationic precursors of the NHCs have a chemical shift of about δ = 135 – 180 ppm in the ^{13}C NMR spectrum. The carbene carbon shift is between δ = 205 – 300 ppm, more specifically between δ = 205 –

220 ppm for unsaturated heterocyclic carbenes. The carbene carbon in the saturated analogue can usually be found between δ = 235 – 245 ppm.[7,11–14]

There are many varieties of NHCs. Most common are the imidazole **F** and the imidazolin-ylidene **G**. The backbone can be modified as in the triazolin-5-ylidene **H**. For enantioselective catalysis it is convenient to use chiral ligands like **I** or **J** as pictured in Figure 5.

Tethered NHCs as for example **K** with an O, S or N tether have the advantage of being able to bind strongly to the metal, especially f-block metals, thereby anchoring the carbene close to the metal centre.

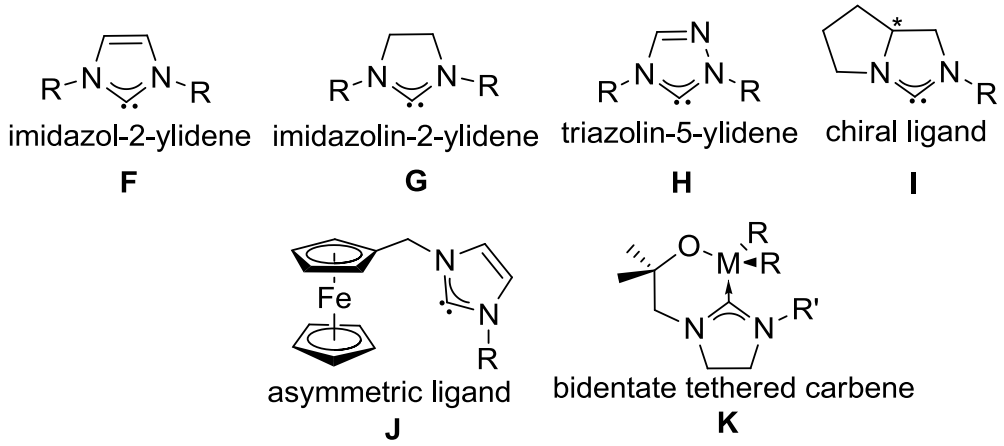

Figure 5 Examples of NHCs

1.1.3 Metal NHC complexes

The NHC carbene is a strong Lewis base and the metal is a Lewis acid. This system enables bifunctional catalysis as has been shown by the Arnold group, by successfully polymerising racemic lactide with an yttrium and a titanium NHC, which is schematically shown in Eq. (3).[15]

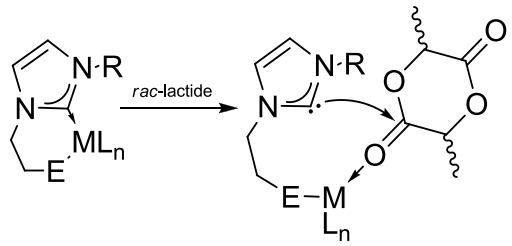

(3)

The Lewis-basic NHC carbene is bound *via* a tether E (E = S, O) to the Lewis-acidic metal M. This combination allows a nucleophilic attack of the ester carbon by the carbene while the metal can act as an electron pair acceptor towards the oxygen atom of the ester CO group.

1.1.4 Activity of NHCs

It was further shown that zinc and magnesium NHC complexes of an imidazolinium carbene and an alkoxy tether are able to polymerise racemic lactide, Eq. (4).[16]

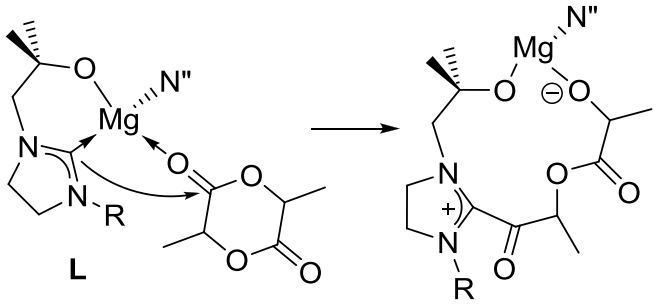

(4)

NHCs themselves can act as oragnocatalysts as has been shown by Zhang and coworkers.[17] They showed that an NHC performs as a catalyst for hydrosilylation of a silane with carbon dioxide with methanol as a byproduct, schematically shown in Scheme 1. They believe that the NHC forms an adduct **M** with the carbon dioxide that can react with the silane.

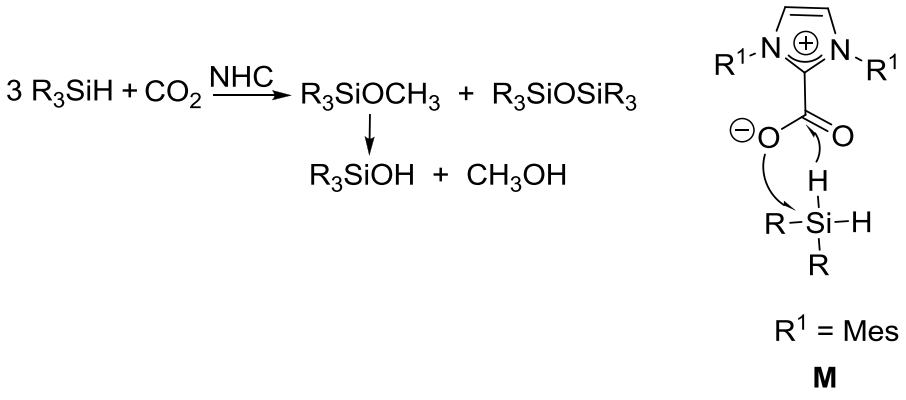

Scheme 1 Hydrosilylation of a silane with CO_2

NHCs are widely used in catalysis as ligands for different catalysed reactions such as olefin metathesis. They have been proven to be better ligands than phosphines in catalysis because of their ability to form strong σ-bonds whilst being a weak π-acceptor.

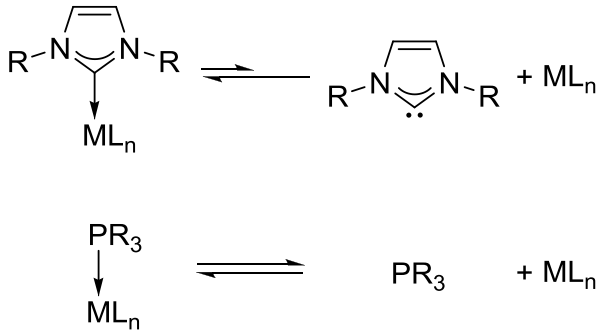

Scheme 2 Comparison of the ability to form σ-bonds between phosphines and NHCs

NHCs are nucleophilic enough to form carbene phosphinide adducts (reported by Arduengo)[11] and also carbene borane adducts. These Lewis acid-base adducts can act as frustrated Lewis pairs when their ability to form stable donor-acceptor adducts is suppressed by steric factors.[18–20] This allows activation of small molecules such as dihydrogen, olefins and tetrahydrofuran. Tamm reported the frustrated Lewis pair **N** which can activate C-O, H-H and N-H bonds, Eq. (5).[21,22]

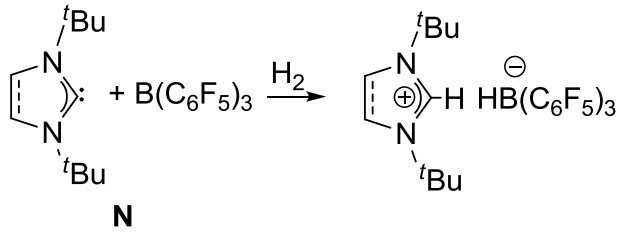

(5)

N

1.2 Ce^{IV} organometallic complexes

The lanthanides form mostly trivalent complexes. This is partly due to the ionisation energy, as $I_4 \rangle (I_3 + I_2 + I_1)$. Another reason is the enthalpy of atomisation, as $\Delta_{at}H$ follows the inverse trend to I_3. The enthalpy of hydration also follows a $Ln^{4+} \rangle Ln^{3+} \rangle Ln^{2+}$ trend, this is due to the ions with a larger charge having a greater charge density. The smooth ionic-size-based trend shows that the hydration energy increases with an increasing atomic number as the ions become smaller and their attraction for water

molecules increases. The enthalpy of formation show a smooth trend based on size effects.

Cerium is the only lanthanide with a chemically accessible +IV oxidation state. A lot of research has been undertaken to synthesise tetravalent organometallic cerium f^0 complexes. Ce^{IV} complexes are highly oxidising, the most commonly known and used Ce^{IV} complex is ceric ammonium nitrate (CAN), which is widely used in organic synthesis and catalysis for one-electron oxidation, generation/cleavage of carbon-heteroatom bonds, carbon-carbon bond formation and multicomponent reactions.[23–26] Despite the accessibility of the +IV oxidation state, obtained yields are often low and the synthesis of tetravalent cerium complexes is highly dependent on the choice of solvent, reaction temperature, oxidant and the choice of ligand.[27]

1.3 Oxidation of [{M(THF)$_2$}Ce(binolate)$_3$] (M = Li, Na, K) and the importance of ligand reorganisation

Schelter and co-workers have recently shown that the choice of the ligand has a big influence on the oxidation chemistry of Ce^{III}.[27] The ligand's ability to reorganise is a key factor in the chemical oxidation rate of a heterobimetallic Ce^{III} complex. The heterobimetallic framework was designed by Shibasaki and the authors extended this to the [{M(THF)$_2$}$_3$Ce(binolate)$_3$] (M = Li, Na or K) cerium complex **O**, Scheme 3. Studies of the electrochemistry and electron transfer rate k_S of $\mathbf{O^{Li\text{-}K}}$ showed that k_S (K^+) › k_S (Na^+) › k_S (Li^+). In contrast, the chemical oxidation of **O** showed that under pseudo first-order rate conditions k_{obs} (K^+) ‹ k_{obs} (Na^+) ‹‹ k_{obs} (Li^+). Depending on the nature of M a different reaction product is observed when **O** is treated with Ph_3CCl.

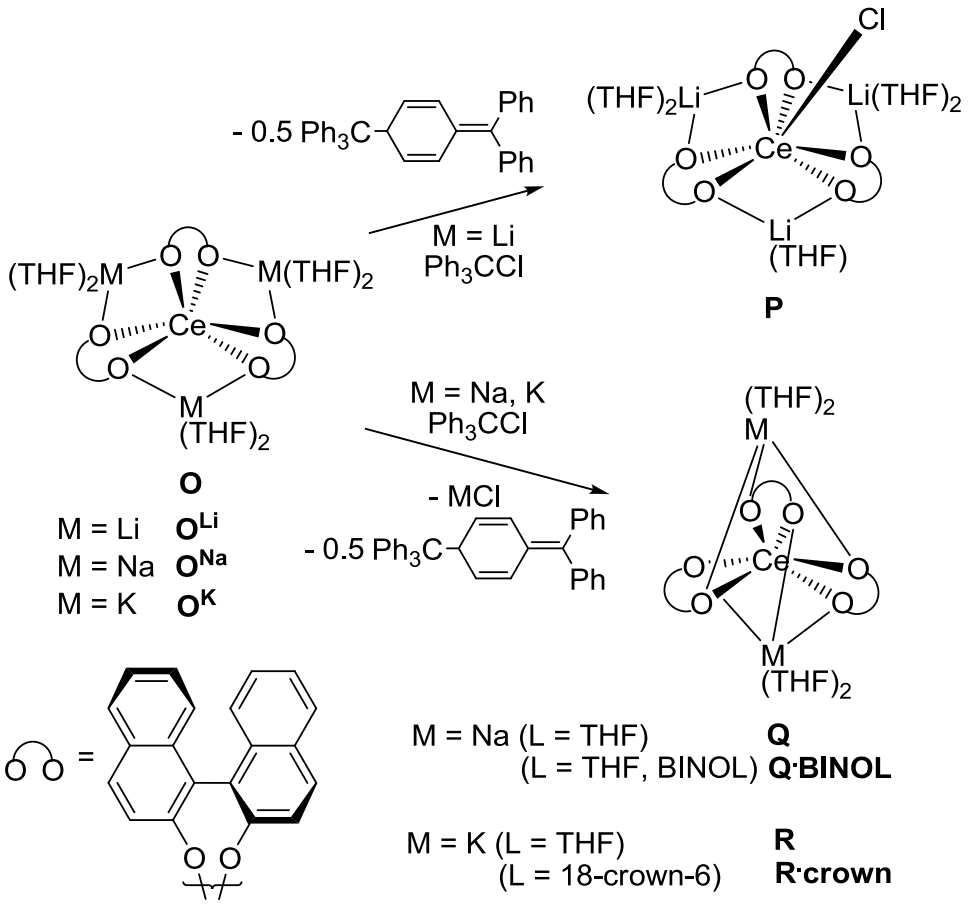

Scheme 3 Synthesis of **P**, **Q** and **R**

If M = Li the obtained product is the $[\{Li(THF)_2\}_2\{Li(THF)\}Ce^{IV}(binolate)_3Cl]$ complex **P**. If instead M = Na or K one equivalent of MCl is eliminated and the $[\{M(THF)_2\}_2Ce^{IV}(binolate)_3]$ complexes **Q** and **R** are afforded. This difference in reactivity and k_{obs} is explained by the reorganisation of the coordination spheres of $\mathbf{O^{Li\text{-}K}}$ and the accessibility of the Ce^{III} cation.

1.4 Oxidation of Ce^{III} amide complexes

Scott and co-workers published the oxidation of a Ce^{III} amide complex $[Ce(NN')_3]$ (NN' = $N(CH_2CH_2NSiMe_2{}^tBu)_3$) **S** by treatment with iodine to form the Ce^{IV} complex $[Ce(NN')_3I]$ **T**. Treatment of $[Ce(NN')_3]$ with bromine or chlorine yielded the mixed valence $Ce^{III/IV}$ complexes $[\{Ce(NN')_3\}_2(\mu\text{-Cl})]$ and $[\{Ce(NN')_3\}_2(\mu\text{-Br})]$ $\mathbf{U^{Cl,Br}}$, Scheme 4.[28]

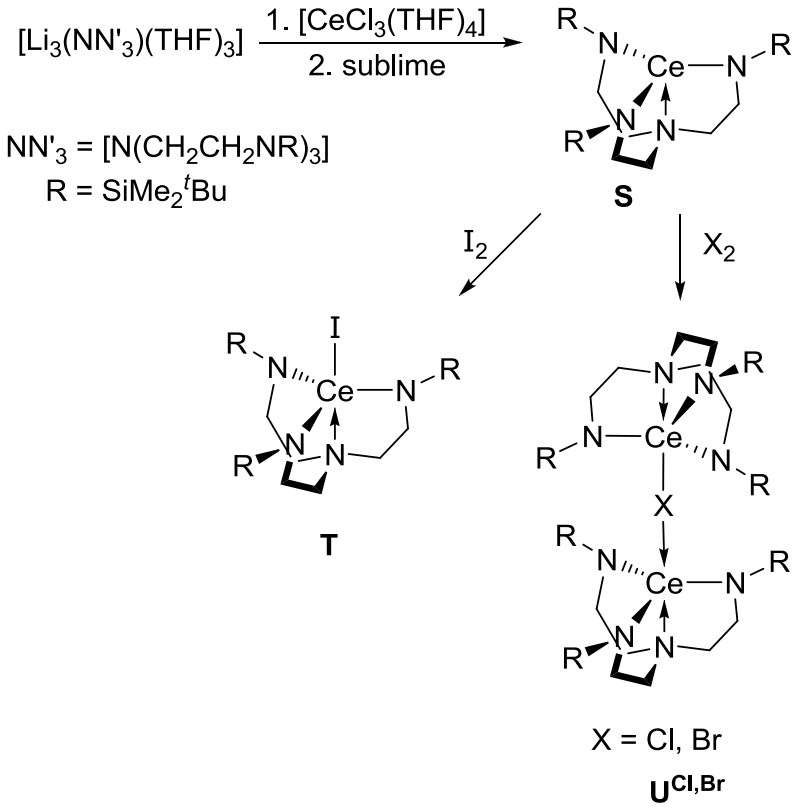

Scheme 4 Synthesis of [Ce(NN'$_3$)I] **T** and [{Ce(NN'$_3$)}$_2$(μ-X)] **U**

The trivalent complexes [Ce(N")$_3$] (N" = N(SiMe$_3$)$_2$) and [Ce(η-C$_5$H$_5$)$_3$] cannot be oxidised by chlorine despite being less sterically hindered than **S**. The authors suggest that the stability of **T** is explained by the ligand forming a pseudo-trigonal monopyramidal complex with cerium which does not have to be rearranged in order to generate a vacant coordination site to bind an incoming ligand and thereby enhancing the Lewis acidity of the cerium. The formation of the mixed valence complexes $\mathbf{U^{Cl}}$ and $\mathbf{U^{Br}}$ compared to the formation of the Ce^{IV} complex **T** is explained by the ability of bromide and chloride as relatively hard bases to form dative bonds with the Ce^{III} ion, thereby compensating the loss of the Ce^{IV}-X bond enthalpy by the formation of a dative Ce^{IV}-X→Ce^{III} bond. Since iodide is a softer base it would form a weak dative bond with Ce^{III} and the loss of the Ce^{IV}-I bond enthalpy could not be compensated, rendering **T** relatively stable.

Lappert and co-workers reported in 2004 the unsuccessful attempt to oxidise [Ce(TMP)$_3$(THF)] (TMP = 2,2,6,6-tetramethylpiperidine) with TeCl$_4$.[29] Instead of the

tetravalent cerium low yields of crystalline TeCl(TMP) and $[CeCl_2(THF)_5][TeCl_5(THF)]$ were observed. Possibly, the TMP ligand is too big and sterically hinders oxidation of the cerium.

Lappert and coworkers later reported the first homoleptic Ce^{IV} amide complex $[Ce(NCy_2)_4]$ **V** in 2006, Scheme 5.[30]

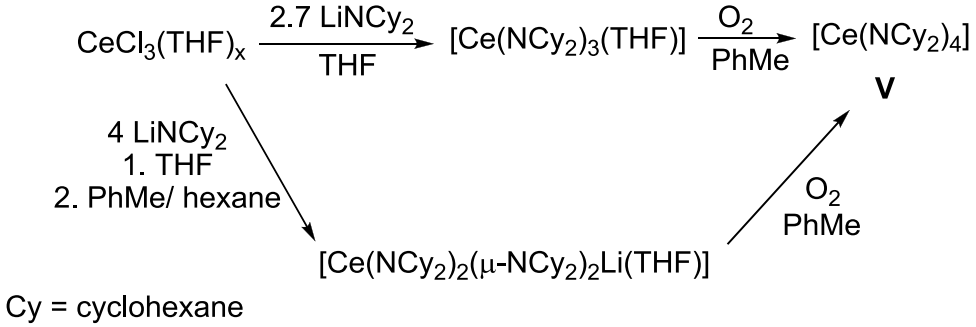

Scheme 5 Synthesis of $[Ce(NCy_2)_4]$ **V**

V is synthesised from trivalent cerium amides that were obtained by salt elimination reactions from $[CeCl_3(THF)_x]$ with either 2.7 or 4 equivalents of $LiNCy_2$ respectively. These Ce^{III} amides are very air sensitive and easily react with trace amounts of oxygen. When a measured amount of O_2 was added to toluene solutions of the amides the dark blue Ce^{IV} amide formed immediately in a moderate yield of 35%. The structure was confirmed by single crystal X-ray diffraction.

In 2010 Lappert and co-workers reported unprecedented amido Ce^{IV} complexes **X** – **AH** and the side-on bridging dioxygen complexes **AI** and **AI'**.[31] They found that the homoleptic $[Ce(N'')_3]$ can be oxidised with O_2 at low temperatures of -27 ˚C to form complex **X** in a 38% yield. The cyclotriceroxane complex **Y** is a result of the reaction of **W** with 2,6-di-^{t}Bu-1,4-benzoquinone at room temperature in a low crystalline yield of 10%, Scheme 6. **Y** is very sensitive towards thermal decomposition at room temperature.

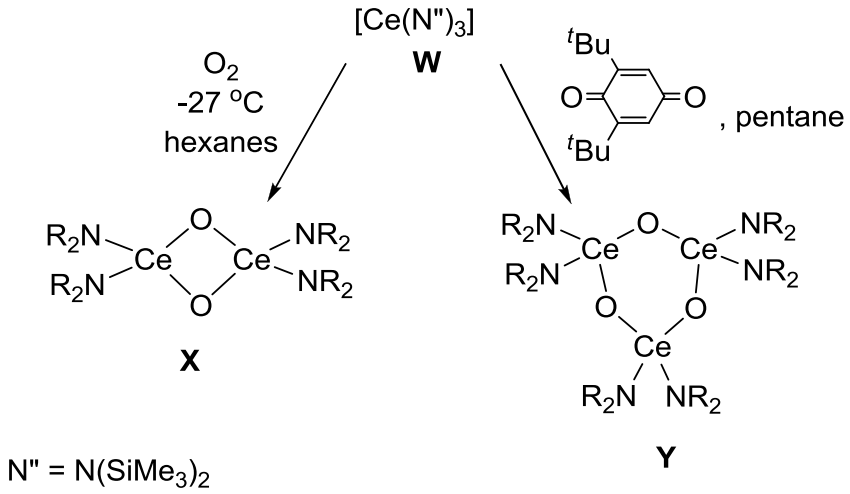

Scheme 6 Synthesis of the Ce^{IV} amide complexes **X** and **Y**

The formation of **X** is explained by Lappert and co-workers *via* the pathway shown in Scheme 7.

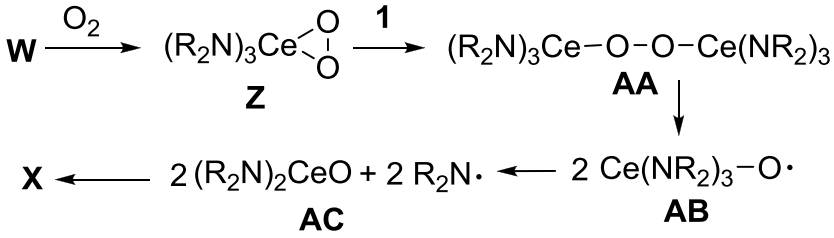

Scheme 7 Plausible reaction pathway for the formation of **X**[31]

According to the authors **W** reacts with O_2 to form the superoxide **Z** which can be treated with another equivalent of **W** to give the peroxide **AA**. No attempts to trap the postulated amide radical were reported.

The tetrametallic complex **AE** was isolated in very low yields as an accidental by-product with moisture or traces of oxygen from the synthesis of **AD** from the reaction of $[CeCl_3(THF)_x]$ with Li(TMP) (TMP = 2,2,6,6-tetramethylpiperidine), Eq (6).

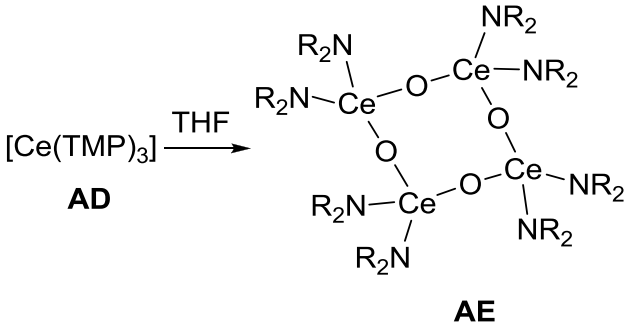

(6)

The alkali metal bis(trimethylsilyl)amido(oxy)cerate complexes **AF** and **AG** were synthesised by connecting a Schlenk tube containing dioxygen to a Schlenk tube containing a solution of **W** with NaN" or KN" respectively at -27 ˚C. Crystals could be isolated from this slow diffusion reaction in a 17% (**AF**) and 23% (**AG**) yield, Scheme 8.

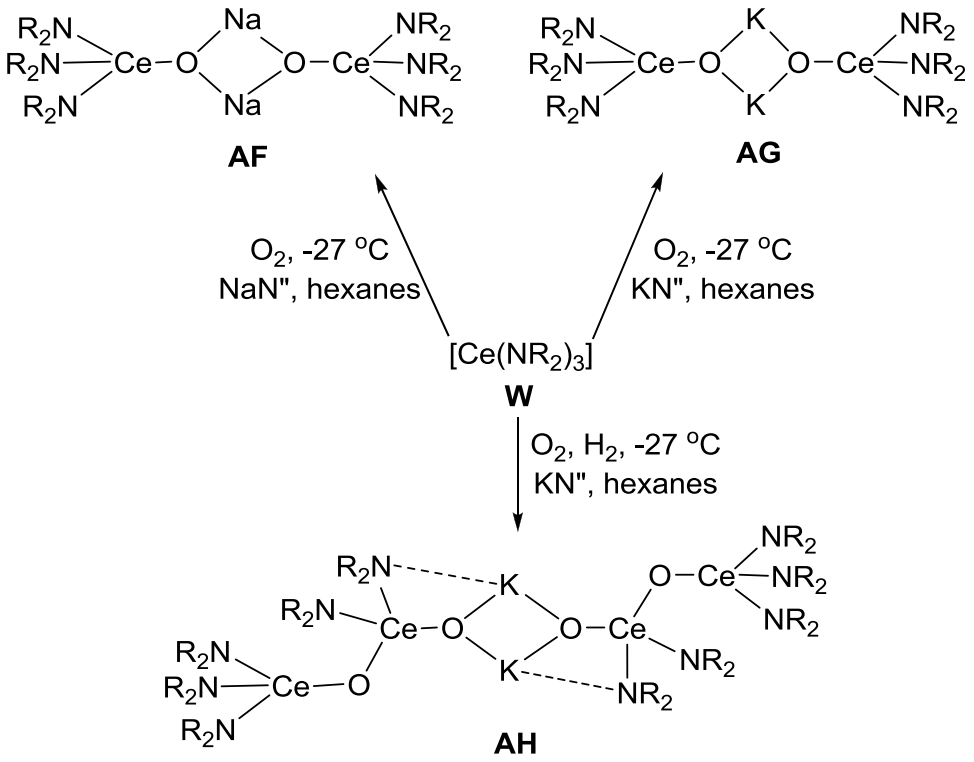

Scheme 8 Synthesis of the Ce^{IV} amide complexes **AF**-**AH**

Complex **AH** was obtained when the synthesis of **AG** was modulated by additionally connecting a Schlenk tube filled with dihydrogen at atmospheric pressure. The crystalline product was obtained in a 10% yield after several days.

The side-on bridging complexes **AI** and **AI'** could be isolated in a 20% yield by treating **W** with O_2 at -27 ˚C in hexane (**AI**) or pentane (**AI'**), Eq. (7).

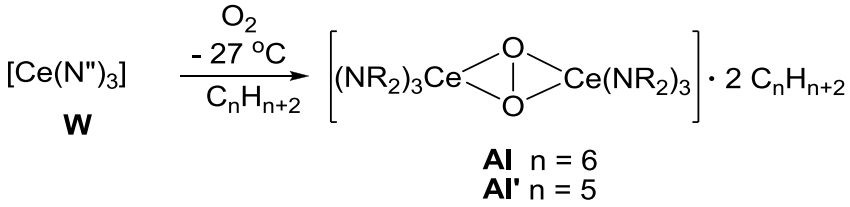

(7)

It is postulated that **AI** and **AI'** form *via* the superoxo complex **Z** and are a possible precursor to the linear complex **AA**, Scheme 7. All complexes **X** – **AI** are thermally unstable and decompose after a few hours at ambient temperature, especially in solution.

Andersen and co-workers reported the synthesis of cerium macrocyclic complexes with a tetramethyldibenzotetraaza[14]annulene (tmtaaH_2) ligand.[32]

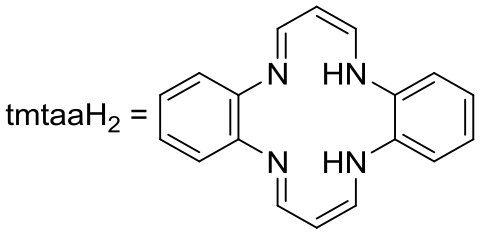

Figure 6 tmtaaH_2 ligand

Depending on stoichiometry, solvent and temperature [Ce(tmtaa)(tmtaaH)], [Ce_2(tmtaa)$_3$] or [Ce(tmtaa)$_2$] were obtained from the reaction of [Ce(N")$_3$] and tmtaaH_2, Scheme 9.

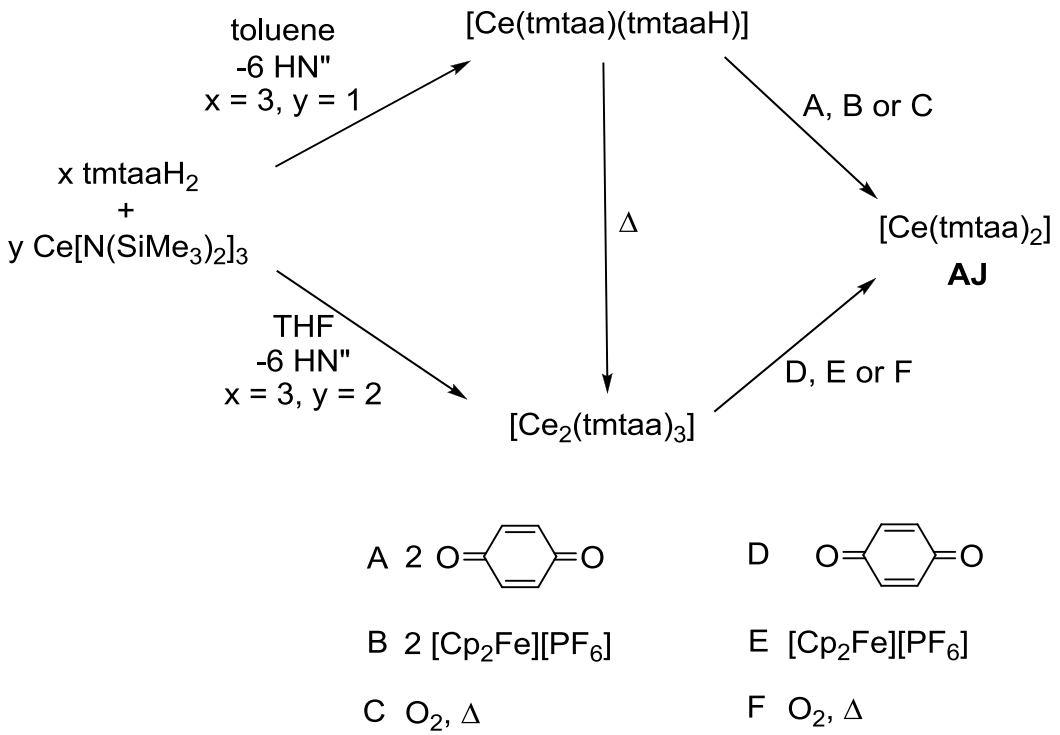

Scheme 9 Synthesis of $[Ce(tmtaa)_2]$ **AJ**

Complex **AJ** can be synthesised in a 56% yield from $[Ce_2(tmtaa)_3]$ or [Ce(tmtaa)(tmtaaH)] by treatment with 1,4-benzoquinone, $[Cp_2Fe][PF_6]$ or traces of O_2.

Analysis of the temperature dependence of the magnetic susceptibility of **AJ** showed that it is not a diamagnetic cerium (IV) but behaves in the solid state as a temperature independent paramagnet analogous to $[Ce(COT)_2]$ (see section 1.5.1), Figure 7.

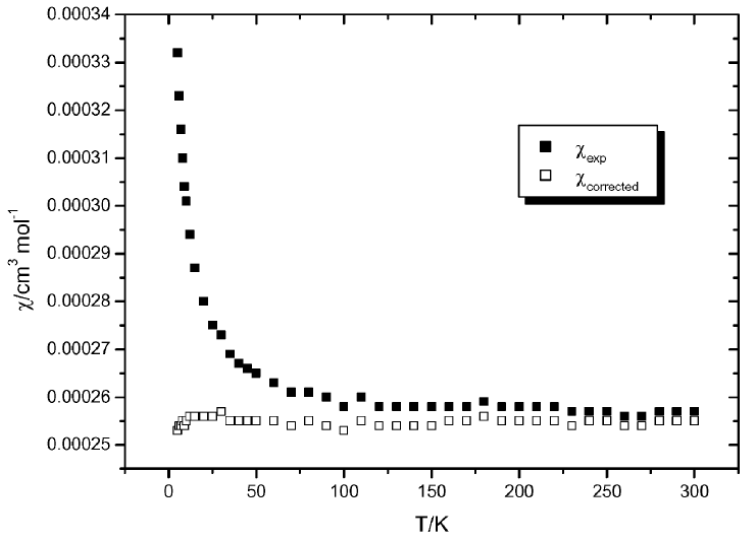

Figure 7 χ vs T plot for **AJ** at 40 kG. Reproduced from reference 32.

Apart from a small amount of impurity of Ce^{III} the χ vs T plot (χ = magnetic susceptibility) with the corrected plot for $\chi_{corrected}$ of **AJ** shows the typical behaviour of a TIP with $\chi_0 = (2.55 \pm 0.02) \times 10^{-4}$ cm^3/mol.

Lappert and co-workers reported the synthesis of a homoleptic dithiocarbamate Ce^{IV} complex $[Ce(\kappa^2\text{-}S_2CNEt_2)_4]$ **AK** from $[Ce(N'')_3]$,
Scheme 10.[33]

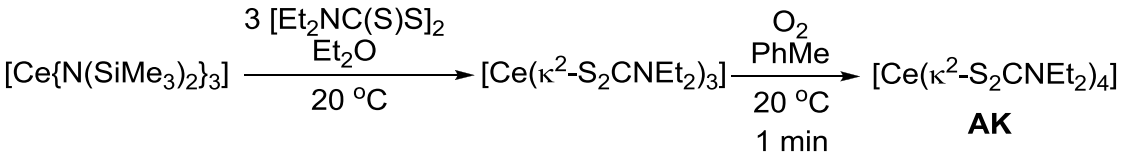

Scheme 10 Synthesis of $[Ce(\kappa^2\text{-}S_2CNEt_2)_4]$ **AK**

The yellow trivalent **AK** was synthesised in 72% yield by treating a diethyl ether solution of diethylammonium diethyl dithiocarbamate with a diethyl ether solution of $[Ce(N'')_3]$. When O_2 was bubbled through a yellow suspension of $[Ce(\kappa^2\text{-}S_2CNEt_2)_3]$ in toluene at room temperature the colour of the solution changed immediately to black. Black crystals of **AK** could be isolated in a 74% yield, suggesting that this is the major product. The byproduct is suggested to have been either Ce_2O_3 or CeO_2.

Additionally, it was observed that a suspension of six - eight equivalents of tetramethylthiuram disulfide with a THF solution of [Ce(N")$_3$] changed colour to purple after 3 h. No crystals suitable for X-ray crystallography could be isolated but ^{1}H NMR and ^{13}C NMR spectroscopy suggest the diamagnetic Ce^{IV} complex [Ce{N(SiMe$_3$)$_2$}$_2$(κ^2-S$_2$CNEt$_2$)$_2$], Eq. (8).

$$[Ce(N")_3] \xrightarrow[20\ ^oC]{6\ [Me_2NC(S)S]_2,\ THF} [Ce(N")_2(\kappa^2\text{-}S_2CNEt_2)_2]\ ?\ \textbf{AL} \qquad (8)$$

Lappert, Maron and co-workers reported the first oxidation of [Ce(N")$_3$] to the tetravalent heteroleptic [Ce(N")$_3$Cl] **AM** in 2001.[34] They observed that [Ce(N")$_3$] was inert to Cl$_2$ but would react with 0.25 equivalents of TeCl$_4$ to give dark purple needles of **AM** in a relatively low yield of 24-30%. Lappert and co-workers followed this up in a publication in 2004 where they reported the inertness of [CeN"$_3$] towards I$_2$ and Br$_2$ and the oxidation of [CeN"$_3$] with dibromotriphenylphosphorane Ph$_3$PBr$_2$ to yield 30% of the tetravalent dark-purple complex [Ce(N")$_3$Br] **AN**, Scheme 11.[35]

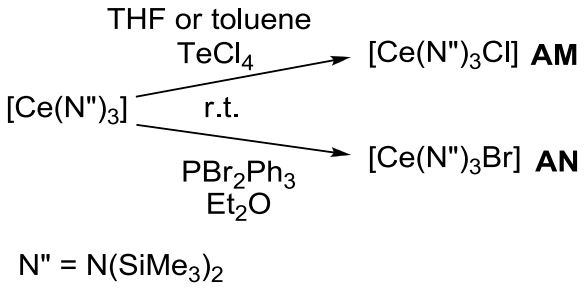

Scheme 11 Synthesis of [CeN"$_3$Cl] **AM** and [CeN"$_3$Br] **AN**

They also found that prolonged storage of the bromide **AN** would lead to decomposition of the tetravalent complex and the assumed formation of [CeBr$_3$(Et$_2$O)$_2$] which could be crystallised as [CeBr$_3$(THF)$_4$]. The attempt to synthesise **AN** from TeBr$_4$ and [Ce(N")$_3$] in THF at room temperature yielded the trivalent [Ce(Br)$_2$N"(THF)$_3$] complex and was therefore deemed as an inappropriate oxidising agent. A number of alternate oxidising agents such as NBS, NCS, AgBF$_4$, AgCN, Hg(C$_6$F$_5$)$_2$, PbCl$_2$ and ^{t}BuO^{t}Bu were tried with the goal of forming a tetravalent cerium complex, however,

all attempts were unsuccessful. The authors speculate that the reason for the success of $TeCl_4$ and PBr_2Ph_3 lies in the fact that they dissociate in solution to form the halogenium ions $[TeCl_3]^+$ and $[PBrPh_3]^+$ respectively, thereby enhancing their electrophilicity in coordinating solvents. Thus the barrier for an electron transfer from the metal to the main group centre could be lowered.[36]

In 2010 the Arnold group showed that it is possible to oxidise $[Ce(N'')_3]$ to $[Ce(N'')_3Cl]$ in a 100% conversion with the commercially available trityl chloride yielding Gomberg's dimer ($Ph_3CCH(C_6H_4)CPh_2$) **AO** as the only byproduct, Scheme 12.[37]

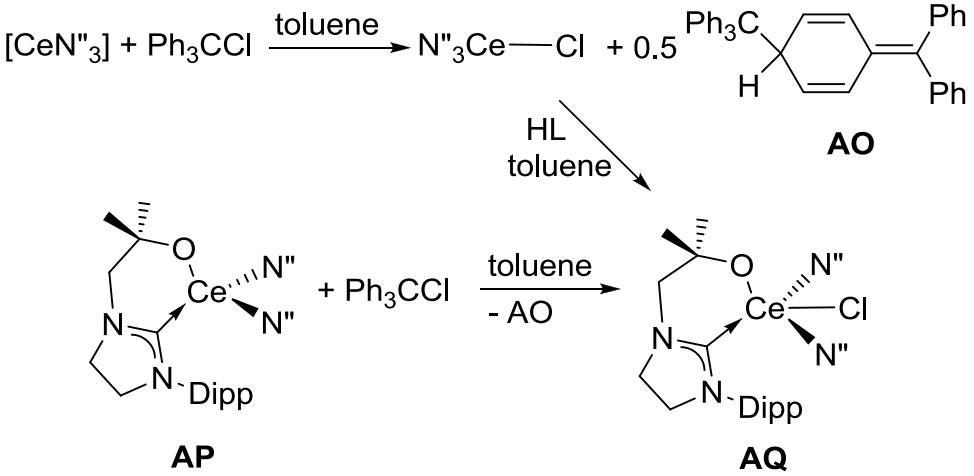

Scheme 12 Synthesis of $[N''_3CeCl]$ and $[Ce(L)N''_2Cl]$

The yellow NHC Ce^{III} complex **AP** can be oxidised in the same manner as $[Ce(N'')_3]$ to form the dark red Ce^{IV} complex $[Ce(L)(N'')_2Cl]$ **AQ** in a 34% yield. The yield can be improved to 67% if **AQ** is synthesised by eliminating HN'' in an equimolar reaction of $[Ce(N'')_3Cl]$ and HL. Attempts to oxidise **AP** with $TeCl_4$ did not yield a reaction.

Anwander and co-workers reported the one-electron oxidation of homoleptic Ce^{III} complexes with $PhICl_2$, Scheme 13.[38] The $[CeX_3]$ complexes where X = $N(SiMe_3)_2$

(a), [*p*-$MeOC_6H_4C(NSiMe_3)_2]_3$ (b), Cp (c), were treated with stoichiometric amounts of $PhICl_2$.

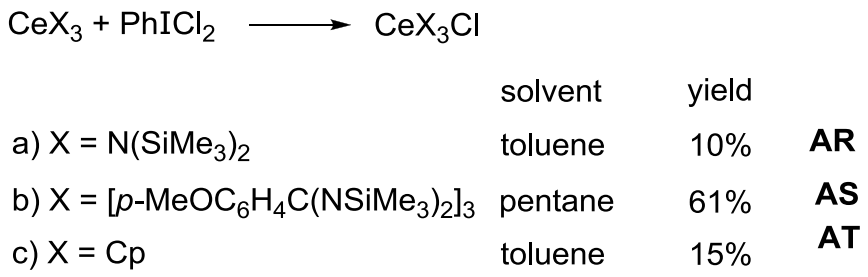

Scheme 13 Reactions of CeL_3 with $PhICl_2$

Reaction a) yielded poor results with a yield of only 10% of $[Ce(N'')_3Cl]$ compared to the oxidations with $TeCl_4$ and Ph_3CCl mentioned above. In a slight variation of the synthesis a), N≡C-*p*-C_6H_4OMe was used as a coordinating solvent thereby improving the yield to 45%. The Ce^{IV} amidinate product **AS** of synthesis b) could be isolated in a 61% yield as dark-brown crystals and the structure was confirmed by X-ray crystallography. The most interesting reaction described is the oxidation of $[CeCp_3]$ to $[Ce(Cp)_3Cl]$ **AT**, which could be isolated in a 10% yield as black crystals. This new cyclopentadienyl complex allows comparisons to the uranium analogue $[U(Cp)_3Cl]$.

Baudry and co-workers reported the Ce^{IV} triflimidate complex $[Ce(NTf_2)_4]$ that can catalyse the oxidation of aromatic ketones to the corresponding carboxylic acids.[39]

1.5 Mixed valence cerium complexes

1.5.1 Cerocenes

Cerocenes are sandwich complexes of the form $[Ce(\eta^8\text{-}COT)_2]$ (COT = cyclooctatetraenyl = η^8-C_8H_8). The cerium is sandwiched between the metals in a D_{8h} orientation. $[Ce(\eta^8\text{-}C_8H_8)_2]$ was first synthesised by Cesca and co-workers.[40] Full characterisation of this compound and the methylsubstituted derivative $[Ce(\eta^8\text{-}C_8H_7Me)_2]$ synthesised by Streitwieser and coworkers were achieved.[41] Unfortunately reactivity studies of these compounds proved to be difficult due to their poor solubility in organic solvents. The trimethylsilyl substituted complex **AU** can be synthesised from a Ce^{III} salt by an oxidation reaction published by Edelmann and co-workers and shows good solubility.[42]

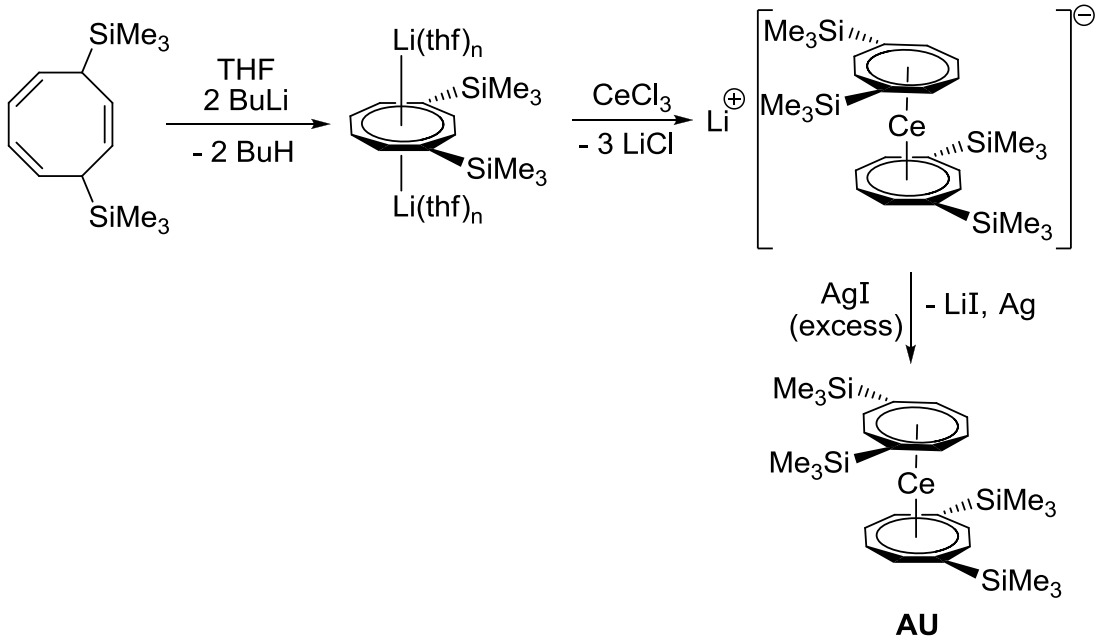

Scheme 14 Synthesis of [Ce(COT")$_2$] **AU**

This complex is very intriguing because of the very reducing nature of the COT ligand and the strongly oxidising nature of the Ce^{4+}. The compound was initially reported to be a tetravalent ionic compound.[43] Theoretical studies of this compound have been carried out which suggest that it has in fact a mixed valence cerium centre and should be described as having an about 80% Ce^{III} $4f^1$ character and 20% Ce^{IV} $4f^0$ character and should be described as a [$Ce^{3+}(COT^{-1.5})_2$] complex.[44–46] The theoretical findings were tested by Edelstein and co-workers using K-edge absorption spectroscopy *XANES* (X-ray adsorption near-edge structure) on a series of substituted cerocenes bis[1,4-bis-(trimethylsilyl)cyclooctatetraene]cerium [Ce(COT")$_2$], bis[1,3,6-tris-(trimethylsilyl)cyclooctatetraene]cerium [Ce(COT"')$_2$], their related trivalent cerocene salts Li[Ce(COT")$_2$] and K[Ce(COT")$_2$] and some cerium compounds used as standards ([CeO_2], [$Ce(NH_4)_4(SO_4)_4 \cdot 2H_2O$], [$CeCl_3 \cdot 6H_2O$] and others).[47] The *XANES* data showed that the oxidation state of cerium in substituted cerocenes is +3. However, Kaltsoyannis recently followed up this publication with DFT calculations of the [$CePn_2$] (Pn = pentalene = η^8-C_8H_6) complex which has a very similar electronic structure to cerocene. It was found that these complexes are best described as Ce^{IV} complexes in which a significant metal 4f density is the consequence of the transfer of electron density from ligand to metal through partial occupation of a metal dominated orbital. It is further

stated that the *XANES* data do not contradict this statement but is an indication of the fact that "experimental measurements of the effective oxidation state cannot necessarily be used to unambiguously define the detailed electronic structure of complexes such as $[Ce(\eta^8\text{-}C_8H_6)_2]$".[48]

A new cerocene **AV** with superbulky triphenylsilylgroups as substituents has been synthesised recently by Evans and coworkers in a slight variation of the procedure published by Edelmann.[49] ^{1}H NMR and ^{13}C NMR spectroscopy data suggest that **AV** is a diamagnetic complex.

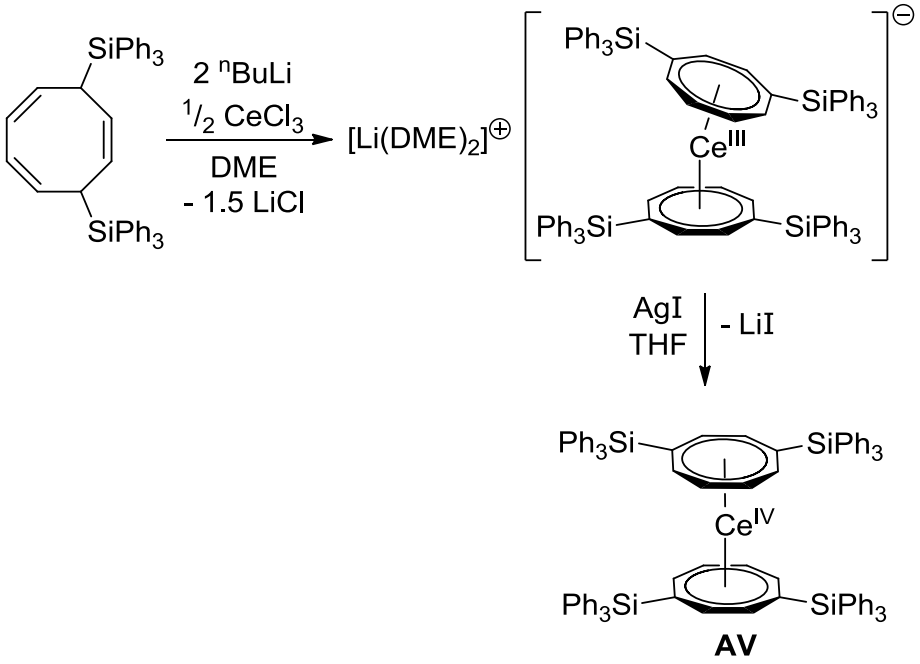

Scheme 15 Synthesis of $[Ce(COT^{BIG})_2]$ **AV**

1.5.2 [Ce(η^8-pentalene)$_2$] sandwich complex

The 1,4-trialkylsilyl substituted pentalene cerium sandwich complex **AW** was synthesised by Balasz and co-workers in order to make comparisons with the related cerocene complexes.[50]

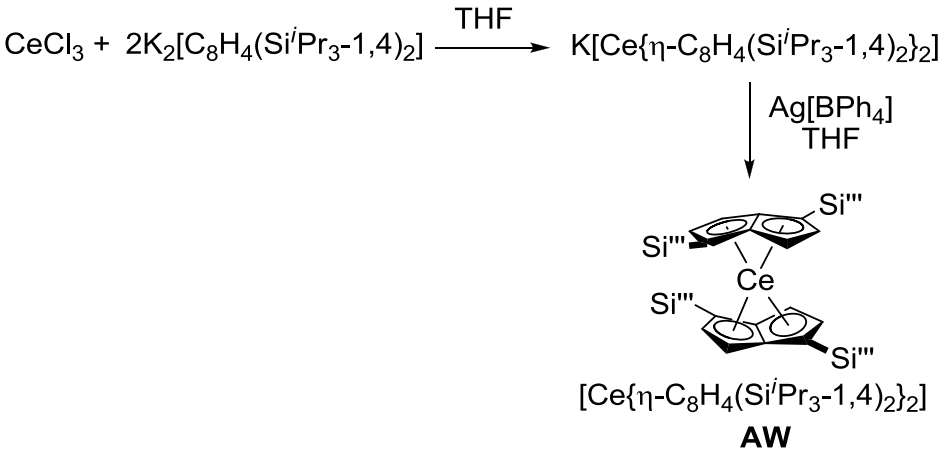

Scheme 16 Synthesis of [Ce(η^8-pentalene)$_2$] **AW**

The authors suggest that the findings from magnetic studies, K-edge *XANES* spectroscopy, UV-Vis spectroscopy, gas-phase electron spectroscopy and DFT calculations indicate that the [Ce{η-C_8H_4(Si^iPr_3-1,4)$_2$}$_2$] **AW** complex has a multi-configuration ground state but recommend a +IV oxidation state. In contrast to those findings the methyl substituted complex [Ce(η^8-C_8Me_6)$_2$] **AX** was studied by members of the same group and the cerium was found to be close to a trivalent nature. *XANES* data indicated the formation of a Ce^{III} complex, whereas ^{13}C NMR spectroscopy suggests a diamagnetic compound with a paramagnetic contribution to the shielding of some nuclei. Variable temperature NMR spectroscopy between -100 ˚C and 80 ˚C shows no change in the chemical shifts, indicating that any paramagnetic contribution is temperature independent. Solid state magnetic measurements confirm that **AX** is a temperature independent paramagnet (TIP).[51]

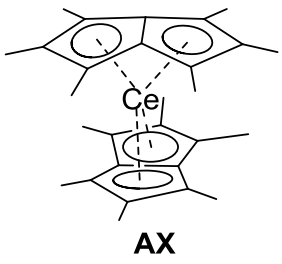

Figure 8 [Ce(η^8-C_8Me_6)$_2$]

Further investigations must be carried out before a definite answer can be found to describe the electronic configuration of cerium in these sandwich complexes. The findings for complexes **AV** – **AX** are summarised in Table 1.

Table 1 Analytic data for complexes **AV** – **AX**

	XANES	DFT	NMR	SQUID
$[Ce(COT)_2]$ **AV**	$4f^1$	80% $4f^1$ 20% $4f^0$	diamagnetic	TIP $\chi(T) = 1.4 \times 10^{-4}$ emu mol^{-1}
$[Ce\{\eta\text{-}C_8H_4(Si^iPr_3\text{-}1,4)_2\}_2]$ **AW**	$4f^1$	multiconfiguration ground state	paramagnetic	TIP $\chi(T) = (4.5 \pm 0.3) \times 10^{-4}$ emu mol^{-1}
$[Ce(\eta\text{-}C_8Me_6)_2]$ **AX**	$4f^1$	multiconfiguration ground state	diamagnetic with a paramagnetic contribution	TIP $\chi(T) = (25 \pm 0.1) \times 10^{-4}$ emu mol^{-1}

The UV-vis data of Ce^{IV} complexes and mixed valence cerium complexes will be discussed in section 1.13.

1.5.3 Mixed valence phthalocyaninato cerium complexes

Another type of cerium sandwich complex is the double-decker cerium phthalocyanine complex. These complexes have been reported to be of a radical nature with the trivalent cerium between a dianionic and a radical phthalocyanine ring, Figure 9.

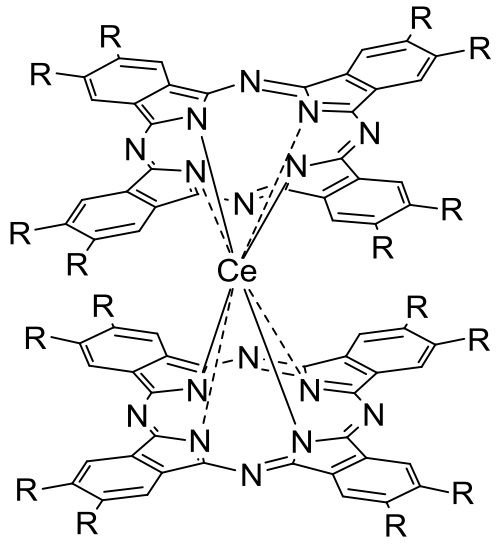

R = alkyl, alkoxy, thioalkyl

AY

Figure 9 Cerium phthalocyanine double-decker complex

In contrast, Nekelson and co-workers report the phthalocyanine cerium sandwich complexes as having a tetravalent cerium centre when the R groups were thioalkyls.[52,53] Isago and Shimoda studied the cerium bis(phthalocyaninato) complex with IR spectroscopy and cerium 3d XPS spectroscopy (X-ray photoelectron spectroscopy) and concluded that the cerium centre is neither tri- nor tetravalent and that the Ce 4f electron is delocalized in a phthalacyanine π orbital.[54] A study carried out by by Bian and co-workers compared a series of 7 cerium double-decker complexes with tetrapyrrole ligands including porphyrinates and phthalocyaninatos with different electronic properties. Spectroscopic, electrochemical and structural data show that these are multiconfigurational ground state complexes. A virtually trivalent state was found for the cerium complex with an electron rich naphthalocyaninato ligand. The other cerium complexes showed a predominantly $4f^0$ configuration state.[55]

1.6 Ce^{IV}-silanolate complexes

1.6.1 Synthesis of a Ce^{IV} metallasilsesquioxane complex from $[Ce(N")_3]$

The first tetravalent Ce^{IV} metallasilsesquioxane complex $[Ce\{(c\text{-}C_6H_{11})_8Si_8O_{13}\}_2(py)_3]$ **AZ** was reported by Edelmann and co-workers in 2001.[56] This

diamagnetic Ce^{IV} complex can be synthesised by treating $[Ce(N'')_3]$ with two equivalents of $(c\text{-}C_6H_{11})_8Si_8O_{11}(OH)_2$ in diethyl ether with the addition of an excess of pyridine or by the reaction of $[CeCl_3]$ with two equivalents of $(c\text{-}C_6H_{11})_8Si_8O_{11}(OH)_2$ in THF/pyridine, Scheme 17.

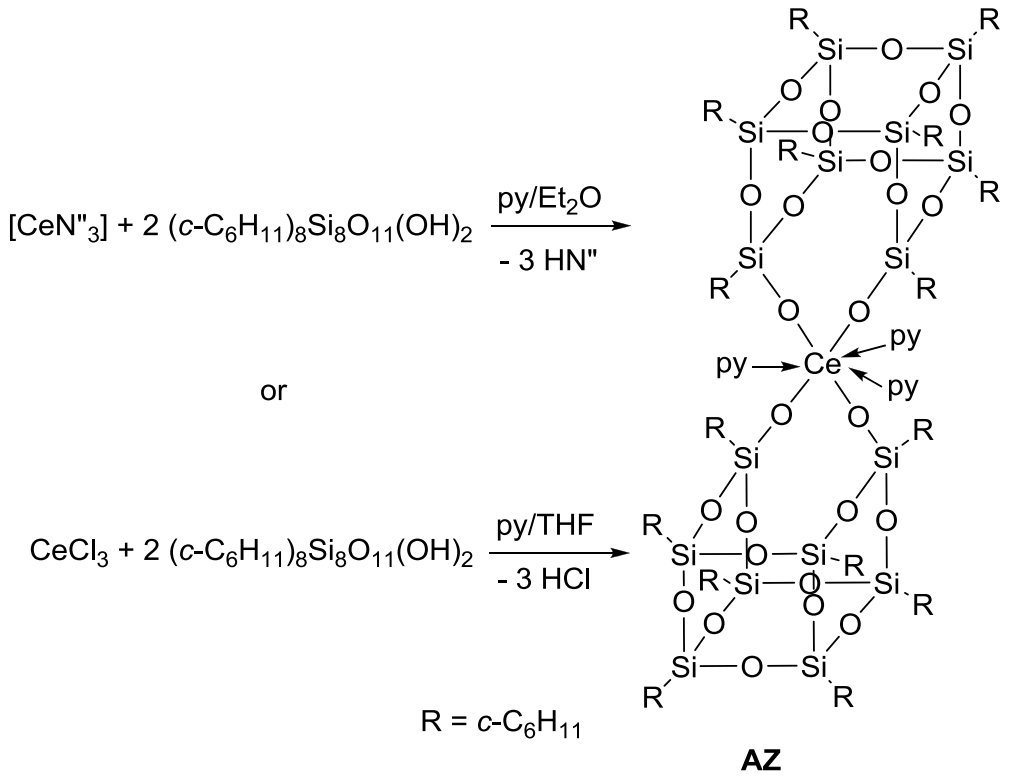

Scheme 17 Synthesis of $[Ce\{(c\text{-}C_6H_{11})_8Si_8O_{13}\}_2(py)_3]$ **AZ**

The authors speculate that initially an anionic Ce^{III} complex (Hpy)-$[Ce\{(c\text{-}C_6H_{11})_8Si_8O_{13}\}_2(py)_x]$ is formed in which the silanolate ligands confer an extended degree of Lewis acidity. Further, it is proposed that the Ce^{III} complex is then oxidised by the skeletal oxygen atom of the silsequioxane ligand to give **AZ**.

1.6.2 Cerium silyloxy complexes and heterobimetallic cerium disiloxanediolate complexes

Tetravalent cerium silyloxy complexes were reported by Gradeff and co-workers.[57] An example is the $[Ce(OSiPh_3)_4(DME)]$ complex **BA** which was obtained by treating CAN with 6 equivalents of $NaOSiPh_3$, Eq. (9). The cerium silyloxide complex **BA** can also be synthesised by the reaction between $[Ce(O^iPr)_4]$ and Ph_3SiOH.[58]

$$(NH_4)_2[Ce(NO_3)_6] + 6\ NaOSiPh_3 \xrightarrow{DME} [Ce(OSiPh_3)_4(DME)]\ \mathbf{BA} + 6\ NaNO_3 + 2\ NH_3 + 2\ Ph_3SiOH \quad (9)$$

Edelmann and co-workers published the first synthesis of two heterobimetallic cerium disiloxanediolate complexes $[\{(Ph_2SiO)_2O\}\{K(THF)_2\}]_2Ce(O^tBu)_2$ **BB** and $[\{(Ph_2SiO)_2O\}_2\{(DME)KO^tBu\}\{(Ph_2SiO_2)K\}Ce]_2$ **BC** starting from the Ce^{IV} complex $[(^tBuO)_3Ce(NO_3)_6]$ and two or three equivalents of $(Ph_2SiO)_2K$ respectively in 2007, Scheme 18.[59]

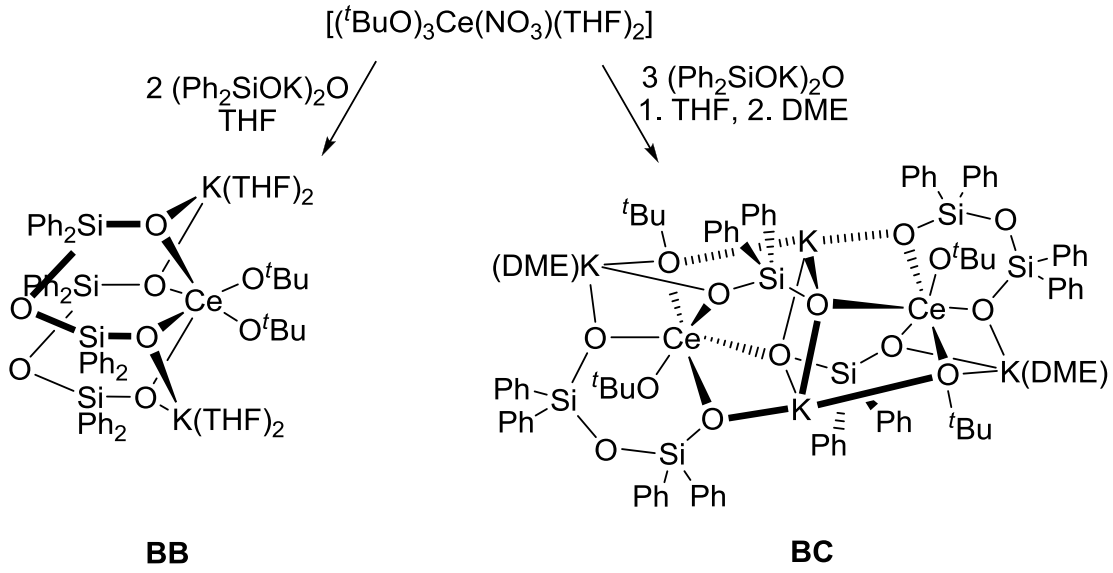

Scheme 18 Synthesis of the cerium(IV) disiloxanediolate complexes **BB** and **BC**

1.7 Ce^{IV} alkoxide complexes

An alternative starting material to CAN are mixed nitrate alkoxide complexes like $[(^tBuO)_3Ce(NO_3)_6]$ **BD**, whose synthesis was first published by Evans and co-workers, Eq. (10).[60]

$$(NH_4)_2[Ce(NO_3)_6] \xrightarrow[-\,2\,NH_3,\ -\,2\,{}^tBuOH,\ -\,n\,NaNO_3]{+\,n\,{}^tBuONa,\ THF} [Ce(O^tBu)_{n-2}(NO_3)_{6-n}(THF)_2]\quad n = 2-6 \quad \textbf{BD} \tag{10}$$

The one-electron oxidation of homoleptic Ce^{III} alkoxides was reported by Sen and co-workers in 1992.[61] They decided to use tri-*tert*-butyl methoxide (OC^tBu_3) as a ligand because of its high steric encumbrance. $[Ce(OC^tBu_3)_3]$ **BE** reacts cleanly with benzoyl peroxide on the NMR-scale in 95% yield to afford the Ce^{IV} complex $[Ce(OC^tBu_3)_3(OC(O)Ph)]$ **BF**, Eq. (11). Scaling up the reaction reduced the yield of **BF** to 60% and resulted in the formation of several Ce^{III} impurities as seen by ^1H NMR spectroscopy.

$$\underset{\textbf{BE}}{2\,Ce(OR)_3} + PhC(O)OOC(O)PH \xrightarrow[r.t.]{C_6D_6} \underset{\textbf{BF}}{2\,Ce(OR)_3(OC(O)Ph)} \qquad R = C^tBu_3 \tag{11}$$

If **BE** is treated with 1 equivalent of di-*tert*-butyl peroxide at 80 – 100 ˚C the Ce^{IV} complex $[Ce(OC^tBu_3)_2(O^tBu)_2]$ **BG** is obtained. The byproducts were identified as *tert*-butyl containing organics and therefore formulated as $[^tBu_3COOC^tBu_3]$, Eq. (12).

$$Ce(OR)_3 + 2\,{}^tBuOO^tBu \xrightarrow[80\,-\,100\,{}^oC]{C_6D_6} \underset{\textbf{BG}}{[Ce(OR)_2(O^tBu)_2] + [ROOCR]} \qquad R = C^tBu_3 \tag{12}$$

If **BE** is treated with the unsymmetrical peroxide *tert*-butyl peroxybenzoate a mixture of both products **BF** and **BG** is observed, Eq. (13).

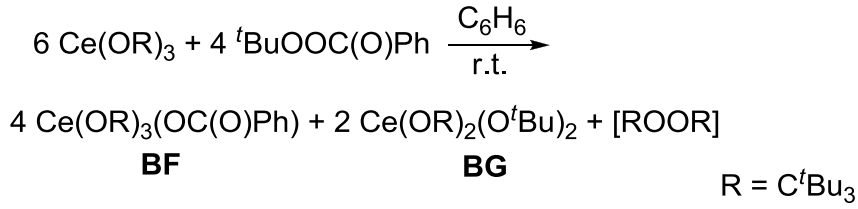

(13)

Further, Sen and co-workers reported the oxidation reaction of **BD** with benzoquinone to form the tetravalent Ce^{IV} complex $[(^tBu_3CO)_3CeOC_6H_4OCe(OC^tBu_3)_3]$ **BH**, Eq. (14).

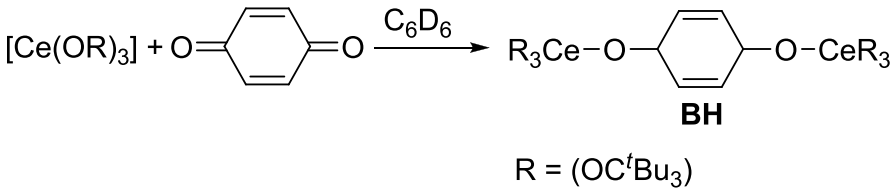

(14)

If **BE** is treated with 2,6-di-*tert*-butylbenzoquinone, only one equivalent of $[Ce(OR)_3]$ (R = C^tBu_3) reacts and the hemiquinone complex $[Ce(OR)_3(O\text{-}2,6\text{-}(^tBu)_2C_6H_2O\cdot]$ **BI** is formed, Eq. (15).

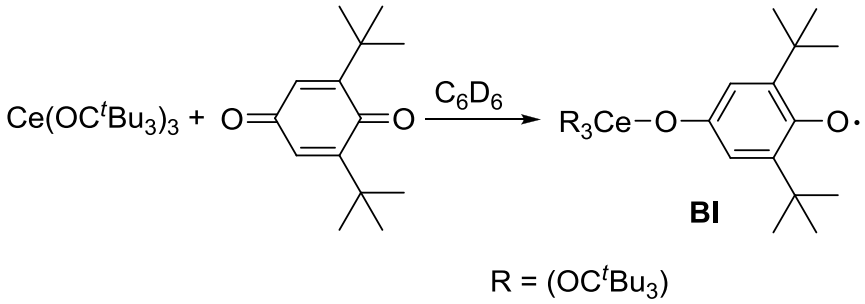

(15)

Since the ^1H NMR spectrum showed extremely broad resonances for the ring-*tert*-butyl groups and no resonances for the 3,5-protons but a typical shift for the $^tBu_3CO$ alkoxide groups the authors assume that the unpaired electron is delocalised about the ring and not the cerium. This was confirmed by ESR measurements. This complex **BI** is stable only for a few hours in solution at room temperature before it decomposes to $^tBu_2CO$ and isobutylene amongst other products.

In conclusion, the authors deem the utility of the (OC^tBu_3) ligand as limited from a synthetic standpoint as the tri-*tert*-butyl methoxide group has a tendency to dissociate

the Ce^{IV} complexes. When Sen and co-workers changed the alkoxy ligand from (OC^tBu_3) to (O^iPr) a tendency to form oligomeric species and bridging alkoxide groups were observed due to the smaller ligand.

A range of Ce^{IV} *tert*-alkoxides were published by Bradley and co-workers in 1957.[62] The heteroleptic Ce^{IV} complexes $[Ce(OR)_3Cl](py)$ **BJ** where R= CMe_3, CMe_2Et were synthesised from $[CeCl_6(py)_2]$ with an azeotropic mixture of benzene and the appropriate alcohol and ammonia, Eq. (16).

$$[CeCl_6(py)_2] + ROH/C_6H_6 \xrightarrow[NH_3]{\text{r.t.}} \underset{\textbf{BJ}}{[Ce(OR)_3Cl](py)} \quad (16)$$

$$R = CMe_3,\ CMe_2Et \qquad -\ 5\ NH_4Cl$$

Alcohol exchange was used to synthesise the tetravalent cerium alkoxides $[Ce(OR)_4]$ **BK** where R = CMe_3, CMe_2Et, CEt_3, $CMe_2{}^nPr$, $CMe_2{}^iPr$, $CMeEt{}^nPr$, Eq. (17).

$$[Ce(O^iPr)_4] + ROH/C_6H_6 \xrightarrow{\text{reflux, 12 h}} \underset{\textbf{BK}}{[Ce(OR)_4]} \quad (17)$$

$$R = CMe_3,\ CMe_2Et,\ CEt_3,\ CMe_2{}^nPr,\ CeMe_2{}^iPr,\ CMeEt{}^nPr$$

These cerium tetra-*tert*-alkoxides have boiling points between 130 – 150 ˚C at 0.05 mm Hg apart from R = CMe_2Et which has an observed boiling point of 240 ˚C at 0.1 mm Hg and are sensitive to water.

Cesca and co-workers reported in 1976 the first synthesis of $[Cp_3CeO^iPr]$ **BL** from $MgCp_2$ and $[Ce(O^iPr)_4]$ albeit in a very low yield, under 5%.[40]

$$3\ Cp_2Mg + 2\ Ce(O^iPr)_4 \xrightarrow[20\ ^oC]{C_6H_6} \underset{\textbf{BL}}{2\ Cp_3CeO^iPr} + 3Mg(O^iPr)_2 \quad (18)$$

This procedure was improved by Marks and co-workers by treating $[Ce(O^iPr)_4]$ with Me_3SnCp to give a 69% yield of $[Cp_3CeO^iPr]$.[63]

Evans and co-workers reported the conversion of mixed ligand cerium(IV)-*tert*-butoxide nitrate complexes to the cerium(IV)-*tert*-butoxide cyclopentadienyl complexes in a 90% yield for **BM** and a 50% yield for **BN**.[64]

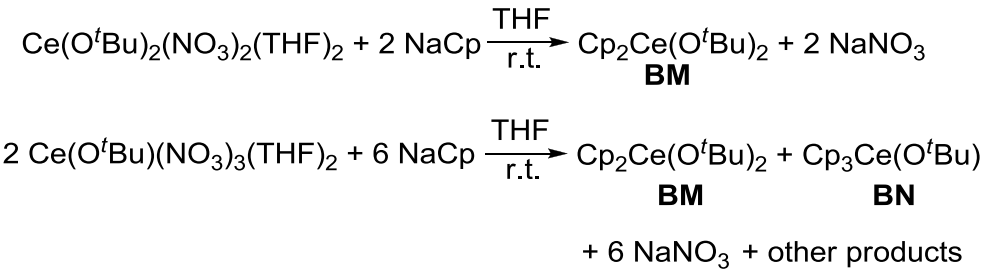

Scheme 19 Synthesis of cerium(IV)-*tert*-butoxide cyclopentadienyl complexes **BM** and **BN**

A mixed valence trinuclear cluster was reported by Lappert and co-workers as the result of treating [Ce(O^{t}Bu)$_4$(THF)$_2$] or [Ce(O^{t}Bu)$_3$(NO$_3$)] with three equivalents of [SnCp"Me$_3$] in an attempt to replace the -O^{t}Bu or -NO$_3$ ligand with -Cp".[36] Instead [{Ce(O^{t}Bu)$_2$}$_2$(μ_3-O^{t}Bu)$_2${Ce(O^{t}Bu)(κ^2-NO$_3$)}] **BO** was obtained, Figure 10.

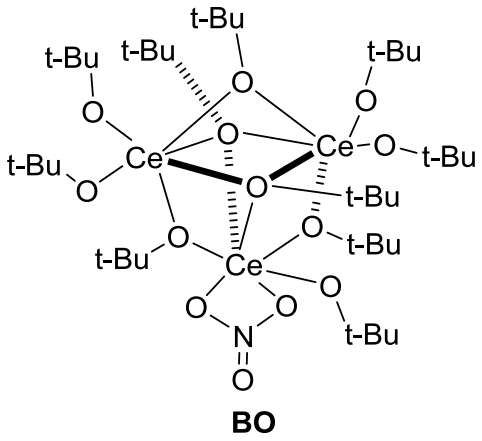

BO

Figure 10 Trinuclear complex [{Ce(O^{t}Bu)$_2$}$_2$(μ_3-O^{t}Bu)$_2${Ce(O^{t}Bu)(κ^2-NO$_3$)}] **BO**

The nitrate coordinated Ce atom has a formal oxidation state of (III) while the other two Ce cations are tetravalent.

1.8 Ce^{IV} complexes in a Schiff base ligand framework

Several cerium (IV) Schiff base ligand complexes have been reported, many of them bearing a variation of the H$_2$salen **BP** or H$_2$saloph **BQ** ligand, Figure 11.[65–68]

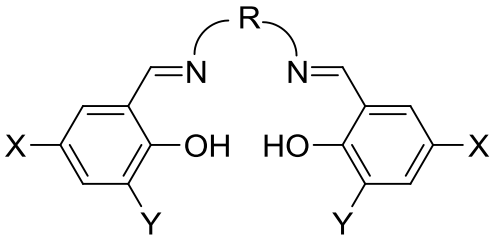

	R	X	Y	
H_2salen	CH_2CH_2	H	H	**BP**
H_2saloph	*o*-C_6H_4	H	H	**BQ**

Figure 11 H_2salen and H_2saloph

The related complex [Ce(salfen)(O^{t}Bu)$_2$], (salfen: R = Fe(C_5H_5)$_2$, X = Y = ^{t}Bu) can act as a catalyst for polymerisation reactions such as ring-opening polymerisation and was first reported by Diaconescu and Broderick in 2009.[69] It was found that the salfen compound is less active than [Ce(O^{t}Bu)$_4$(THF)$_2$] and only reacts with ε-caprolactone and L-lactide at 70 ˚C with an 80% conversion after 4 h and a mechanism that is described as 'complicated' by the authors.

Ce^{IV} Schiff-base ligand complexes are also known to form polymers such as [Ce(tsdb)]$_n$ (H_2tsdb: R = C_6H_4, X = Y = H), [Ce(tstm)]$_n$ ([Ce(tstm)]$_n$ = *catena*-poly[cerium(IV)-*μ*-*N*,*N*′,*N*″,*N*‴-tetrasalicylidene-3,3',4,4'-tetraaminodiphenylmethanato-O,N,N',O',O'',N'',N''',O''']) and [Ce(tsts)]$_n$ (Ce(tsts = *catena*-poly[cerium(IV)-*μ*-*N*,*N*′,*N*″,*N*‴-tetrasalicylidene-3,3',4,4'-tetraaminodiphenylsulfonato-O,N,N',O',N'',N'',N''',O''']) reported by Archer and co-workers.[70,71]

Other reported Schiff-base ligands used to make Ce^{IV} complexes include H_6TrenSal (H_6TrenSal = tris-((2-hydroxybenzyl)-aminoethyl)amine), Figure 12.

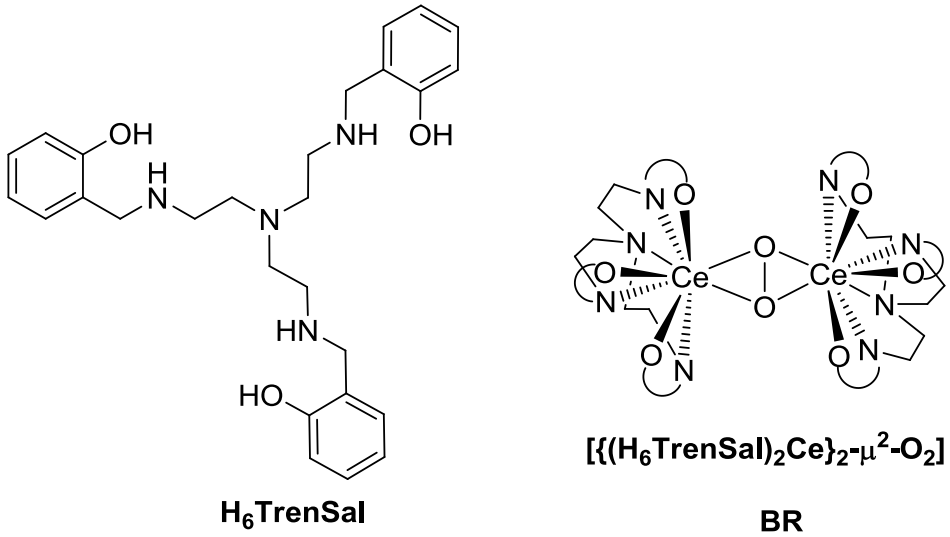

H_6TrenSal **[{(H_6TrenSal)$_2$Ce}$_2$-μ^2-O_2]**

BR

Figure 12 H_6TrenSal and [{(H_6TrenSal)Ce}$_2$-μ^2-O_2] **BR**

H_6TrenSal was reported by Reglinski and co-workers to form the peroxocomplex [{(H_6TrenSal)Ce}$_2$-μ^2-O_2] **BR**.[72] Since the magnetic moment of this complex is 1.3 BM at room temperature, whereas the expected moment for a Ce^{III} complex would be 2.2 BM, the authors propose that this is a mixed valence $Ce^{III/IV}$ complex.

Very similar to the H_6TrenSal ligand is the tripodal heptadentate Schiff-Base ligand that stabilises heteroleptic Ce^{IV} complexes that was reported by Dröse and Gottfriedsen, Eq. (19).[73]

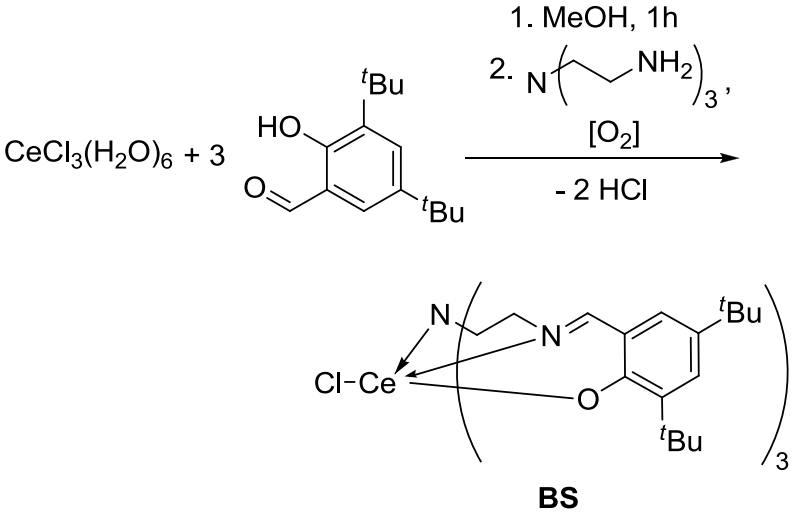

(19)

BS

The [CeN(L)$_3$Cl] complex **BS** is synthesised in a 53% yield from [CeCl$_3$(H$_2$O)$_6$]. The NO_3 equivalent [CeN(L)$_3$NO$_3$] can be synthesised from CAN in a 50% yield.

Gottfriedsen reported the synthesis and structure of [(THF)$_2$KCe(salen')$_2$] and the oxidation to the Ce^{IV} compound [Ce(salen')$_2$] **BT** by reaction with *p*-benzoquinone and air.[74]

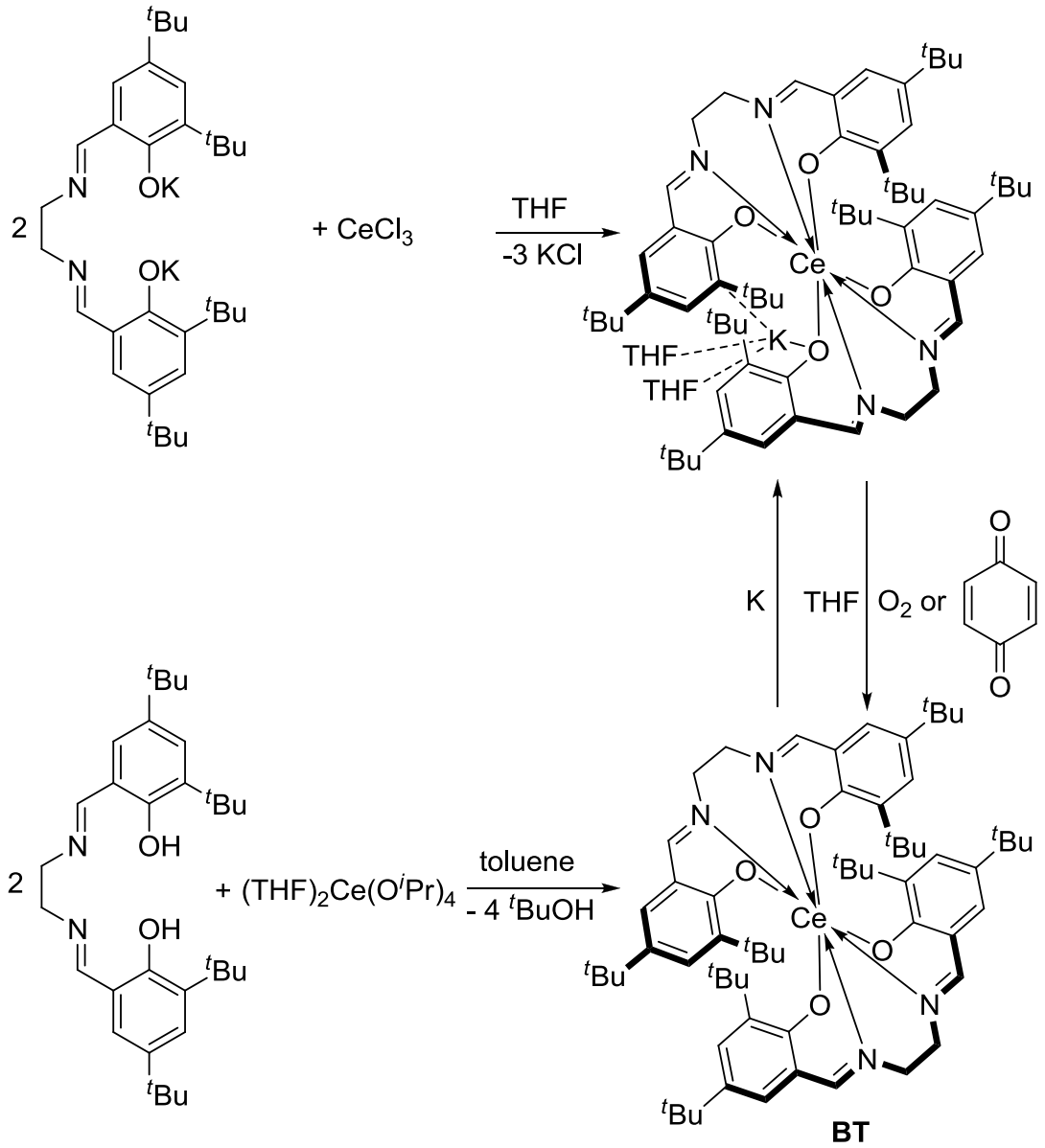

Scheme 20 Synthesis of [Ce(Salen')$_2$] **BT** and [(THF)$_2$KCe(Salen')$_2$]

1.9 First Ce^{IV} cationic complex with a Schiff-base ligand framework

The first cationic tetravalent cerium coordination complex and first tetravalent cerium azide compound were recently synthesised by Dröse and co-workers in 2011.[75] They are synthesised from a blue-purple Ce^{IV} complex with a tripodal Schiff-base ligand TRENDSAL (= $N[CH_2CH_2N{=}CH9C_6H_2{}^tBu_2\text{-}3,5\text{-}O\text{-}2]_3$ that is coordinated to the cerium metal ion, Scheme 21.

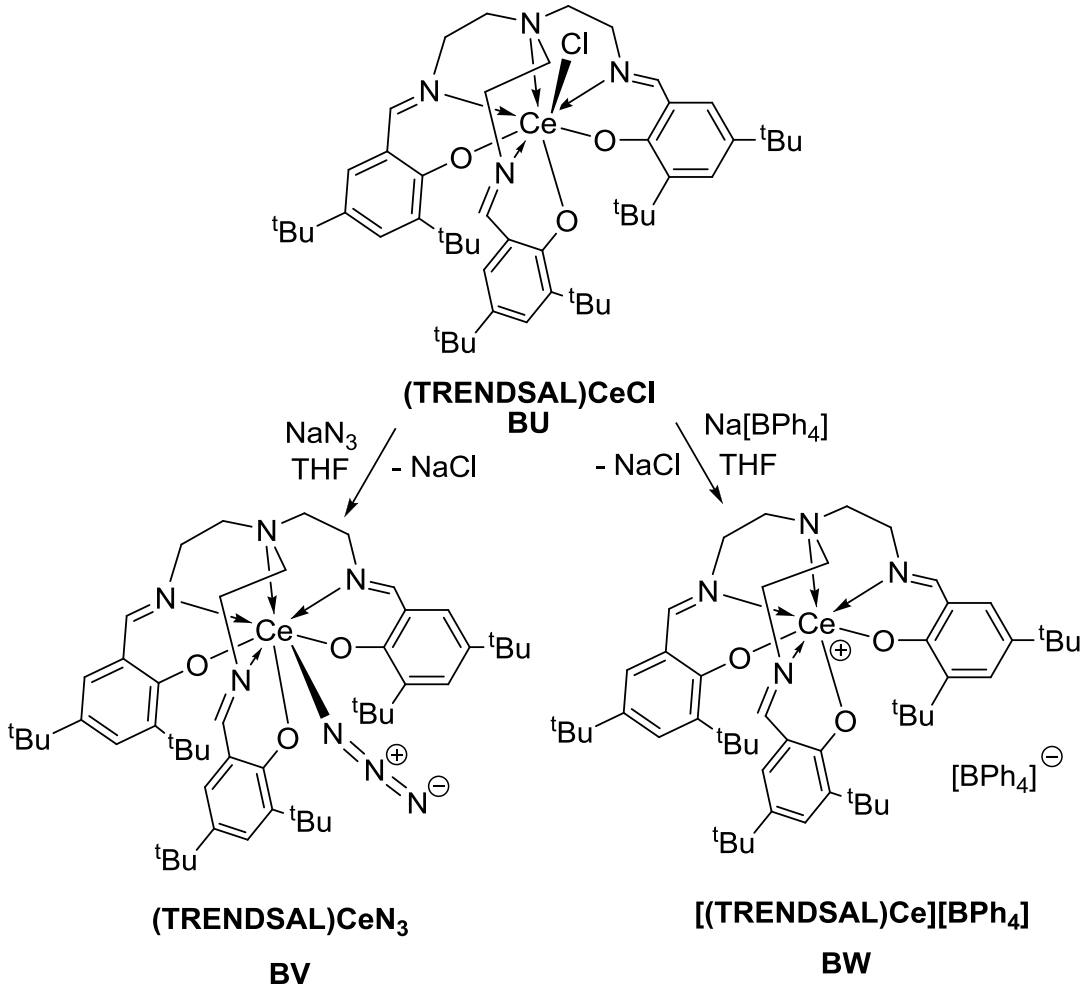

Scheme 21 The first Ce^{IV} cationic species by Dröse and coworkers

[(TRENDSAL)CeCl] **BU** is synthesised in a one-pot reaction from $[CeCl_3(H_2O)_6]$ or $(NH_4)_2[Ce(NO_3)_6]$ with tris(2-aminoethyl)amine and 3,5-di-*tert*-butylsalicylaldehyde. A THF solution of [(TRENDSAL)CeCl] was treated with an excess of NaN_3 to afford a dark purple solution from which crystals of air- and moisture-

stable [(TRENDSAL)CeN_3] **BV** can be obtained in a 53% yield. The strong azido stretch found in the IR spectrum at 2044 cm^{-1}, mass spectrometry and X-ray crystallography confirm the formation of the Ce^{IV} azide complex. Of note is the considerably longer Ce-N_{N3} bond length of 2.437(3) and 2.423(2) Å than the Ce-N_{amide} bond length of [$ClCe(N'')_3$] of 2.217(3) Å.[34]

The cationic [(TRENDSAL)Ce][BPh_4] **BW** was obtained in an 89% yield from a red-purple THF solution of the reaction of one equivalent of **BU** with an equimolar amount of $NaBPh_4$. Black crystals of the Ce^{IV} cationic species could be grown from an acetonitrile solution, Figure 13.

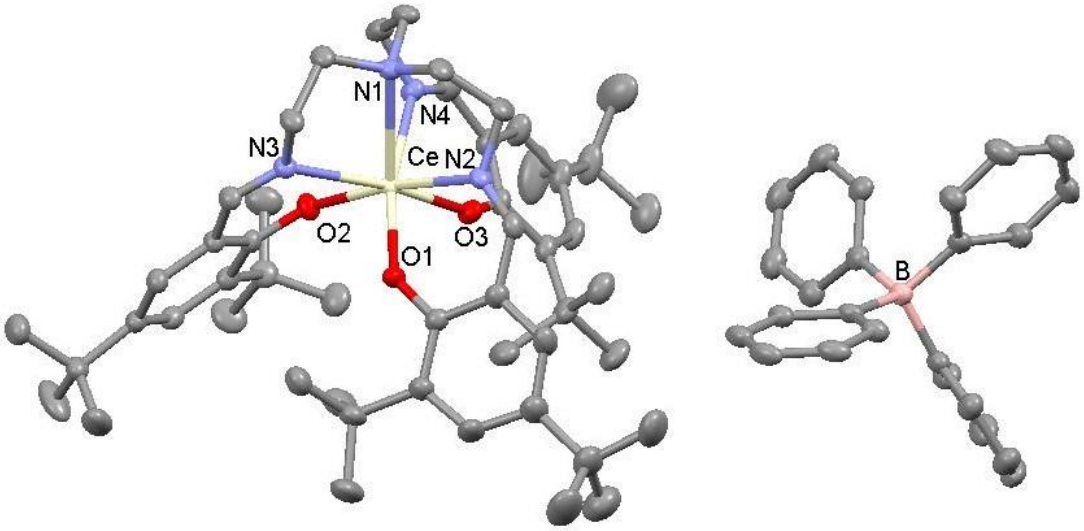

Figure 13 Solid state molecular structure of [(TRENDSAL)Ce][BPh_4] **BW**

The average Ce-N_{imine} bond distances of 2.482(9) Å are considerably shorter than in the Ce^{IV} azido complex with an average Ce-N_{imine} bond distance of 2.581 Å. The flexibility and the steric demand of the TRENDSAL Schiff-base ligand appear to be the important factor in stabilising the Ce^{IV} cation. The flexibility of the two chelating arms enables the rearrangement of the ligand, enabling it to satisfy the coordination sphere around the cerium cation once the chloride is removed. This presents an opposing argument to Schelter's work that was previously described in section 1.3 where the authors base the stabilisation of the Ce^{IV} complex on ligand rearrangement.

1.10 Tetravalent cerium NHC complexes

In 2007 our group showed that the Ce^{III} alkoxy-functionalised NHC complex $[CeL_3]$ (L = C{(N^{i}Pr)-CHCHN}CH_2CMe_2O) **BX** could be oxidised with benzoquinone to afford the Ce^{IV} complex $[CeL_4]$ **BY** in 78% yield, a complex which contains two pendant carbenes in the solid state, Scheme 22.[76]

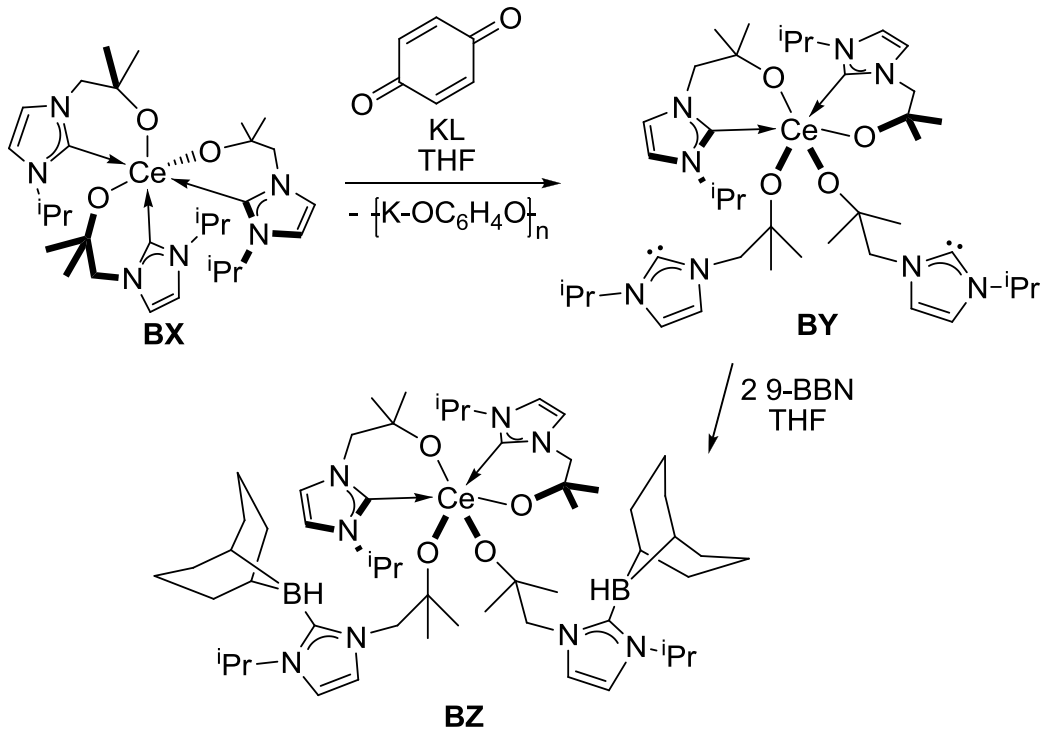

Scheme 22 Synthesis of the tetravalent Ce complexes **B** and **C**

The fluxionality of the pendant carbenes in **BY** can be 'frozen out' by adding two equivalents of 9-borabicyclo[3.3.1]nonane (9-BBN), yielding 80% of yellow crystals of **BZ**.

BX and **BY** were also afforded when $[Ce(OTf)_4]$ was combined with four equivalents of KL in a 3:1 ratio, Eq.(20).

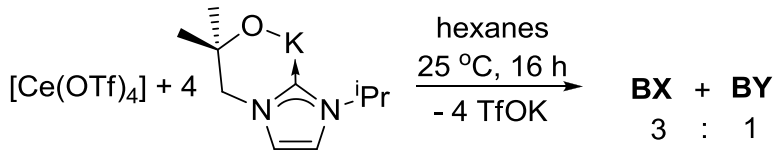

(20)

Other oxidants such as $TeCl_4$, I_2 and PBr_2Ph_3 were tested for their reactivity towards **BX** but no reaction was observed. The oxidants XeF_2 and $[FeCp_2][OTf]$ gave the product **BY** as a yellow solid in low yields of 32% and less than 10% respectively.

It was also found that $[CeL_4]$ **BY** could be synthesised from $[Ce(OTf)_4]$ and the potassium salt of the ligand [KL] and benzoquinone when they were treated in a 4:17.5:1.5 ratio.[77] Attempts to synthesise **BY** from a $[Ce(O^tBu)_4]$ starting material and HL (saturated and unsaturated NHC backbone) led to the formation of $[Ce(O^tBu)_4]_2(\mu$-LH) **CA**, Scheme 23. Subsequent attempts to eliminate ^{t}BuOH from the complex to obtain **CB** did not lead to the desired result.

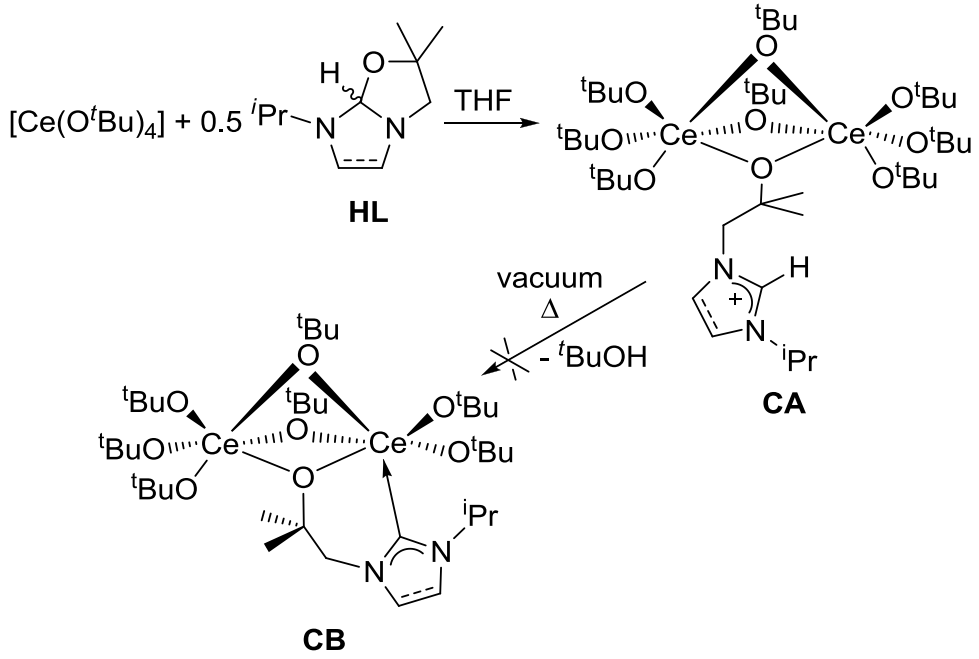

Scheme 23 Addition of [HL] to $[Ce(OtBu)_4]$

1.11 Ce^{IV} double-decker porphyrin complexes

Tetravalent cerium double-decker porphyrin complexes have received attention because of their potential electrochromic properties. One example is the bis(2,3,7,8,12,13,17,18-ocatethylporphyrinato)cerium(IV) ($[Ce(OEP)_2]$) complex that was reported in 1986 by Buchler and co-workers.[78] Aida and co-workers reported the structurally very similar $[Ce(dtp)_2]$ (dtp = ditolylporphoryn) **CC** and $[Ce(motp)_2]$ (motp = methoxyphenyl ditolylporhyrin) **CD** complexes, Scheme 24.[79] **CC** and **CD** have D_2 symmetry in the solid state and are chiral. The rotatability of these complexes was investigated with variable-temperature NMR spectroscopy. The **CD** enantiomers could

successfully be separated but slowly racemise at 10 ˚C, and show optical activity for 7.5 h, whereas the **CC** complex shows no optical resolution. Attempts to obtain the heteroleptic [Ce(dtp)(motp)] complex were not successful.

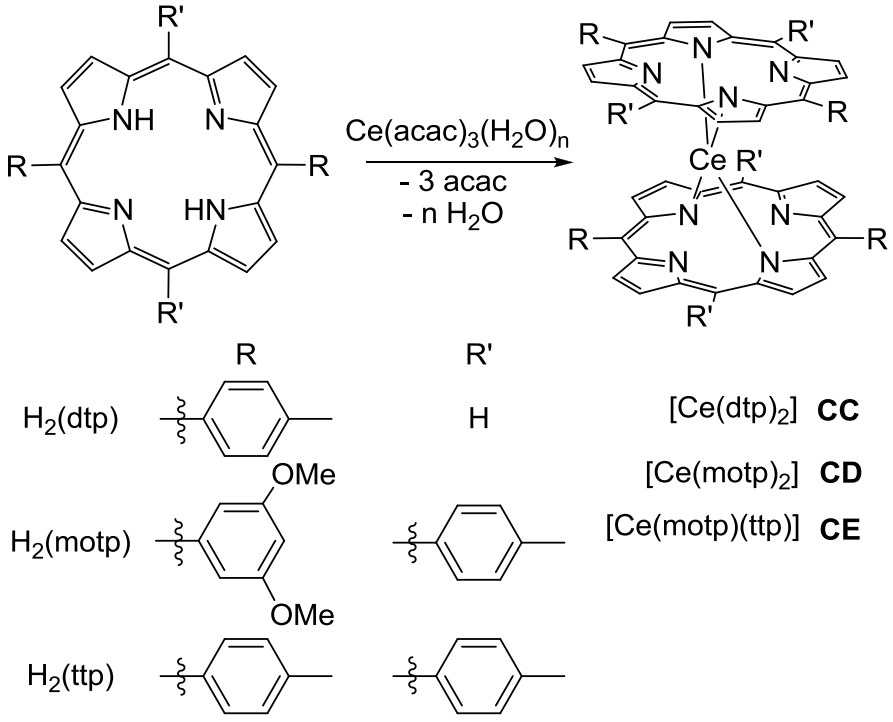

Scheme 24 Synthesis of chiral cerium *bis*porphyrins

Buchler and co-workers also published an example of tetravalent cerium sandwich complexes with porphyrin ligands that are bridged by aliphatic diether bridges, Figure 14.[80]

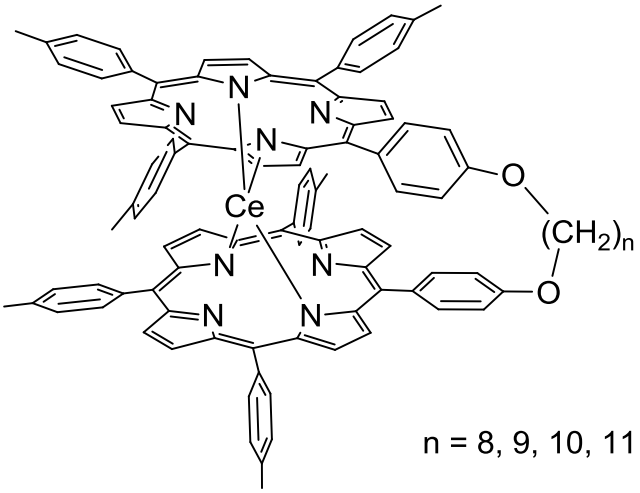

CF$^{8, 9, 10, 11}$

Figure 14 Aliphatic diether bridged Ce^{IV} bisporphyrin complex **CF**

Yang and co-workers reported the 2-butenedioic acid (Z)-monophenyl ester Ce^{IV} complex with a coordinated ethereal oxygen atom, Figure 15.[81] The complex was synthesised from CAN and the protonated ligand.

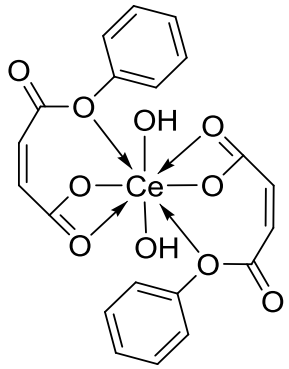

CG

Figure 15 2-butenedioic acid (Z)-monophenyl ester cerium complex

Ce^{IV} complexes such as a Ce^{IV}/EDTA complex reported by Komiyama and Sumaoka and a monolayer protected gold nanoparticle Ce^{IV} complex reported by Mancin and co-workers were investigated towards their reactivity for phosphodiester cleavage.[82,83]

1.12 ß-diketonate Ce^{IV} complexes

Homoleptic Ce^{IV} tetrakis ß-diketonate complexes show good air stability and often have good volatility. Because of these properties they have been used as CVD (chemical vapour deposition) and MOCVD (metal-organic chemical vapour deposition) precursors for the growth of CeO_2 fims. A wide range of homoleptic Ce^{IV} tetrakis ß-diketonate complexes have been synthesised and fully characterised, for example complexes **CH**-**CL**, Figure 16.[84–91]

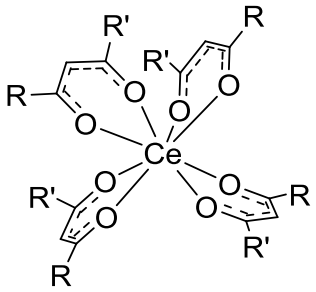

CH $Ce(acac)_4$ R, R' = CH_3
CI $Ce(thd)_4$ R, R' = $(CH_3)_3$
CJ $Ce(fdh)_4$ R = $(CH_3)_3$, R' = CF_3
CK $Ce(pmhd)_4$ R = Ph R' = $CH_2CH(CH_3)_2$
CL $Ce(fod)_4$ R = $(CH_3)_3$, R' = $CF_3(CF_2)_2$

Figure 16 ß-diketonate cerium complexes A - G

Leung and co-workers reported the synthesis of tetravalent cerium oxo and peroxo complexes supported by an imidophosphinate ligand **CM**.[92]

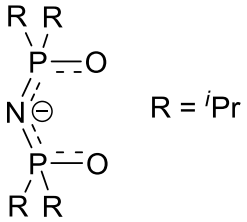

CM

Figure 17 imidophosphinate ligand **A**

The air-stable cerium di-μ-peroxo complex $[Ce\{N(^iPr_2PO)_2\}_2]_2(\mu\text{-}\eta^2\text{:}\eta^2\text{-}O_2)_2$ **CN** could be synthesised from the Ce^{IV} alkoxide $[Ce_2(O^iPr)_8(^iPrOH)_2]$ treated with $HN(^iPr_2PO)_2$ or from the oxidation of $[Ce\{N(^iPr_2PO)_2\}_3]$ with H_2O_2, Scheme 25.

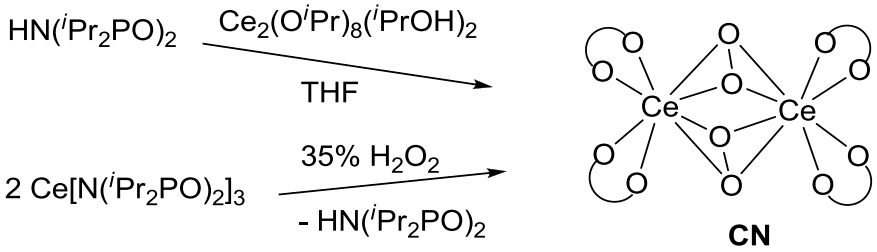

CN

Scheme 25 Synthesis of cerium peroxo complex **CN**

If three equivalents of $KN(^{i}Pr_2PO)_2$ are reacted with $(Et_4N)_2[CeCl_6]$ in acetonitrile the tetravalent $[Ce\{N(^{i}Pr_2PO)_2\}_3Cl]$ complex **CP** is obtained, Scheme 26.

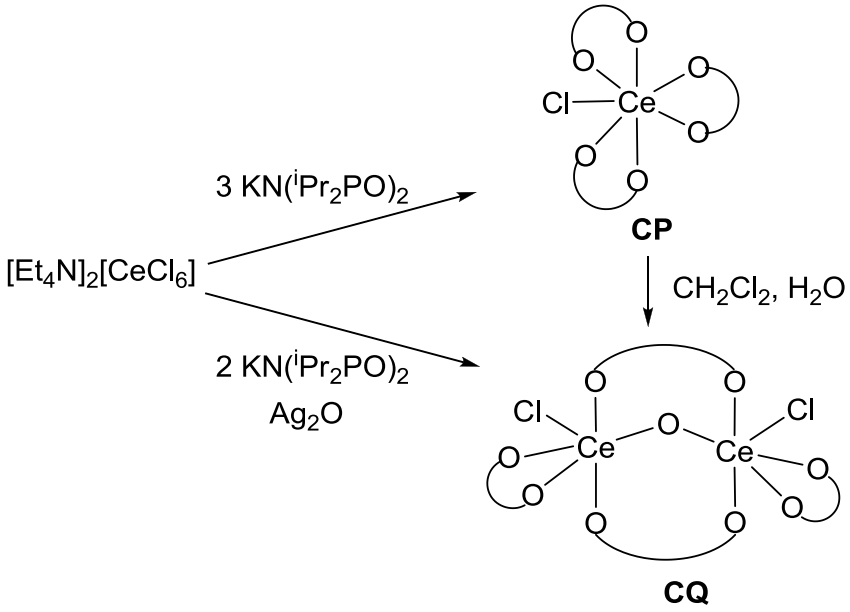

Scheme 26 Synthesis of cerium oxo complexes **CP** and **CQ**

If only two equivalents of $KN(^{i}Pr_2PO)_2$ were used an air-sensitive diamagnetic substance was isolated which is speculated to be the dichloride complex $[Ce\{N(^{i}Pr_2PO)_2\}Cl]$ with a small amount of **CP** as a byproduct. If this compound was allowed to slowly hydrolyse the μ-oxo complex $[Ce\{N(^{i}Pr_2PO)_2\}\text{-}Cl]_2[\mu\text{-}N(^{i}Pr_2PO)_2](\mu\text{-}O)$ **CQ** was obtained in a 10% yield. An improved yield of 45% was achieved when half an equivalent of Ag_2O was added to the reaction mixture. Complex **CQ** is stable under nitrogen but slowly reacts in air to form **CP** and an unknown byproduct that is postulated to be a polynuclear Ce^{IV} oxide.

1.13 UV-vis data of Ce^{IV} complexes and mixed valence cerium complexes

It has been reported that Ce^{IV} complexes often are of an intense purple colour compared to the mostly yellow and orange Ce^{III} complexes. Collected UV-vis data for Ce^{IV} complexes are shown in Table 2. The spectra typically consist of a strong B (Soret) band and Q(0,0) bands.

Table 2 UV-vis data for Ce^{IV} complexes

complex		λ / nm	reference
$[Ce(dtp)_2]$	**CC**	384, 482, 530.5	[79]
$[Ce(motp)_2]$	**CD**	401.5, 482.5, 543.5, 635.5	[79]
[Ce(motp)(tpp)]	**CE**	398, 487, 542, 628.5	[79]
$[Ce(OEP)_2]$	**CQ**	378, 530, 573	[78]
$[Ce(porphyrinato)_2]$	**CF[8]**	398, 483, 544, 586, 647	[80]
"	**CF[9]**	398, 483, 544, 586, 647	[80]
"	**CF[10]**	398, 480, 544, 582, 648	[80]
"	**CF[11]**	398, 478, 545, 584, 648	[80]
$[Ce(sal)_4]$	**CR**	381	[70]
$[\{(H_6TrenSal)Ce\}_2\text{-}\mu^2\text{-}O_2]$	**BR**	431	[72]
$[\{Ce(O^tBu)_2\}_2(\mu_3\text{-}O^tBu)_2(\mu\text{-}O^tBu)_3\{Ce(O^tBu)(NO_3)\}]$	**BO**	220, 258, 278, 336	[93]

OEP = octaethylporphyrinate; sal = salicylaldehydato

Very little data has been collected for the UV-vis analysis of molecular Ce^{IV}-complexes. A definite trend can be seen in the porphyrinato and Schiff-base ligand cerium complexes **CC**-**BR**. They all display a Soret band at around 400 nm, the weakest displayed by **CQ** with 378 nm and the most intense displayed by **BR** with 431 nm. The trinuclear complex **BO** with two Ce^{IV} and one Ce^{III} centre shows a hypsochromic shift compared to **CC**-**BR**.

The data in Table 3 are collected UV-vis data for mixed valence cerium compounds that were described in this chapter.

Table 3 Collected UV-vis data for mixed valence cerium compounds

complex		λ / nm	reference
$[Ce(\eta^8\text{-}C_8Me_6)_2]$	**AX**	530	[51]
$[Ce(COT)_2]$	**CS**	469	[51]
$[Ce(\eta^8\text{-}C_8H_7Me)_2]$	**CT**	570	[41]
$[Ce\{Pc(OC_{12}H_{25})_8\}_2]$	**CU**	357, 500, 650, 686, 1650	[55]
[Ce(Pc)(TPyP)]	**CV**	331, 398, 438, 465, 526, 633, 832	[55]
[Ce(Nc)(TBPP)]	**CW**	323, 413, 479, 632, 685, 911	[55]
[Ce(Nc)(OEP)]	**CX**	324, 392, 467, 610, 660, 935	[55]
$[Ce\{(C_{18}H_{37}S)_8Pc\}_2]$	**AY**	312, 370, 494, 687	[52]

OEP = octaethylporphyrinate; sal = salicylaldehydato; COT = cyclooctatetraenide, Pc = phthalocyaninate; TPyP = *meso*-tetra(4-pyridyl)porphyrinate; TBPP = *meso*-tetrakis(4-*tert*-butylphenyl)porphyrinate; Nc = 2,3-naphthalocyaninate

In contrast to the data collected in Table 2 the complexes **AX**-**AY** show B-bands between 312 nm and 357 nm (**CU**-**AY**) and B-bands at a higher wavelength of 469 nm to 570 nm (**AX**-**CT**).

1.14 Outlook

This thesis describes the synthesis of electropositive metal N-heterocyclic carbene complexes and examines their reactivity towards small molecules. The oxidation chemistry of Ce^{III} and Pr^{III} complexes and the magnetic properties of dinculear cerium and praseodymium complexes is also discussed. Lastly, the issue of functionalisation of the uranyl oxo groups is discussed.

1.15 References

1. P. L. Watson, *J. Am. Chem. Soc.*, 1983, **105**, 6491–6493.
2. E. O. Fischer and A. Maasböl, *Angew. Chem. Int. Edit.*, 1964, **3**, 580–581.
3. W. von E. Doering and A. Kentaro Hoffmann, *J. Am. Chem. Soc.*, 1954, **76**, 6162–6165.
4. A. Igau, H. Grutzmacher, A. Baceiredo, and G. Bertrand, *J. Am. Chem. Soc.*, 1988, **110**, 6463–6466.
5. B. Pötter and K. Seppelt, *Angew. Chem. Int. Edit.*, 1984, **23**, 150–150.
6. H.-W. Wanzlick and H.-J. Kleiner, *Angew. Chem.*, 1961, **73**, 493–493.

7. A. J. Arduengo, H. V. R. Dias, R. L. Harlow, and M. Kline, *J. Am. Chem. Soc.*, 1992, **114**, 5530–5534.
8. R. W. Alder, P. R. Allen, M. Murray, and A. G. Orpen, *Angew. Chem. Int. Edit.*, 1996, **35**, 1121–1123.
9. C. Heinemann, T. Müller, Y. Apeloig, and H. Schwarz, *J. Am. Chem. Soc.*, 1996, **118**, 2023–2038.
10. C. Boehme and G. Frenking, *J. Am. Chem. Soc.*, 1996, **118**, 2039–2046.
11. A. J. Arduengo, III, H. V. R. Dias, and J. C. Calabrese, *Chem. Lett.*, 1997, 143–144.
12. A. J. Arduengo III, J. R. Goerlich, R. Krafczyk, and W. J. Marshall, *Angew. Chem. Int. Edit.*, 1998, **37**, 1963–1965.
13. A. J. Arduengo, J. R. Goerlich, and W. J. Marshall, *J. Am. Chem. Soc.*, 1995, **117**, 11027–11028.
14. A. J. Arduengo, F. Davidson, H. V. R. Dias, J. R. Goerlich, D. Khasnis, W. J. Marshall, and T. K. Prakasha, *J. Am. Chem. Soc.*, 1997, **119**, 12742–12749.
15. D. Patel, S. T. Liddle, S. A. Mungur, M. Rodden, A. J. Blake, and P. L. Arnold, *Chem. Commun.*, 2006, 1124.
16. P. L. Arnold, I. J. Casely, Z. R. Turner, R. Bellabarba, and R. B. Tooze, *Dalton Trans.*, 2009, 7236.
17. S. N. Riduan, Y. Zhang, and J. Y. Ying, *Angew. Chem. Int. Edit.*, 2009, **48**, 3322–3325.
18. S. E. Denmark and G. L. Beutner, *Angew. Chem. Int. Edit.*, 2008, **47**, 1560–1638.
19. A. L. Kenward and W. E. Piers, *Angew. Chem. Int. Edit.*, 2008, **47**, 38–41.
20. D. W. Stephan, *Dalton Trans.*, 2009, 3129.
21. P. A. Chase, A. L. Gille, T. M. Gilbert, and D. W. Stephan, *Dalton Trans.*, 2009, 7179.
22. D. Holschumacher, T. Bannenberg, C. G. Hrib, P. G. Jones, and M. Tamm, *Angew. Chem. Int. Edit.*, 2008, **47**, 7428–7432.
23. D. P. Riley, M. R. Smith, and P. E. Correa, *J. Am. Chem. Soc.*, 1988, **110**, 177–180.
24. J. Jiao, L. X. Nguyen, D. R. Patterson, and R. A. Flowers, *Org. Lett.*, 2007, **9**, 1323–1326.
25. V. Nair, J. Mathew, and J. Prabhakaran, *J. Chem. Soc. Rev.*, 1997, **26**, 127.
26. H.-J. Wang, L.-P. Mo, and Z.-H. Zhang, *ACS Comb. Sci.*, 2011, **13**, 181–185.
27. J. R. Robinson, P. J. Carroll, P. J. Walsh, and E. J. Schelter, *Angew. Chem. Int. Edit.*, 2012, **51**, 10159–10163.
28. C. Morton, N. W. Alcock, M. R. Lees, I. J. Munslow, C. J. Sanders, and P. Scott, *J. Am. Chem. Soc.*, 1999, **121**, 11255–11256.
29. P. B. Hitchcock, Q.-G. Huang, M. F. Lappert, and X.-H. Wei, *J. Mater. Chem.*, 2004, **14**, 3266.
30. P. B. Hitchcock, M. F. Lappert, and A. V. Protchenko, *Chem. Commun.*, 2006, 3546.
31. M. P. Coles, P. B. Hitchcock, A. V. Khvostov, M. F. Lappert, Z. Li, and A. V. Protchenko, *J. Chem. Soc. Dalton*, 2010, **39**, 6780.
32. M. D. Walter, R. Fandos, and R. A. Andersen, *New J. Chem.*, 2006, **30**, 1065.
33. P. B. Hitchcock, A. G. Hulkes, M. F. Lappert, and Z. Li, *Dalton Trans.*, 2004, 129.
34. O. Eisenstein, P. B. Hitchcock, A. G. Hulkes, M. F. Lappert, and L. Maron, *Chem. Commun.*, 2001, 1560–1561.
35. P. B. Hitchcock, A. G. Hulkes, and M. F. Lappert, *Inorg. Chem.*, 2004, **43**, 1031–1038.
36. M. Cristina Cassani, Y. K. Gun'ko, P. B. Hitchcock, A. G. Hulkes, A. V. Khvostov, M. F. Lappert, and A. V. Protchenko, *J. Organomet. Chem.*, 2002, **647**, 71–83.
37. P. L. Arnold, Z. R. Turner, N. Kaltsoyannis, P. Pelekanaki, R. M. Bellabarba, and R. P. Tooze, *Chem.-Eur. J.*, 2010, **16**, 9623–9629.

38. P. Dröse, A. R. Crozier, S. Lashkari, J. Gottfriedsen, S. Blaurock, C. G. Hrib, C. Maichle-Mössmer, C. Schädle, R. Anwander, and F. T. Edelmann, *J. Am. Chem. Soc.*, 2010, **132**, 14046–14047.
39. D. B. Baudry, A. Dormond, F. Duris, J. M. Bernard, and J. R. Desmurs, *J. Fluorine Chem.*, 2003, **121**, 233–238.
40. A. Greco, S. Cesca, and W. Bertolini, *J. Organomet. Chem.*, 1976, **113**, 321–330.
41. T. R. Boussie, D. C. Eisenberg, J. Rigsbee, A. Streitwieser, and A. Zalkin, *Organometallics*, 1991, **10**, 1922–1928.
42. U. Kilimann, R. Herbst-Irmer, D. Stalke, and F. T. Edelmann, *Angew. Chem. Int. Edit.*, 1994, **33**, 1618–1621.
43. A. Streitwieser, S. A. Kinsley, J. T. Rigsbee, I. L. Fragala, and E. Ciliberto, *J. Am. Chem. Soc.*, 1985, **107**, 7786–7788.
44. M. Dolg, P. Fulde, H. Stoll, H. Preuss, A. Chang, and R. M. Pitzer, *Chem. Phys.*, 1995, **195**, 71–82.
45. M. Dolg, P. Fulde, W. Küchle, C.-S. Neumann, and H. Stoll, *J. Chem. Phys.*, 1991, **94**, 3011.
46. A. Kerridge, R. Coates, and N. Kaltsoyannis, *J. Phys. Chem. A*, 2009, **113**, 2896–2905.
47. N. M. Edelstein, P. G. Allen, J. J. Bucher, D. K. Shuh, C. D. Sofield, N. Kaltsoyannis, G. H. Maunder, M. R. Russo, and A. Sella, *J. Am. Chem. Soc.*, 1996, **118**, 13115–13116.
48. A. Kerridge and N. Kaltsoyannis, *Comptes Rendus Chimie*, 2010, **13**, 853–859.
49. V. Lorenz, B. M. Schmiege, C. G. Hrib, J. W. Ziller, A. Edelmann, S. Blaurock, W. J. Evans, and F. T. Edelmann, *J. Am. Chem. Soc.*, 2011, **133**, 1257–1259.
50. G. Balazs, F. G. N. Cloke, J. C. Green, R. M. Harker, A. Harrison, P. B. Hitchcock, C. N. Jardine, and R. Walton, *Organometallics*, 2007, **26**, 3111–3119.
51. A. Ashley, G. Balazs, A. Cowley, J. Green, C. H. Booth, and D. O'Hare, *Chem. Commun.*, 2007, 1515.
52. F. Nekelson, H. Monobe, and Y. Shimizu, *Chem. Commun.*, 2006, 3874.
53. F. Nekelson, H. Monobe, M. Shiro, and Y. Shimizu, *J. Mater. Chem.*, 2007, **17**, 2607.
54. H. Isago and M. Shimoda, *Chem. Lett.*, 1992, 147–150.
55. Y. Bian, J. Jiang, Y. Tao, M. T. M. Choi, R. Li, A. C. H. Ng, P. Zhu, N. Pan, X. Sun, D. P. Arnold, Z.-Y. Zhou, H.-W. Li, T. C. W. Mak, and D. K. P. Ng, *J. Am. Chem. Soc.*, 2003, **125**, 12257–12267.
56. Y. K. Gun'ko, R. Reilly, F. T. Edelmann, and H.-G. Schmidt, *Angew. Chem. Int. Edit.*, 2001, **40**, 1279–1281.
57. P. S. Gradeff, K. Yunlu, T. J. Deming, J. M. Olofson, R. J. Doedens, and W. J. Evans, *Inorg. Chem.*, 1990, **29**, 420–424.
58. P. S. Gradeff, K. Yunlu, A. Gleizes, and J. Galy, *Polyhedron*, 1989, **8**, 1001–1005.
59. S. Giessmann, S. Blaurock, V. Lorenz, and F. T. Edelmann, *Inorg. Chem.*, 2007, **46**, 8100–8101.
60. W. J. Evans, T. J. Deming, J. M. Olofson, and J. W. Ziller, *Inorg. Chem.*, 1989, **28**, 4027–4034.
61. A. Sen, H. A. Stecher, and A. L. Rheingold, *Inorg. Chem.*, 1992, **31**, 473–479.
62. D. C. Bradley, A. K. Chatterjee, and W. Wardlaw, *J. Chem. Soc.*, 1957, 2600.
63. A. Gulino, M. Casarin, V. P. Conticello, J. G. Gaudiello, H. Mauermann, I. Fragala, and T. J. Marks, *Organometallics*, 1988, **7**, 2360–2364.
64. W. J. Evans, T. J. Deming, and J. W. Ziller, *Organometallics*, 1989, **8**, 1581–1583.
65. A. Terzis, D. Mentzafos, and H. A. Tajmir-Riahi, *Inorg. Chim. Acta*, 1984, **84**, 187–193.
66. K. Kubono, N. Hirayama, H. Kokusen, and K. Yokoi, *Anal. Sci.*, 2001, **17**, 193–197.

67. E. Szłyk, A. Wojtczak, L. Dobrzańska, and M. Barwiołek, *Polyhedron*, 2008, **27**, 765–776.
68. J. Gottfriedsen, M. Spoida, and S. Blaurock, *Z. Anorg. Allg. Chem.*, 2008, **634**, 514–518.
69. E. M. Broderick and P. L. Diaconescu, *Inorg. Chem.*, 2009, **48**, 4701–4706.
70. H. Chen, J. A. Cronin, and R. D. Archer, *Macromolecules*, 1994, **27**, 2174–2180.
71. H. Chen, J. A. Cronin, and R. D. Archer, *Inorg. Chem.*, 1995, **34**, 2306–2315.
72. A. Mustapha, J. Reglinski, and A. R. Kennedy, *Inorg. Chim. Acta*, 2009, **362**, 1267–1274.
73. P. Dröse and J. Gottfriedsen, *Z. Anorg. Allg. Chem.*, 2008, **634**, 87–90.
74. J. Gottfriedsen, M. Spoida, and S. Blaurock, *Z. Anorg. Allg. Chem.*, 2008, **634**, 514–518.
75. P. Dröse, J. Gottfriedsen, C. G. Hrib, P. G. Jones, L. Hilfert, and F. T. Edelmann, *Z. Anorg. Allg. Chem.*, 2011, **637**, 369–373.
76. I. J. Casely, S. T. Liddle, A. J. Blake, C. Wilson, and P. L. Arnold, *Chem. Commun.*, 2007, 5037.
77. P. L. Arnold, I. J. Casely, S. Zlatogorsky, and C. Wilson, *Helv. Chim. Acta*, 2009, **92**, 2291–2303.
78. J. W. Buchler, A. De Cian, J. Fischer, M. Kihn-Botulinski, H. Paulus, and R. Weiss, *J. Am. Chem. Soc.*, 1986, **108**, 3652–3659.
79. K. Tashiro, K. Konishi, and T. Aida, *Angew. Chem. Int. Edit.*, 1997, **36**, 856–858.
80. J. W. Buchler and T. Dippell, *Eur. J. Inorg. Chem.*, 1998, **1998**, 445–449.
81. Y. Zheng, Y. Yang, Y. Cui, and F. Dang, *J. Coord. Chem.*, 2006, **59**, 1921–1928.
82. M. Komiyama and J. Sumaoka, *B. Chem. Soc. Jpn.*, 2012, **85**, 533–544.
83. R. Bonomi, P. Scrimin, and F. Mancin, *Org. Biomol. Chem.*, 2010, **8**, 2622.
84. M. Becht, K.-H. Dahmen, V. Gramlich, and A. Marteletti, *Inorg. Chim. Acta*, 1996, **248**, 27–33.
85. H. Titze, L. Pettersson, N. Nigri, A. Kjekshus, B. Klewe, and D. L. Powell, *Acta Chem. Scand.*, 1974, **28a**, 1079–1088.
86. H. Titze, G. Gårdhammar, E. Rundcrantz, S. Sunner, A. A. Lindberg, G. Jansen, B. Lamm, and B. Samuelsson, *Acta Chem. Scand.*, 1969, **23**, 399–408.
87. M. DelaRosa, K. Bousman, J. Welch, and P. Toscano, *J. Coord. Chem.*, 2002, **55**, 781–793.
88. I. Baxter, J. A. Darr, M. B. Hursthouse, K. M. A. Malik, D. M. P. Mingos, and J. C. Plakatouras, *J. Chem. Crystallogr.*, 1998, **28**, 267–276.
89. M. Becht, T. Gerfin, and K. H. Dahmen, *Chem. Mater.*, 1993, **5**, 137–144.
90. B. Matković and D. Grdenić, *Acta Crystallogr.*, 1963, **16**, 456–461.
91. J. McAleese, J. C. Plakatouras, and B. C. H. Steele, *Thin Solid Films*, 1996, **280**, 152–159.
92. G.-C. Wang, H. H. Y. Sung, I. D. Williams, and W.-H. Leung, *Inorg. Chem.*, 2012, **51**, 3640–3647.
93. Y. K. Gun'ko, S. D. Elliott, P. B. Hitchcock, and M. F. Lappert, *J. Chem. Soc. Dalton*, 2002, 1852–1856.

Chapter 2 Reactivity of Ce^{III} and $U^{III/IV}$ NHC complexes

2.1 Introduction

Transition metal NHC complexes are effectively and widely used in homogenous catalysis.[1–6] The most common oxidation state for cerium is Ce^{3+}, the electronic configuration of which is $[Xe]4f^1$ with Ce^{4+} also being chemically accessible. The uranium complexes discussed in this chapter are in the oxidation state U^{3+} and U^{4+}. The ionic radii for six coordinate, octahedral Ce^{3+}, U^{3+} and U^{4+} are very similar with 115 pm (Ce^{III}), 116.5 pm (U^{III}) and 114 pm (U^{IV})[7], allowing for comparisons between the 4f and 5f metal complexes in regards to their reactivity and bonding. The standard redox potential for $Ce^{3+/4+}$ is 1.4 V and –0.61 V for $U^{3+/4+}$.[8,9] Different affinities of an NHC ligand towards a lanthanide and actinide compound [Cp'MI] (M = U, Ce; Cp' = $C_5H_4{}^tBu$) have been observed by Berthet and Ephritikine.[10] DFT studies investigating selective lanthanide/actinide complexation by tridentate bis(NHC)pyridyl ligands have been carried out by Maron showing that the formation of the mono-adducts were predicted to be thermodynamically favoured for the lanthanides.[11] It was also shown by the Arnold group that an NHC-alkoxide formed a six-coordinated [CeL_4] (L = [$OCMe_2CH_2${CN CHCHN^{i}Pr}]) compound with two of the NHC bound whereas the [UL_4] complex, which was expected to be isostructural with [CeL_4], was seven-coordinate with three of the NHCs bound.[12–14]

2.2 Ce^{III}-NHC complex addition-elimination chemistry

2.2.1 Synthesis and characterisation of the Ce^{III}-NHC complexes

The ligand that was used for the synthesis of the Ce-NHC complexes is a bicyclic alkoxy-tethered NHC with a saturated backbone [L^M] (L^M = $OC(CH_3)_2CH_2(CNCH_2CH_2NMes)$) that was synthesised by the Arnold group;[15] shown in Figure 1.

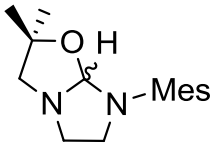

Figure 1 Alkoxy-tethered proligand **[HL^{M}]**

The proligand [HL^{M}] was designed due to the discovery that the neodymium complex **A** (a bicyclic NHC with an unsaturated backbone) could be functionalised at the carbene backbone when treated with substrates such as Me_3SiI, forming **C**, see Scheme 1, instead of binding to the carbene carbon. **A** was anticipated to react with Me_3SiI to form **[Nd(L)N"(μ-I$_2$)]** and $N(SiMe_3)_3$ as a byproduct.[16] Instead **A** reacts with Me_3SiI to form **B** with HN" as a byproduct. To prevent this unwanted side-reaction [HL^{M}] was synthesised.

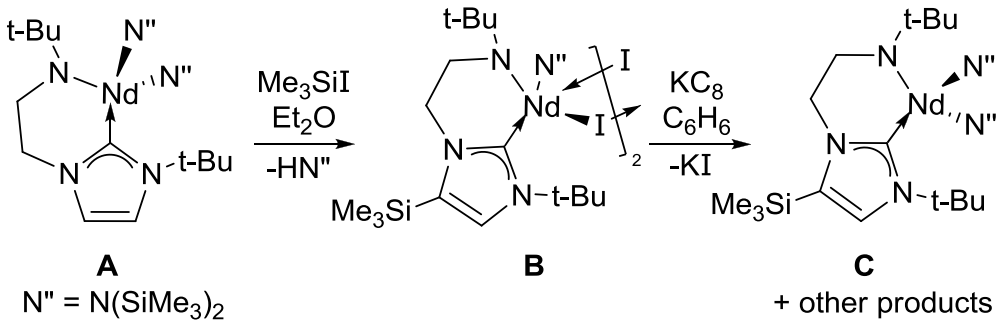

Scheme 1 Addition of $SiMe_3$ to the unsaturated carbene backbone

2.2.1.1 Synthesis of the Ce^{III}-NHC complexes

The mono-ligand cerium complex [Ce(L^{M})(N")$_2$] **1** (N" = N(SiMe$_3$)$_2$ and the bis-ligand cerium complex [Ce(L^{M})$_2$N"] **2** were synthesised by a protonolysis reaction of [Ce(N")$_3$] with one or two equivalents of [HL^{M}][17], Scheme 2.

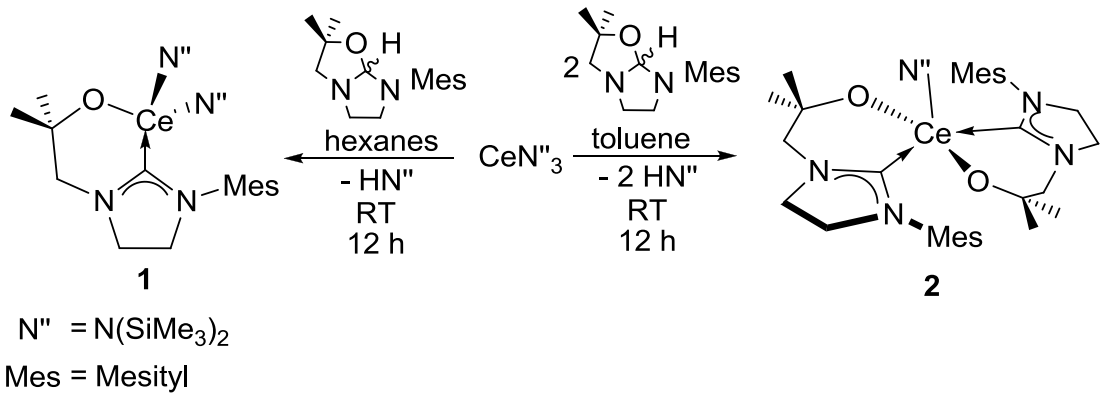

Scheme 2 Syntheses of the mono-ligand cerium amide complex **1** and bis-ligand cerium amide complex **2**

Complex **2** has been fully characterised by Dr. Ian Casely, a former member of the Arnold group.[18] The synthesis of the mono-ligand carbene cerium complex **1** was carried out at room temperature in hexane solution in the reaction of [HL^M] with [$Ce(N")_3$], over 16 hours, with a 72% yield.

2.2.1.2 X-ray crystal structure of [Ce(L^M)N"$_2$(py)] and comparison to [Ce(L^M)$_2$N"]

Single crystals of [Ce(L^M)(N")$_2$(py)] $\mathbf{1_{py}}$ (py = pyridine) that were suitable for X-ray crystallography were obtained from a saturated pyridine solution of **1** at -30 °C. The molecular structure is shown in Figure 2 and selected bond distances and angles are displayed in Table 1.

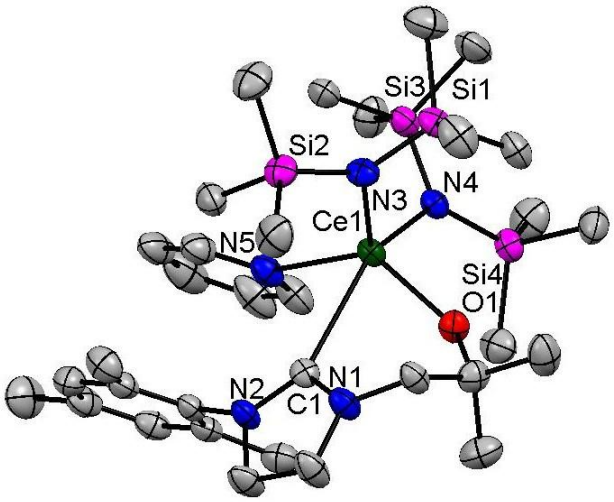

Figure 2 Displacement ellipsoid drawing (50%) of $\mathbf{1_{py}}$, H-atoms and one pyridine solvent molecule omitted for clarity

The colour scheme for the crystal structures in this chapter is as follows:
Carbon ■ Nitrogen ■ Oxygen ■ Silicon ■ Cerium ■

The cerium centre is five-coordinate and adopts a highly distorted trigonal bipyramidal geometry, the axial atoms being $C1_{carbene}$, $N3_{amide}$ and $N4_{amide}$ with an axial C1-Ce1-N4 angle of 148.51(13)° and equatorial angles N5-Ce1-N3, N3-Ce1-O1 and O1-Ce1-N5 of 126.28(15)°, 101.31(14)° and 129.00(13)° respectively, with an angle sum of 356.59(12)°. The Ce1-O1 and the Ce1-C1 bond distances are 2.155(3) Å and 2.844(5) Å respectively. The crystal structure of the bis-ligand cerium complex has been obtained by I. J. Casely, Figure 3.

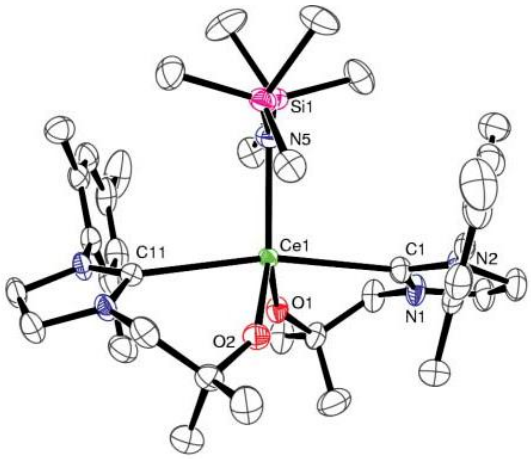

Figure 3 Displacement ellipsoid drawing (50%) of **2**, H-atoms omitted for clarity

To compare the structures of $\mathbf{1_{py}}$ and **2** selected bond distances (Å) and angles (˚) are displayed in Table 1.

Table 1 Selected bond distances (Å) and angles (˚) in $\mathbf{1_{py}}$ and **2**

$\mathbf{1_{py}}$		**2**	
Ce1-O1	2.155(3)	Ce1-O1,-O2	2.172(3), 2.184(3)
Ce1-C1	2.844(5)	Ce1-C1,-C11	2.786(4), 2.798(4)
$Ce1\text{-}N3_{amide}$,$\text{-}N4_{amide}$	2.398(4), 2.408(4)	$Ce1\text{-}N5_{amide}$	2.442(3)
$N\text{-}C_{av}$	1.342	$N\text{-}C_{av}$	1.336
N1-C1-N2	106.6(4)	$N\text{-}C\text{-}N_{av}$	107.1
$Ce1\text{-}N5_{py}$	2.810(4)		

The Ce1-O1 bond of $\mathbf{1_{py}}$ is 2.155(3) Å *vs* 2.172(3) and 2.184(3) Å for **2**. Therefore the Ce1-O1 bond of $\mathbf{1_{py}}$ is 0.017 - 0.029 Å shorter than in **2**. The Ce1-C1 bond distance for $\mathbf{1_{py}}$ is 2.844(5) Å *vs* 2.786(4) and 2.798(4) Å for **2** and by 0.058 - 0.046 Å longer in $\mathbf{1_{py}}$ than in **2**. The N-C-N angle of 106.6(4)˚ is comparable. The Ce1-N_{amide} bond distances of 2.398(4) Å and 2.408(4) Å are 0.034 - 0.044 Å shorter in $\mathbf{1_{py}}$ than in **2**. The key difference between $\mathbf{1_{py}}$ and **2** is that **2** is sterically encumbered because of the two bound NHCs with sterically demanding mesityl groups as opposed to one in $\mathbf{1_{py}}$. The resulting lack of bulk surrounding $\mathbf{1_{py}}$ results in a bound pyridine solvent molecule on the metal centre. Further differences are the longer Ce-$C_{carbene}$ bond in $\mathbf{1_{py}}$ and slightly shorter Ce-O and Ce-$N_{silylamide}$ bonds in $\mathbf{1_{py}}$. $\mathbf{1_{py}}$ displaying a longer Ce-$C_{carbene}$ bond is slightly counter-intuitive as the steric congestion of the bis-ligand complex could be expected to result in a longer C-$C_{carbene}$ bond distance in **2**. The five coordinate Ce^{III}-amido-NHC complex $[Ce(L)N''(\mu\text{-}I)_2]_2$ (L = ^{t}BuNHCH$_2$CH$_2$[C{^{t}BuNCHCHN}] has a Ce-$C_{carbene}$ bond distance of 2.700(3) Å, which is shorter than for $\mathbf{1_{py}}$. Other cerium carbene complexes, such as the *cis*-1,2-$[(1,2,4\text{-}(Me_3C)_3C_5H_2)_2CeO]_2C_2H_2$ and the *trans* analogue, have a Ce-C_{Cp} bond distance of 2.83(2) Å,[19] which is comparable to the Ce-$C_{carbene}$ bond distance as in $\mathbf{1_{py}}$. The complex $[Ce(C_5Me_5)_2I\text{-}C(NMeCMe_4N_2)]$, one of the first cerium carbene complexes, has a Ce-$C_{carbene}$ bond distance of 2.724(4) Å, which is about 0.1 Å shorter than for $\mathbf{1_{py}}$.[10]

2.2.1.3 The role of pyridine

The coordinated pyridine may be the reason for the elongation of the bond because of π-stacking between the pyridine and the mesityl ring. The two aromatic rings are in a slightly displaced sandwich configuration with a distance between the two centroids of 3.761 Å. The energy from π-π stacking has been modelled and investigated by several research groups.[20–22] Platts *et al.* used a BH&H6-311++G(d,p) basis set to calculate the binding energy between toluene and pyridine to be 11.85 kJ mol^{-1}.[22] The bond dissociation energy (BDE) for the transition metal-pyridine bond has been of interest.[23,24] Zero-Electron-Kinetic-Energy (ZEKE) measurements were applied to measure the BDE of 110.6 kJ mol^{-1} of scandium-pyridine.[24] Further, it is interesting to note that that the Ce1-$N5_{py}$ distance of 2.810(4) Å, is 0.034 Å shorter than the Ce1-C1 distance. Pyridine is an N-donor ligand that acts as a σ-donor and weak π-acceptor.[25] NHCs are also strong σ-donors and weak π-acceptors. Studies by Nolan of saturated and

unsaturated NHC complexes of Group 10 metals showed that the σ-donor properties of the two types of NHCs are much the same.[26] An examination of Pt^{II}-NHC complexes showed that unsaturated NHCs are stronger π-acceptors than the saturated NHC-Pt-complexes, which contain a 10% bonding contribution from backbonding.[27] Another study on Ir-NHC complexes concluded that there is little difference between saturated and unsaturated NHCs and that the biggest contribution to the differences in formed metal complexes is found in the sterics of the ligands.[28] The BDE for M-NHC complexes has received a lot of interest.[29–32] The values range between an experimentally measured 85.4 kJ mol^{-1} for a [(IAd)Ni$(CO)_3$] complex (IAd = [$CN_2C_2H_2$(adamantyl)$_2$] to a with DFT calculated 113.7 kJ mol^{-1} for a [$(TIME^{Me})_2Cu_3$]$(PF_6)_3$ complex ($TIME^{Me}$ = 1,1,1-tris[(3-methylimidazol-2-ylidene)-methyl]ethane.[30,31]

2.2.2 Addition across the metal-carbene bond

The mono-ligand cerium complexes [Ce(L^{Ar})(N")$_2$] (Ar = mesityl, 2,6-diisopropylphenyl) are effective for E-X bond activation and E-N bond formation.[33] Results to date are summarised in Scheme 3.

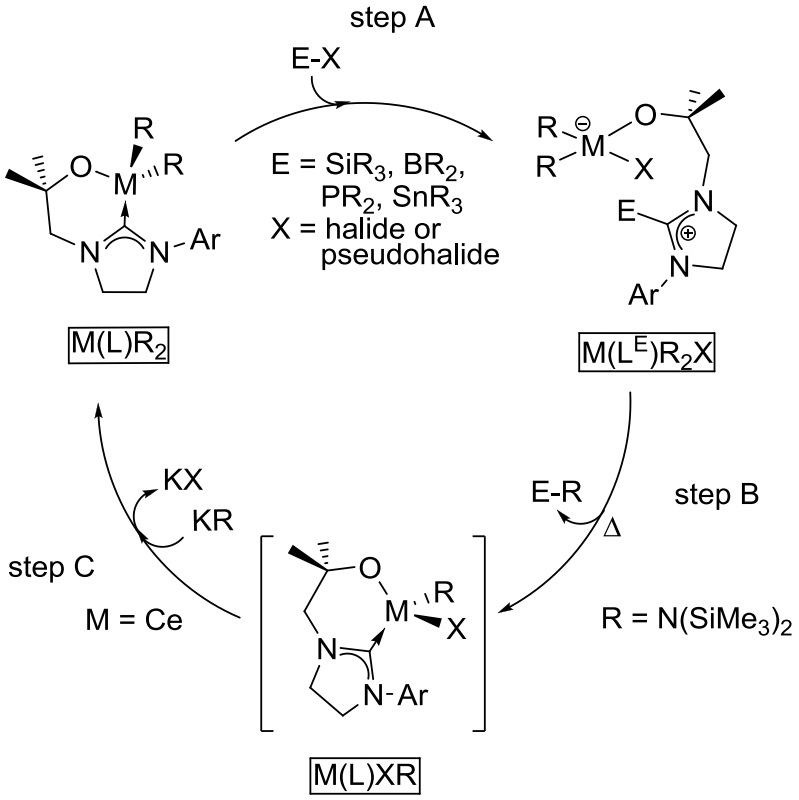

Scheme 3 Reaction of [Ce(L^{Ar})R_2] with E-X substrates to form new E-N bonds

For example the reaction of the mono-ligand complex **1** (= $[M(L)R_2]$) with one equivalent of Me_3SiCl (= (E-X)): In step A, **1** reacts with one equivalent of Me_3SiCl to afford $M(L^E)R_2X$. The Me_3Si-Cl bond is broken heterolytically and the electrophilic trimethylsilyl group binds to the carbene, while the chloride binds to the cerium metal centre. This $[Ce(Me_3SiL^{Ar})N"_2Cl]$ complex can then be heated to 80 ˚C in step B to form one equivalent of $Me_3SiN"$ and one equivalent of the $[Ce(L^M)N"Cl]$ complex with a regenerated metal-carbene bond. In step C the starting $[Ce(L^M)(N")_2]$ complex can be reformed if $[Ce(L^M)N"Cl]$ is reacted with one equivalent of KN" to eliminate KCl.

2.2.2.1 Addition of Me_3SiX (X = N_3, Cl) across the metal-carbene bond

In light of the reactivity of the mono-ligand complex **1**, a study of the reactivity of the bis-ligand complex **2** towards E-X substrates was carried out. In an NMR scale experiment one equivalent of Me_3SiN_3 was added to a solution of **2** in C_6D_6, Scheme 4.

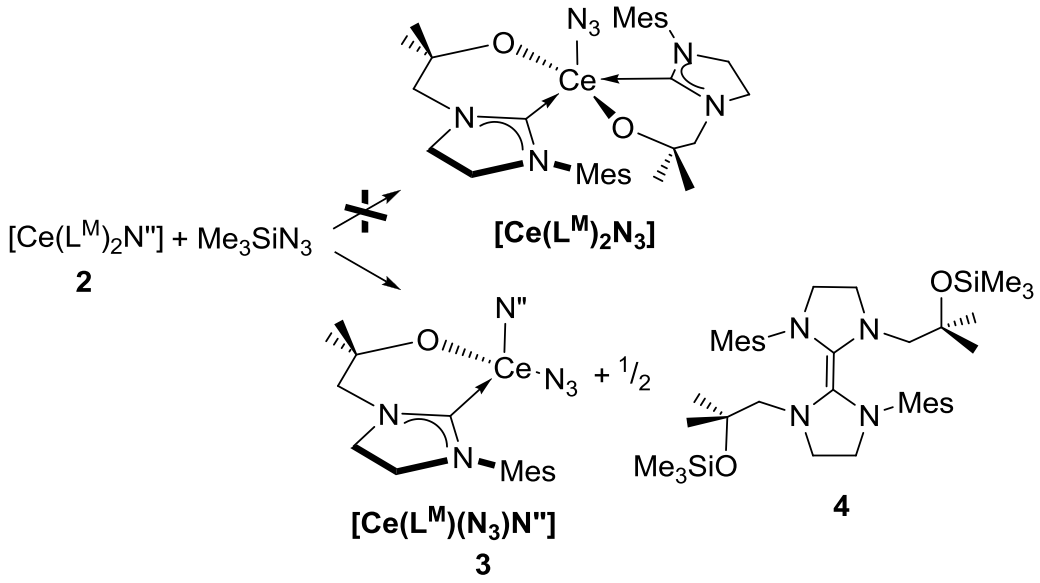

Scheme 4 Reaction of **2** with one equivalent of Me_3SiN_3

Instead of the formation of the addition product $[Ce(L^M)(L^MSiMe_3)(N_3)N"]$ or the $[Ce(L^M)_2N_3]$ complexes that were expected products, the formation of the diamagnetic compound $[L^M]_2$ **4** and the paramagnetic $[Ce(L^M)(N_3)N"]$ **3** were observed by ^1H NMR spectroscopy. A resonance at 243 ppm in the $^{13}C\{^1H\}$ NMR spectrum was further evidence for the alkene **4**. The paramagnetic resonances at 13.74, 11.12. -5.00 and -6.31 ppm in the ^1H NMR spectrum, are no longer detected upon addition of a further equivalent of Me_3SiN_3. This suggests one equivalent of **2** reacts with 2

equivalents of Me_3SiN_3 to form **4** and $[Ce(N_3)_2N'']$ **5** which is most likely polymeric, Eq. (1).

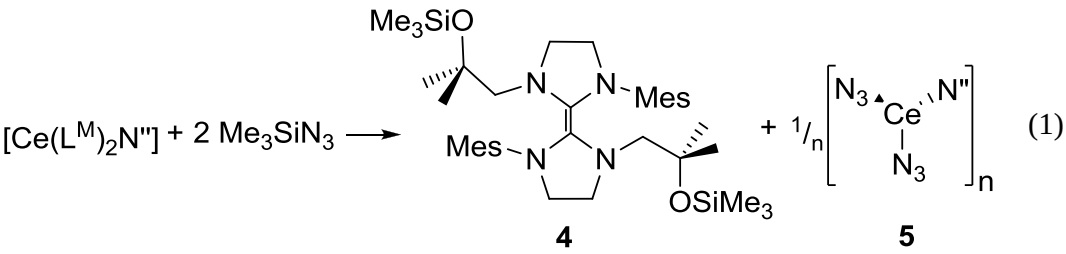

(1)

The possible byproduct of this reaction could be a Ce^{III} azide complex closely related to the U^{IV} complex $[U(N_3)_4(py)_4]$ complex, which has been reported by Mazzanti and co-workers.[34] $[U(N_3)_4(py)_4]$ is the stable decomposition product of an unstable "$Cs_3[U(N_3)_7]$" complex in pyridine. Evidence for the formation of **5** is a very broad resonance at -9.91 ppm in the ^1H NMR spectrum. Further evidence for the formation of **5** can be found in the FTIR spectrum with a distinctive azide stretch found at 2090 cm^{-1}. The ν_{N3} for Me_3SiN_3 is at 2140 cm^{-1}, therefore the observed band is not due to residual Me_3SiN_3.

The reaction was scaled up by warming an orange suspension of **2** in toluene at 60 ˚C for 15 minutes while stirring it vigorously to obtain a clear orange solution. To this solution were added 2 equivalents of Me_3SiN_3 with a syringe. Upon addition the colour of the solution turned from dark orange to red. This solution was cooled down to 3 ˚C over night to obtain single crystals suitable for X-ray crystallography of the dimeric silylated proligand $[Me_3SiL^M]_2$ **4** of the ligand redistribution reaction in a 62% yield, see Figure 4.

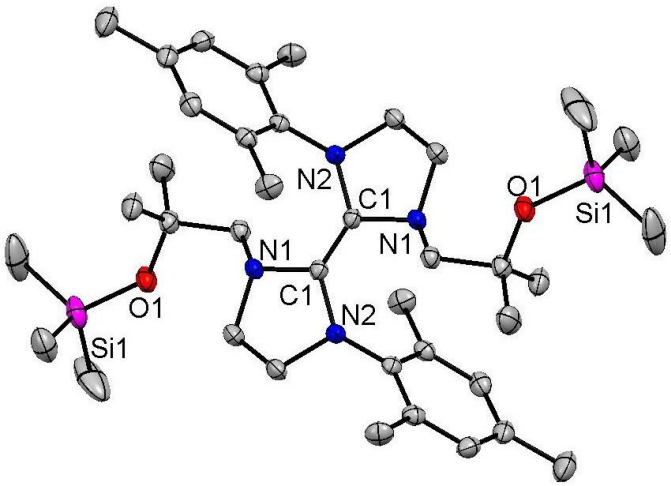

Figure 4 Displacement ellipsoid drawing (50%) of the $[Me_3SiL^M]_2$ dimer **4**, H-atoms omitted for clarity

The asymmetric unit of **4** contains half of the dimer. The two C1, formerly carbene carbons in **4** are bound with a double bond as is shown by the distinctively short bond distance of 1.350(2) Å.

Selected bond distances (Å) and angles (˚) for **4** are displayed in Table 2.

Table 2 Selected bond distances (Å) and angles (˚) for $[Me_3SiL^M]_2$ **4**

C1-C1	1.350(2)
Si-O	1.6396(10)
N-C-N	108.49(10)

These enetetramines were studied by Lappert and co-workers who used these electron rich alkenes to form metal NHC complexes (metal = Cr, Mo, W, Rh).[35] A variety of NHC dimers have been synthesised, see Figure 5.[36–39]

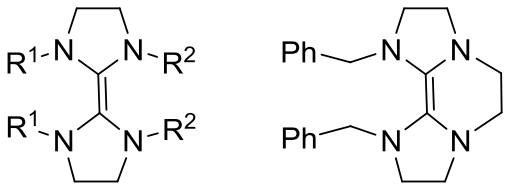

D $R^1 = R^2 =$ Me
E $R^1 = R^2 =$ Ph
F $R^1 = R^2 =$ benzyl
G $R^1 = R^2 =$ naphthalenyl
H $R^1 =$ Ph, $R^2 =$ Me

I

Figure 5 NHC dimers

To compare the structures of these electron rich alkenes, the distance of the carbene-carbene bonds and the N-C-N angles have been collected for a range of the enetetramines in Graph 1.

Graph 1 N-C-N angles (˚) and C-C bond distances (Å) for electron-rich alkene 4 and enetetramines in literature

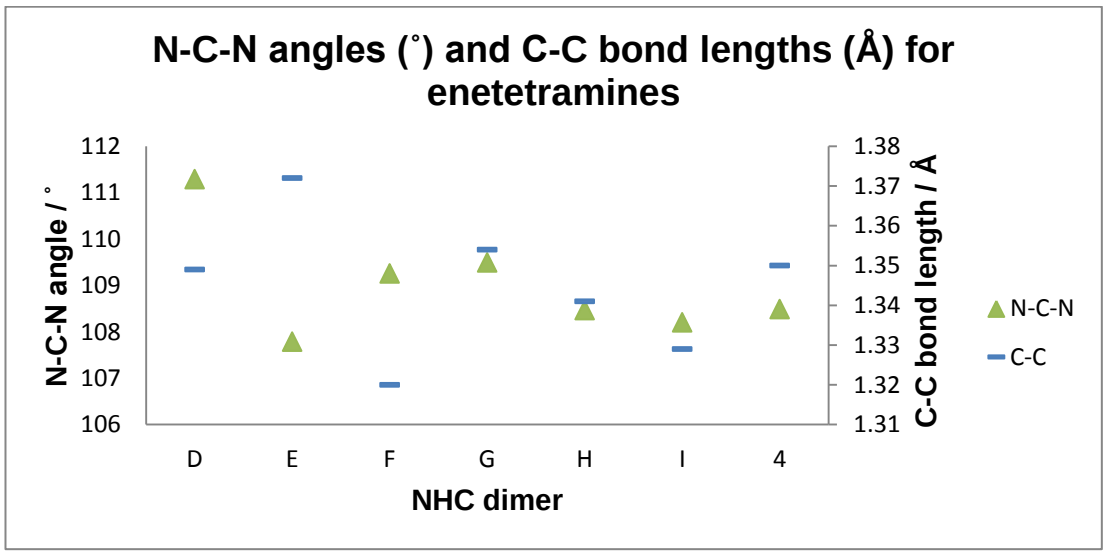

4 has a $C_{carbene}$-$C_{carbene}$ bond distance of 1.350(2) Å and an N-C-N angle of 108.49(10)˚. The structural parameters bear greatest similarity to compound **H**, which has a C-C bond distance of 1.341 Å and has N-C-N angle of 108.468˚. **H** is also structurally the most similar, R^1 = a phenyl group, compared to the mesityl group of the ligand and R^2 a methyl group compared to the alkyl group of the alkoxysilyl of **4**. Ethene has a C-C bond distance of 1.33 Å which is 0.2 Å shorter than the C-C bond distance in

4.[40] Tetrakis(dimethylamino)ethane has a bond distance of 1.351(2) Å which is a similar bond distance as in **4**.[41]

The proposed mechanism for the reaction of 2 with Me_3SiN_3 is shown in Scheme 5.

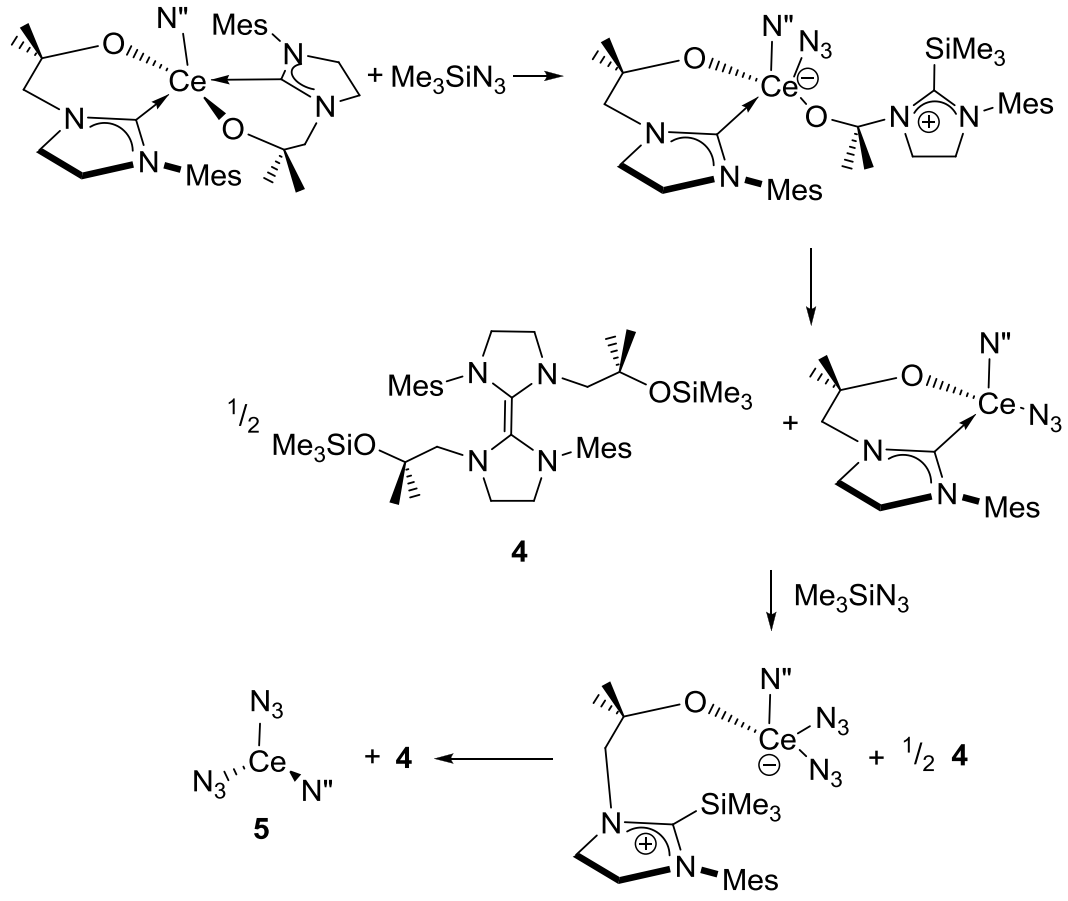

Scheme 5 Proposed mechanism for the reaction of $[Ce(L^M)_2N"]$ with Me_sSiN_3

To find experimental evidence for this proposed mechanism an NMR-scale reaction of $[Ce(L^M)_2N"]$ with one equivalent of Me_3SiN_3 in C_6D_6 was carried out and monitored by ^1H NMR spectroscopy, Figure 6. Resonances with the letters a-h between 0.15 ppm and 6.81 ppm correspond to **4**, i*-p* between -6.29 ppm and 13.74 ppm correspond to $[Ce(L^M)N"(N_3)]$.

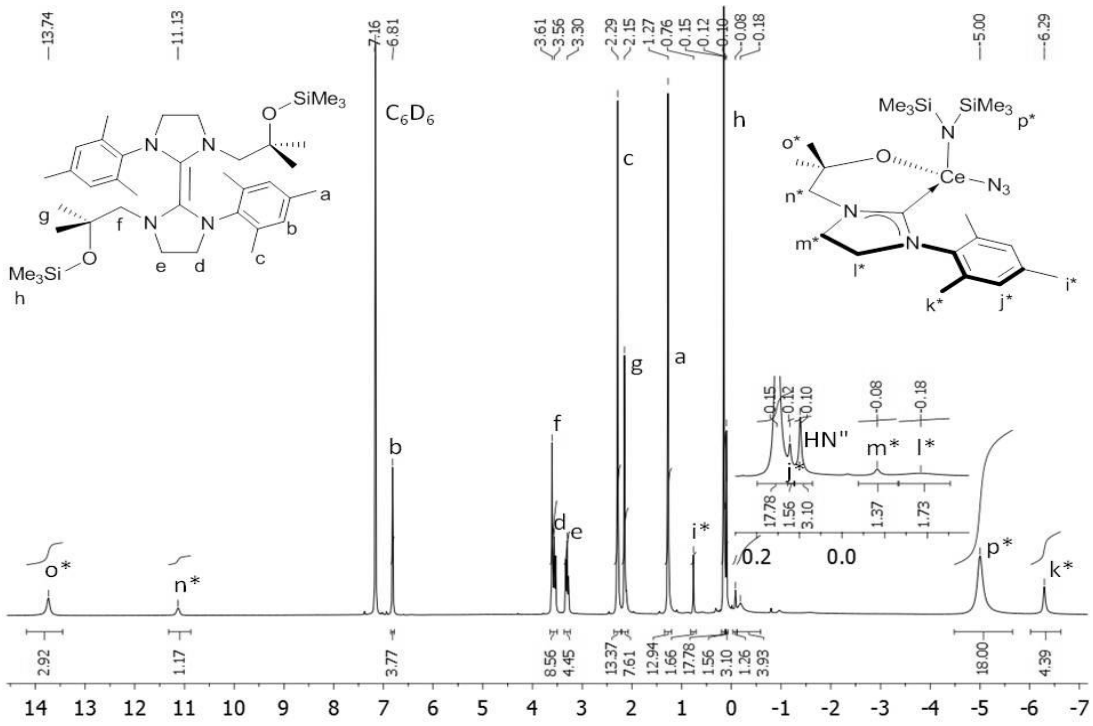

Figure 6 ^{1}H NMR spectrum of the reaction of [Ce(L^{M})$_2$(N")] + Me_3SiN_3 in C_6D_6

Due to solubility problems, the integrals for [Ce(L^{M})N"(N_3)] are not in the expected ratio with respect to **4**. A fine precipitate in the NMR tube formerly assumed to be unreacted starting material [Ce(L^{M})$_2$N"] supports this assumption.

If this reaction is carried out with two equivalents of Me_3SiCl instead of Me_3SiN_3 with **2** an almost identical ^{1}H NMR spectrum is gained, Eq. (2).

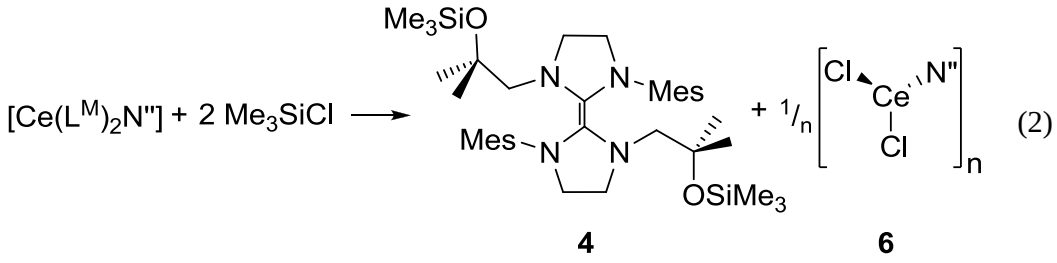

4 **6** (2)

When the FTIR spectrum of a crude mixture of **4** and **6** was compared to that of a crude mixture of **4** and **5** the IR spectra of the both compounds show the same bands in the fingerprint region. No azide stretch can be detected in the infrared spectrum of **4** and **6** which is further confirmation of the formation of **5** and **6**.

Further evidence of the formation of **4** as a main product, is the reaction of [Pr(L^M)$_2$N"] with either Me_3SiCl or Me_3SiN_3 which shows exactly the same resonances between 0 ppm and 8 ppm in the ^{1}H NMR spectrum as the reaction of [Ce(L^M)$_2$N"] with either Me_3SiCl or Me_3SiN_3.

2.2.2.2 Reaction of [Ce(L^M)$_2$N"] with I-BBN

One equivalent of an orange toluene suspension of **2** was treated with two equivalents of a purple solution of 9-iodo-9-boracyclo[3.3.3]nonane in hexanes (I-BBN), resulting in a brown mixture. The reaction was stirred for 12 hours at room temperature, the solution extracted and the solution was concentrated under reduced pressure. From this saturated solution single crystals suitable for X-ray crystallography were grown at 3 ˚C in a 66% yield. The crystals were the products of ligand abstraction, complex **8**, see Scheme 6. **2** reacts with one equivalent of I-BBN to form [Ce(L^M)N"(I)] and one equivalent of [L^MBBN] **8**. This reacts with another equivalent of I-BBN to form [CeN"I_2] and another equivalent of **8**.

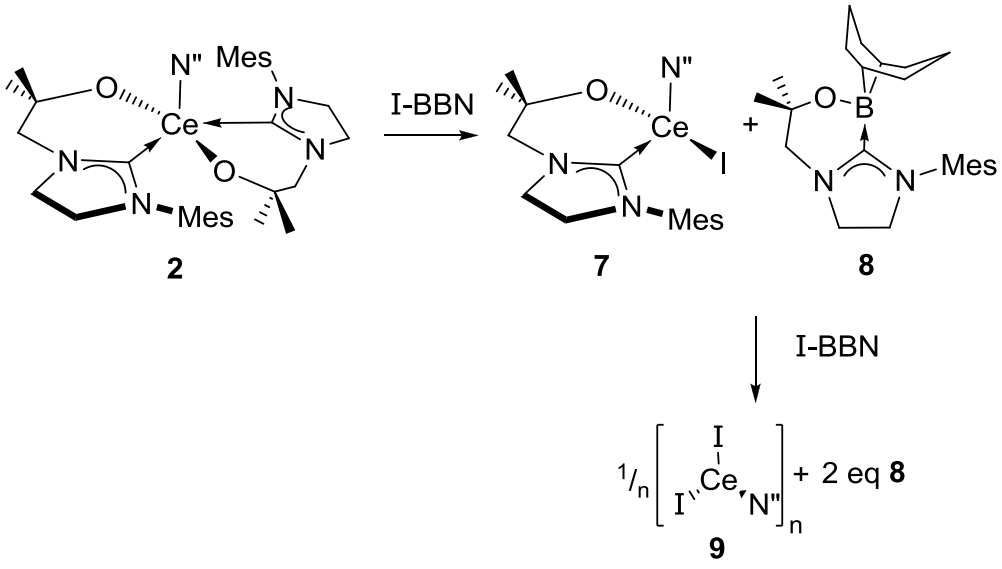

Scheme 6 Reaction of [Ce(L^M)$_2$N"] with 9-iodo-9-boracyclo[3.3.3]nonane

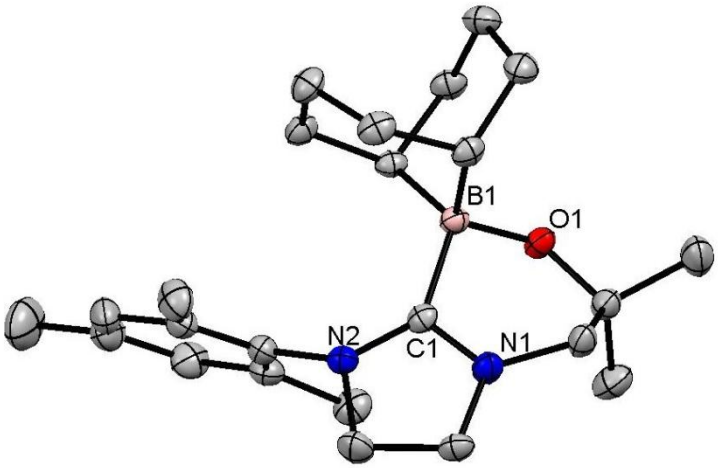

Figure 7 Displacement ellipsoid drawing (50%) of [L^{M}BBN] **8**, H atoms omitted for clarity

The boron centre is four-coordinate and surrounded in a distorted tetrahedral geometry by O1, C1 and the two carbons of the BBN-group. The B1-C1 distance of 1.658(3) Å and the N1-C1-N2 angle of 108.49(15)˚ are typical for a bound imidazoline.

Selected bond distances (Å) and angles (˚) for [BBNL^{M}] **8** are displayed in Table 3.

Table 3 Selected bond distances (Å) and angles (˚) for **8**

C1-B1	1.658(3)
B1-O1	1.508(2)
N1-C1-B1	115.30(14)
B1-C1-N2	135.92(15)
N1-C1-N2	108.49(15)

The boron functionalised NHC synthesised by Piers is synthesised from the (2-(3-(2,6-diisopropylphenyl)-4,5-dihydro-*1H*-imidazol-3-ium-1-yl)phenyl)trifluoroborate with one equivalent of KN" to form **J**, Eq. (3).[42]

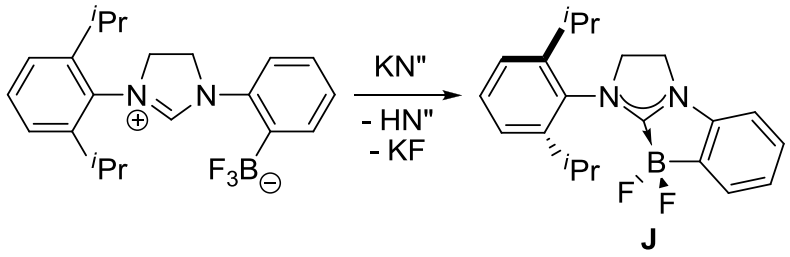

(3)

The B-C bond distance of **J** is 1.682(2) Å, comparable to **8** with a B1-C1 bond distance of 1.658(3) Å. The synthesis of **J** is suggested to proceed through the formation of the potassium carbene complex.

Other boron-functionalised NHCs include complexes **K** and **L**, synthesised by Braunschweig, Eq. (4).[43]

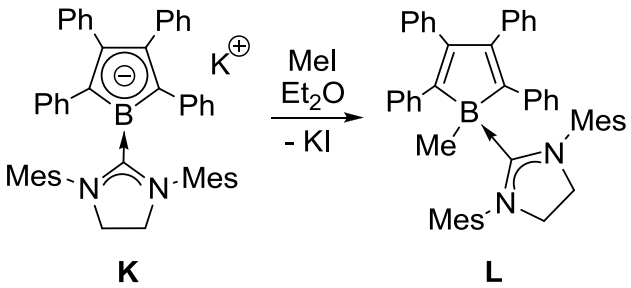

(4)

More examples of boron-NHC complexes can be seen in Figure 8, complexes **L**-**O**.[44–46,43]

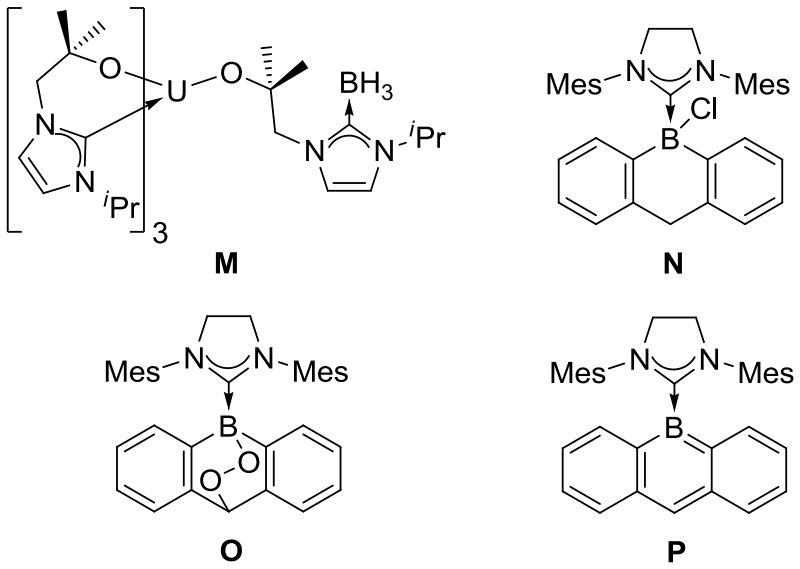

Figure 8 Boron functionalised NHC complexes

The bond distances (Å) for the B-C bonds of the NHC complexes are displayed in Table 4.

Table 4 Bond distances (Å) for B-C bonds in NHC complexes

8	1.658(3)
J	1.68
K	1.541(2)
L	1.647(2)
M	1.609(7)
N	1.666(3)
O	1.657(3)
P	1.607(4)

The B-C bond distances vary from 1.541(2) Å to 1.68 Å. As displayed in the B-NHC complex **J**, 1.68 Å is the closest in B-C bond distance to **8** with 1.658 Å.

2.2.3 Steric and electrochemical comparisons of $[Ce(L^M)(N"_2)_2]$ to $[Ce(L^M)_2N"]$

To establish why **1** was showing such a different reactivity towards E-X than **2**, steric and electronic factors were considered, and the oxidation potential electrochemically investigated.

2.2.3.1 Electrochemical investigations

Electrochemical investigations by cyclic voltammetry of **1** and **2** were performed. All experiments were conducted in dry CH_2Cl_2 with $[Bu_4N][BF_4]$ electrolyte (0.2 M) and the respective complex (1.0 mmol L^{-1}) under an atmosphere of N_2 and referenced to ferrocene.

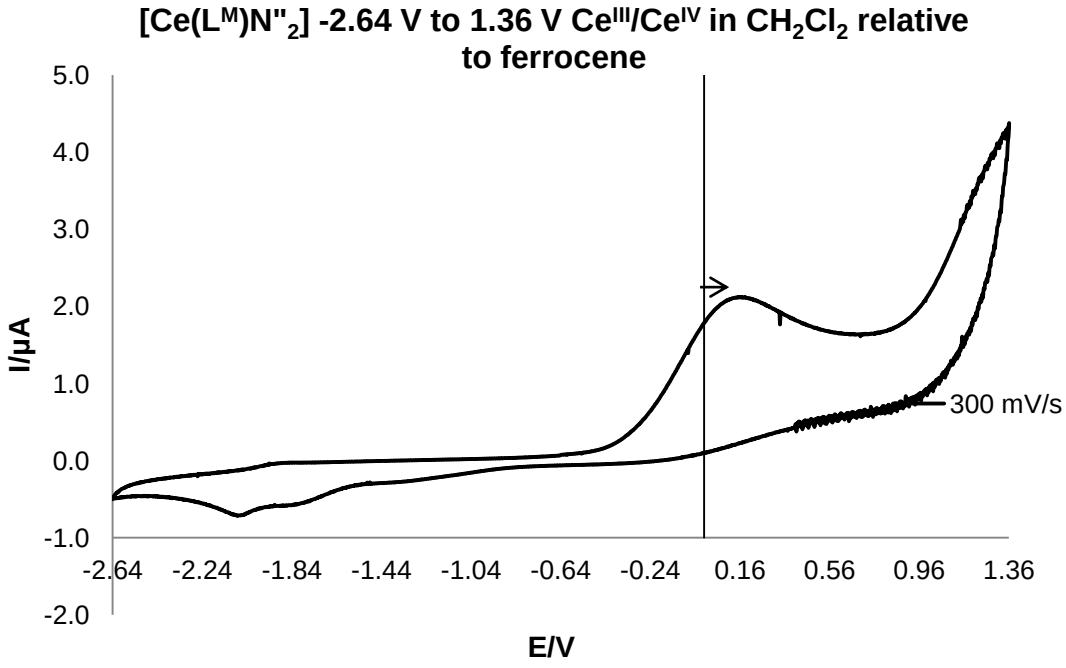

Figure 9 Cyclic voltammogram for $[Ce(L^M)N"_2]$ from -2.64 V to 1.36 V for Ce^{III}/Ce^{IV} in CH_2Cl_2 relative to ferrocene

The irreversible oxidation potential for **1** is 0.12 V. No oxidation potential could be detected for **2** between -2 V and 3 V in DCM or THF.

2.2.3.2 Steric considerations, calculation and comparison of the percent buried volume of [L^{M}], [L^{D}], [L^{iPr}] and [N"]

Investigations have shown that there are steric effects involved in the susceptibility to oxidation in NHC ligand complexes as shown by Sigman and Dible. They investigated steric effects in the aerobic oxidation of π-allylnickel(II) complexes with NHCs.[47] In their studies they compared fourteen different imidazoles and imadozolines with different substituents on the nitrogen atoms, Figure 10.

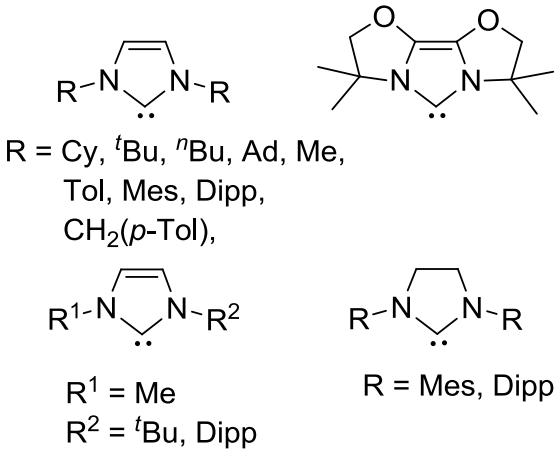

Figure 10 N-substituted NHCs discussed by Sigman and Dieble

Earlier studies carried out on the Tolman electronic parameter (TEP),[48] which is a measurement of the electron donating or withdrawing efficacy of a ligand, by Crabtree[28] and Nolan[26] showed that the TEPs for NHCs did not differ significantly in value (less than 2 cm^{-1}). This lead Sigman and Dible to conclude that steric effects are the dominant factor in the oxidation of Ni-NHC complexes. They found that reported reactions of the N-substituted NHCs (shown in Figure 10) with $Ni(CO)_4$ and $Ni(cod)_2$ which form a variety of (NHC)nickel(II) complexes, showed a difference in reactivity. This difference mostly coincided with the steric demand of the NHCs. To further investigate this O_2 binding to π-allylchloro(NHC)nickel(II) (NHCs shown in Figure 10) complexes was examined. They found that the bulkier NHCs, such as *tert*butyl and adamantyl substituted NHCs prevented O_2 binding; whereas mesityl or diisopropylphenyl substituted imidazoles reacted with O_2 to form $[(\mu_2\text{-OH})Ni(NHC)Cl]_2$ complexes within minutes. They explain the difference in reactivity with the inhibited rotation about the M-C bond in the bulkier NHCs thereby blocking empty axial sites for oxidation.

Calculation and comparison of the percent buried volume of [L^{M}], [L^{D}], [L^{iPr}] and [N"]

The steric bulk of NHC ligands can be expressed in 'percent buried volume' $\%V_{bur}$, which is defined as the total volume of a sphere occupied by the NHC. This technique, developed by Nolan and Cavallo uses crystallographic data to calculate $\%V_{bur}$. [49–51] Cavallo and co-workers created Samb*V*ca (Salerno molecular buried volume calculation), a software to calculate the spatial occupation value of the ligand and is available online.[52,53] This software is also applicable for ligands other than phosphines and NHCs for which it was originally developed. Information to input into the program includes a crystallographic data file, such as the .cif, with all coordinates removed that do not belong to the ligand. Further, the sequence number of the atom binding to the metal ($C_{carbene}$ in the case of NHCs), the number of atoms required to form the coordination axis (N1 and N2 for **1$_{py}$**) and their respective sequence number must be input. For comparison the $\%V_{bur}$ of the NHCs [L^{D}] and [L^{iPr}] ([L^{D}] = [OCMe$_2$CH$_2${CNCH$_2$CH$_2$NDipp}], [L^{iPr}] = [OCMe$_2$CH$_2${CNCHCHN^{i}Pr}]) were calculated as the Ce^{III} complexes [Ce(L^{D})$_2$N"] and [Ce(L^{iPr})$_3$] as well as the Ce^{IV} complex [Ce(L^{iPr})$_4$] have been synthesised and structurally characterised.[17,14]

For calculation of $\%V_{bur}$ for [L^{M}] in **1$_{py}$** the following information was entered into Samb*V*ca:

- Atom coordinated at the centre of the sphere: 1 ($C_{carbene}$)
- Number of atoms for axis definition: 2
- Atom indexes: 2 3 (**N**-$C_{carbene}$-**N**)
- Sphere radius: 3.5 (default)
- Distance from the centre of the sphere: 2.85 (Ce1-C1)
- Mesh spacing: 0.05
- Include H-atoms: yes

The Bondi radii were set to: Bondi radii scaled by 1.17.

$\%V_{bur}$ for [L^{M}] = 25.5

The same approach was taken to calculate $\%V_{bur}$ for [L^{D}], [L^{iPr}] and [N(SiMe$_3$)$_2$]. Results of the calculations can be seen in Figure 11.

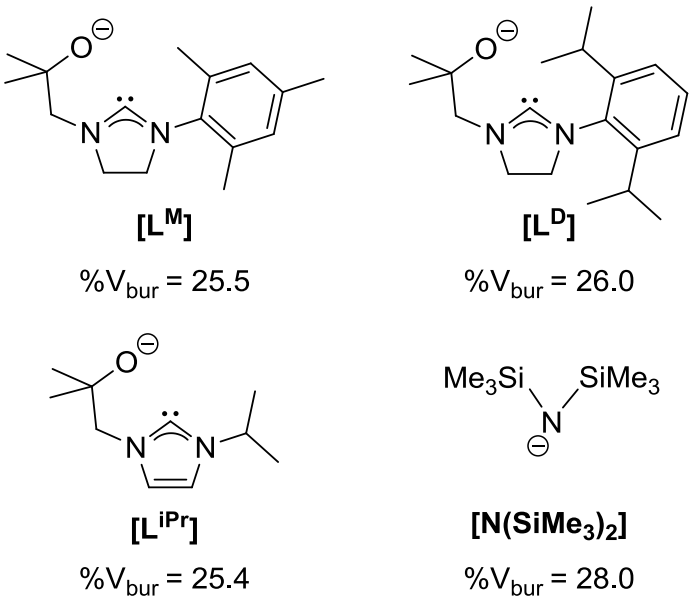

Figure 11 $\%V_{bur}$ for [L^{M}], [L^{D}], [L^{iPr}] and [$N(SiMe_3)_2$]

Changes made to above input for [L^{D}] and [L^{iPr}] were: Distance from the centre of the sphere: 2.855 for [L^{D}] and 2.697 for [L^{iPr}]. Changes made to above input for [$N(SiMe_3)_2$] were: the coordinated atom (N3), the atoms for axis definition (Si1 and Si2) and the distance from the metal centre (2.40 Ce-N_{amide}).

The results for $\%V_{bur}$ were 25.5 for [L^{M}], 26.0 for [L^{D}], 25.4 for [L^{iPr}] and 28.0 for [$N(SiMe_3)_2$]. [L^{D}] is only 0.5 $\%V_{bur}$ larger than [L^{M}]. Both form mono and bis-ligand cerium amide complexes and react towards small molecules in the same manner, therefore this small difference in sterics does not seem to influence the reactivity of the metal complexes. On the other hand [L^{iPr}] is only marginally smaller than [L^{M}] by only 0.1 $\%V_{bur}$, yet it is possible to form the tri-ligand and the tetra-ligand Ce complexes with it, which is impossible for [L^{D}] or [L^{M}]. This could mean that the steric demand of the ligands do not play an important role in the formation of the complexes. Alternatively, the method of calculation does not take into consideration that the sterics of [L^{M}] and [L^{D}] do not allow packing as well as the sterics of [L^{iPr}].

In respect to $\mathbf{1_{py}}$ $\%V_{bur}$ for both silylamide groups is 56% and $\%V_{bur}$ for [L^{M}] is 25.5 %.

This information could help further explain the differences in the reactivity of the cerium complexes [Ce(L^{M})N"$_2$py] **1** and [Ce(L^{M})$_2$N"] **2**. Figure 12 and Figure 13 show

spacefill diagrams of $\mathbf{1_{py}}$ and **2**. The Van der Waals radius that is used to calculate the spacefill for Ce is 181 pm.

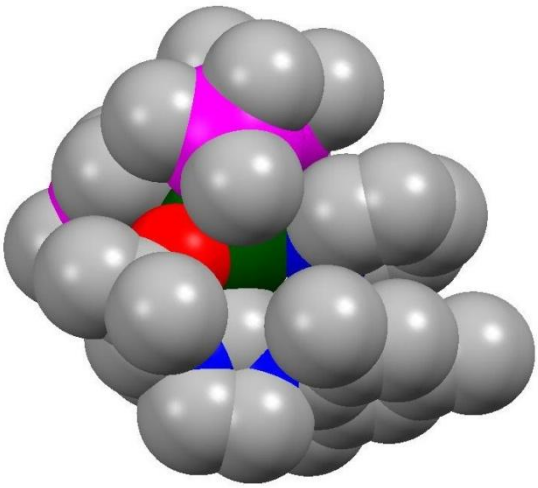

Figure 12 Spacefill of $\mathbf{1_{py}}$, H atoms omitted for clarity

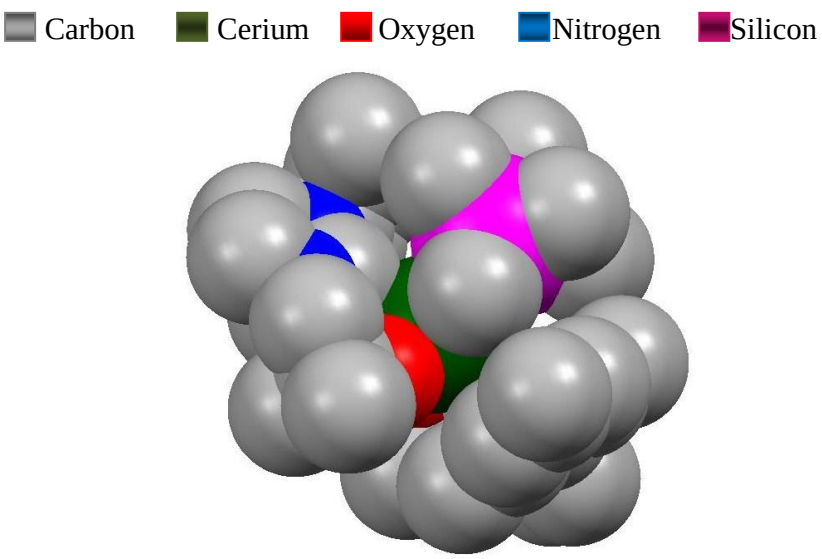

Figure 13 Spacefill of **2**, H atoms omitted for clarity

2 is considerably more sterically crowded than $\mathbf{1_{py}}$, as the mesityl substituted alkoxy tethered imidazole is sterically more demanding than the silylamide group. This is observed in the crystal structures for each compound, where the mono-ligand cerium complex $\mathbf{1_{py}}$ has enough space on the metal centre to coordinate a pyridine to the metal centre whereas the bis-ligand compound **2** does not. Consequently, $\mathbf{1_{py}}$ has the necessary space to allow a reaction to occur whereas **2** is sterically too hindered to allow a reaction.

When the bis-ligand complex reacts with a substrate, e.g. Me_3SiCl, one ligand is abstracted and the resulting [Ce(L^M)N"Cl] compound does not react in the same way as [Ce(L^M)N"$_2$], i.e. reacting with another equivalent of the Me_3SiCl. Instead of adding across the metal-carbon bond and forming a N-Si bond, the ligand is abstracted again. This results in a different system, which now favours ligand abstraction to form the more stable [Ce(Cl)$_2$(N")] complex and **4** with a strong Si-O bond. The bond enthalpies for gaseous diatomic E-O bonds are displayed in Table 5.[54]

Table 6 Bond enthalpies of in gaseous diatomic species E-O in kJ mol^{-1} at 298 K

Ce-O	795 ± 8
Si-O	799.6 ± 13.4
B-O	808.8 ± 20.9
P-O	599.1 ± 12.6
Ce-N	519 ± 21

The bond enthalpies for these species refer to neutral diatomic molecules in the gas phase and might differ from single bond energies in a solid. Still, it is an indication of the stability of the formed compounds. As can be seen from the table, the Ce-O bond with 795 ± 8 kJ mol^{-1} is approximately the same as the Si-O bond with 799.6 ± 13.4 kJ mol^{-1} and the B-O bond with 808.8 ± 20.9 kJ mol^{-1}. This may be an additional reason for the ligand abstraction in the [Ce(L^M)$_2$N"] complex. The P-O bond enthalpy is 559.1 ± 12.6 kJ mol^{-1} which is 236 kJ mol^{-1} weaker than the Ce-O bond. Therefore a reaction with a P substrate may be more likely to give the desired addition across the M-C bond.

2.2.4 Friedel-Crafts acylation with [Ce(L^M)N"]

The Friedel-Crafts acylation is an electrophilic aromatic substitution reaction between arenes and acyl chlorides or anhydrides in the presence of a catalyst, Eq. (5). In preparative organic synthesis the most common Lewis acid catalyst used for this reaction is $AlCl_3$.

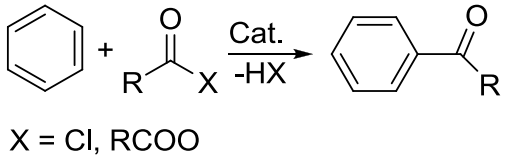

(5)

Other catalysts that have been successfully used for this reaction are bis(trifluoromethylsulfonylimino)trifluoromethanesulfonic acid,[55] activated hematite[56] and lanthanide trifluoromethanesulfonates.[57]

When a benzene solution of **2** was layered with a hexanes solution of an excess of benzoylchloride, yellow single crystals of $[(Ph_2CO)_2H]_3[CeCl_6]$ **10** could be isolated in a 20% yield., Eq. (6).

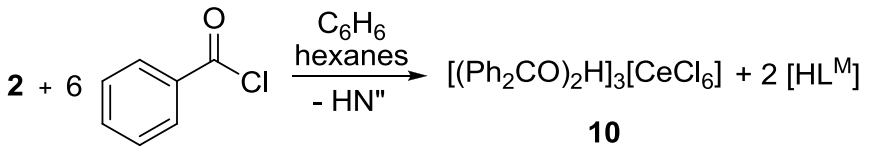

(6)

The counterion to the $[CeCl_6]^{3-}$ anion is the protonated benzophenone cation $[(Ph_2CO)_2H]^+$. It is postulated that **2** activates benzoyl chloride by forming an NHC-acyl and Ce-Cl bond before the acyl can react with deuterated benzene to form the $[(d_5PhC(O)Ph)_2H]$ cation. The crystal structure of **10** is shown in Figure 14.

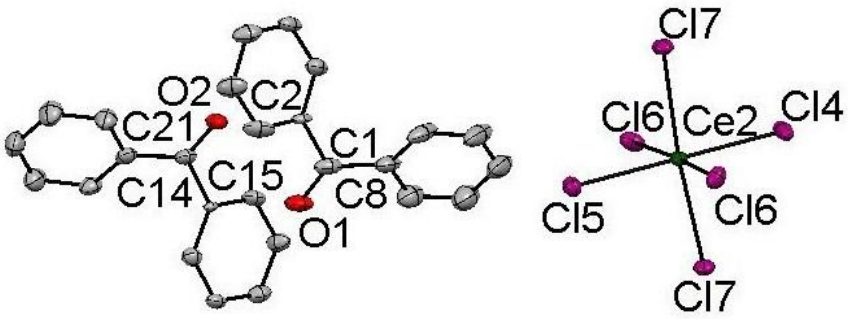

Figure 14 Displacement ellipsoid plot (50 %) of $[(Ph_2CO)_2H]_3[CeCl_6]$ **10**, H-atoms omitted for clarity

It is assumed that $[(Ph_2CO)_2H]^+$ forms the counterion as the distance between O1 and O2 is 3.031 Å, which accounts for a hydrogen bond between those two atoms.

Selected bond distances (Å) and angles (˚) for compound **10** are displayed in Table 7.

Table 7 Selected bond distances (Å) and angles (˚) for **10**

Ce1-Cl1	2.7651(8)	Cl1-Ce1-Cl1	180.00
Ce1-Cl2	2.7527(8)	Cl1-Ce1-Cl2	91.31(2)
Ce1-Cl3	2.7821(9)	Cl1-Ce1-Cl3	87.37(2)
Ce2- Cl4	2.7368(12)	Cl2-Ce1-Cl3	89.59(3)
Ce2- Cl5	2.7876(11)	Cl4-Ce2-Cl5	180.00
Ce2-Cl6	2.7976(9)	Cl4-Ce2-Cl6	92.336(19)
Ce2-Cl7	2.7490(8)	Cl4-Ce2-Cl7	87.357(18)
C1-O1	1.203(4)	Cl6-Ce2-Cl7	91.02(3)
C14-O2	1.194(4)	O1-O2	3.031(3)
C1-C2	1.487(5)	C14-C15	1.497(4)
C1-C8	1.470(6)	C14-C21	1.465(5)

The cerium centre is in an octahedral geometry surrounded with six chloride atoms with an average bond distance of 2.767 Å. The equatorial chloride atoms stand in a nearly 90˚ angle to the axial chloride atoms (87.37(2)˚ and 92.336(19)˚). The C-O distances of the ketyl groups in the benzophenones are 1.203(4) Å and 1.194(4) Å which is a standard distance for a ketone but significantly shorter than reported C-O bond distances of 1.246-1.211 Å for benzophenone.[58,59] Reed and co-workers also observed the formation of $[(Ph_2CO)_2H]^+$ as a counterion to $CHB_{11}R_5X_6^-$ (R = H, Me; X = Cl, Br).[60] They report shorter O-O distances of 2.470(3) Å and longer C-O bond distances of 1.274(4) Å and 1.258(4) Å.

There are DFT calculations concerning the bond structure and properties of 4f compounds and specifically cerium hexahalides.[61–63] A search of the literature shows that molecular trivalent cerium hexahalides are not common. No crystal structures of the hexabromides or iodides and only one example of a cerium hexafluoride compound was found.[64]

Only a few other crystallographic examples of the $[CeCl_6]^{3-}$ anion were published. Tris(2,4,6-trimethylpyridinium) hexachloride, Figure 15, and various other lanthanide hexachlorides were synthesised by J. Hallfeldt and are described in his Ph.D. thesis.[65]

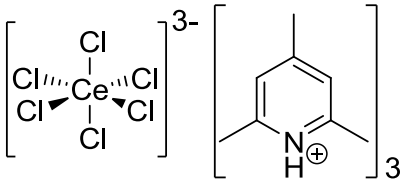

Q

Figure 15 Tris(2,4,6-trimethylpyridinium) hexachlororide

The average Ce-Cl bond distance in **Q** is 2.766 Å which is in excellent accordance with the average Ce-Cl bond distance of **10** of 2.767 Å.

2.2.5 Reaction with gases

The reactivity of the mono-ligand cerium $[Ce(L^M)(N'')_2]$ **1** and uranium carbene complexes $[U(L^M)(N'')_2]$, as well as the bis-ligand cerium carbene complex $[Ce(L^M)_2N'']$ **2** were studied towards small molecules such as CO_2, COS and NO.

All three compounds displayed a very similar reaction when CO_2 or COS were added to a solution of the complexes. A precipitate formed immediately upon addition of gas.

A similar reactivity had been reported by Gambarotta and coworkers when treating a magnesium cation with CO_2.[66] They added a $AlMe_3$ solution in toluene to a solution of $[\{[(Me_3Si)_2N]Mg[\mu\text{-}N(SiMe_3)_2]\}_2]$ in THF that was cooled in an ice bath and stirred under a carbon dioxide atmosphere. The intermediates formed in the first step are $[\{[Me_3SiO]Mg[[\mu\text{-}OSiMe_3]\}_2]$ and 2 Me_3SiNCO which then further react with the $AlMe_3$ to form colourless crystals of the product after cooling the solution in a freezer for 5 days.

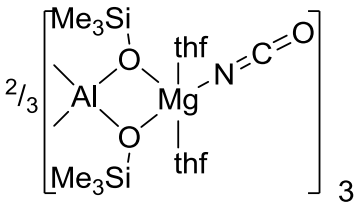

Figure 16 Product of CO_2 reaction described by Gambarotta

The reaction of the compounds with COS and CO_2 follow the same reaction path to afford $[Ce(L^M)_2OSiMe_3]$ **11** and liberating an isocyanate/isothiocyanate; confirmed by

the characteristic stretch of the isocyanate or isothionate compound in the IR spectra, Eq. (7).

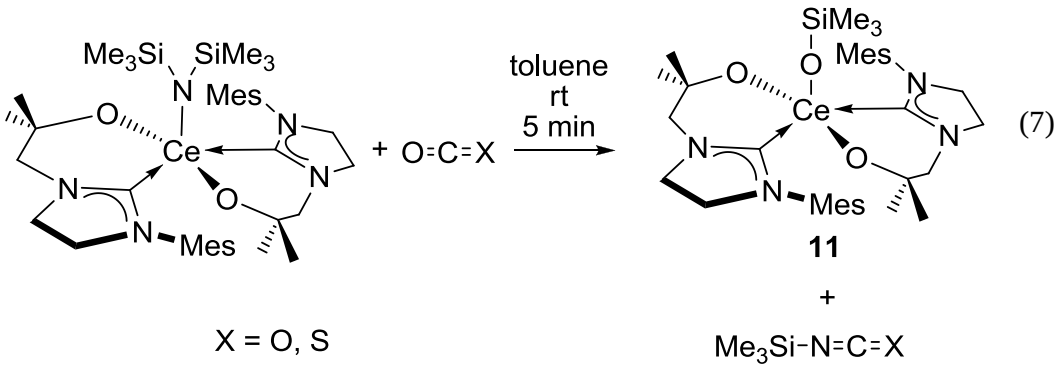

(7)

The products are insoluble in aromatic solvents, infrared spectroscopy was therefore used to characterise the afforded compounds. The N=C=S stretch and the N=C=O stretch of the by-product of this reaction are clearly assignable in the IR spectrum at 2278 cm^{-1} and 2128 cm^{-1} respectively.

It is known from literature that metal silylamides react with CO_2, CS_2 and COS as shown in Eq. (8).[67]

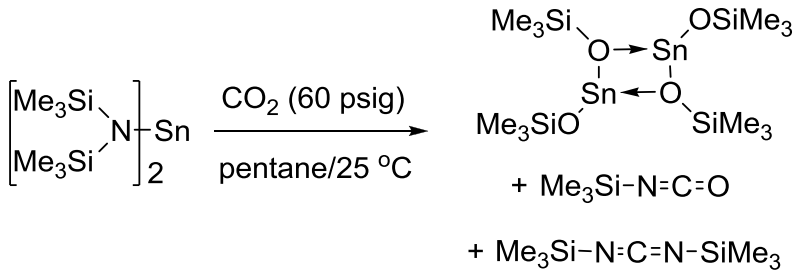

(8)

Therefore, a possible mechanism for this reaction is as follows.

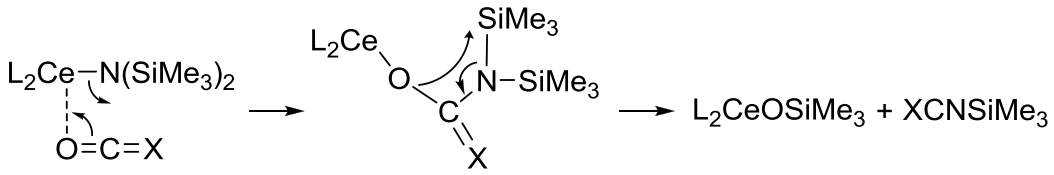

Scheme 7 Possible mechanism for the reaction of **2** with CO_2

NO and H_2 showed no reactivity towards **1** or **2**.

2.3 Attempted Ce=N double bond formation

Before it was established that the reaction of **2** with one equivalent of Me_3SiN_3 formed **4** as a main product, the possibility of the formation of a Ce=N double bond was entertained as Me_3SiN_3 is known to be able to oxidise metalloid complexes such as germanium compounds and transition metal compounds such as as zirconium and tin complexes to form terminal metal imido bonds.[68–70] It is possible to oxidise $[U(N'')_3]$ with trimethylsilyl azide to form the U^V imido complex $[(N'')_3UNSiMe_3]$.[71] It was also shown by Scott that a U^{III} triamidoamine complex can be oxidised to the U^V imido complex.[72] The formation of lanthanide-main group element multiple bonds are of academic interest since the involvement of the valence orbitals in f-block chemistry bonds is still poorly understood. Cerium was chosen as the metal because of its chemically accessible Ce^{IV} oxidation state. DFT studies on a Cp_2CeZ system (Z = F^-, O, NH, CH^-, CH_2) show that it should be possible to synthesise such a compound and that it would be reasonably stable. Still, the bonding interactions are quite polarised and aggregation to an oligomeric species presents a likely problem.[73] In 2010 the first rare earth metal terminal imido complex was isolated and structurally characterised. It was synthesised from a Me(L)Sc(anilide) complex **S** that was reacted with DMAP to form the scandium terminal imido complex **T**, Scheme 8.[74]

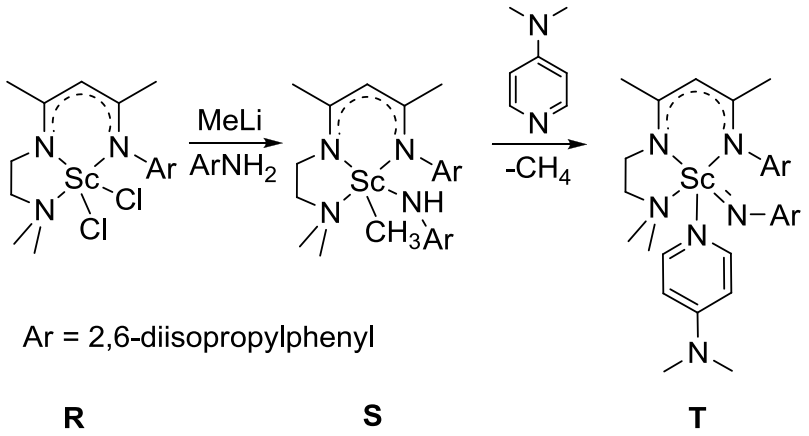

Scheme 8 Formation of the scandium terminal imido complex **T**

Boncella and coworkers reported the synthesis of a complex containing a U=N double bond by treatment of a uranium tetrahalide with a lithium or potassium amide via a salt elimination route which was followed by spontaneous HCl elimination, Scheme 9.[75]

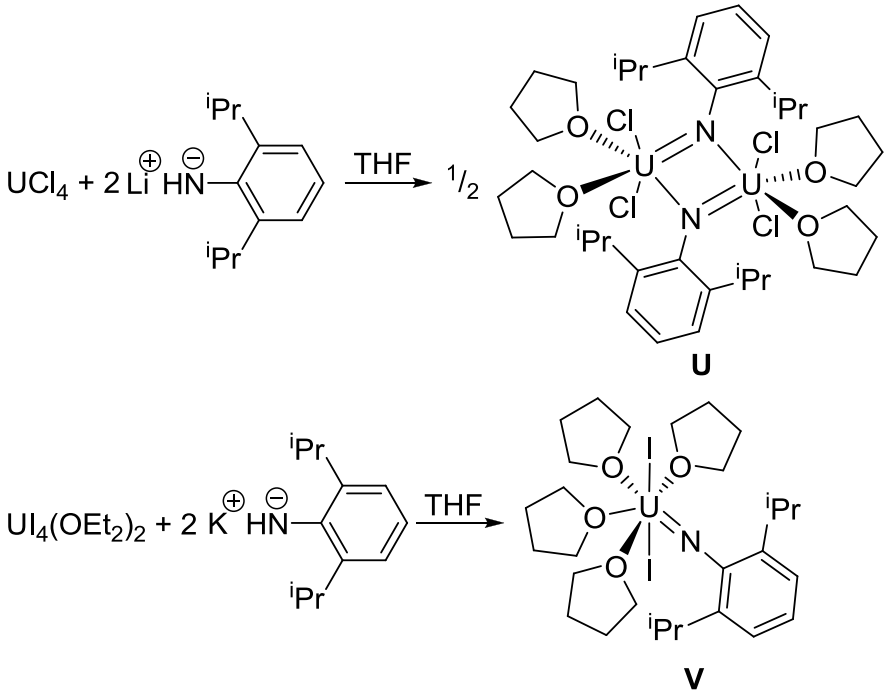

Scheme 9 Synthesis of monoimidouranium(IV) dihalides

Taking inspiration from this work, another attempt at the formation of a Ce=N double bond was made this time *via* a salt elimination route. [Ce(L^M)(N''_2)Cl] was treated with an equivalent of LiN(H)^{t}Bu, lithium chloride formation was evident, but instead of formation of the desired product, reduction of the Ce^{IV} compound to the Ce^{III} starting material was observed, Scheme 10.

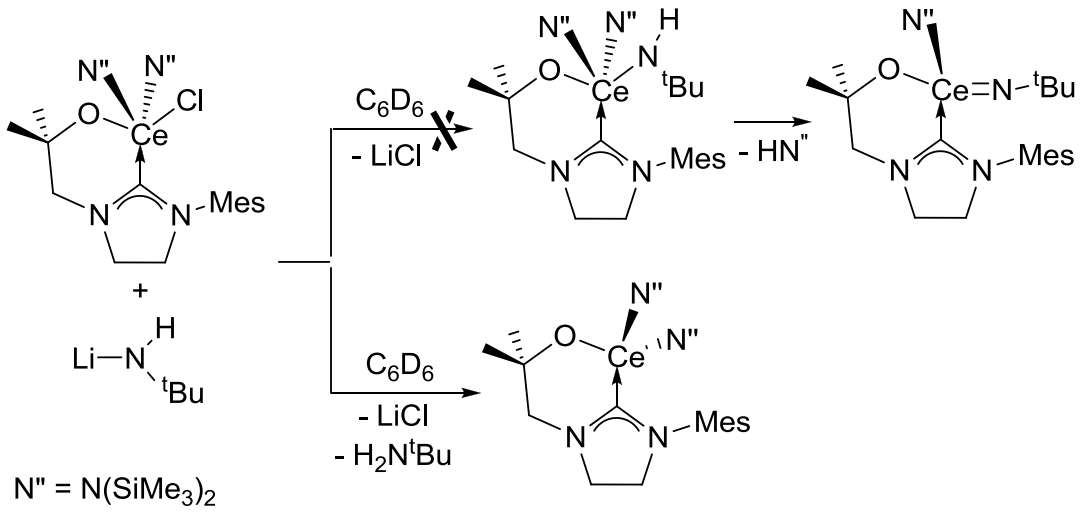

Scheme 10

Single-electron reduction with lithium amides has been observed previously. It was shown by the Arnold and Love groups that lithium amide can act as a single-electron reductant when added to the uranyl ion in a 'Pacman' complex by coordination to the U=O bond.[76]

2.4 NHC functionalisation

2.4.1 Synthesis and crystal structure of the lithium salt of the proligand $[Li(L^M)]_4$

Many of the most readily available lanthanide and actinide starting materials are the halide salts of the respective metal, e.g. $[CeCl_3(H_2O)_6]$, $[YCl_3(H_2O)_6]$ or $[PrCl_3(H_2O)_6]$. These can be dried and converted into the THF solvated halide salts of the corresponding metal such as $[CeCl_3(THF)_{3.5}]$. Further, $[UI_3]$ and $[UO_2Cl_2(THF)_2]$ are often used starting materials. Thus it is desirable to synthesise the alkali metal salt of the proligand in order to carry out salt elimination reactions with the halide salts of the lanthanide and actinide metals.

Initial attempts at deprotonating the bicyclic proligand $[HL^M]$ included the reaction of $[HL^M]$ with one equivalent of *n*-butyllithium, benzylpotassium, potassium-*tert*-butoxide and potassium hydride and different combinations thereof, as e.g. Lochmann-Schlosser base (KO^tBu + nBuLi). Since these attempts were unsuccessful, 1.6 equivalents of n-butyllithium were added to a THF solution of $[HL^M]$ in the presence of 1.3 equivalents of tetramethylethylenediamine (TMEDA) at 0 ˚C, Eq. (9).

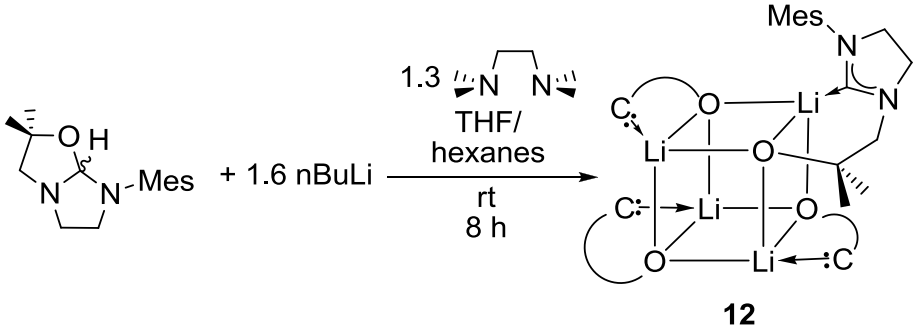

12 (9)

It is a well known fact that the Li/H exchange can be accelerated by adding strong σ-donors such as tetramethylenediamine (TMEDA) which enhances the kinetic

C-H-acidity.[77–81] TMEDA is able to split the *n*-butyllithium oligomer. By complexation of the Li^+-cation it is able to polarise the Li-C bond thereby amplifying the carbanion character of the butyl anion and hence its reactivity rises. Upon addition of *n*-butyllithium, the solution immediately started to turn red. After complete addition the solution was warmed to room temperature and stirred for at least 8 hours after which the volatiles were removed under reduced pressure to yield a brown solid. This solid was washed with hexanes and removal of the volatiles afforded $[Li(L^M)]_4$ **12** in a 52% yield as a yellow solid. The compound had to be dried with stirring over night to yield TMEDA free product. The carbene carbon resonance in the ^{13}C NMR spectrum is shifted to 195 ppm and a lithium resonance in the ^{7}Li-NMR spectrum shifted to 0.23 ppm. $[Li(L^M)]_4$ is a tetramer and so the resonances in the ^{1}H NMR spectrum are very broad and difficult to assign. The resonances in the ^{13}C NMR spectrum are easier to assign when TMEDA or THF are coordinated to the complex. Even when heating the NMR sample to 60 ˚C the ^{1}H NMR spectrum does not resolve.

Confirmation of the tetrameric structure of **12** was obtained when single crystals suitable for X-ray crystallography were isolated in a 56% yield from a reaction of $Li[LaN''_4]$, thought to be $[La(N'')_3]$, with one equivalent of $[HL^M]$, Eq. (10).

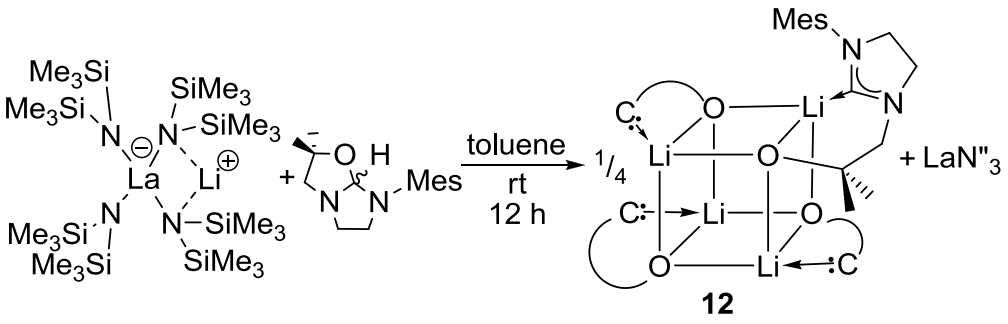

(10)

The $[La(N'')_3]$ had been synthesised from $[LaCl_3(THF)_3]$ and 3 equivalents of LiN" in THF at room temperature with continous rigorous stirring and sonicating for 72 hours and subsequent sublimation at 105 ˚C and 2×10^{-5} torr. This was then dissolved in toluene and reacted with one equivalent of $[HL^M]$ at room temperature and stirred over night. Reducing the volume of the solution afforded colourless crystals suitable for X-ray crystallography. These crystals were of the tetramer **12**, Figure 17.

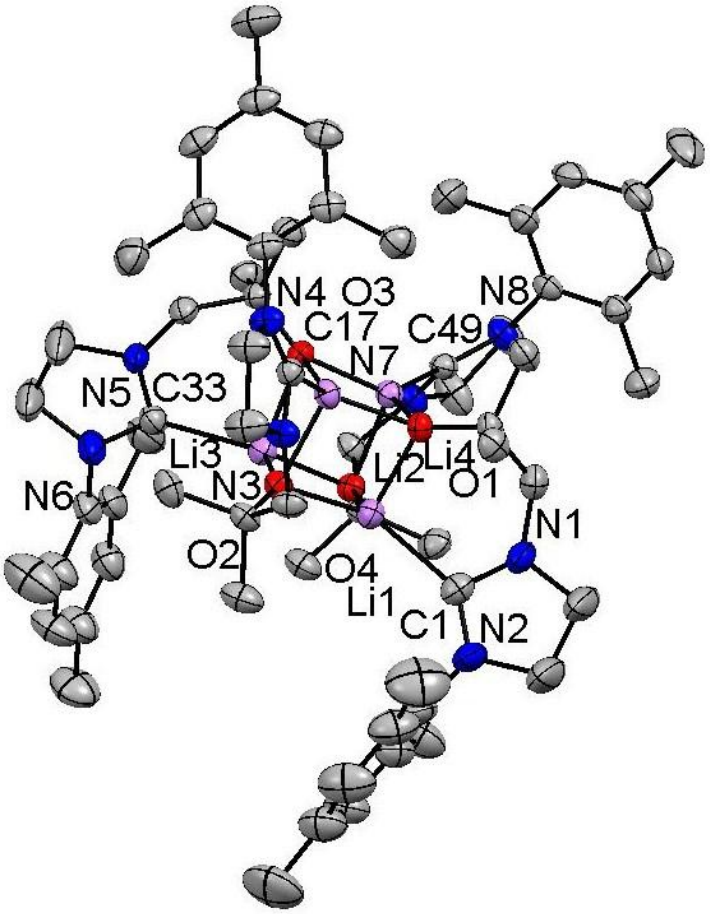

Figure 17 Displacement ellipsoid drawing (50%) of $[Li(L^M)]_4$ **12**, H-atoms omitted for clarity

The core of the displacement ellipsoid plot (50%) of **12** is displayed in Figure 18.

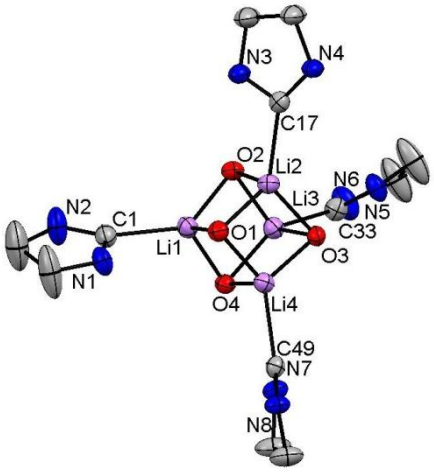

Figure 18 Displacement ellipsoid drawing (50 %) of the core of **12**

The four lithium atoms and the four alkoxy oxygen atoms form a cubane-like structure with alternating Li and O atoms on each corner. Every lithium atom is surrounded by three oxygen atoms and a carbene carbon in a distorted tetrahedral geometry. The oxygen atoms are each surrounded by three lithium atoms and the alkyl-tether of the ligand. This also takes on a distorted tetrahedral geometry. Selected bond distances (Å) and angles (˚) are displayed in Table 8.

Table 8 Selected bond distances (Å) and angles (˚) for **12**

Li1-C1	2.212(4)	Li1-O1	1.947(3)
Li2-C17	2.217(3)	Li2-O2	1.964(3)
Li3-C33	2.195(4)	Li3-O3	1.961(3)
Li4-C49	2.210(3)	Li4-O4	1.977(3)
Li1-O1	1.947(3)	O3-Li2	1.960(3)
Li1-O2	1.976(3)	O3-Li3	1.961(3)
Li1-O4	1.926(3)	O3-Li4	1.905(3)
N1-C1-N2	106.07(18)	N5-C33-N6	106.30(17)
N3-C17-N4	105.93(15)	N7-C49-N8	106.36(15)

A lithium-NHC cluster has been synthesised in the Arnold group previously by Mark Rodden,[82] a lithium halide cluster with an unsaturated version of the alkoxy tethered ligand. A picture of the X-ray structure can be seen in Figure 19. It is a dimer of the lithium carbene complex with stoichiometric incorporation of a lithium iodide byproduct, where the lithium cations form a tetramer capped by two iodides and two oxygen atoms.

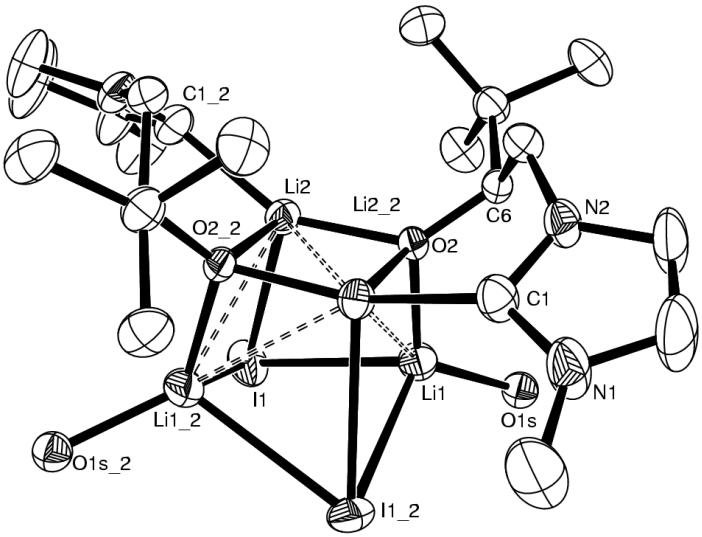

Figure 19 Thermal ellipsoid plot of $LiL^4 \cdot LiI(Et_2O)$

The Li-O bond distances are all between 1.90 Å and 1.97 Å, which is longer compared to the bond distance of 1.887(6) Å in **$LiL^4 \cdot LiI$**. The average N-C-N angle of 106˚ is consistent with an imidazoline and comparable to the N-C-N angle of 106.6˚ in complex **1**. The Li-C bond distance ranges from 2.195(4) Å to 2.217(3) Å, much longer than the reported Li-$C_{carbene}$ bond of 2.130(6) Å in **$LiL^4 \cdot LiI$**, which is the shortest reported Li-NHC bond. The distortion of the anticipated trigonal planar carbon geometry can be quantified by the pitch and the yaw angle. They form because of steric crowding of unsymetrically coordinated NHC ligands[83] The pitch angle is the deviation of the M-C bond from the plane formed by the NHC atoms and the yaw angle is the horizontal distortion of the M-C bond. For **11** the pitch is 3˚ and the yaw is 16˚.

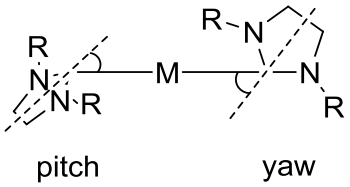

Figure 20 Pitch and yaw angles for NHCs

Other Li-NHCs synthesised and reported in literature include **W**, **X**, **$Y^{tBu, Mes}$** and **$Z^{Sc, Y}$**. The Li-NHC complexes **W**, **Y^{tBu}** and **Y^{Mes}** form dimers. All complexes are formed

with unsaturated NHCs. In the case of **W**, synthesised by Yao and co-workers, each Li is surrounded by a tridentate bulky NHC with an alkoxy tether binding to the metal.[84] The complexes **Y** and **Z** have been synthesised by the Arnold group;[82] **Y** bears a lithium coordinated amido group. The unusual lithium carbene adduct **X** has been reported by Asay, Bertrand and coworkers[85] but never characterised by X-ray crystallography.

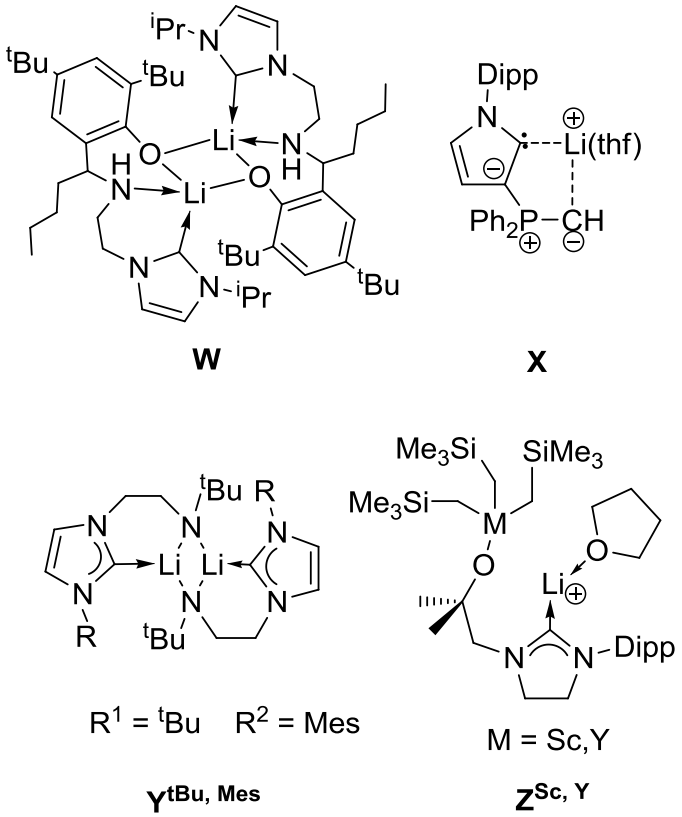

Figure 21 Li-NHC complexes

2.4.2 NHC-boron complex

Treatment of the proligand with an excess of trimethyl amino borane $Me_3N{\cdot}BH_3$ in deuterated benzene gave no reaction at room temperature but under harsher conditions (80 °C for 5 days) gave a colourless solution. The NMR and IR spectrum indicate that the product afforded is the borane-bound carbene **13**.

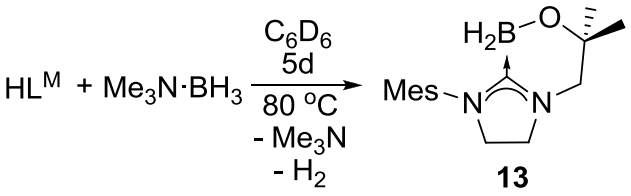

13 (11)

The proton NMR spectrum is very clean and easily assignable. It is even clearer after removing the solvent in vacuo and redissolving it in deuterated benzene confirming that the byproduct is trimethylamine which can be removed in *vacuo*. There is one set of ligand resonances, with one singlet in the aromatic region at 6.84 ppm from the aromatic meta protons of the mesityl group. The -NCH_2CH_2N- backbone resonances are two triplets at 2.93 and 3.17 ppm. The B-H resonances are in the region of 1-4 ppm but are difficult to analyse as they are hidden by the -CH_2CH_2- backbone, the NCH_2 arm and the aromatic methyl groups. The ^{11}B NMR spectrum is a little harder to interpret. A weak resonance is observed at -19 ppm which is most likely the product. In the IR spectrum a distinct B-H stretch is visible at 2279 cm^{-1}, which was compared with Me_3NBH_3 that has distinct signals at 2925 and 2855 cm^{-1}.

2.5 Reactions of [Li(L^M)]$_4$ with uranium iodides

2.5.1 Reaction of [Li(L^M)]$_4$ with uranium iodides

When half an equivalent of **12** is treated with uranium trisiodide in C_6D_6, a brown insoluble precipitate was formed and the NMR spectrum showed only diamagnetic signals. However, if a blue solution of [$UI_3(THF)_4$] in THF was treated at room temperature with one equivalent of the lithium salt, a bright pink solution and an insoluble pink precipitate were afforded. The bright pink colour and poor solubility of the product suggested that uranium bis-ligand bis-iodide complex [U(L^M)$_2$I$_2$] **14** was formed in low yields, Scheme 11. **14** had been synthesised in the group previously by treating a dark blue solution of [U(L^M)(N")$_2$] in d_6-benzene with one equivalent of *iso*-propyl iodide. It is also formed from [{L^{M}SiMe$_3$}UIN"$_2$] in benzene at 70 °C that was left for 12 hours. The product always forms as bright pink crystals that are insoluble in aromatic NMR solvents and a brown solid. The byproduct is most likely U^0 and other decomposition products.

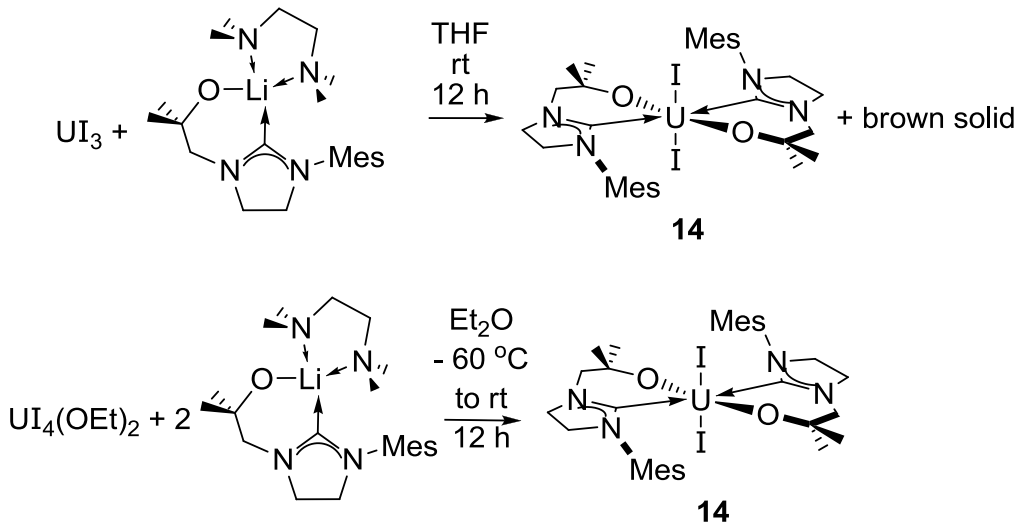

Scheme 11 Pathways to synthesise $[U(L^{M})_2I_2]$ **14**

The same product was afforded when a solution of uranium tetraiodide in diethyl ether was treated at low temperatures of – 60 ˚C with four equivalents of the lithium salt. Instead of the $[U(L^{M})_4]$ complex $[U(L^{M})_2I_2]$ was isolated in a 77% yield as a bright pink insoluble precipitate in a brown solution that was found to be ligand when checked by NMR spectroscopy.

Unfortunately, **14** is highly insoluble and sensitive to high temperatures in solution, therefore further functionalisation of this compound proved to be very difficult.

2.6 Attempted formation of metal-metal bonds

2.6.1 Studies of single crystal growth of the published complex $[Cp_3UFe(CO)_2Cp]$

Marks and Stendal reported the synthesis of an actinide-transition metal bond by reacting $[Cp_3AnCl]$ with $Na[M(CO)_2Cp]$ in THF at room temperature.[86]

$$Cp_3AnCl + CpM(CO)_2Na \xrightarrow[25\ ^{o}C,\ 2\ h]{THF} Cp_3AnM(Cp)(CO)_2 + NaCl \qquad (12)$$

An = Th, U
M = Fe, Ru

The reported reaction has been carried out for the uranium and the thorium analogue of this complex with iron and the ruthenium analogue. Crystals were grown

from a saturated pentane/THF solution for the [$Cp_3ThFe(Cp)(CO)_2$] complex. To ascertain whether it would be possible to grow crystals for the [$Cp_3UFe(Cp)(CO)_2$] complex this experiment was repeated with slightly different starting materials. Instead of [Cp_3UCl] the iodide analogue was used.

$$Cp_3UI + K[Fe(Cp)(CO)_2] \xrightarrow[25\ ^oC,\ 2\ h]{THF} [Cp_3UFe(Cp)(CO)_2] + KI \qquad (13)$$

The reaction is straightforward and after addition of K[$Fe(CO)_2Cp$] to a THF solution of [Cp_3UI] the solution was stirred for 2 hours at room temperature, after which the solvent was removed under reduced pressure and the product extracted with toluene. Removal of solvent under reduced pressure yielded a brown solid which showed the same resonances as reported in literature of -5.60 ppm and -12.82 ppm in the ^{1}H NMR spectrum. A number of techniques, such as cooling the solution to -30 ˚C or -70 ˚C or slow solvent evaporation, were investigated as routes to grow crystals from a saturated solution of this product. Unfortunately, the only single crystals suitable for X-ray crystallography grown from this were of the [$Fe(CO)_2Cp]_2$ dimer. To enhance the reactivity, K[$Fe(CO)_2Cp^*$] was synthesised, but still the only crystals obtained were of the [$Fe(CO)_2Cp^*]_2$ dimer.

2.6.2 Attempted formation of uranium-gold bonds supported by an NHC ligand

The study of heterobimetallic complexes has increased within the last 20 years. These often highly polarised metal-metal bonds present great catalytic activity towards small molecule activation and as a means of tuning redox potentials.[87,88] The combination of a hard, Lewis acidic metal centre and a soft, Lewis basic late metal is interesting for bifunctional catalysis.

Attempts to react [$U(L^M)(N'')_2$] with Au compounds to form a U-Au bond were made. To these means Au-Si complexes were synthesised to perform the suggested reaction in Eq. (14).

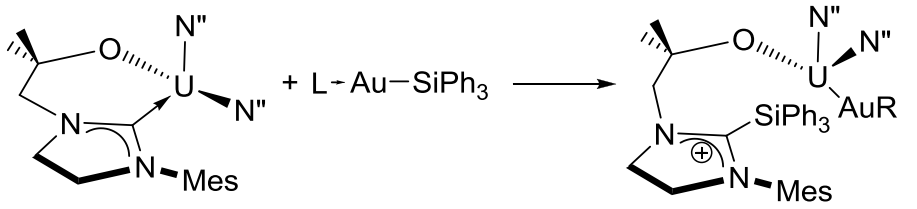

(14)

L = PPh_3

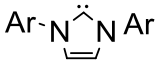

Ar = Diisopropylphenyl

The light sensitive gold compounds were synthesised by reacting RAuCl with $Me_3SnSiPh_3$. The first compound synthesised was the $(Ph_3P)AuSiPh_3$ compound. When reacting $(Ph_3P)AuSiPh_3$ with $[U(L^M)N"_2]$ in benzene, no reaction occured at room temperature. When the solution was heated to 80 ˚C for 12 hours, the solution became greener in colour. Crystals suitable for X-ray crystallography were grown by slow evaporation of the solvent. Unfortunately, the crystals were badly twinned. Nevertheless it seems, that the formed compound was $[Au(L^M)_2]$ **15**.

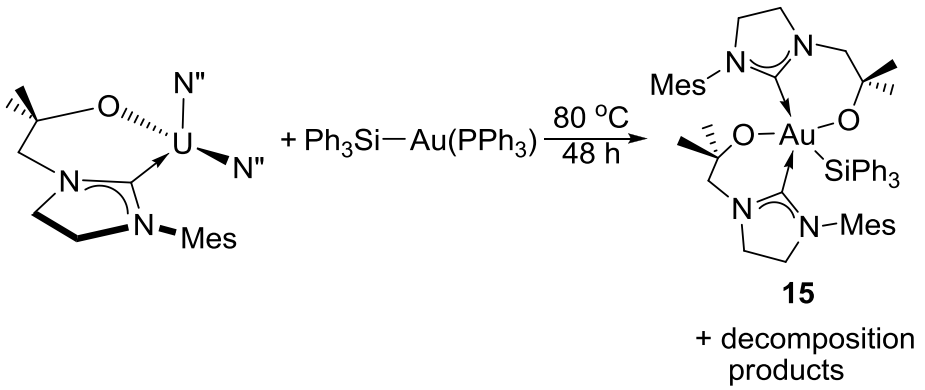

(15)

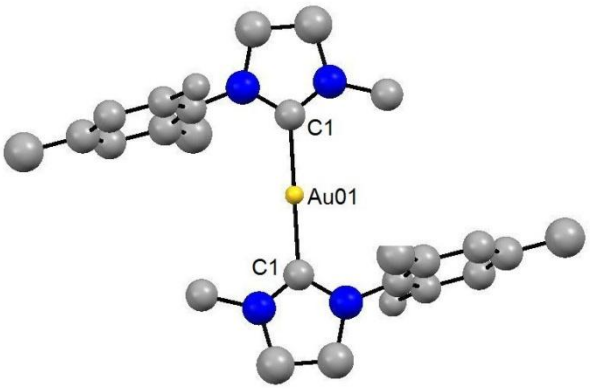

Figure 22 Partial solution of **15**

When the solution was heated for longer at 80 ˚C ^{1}H NMR spectroscopy showed only decomposition of the gold complex. Other attempts at variations of this reaction resulted only in decomposition as the Ph_3P group is very labile. The more strongly coordinating IPr (IPr = 1,3-bis{2,6-bis(diisopropylphenyl)}imidazol-2-ylidene) group was chosen as it had shown use in supporting reactivity of the IPrAuOH compound and its derivatives used in cycloisomerisation and alkyne activation catalysis by the Nolan group.[89–91] When [IPrAuSiPh$_3$] was treated with [U(L^{M})N"$_2$] unfortunately, no reaction occurred at room temperature and heating of the solution only gave decomposition. Due to the thermal instability of the uranium a different uranium compound was chosen. [U(L^{M})(η^5-Cp)$_3$] was reacted with the IPrAu complex at 100 ˚C over a course of four weeks. No reaction occurred that was detectable by ^{1}H NMR spectroscopy.

To ascertain whether the [U(L^{M})(N")$_2$] compound is able to form a U-Fe bond by binding one site with the carbene carbon, it was reacted with K[Fe(CO)$_2$Cp] and [Fe(CO)$_2$Cp]$_2$ but no reaction was observed.

Further attempts were made to react [U(L^{M})(η^5-Cp)$_3$] with [IPrAuSiPh$_3$] but showed no reactivity, see Eq. (16).

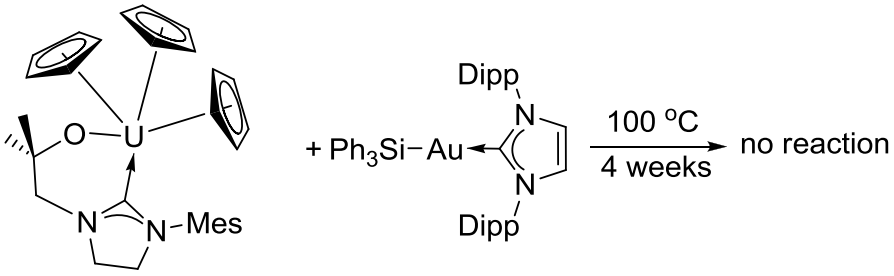

(16)

16

Dipp = Di*iso*propylphenyl

2.7 Addition across the metal-carbene bond of [U(L^M)(η^5-Cp)$_3$]

2.7.1 Activity of [U(L^M)(*η*^{5}-Cp$_3$]

The [U(L^M)(N")$_2$] complex is not an ideal reagent for addition-elimination reaction chemistry because it easily oxidizes to the more stable U^{IV} compound as shown in the reaction of [U(L^M)(N")$_2$] with Me$_3$SiI. This forms the addition product across the metal carbene carbon bond but then rearranges to form the [U(L^M)$_2$I$_2$] complex as seen in Scheme 12.

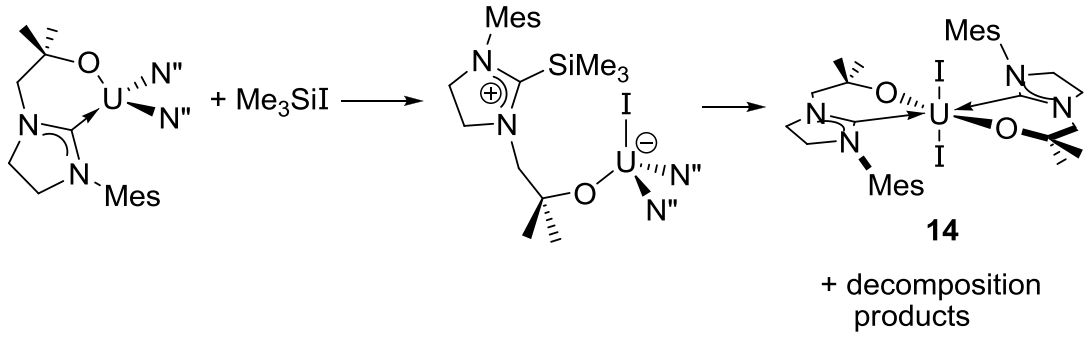

Scheme 12 Reaction of [U(L^M)N"$_2$] with Me$_3$SiI and rearrangement to form [U(L^M)$_2$I$_2$]

In order to avoid this oxidation, a U^{IV} starting material with good leaving groups such as N", Cp, Cp*, indenyl or benzyl was desirable. Therefore [U(L^M)(*η*^{5}-Cp)$_3$] was synthesised in a 71% yield from [Cp$_3$UI] and [Li(L^M)]$_4$ via a salt elimination reaction, Eq. (17).

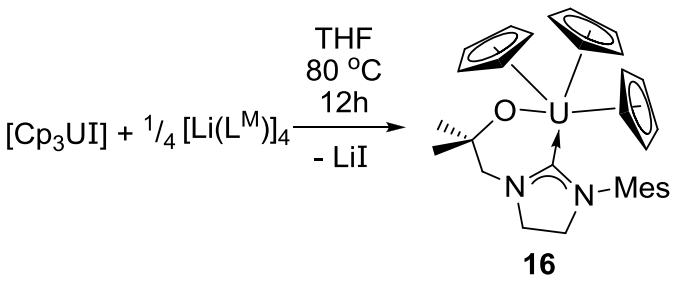

16 (17)

This complex is a potentially ideal starting material for C-X bond activation, see Scheme 13.

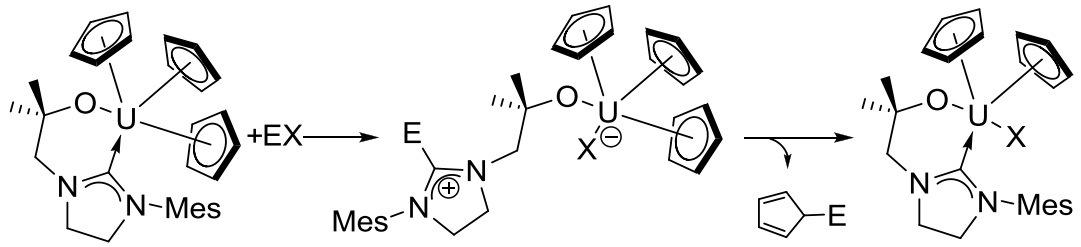

Scheme 13 Reaction of [U(L^M)(η^5-Cp)$_3$] with EX and resulting C-E bond formation

When reacting **16** with Me_3SiI it can clearly be seen in the ^1H NMR spectrum that the starting material completely reacted to form a new product. Simultaneously resonances for Me_3Si-functionalised cyclopentadiene can be recognised in the spectrum.

Further, there clearly is a reaction with I-BBN, Br-catecholborane and H-BBN. The next step is to add in an excess of the Cp monomer to turn this into a cycle as in Scheme 14.

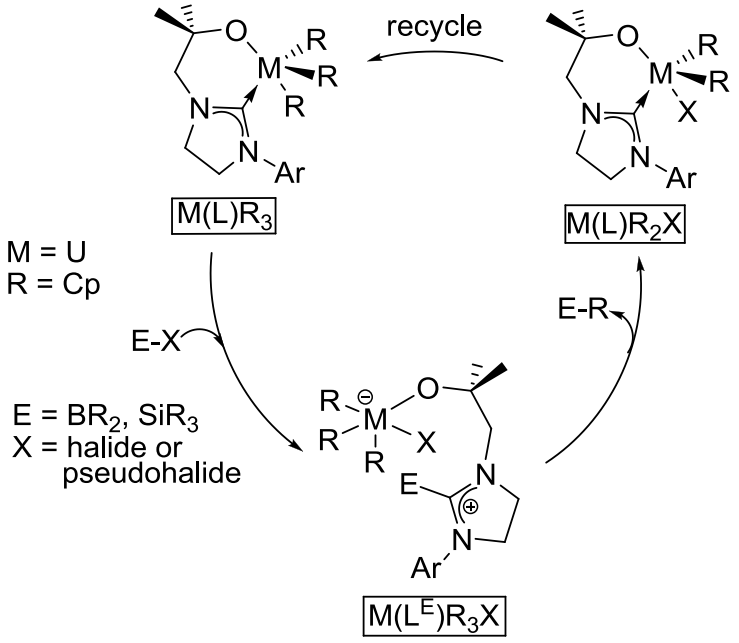

Scheme 14 Cycle for the reaction of $[U(L^{M})(\eta^{5}\text{-}Cp)_3]$ with EX

2.8 Aryloxides

Lanthanide aryloxides have been reported as valuable starting materials to synthesise neutral homoleptic alkyls,[92] cyclopentadienyl and bis(trimethylsilyl)amide lanthanide complexes.[93–95] These compounds can be synthesised by metathesis of the lanthanide aryloxide and appropriate lithium compound. The synthesis of cerium aryloxides is achieved by either salt elimination from the cerium halides or by protonolysis between $[Ce(N'')_3]$ and phenol.

2.8.1 Cerium aryloxide complexes

An attempt was made to synthesise $[Ce(OAr^{3,5\text{-}tBu})_3]$, Eq. (18).

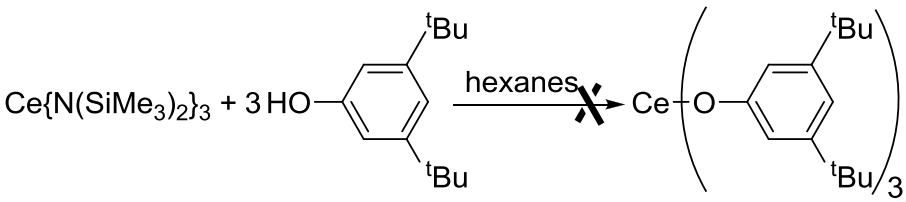

(18)

A solution of $[Ce(N'')_3]$ was treated with a solution of $HOAr^{3,5\text{-}tBu}$. In the ^1H NMR spectrum a multitude of products could be detected. The desired product could not

be isolated by varying the temperature or solvent (coordinating or non), so the known [Ce(OAr$^{2,6\text{-tBu}}$)$_3$] was synthesised instead, Eq. (19).[93]

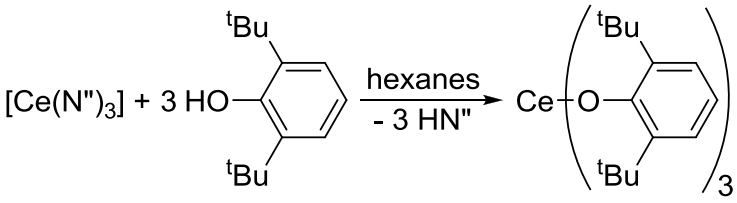

(19)

To form the mono-ligand complex [Ce(L^M)(OAr$^{2,6\text{-tBu}}$)$_2$], [Ce(OAr$^{2,6\text{-tBu}}$)$_3$] was treated with one equivalent of [HL^M] which appeared to give the desired product, as no analysis of the crude product was performed. When [Ce(OAr$^{2,6\text{-tBu}}$)$_3$] was reacted with two equivalents of [HL^M] though, it gave the same product and one set of uncoordinated ligand resonances as detected by ^{1}H NMR spectroscopy, which suggested that the addition product **17** had been formed in a 78% yield. This was confirmed by a structural analysis of single crystals suitable for X-ray crystallography grown from a saturated toluene solution at -30 ˚C.

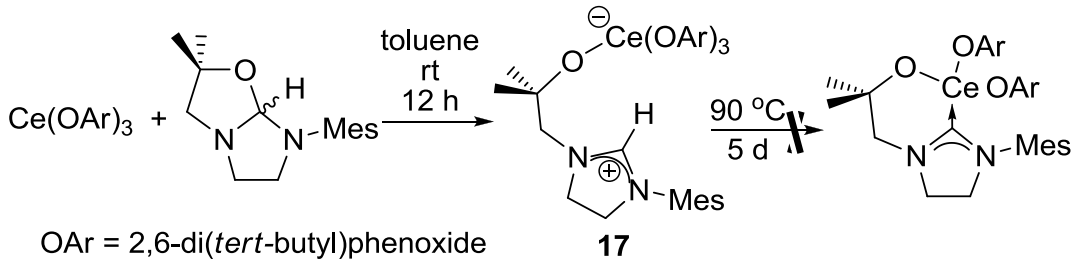

Scheme 15 Formation of **17**

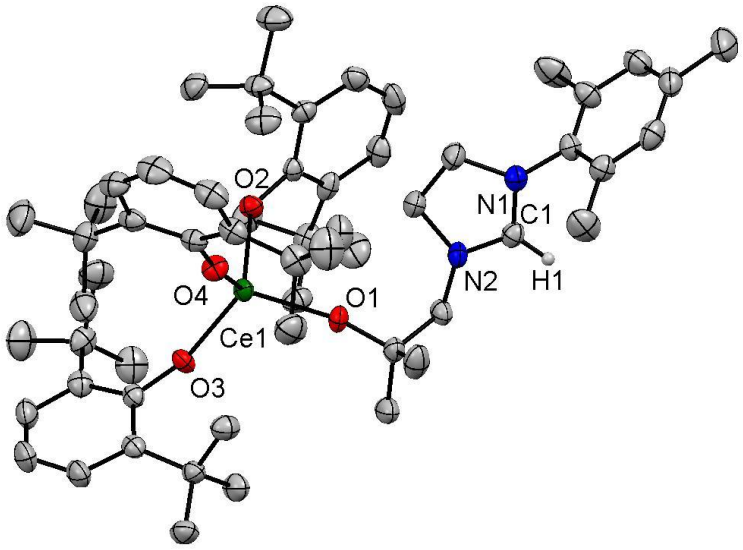

Figure 23 Displacement ellipsoid plot (50%) of [Ce(OAr$^{2,6\text{-tBu}}$)$_3$(HL^{M})] **17**, H-atoms omitted for clarity

The cerium metal is tetrahedrally surrounded by four oxygen atoms. Selected bond distances (Å) and angles (˚) are displayed in Table 9.

Table 9 Selected bond distances (Å) and angles (˚) for **17**

Ce-O(Ar)$_{av}$	2.267(3)
Ce-O1	2.183(3)
N-C-N	114.0(5)

The average bond distance of the metal to the aryloxide oxygen atoms is 2.267 Å which is about 0.1 Å longer than the cerium alkoxide bond of 2.183(3) Å. The average Ce-O(Ar) bond is 0.12 Å longer than the average bond distance of 2.145 Å in [Ce(OAr$^{2,6\text{-tBu}}$)$_3$].[93] The imidazolium is protonated at the C1 carbon, as can be concluded from the N-C-N angle of 114.0(5)˚, which is wider than the N-C-N angle for the deprotonated carbene carbon of 106.6˚ in [Ce(L^{M})N"$_2$(py)] **1$_{py}$** but in accordance with the N-C-N angle of imidazolinium salts of the proligands from 110˚ to 113˚.

A similar compound has been synthesised by the Arnold group from [Ce(O^{t}Bu)$_4$] and [HL^{iPr}], Eq. (20).[12]

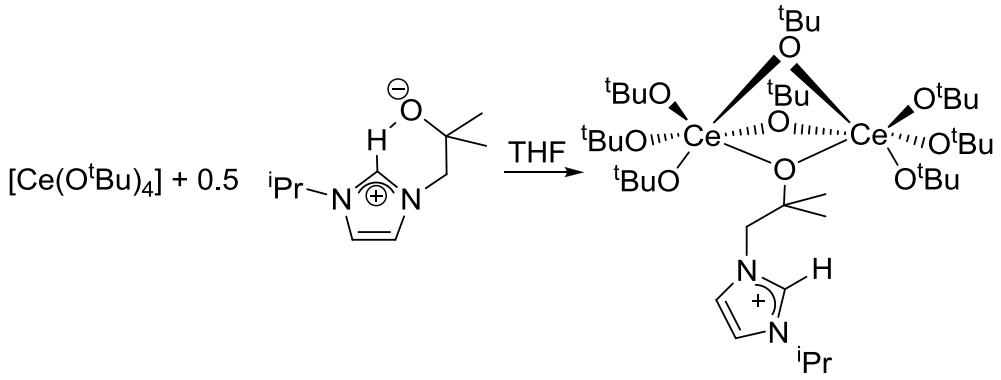

(20)

The product [Ce(OAr$^{2,6\text{-tBu}}$)$_3$(HL^{M})] **17** appears to be thermodynamically stable in solution as it was not possible to convert it to [Ce(OAr$^{2,6\text{-tBu}}$)$_2$(L^{M})] by heating the solution to 100 ˚C. The phenol is not basic enough to deprotonate [HL^{M}] but it was thought that the chelate effect might help in driving the reaction towards [Ce(OAr$^{2,6\text{-tBu}}$)$_2$(L^{M})].

2.8.2 Synthesis of [Ce(L^{M})(OAr)$_2$]

To synthesise the mono-ligand [Ce(OAr$^{2,6\text{-tBu}}$)$_2$(L^{M})], [Ce(OAr$^{2,6\text{-tBu}}$)$_3$] was reacted with [Li(L^{M})]$_4$ in toluene, Eq. (21). After stirring for ten minutes LiOAr$^{2,6\text{-tBu}}$ starts to precipitate out of solution as a colourless solid. Extraction of the toluene solution and removal of the solvent under reduced pressure yields 50% of a yellow solid of **18**.

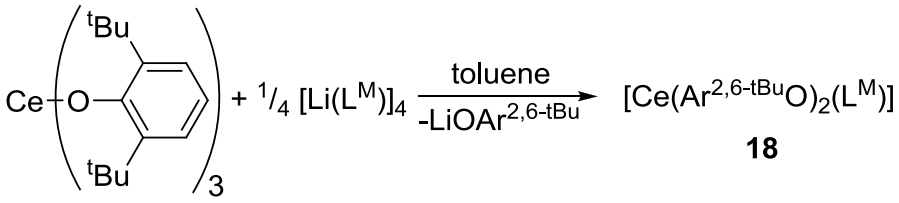

(21)

The product [Ce(Ar$^{2,6\text{-tBu}}$O)$_2$(L^{M})] **18** can be seen in the ^{1}H NMR spectrum and displays nine resonances between 10.08 and -3.81 ppm with the appropriate integrals. The ^{1}H NMR shifts in C_6D_6 are δ: -3.92 (6H, *o*-C*H*$_3$), -1.17 (36H, *tBu*), 1.42-1.63 (8H, C(C*H*$_3$)$_2$, NC*H*$_2$CH$_2$N), 1.65-1.81 (2H, NCH$_2$C*H*$_2$N), 2.44 (2H, NC*H*$_2$C), 3.19 (3H, *p*-C*H*$_3$), 7.34 (2H, *Ar*-*H*), 9.04 (2H, Ar$^{2,6\text{-tBu}}$ p-*H*), 10.12 (4H, Ar$^{2,6\text{-tBu}}$ m-*H*).

2.9 Conclusions

The mono-ligand cerium amide complex $[Ce(L^M)(N'')_2]$ **1** was successfully crystallised and calculations of its percent buried volume were carried out, to show that $[L^M]$ takes up 25.5% of available space surrounding the metal.

The reactivity of $[Ce(L^M)_2N'']$ **2** towards small molecules E-X was tested. Reaction with Me_3SiX (X = Cl, N_3) led to ligand abstraction and the formation of the dimeric carbene $[Me_3SiL^M]$ **4**. Reaction with I-BBN also led to ligand abstraction and the formation of $[L^MBBN]$. The byproduct of these reactions was found to be the respective cerium halide amide complex.

Further comparisons were drawn between $[Ce(L^M)(N'')_2]$ **1** and $[Ce(L^M)_2N'']$ **2** concerning their reactivity, oxidation potential and electronic factors.

It was shown, that $[Ce(L^M)_2N'']$ **2** can be used in a Friedel-Crafts acylation reaction to form benzophenone from benzoyl chloride.

Two different attempts were made at the formation of a Ce=N double bond. Both were unsuccessful.

$[Li(L^M)]_4$ **12** was synthesised successfully and a crystal structure confirmed its tetrameric nature and allowed comparisons to formerly synthesised Li-carbene complexes.

$[Li(L^M)]_4$ **12** was shown to be effective at forming $[UI_2(L^M)_2]$ **14** *via* a direct route from the uranium iodides, which was until recently not possible.

The crystallisation of $[Cp_3UFe(Cp)(CO)_2]$ could not be accomplished. Further investigations into the formation of uranium-metal bonds were also unsuccessful.

The new complex $[U(L^M)(\eta^5\text{-}Cp)_3]$ **16** was synthesised from $[Cp_3UI]$ and $[Li(L^M)]_4$ **12** and was tested for its reactivity towards small molecules E-X and showed promising preliminary results.

Successful synthesis of the cerium aryloxide complexes $[Ce(OAr)_3(L^MH)]$ **17** and $[Ce(L^M)(OAr)_2]$ **18** was accomplished.

2.10 References

1. A. Fürstner, *Angew. Chem. Int. Edit.*, 2000, **39**, 3012–3043.
2. A. Correa, S. P. Nolan, and L. Cavallo, in *Computational Mechanisms of Au and Pt Catalyzed Reactions*, eds. E. Soriano and J. Marco-Contelles, Springer Berlin Heidelberg, Berlin, Heidelberg, 2011, vol. 302, pp. 131–155.

3. N. Marion, O. Navarro, J. Mei, E. D. Stevens, N. M. Scott, and S. P. Nolan, *J. Am. Chem. Soc.*, 2006, **128**, 4101–4111.
4. R. M. Thomas, A. Fedorov, B. K. Keitz, and R. H. Grubbs, *Organometallics*, 2011, 6713–6717.
5. S. Díez-González, *N-heterocyclic carbenes : from laboratory curiosities to efficient synthetic tools*, Royal Society of Chemistry, Cambridge, 2011.
6. O. Kühl, *Functionalised N-heterocyclic carbene complexes*, Wiley, Chichester, U.K., 2010.
7. R. D. Shannon, *Acta Crystallogr. A*, 1976, **32**, 751–767.
8. A. Paulenova, S. E. Creager, J. D. Navratil, and Y. Wei, *J. Power Sources*, 2002, **109**, 431–438.
9. S. Kihara, Z. Yoshida, H. Aoyagi, K. Maeda, O. Shirai, Y. Kitatsuji, and Y. Yoshida, *Pure Appl. Chem.*, 1999, **71**, 1771–1807.
10. T. Mehdoui, J.-C. Berthet, P. Thuéry, and M. Ephritikhine, *Chem. Commun.*, 2005, 2860.
11. L. Maron and D. Bourissou, *Organometallics*, 2009, **28**, 3686–3690.
12. P. L. Arnold, I. J. Casely, S. Zlatogorsky, and C. Wilson, *Helv. Chim. Acta*, 2009, **92**, 2291–2303.
13. P. L. Arnold, A. J. Blake, and C. Wilson, *Chem.-Eur. J.*, 2005, **11**, 6095–6099.
14. I. J. Casely, S. T. Liddle, A. J. Blake, C. Wilson, and P. L. Arnold, *Chem. Commun.*, 2007, 5037.
15. P. L. Arnold, I. J. Casely, Z. R. Turner, and C. D. Carmichael, *Chem.-Eur. J.*, 2008, **14**, 10415–10422.
16. P. L. Arnold and S. T. Liddle, *Chem. Commun.*, 2005, 5638.
17. P. L. Arnold, Z. R. Turner, A. I. Germeroth, I. J. Casely, R. Bellabarba, and R. P. Tooze, *Dalton Trans.*, 2010, **39**, 6808.
18. Casely, I. J., University of Edinburgh, 2009.
19. E. L. Werkema, L. Maron, O. Eisenstein, and R. A. Andersen, *J. Am. Chem. Soc.*, 2007, **129**, 2529–2541.
20. J. M. Sanders, *J. Phys. Chem. A*, 2010, **114**, 9205–9211.
21. P. Mignon, S. Loverix, F. De Proft, and P. Geerlings, *J. Phys. Chem. A*, 2004, **108**, 6038–6044.
22. M. P. Waller, A. Robertazzi, J. A. Platts, D. E. Hibbs, and P. A. Williams, *J. Comput. Chem.*, 2006, **27**, 491–504.
23. D.-Y. Wu, B. Ren, X. Xu, G.-K. Liu, Z.-L. Yang, and Z.-Q. Tian, *J. Chem. Phys.*, 2003, **119**, 1701.
24. S. A. Krasnokutski and D.-S. Yang, *J. Chem. Phys.*, 2009, **130**, 134313.
25. C. Elschenbroich, *Organometallics : a concise introduction*, VCH Verl.-Ges., Weinheim [u.a.], 2., rev. ed., 4. reprint., 2001.
26. R. Dorta, E. D. Stevens, N. M. Scott, C. Costabile, L. Cavallo, C. D. Hoff, and S. P. Nolan, *J. Am. Chem. Soc.*, 2005, **127**, 2485–2495.
27. S. Fantasia, J. L. Petersen, H. Jacobsen, L. Cavallo, and S. P. Nolan, *Organometallics*, 2007, **26**, 5880–5889.
28. A. R. Chianese, X. Li, M. C. Janzen, J. W. Faller, and R. H. Crabtree, *Organometallics*, 2003, **22**, 1663–1667.
29. H. Aktas, J. C. Slootweg, A. W. Ehlers, M. Lutz, A. L. Spek, and K. Lammertsma, *Organometallics*, 2009, **28**, 5166–5172.
30. S. Díez-González and S. P. Nolan, *Coord. Chem. Rev.*, 2007, **251**, 874–883.

31. X. Hu, I. Castro-Rodriguez, K. Olsen, and K. Meyer, *Organometallics*, 2004, **23**, 755–764.
32. H. Jacobsen, A. Correa, A. Poater, C. Costabile, and L. Cavallo, *Coord. Chem. Rev.*, 2009, **253**, 687–703.
33. P. L. Arnold, Z. R. Turner, R. Bellabarba, and R. P. Tooze, *J. Am. Chem. Soc.*, 2011, **133**, 11744–11756.
34. G. Nocton, J. Pécaut, and M. Mazzanti, *Angew. Chem. Int. Edit.*, 2008, **47**, 3040–3042.
35. M. F. Lappert, *J. Organomet. Chem.*, 1988, **358**, 185–213.
36. P. B. Hitchcock, *J. Chem. Soc. Dalton*, 1979, 1314.
37. X. Luan, R. Mariz, M. Gatti, C. Costabile, A. Poater, L. Cavallo, A. Linden, and R. Dorta, *J. Am. Chem. Soc.*, 2008, **130**, 6848–6858.
38. M. K. Denk, A. Thadani, K. Hatano, and A. J. Lough, *Angew. Chem. Int. Edit.*, 1997, **36**, 2607–2609.
39. P. B. Hitchcock, M. F. Lappert, and P. L. Pye, *J. Chem. Soc. Dalton*, 1977, 2160.
40. N. C. Craig, P. Groner, and D. C. McKean, *J. Phys. Chem. A*, 2006, **110**, 7461–7469.
41. H. Bock, H. Borrmann, Z. Havlas, H. Oberhammer, K. Ruppert, and A. Simon, *Angew. Chem. Int. Edit.*, 1991, **30**, 1678–1681.
42. A. L. Gott, W. E. Piers, R. McDonald, and M. Parvez, *Inorg. Chim. Acta*, 2011, **369**, 180–189.
43. H. Braunschweig, C. Chiu, K. Radacki, and T. Kupfer, *Angew. Chem. Int. Edit.*, 2010, **49**, 2041–2044.
44. T. K. Wood, W. E. Piers, B. A. Keay, and M. Parvez, *Angew. Chem. Int. Edit.*, 2009, **48**, 4009–4012.
45. P. L. Arnold, A. J. Blake, and C. Wilson, *Chem.-Eur. J.*, 2005, **11**, 6095–6099.
46. T. K. Wood, W. E. Piers, B. A. Keay, and M. Parvez, *Chem.-Eur. J.*, 2010, **16**, 12199–12206.
47. B. R. Dible and M. S. Sigman, *Inorg. Chem.*, 2006, **45**, 8430–8441.
48. C. A. Tolman, *Chem. Rev.*, 1977, **77**, 313–348.
49. A. C. Hillier, W. J. Sommer, B. S. Yong, J. L. Petersen, L. Cavallo, and S. P. Nolan, *Organometallics*, 2003, **22**, 4322–4326.
50. L. Cavallo, A. Correa, C. Costabile, and H. Jacobsen, *J. Organomet. Chem.*, 2005, **690**, 5407–5413.
51. S. Díez-González and S. P. Nolan, *Coord. Chem. Rev.*, 2007, **251**, 874–883.
52. https://www.molnac.unisa.it/OMtools/sambvca.php
53. A. Poater, B. Cosenza, A. Correa, S. Giudice, F. Ragone, V. Scarano, and L. Cavallo, *Eur. J. Inorg. Chem.*, 2009, **2009**, 1759–1766.
54. W. Haynes, *CRC handbook of chemistry and physics : a ready-reference book of chemical and physical data*, CRC Press, Boca Raton FL., 92nd ed., 2011.
55. A. G. Posternak, R. Y. Garlyauskayte, and L. M. Yagupolskii, *Tetrahedron Lett.*, 2009, **50**, 446–447.
56. H. Sharghi, M. Jokar, M. M. Doroodmand, and R. Khalifeh, *ADV. Synth. Catal.*, 2010, **352**, 3031–3044.
57. A. Kawada, S. Mitamura, and S. Kobayashi, *J. Chem. Soc. Chem. Commun.*, 1993, 1157.
58. E. B. Fleischer, N. Sung, and S. Hawkinson, *J. Phys. Chem.-Us*, 1968, **72**, 4311–4312.
59. H. Kutzke, H. Klapper, R. B. Hammond, and K. J. Roberts, *Acta Crystallogr. B*, 2000, **56**, 486–496.
60. D. Stasko, S. P. Hoffmann, K.-C. Kim, N. L. P. Fackler, A. S. Larsen, T. Drovetskaya, F. S. Tham, C. A. Reed, C. E. F. Rickard, P. D. W. Boyd, and E. S. Stoyanov, *J. Am. Chem. Soc.*, 2002, **124**, 13869–13876.

61. Z. Barandiarán, N. M. Edelstein, B. Ordejón, F. Ruipérez, and L. Seijo, *J. Solid State Chem.*, 2005, **178**, 464–469.
62. J. C. Krupa, *J. Solid State Chem.*, 2005, **178**, 483–488.
63. F. Ferraro and R. Arratia-Pérez, *Polyhedron*, 2011, **30**, 860–863.
64. R. E. Sykora and T. E. Albrecht-Schmitt, *Chem. Mater.*, 2001, **13**, 4399–4401.
65. J. Hallfeldt, Ph.D. thesis, Universität Hannover, 2003.
66. H. Phull, D. Alberti, I. Korobkov, S. Gambarotta, and P. H. M. Budzelaar, *Angew. Chem. Int. Edit.*, 2006, **45**, 5331–5334.
67. C. A. Stewart, D. A. Dickie, M. V. Parkes, J. A. Saria, and R. A. Kemp, *Inorg. Chem.*, 2010, **49**, 11133–11141.
68. P. B. Hitchcock, M. F. Lappert, A. V. Protchenko, and P. G. H. Uiterweerd, *J. Chem. Soc. Dalton*, 2009, 353.
69. A. Jana, H. W. Roesky, and C. Schulzke, *J. Chem. Soc. Dalton*, 2010, **39**, 132.
70. Y. Wielstra, A. Meetsma, S. Gambarotta, and S. Khan, *Organometallics*, 1990, **9**, 876–879.
71. C. J. Burns, W. H. Smith, J. C. Huffman, and A. P. Sattelberger, *J. Am. Chem. Soc.*, 1990, **112**, 3237–3239.
72. P. Roussel, R. Boaretto, A. J. Kingsley, N. W. Alcock, and P. Scott, *J. Chem. Soc. Dalton*, 2002, 1423–1428.
73. D. L. Clark, J. C. Gordon, P. J. Hay, and R. Poli, *Organometallics*, 2005, **24**, 5747–5758.
74. E. Lu, Y. Li, and Y. Chen, *Chem. Commun.*, 2010, **46**, 4469.
75. R. E. Jilek, L. P. Spencer, D. L. Kuiper, B. L. Scott, U. J. Williams, J. M. Kikkawa, E. J. Schelter, and J. M. Boncella, *Inorg. Chem.*, 2011, **50**, 4235–4237.
76. P. L. Arnold, A.-F. Pécharman, E. Hollis, A. Yahia, L. Maron, S. Parsons, and J. B. Love, *Nat. Chem.*, 2010, **2**, 1056–1061.
77. D. Seebach, *Angew. Chem. Int. Edit.*, 1988, **27**, 1624–1654.
78. P. Beak and V. Snieckus, *Acc. Chem. Res.*, 1982, **15**, 306–312.
79. P. Beak and A. I. Meyers, *Acc. Chem. Res.*, 1986, **19**, 356–363.
80. V. Snieckus, *Chem. Rev.*, 1990, **90**, 879–933.
81. P. Beak, W. J. Zajdel, and D. B. Reitz, *Chem. Rev.*, 1984, **84**, 471–523.
82. P. L. Arnold, M. Rodden, K. M. Davis, A. C. Scarisbrick, A. J. Blake, and C. Wilson, *Chem. Commun.*, 2004, 1612.
83. O. Kühl, *Coord. Chem. Rev.*, 2009, **253**, 2481–2492.
84. H. Yao, J. Zhang, Y. Zhang, H. Sun, and Q. Shen, *Organometallics*, 2010, **29**, 5841–5846.
85. M. Asay, B. Donnadieu, A. Baceiredo, M. Soleilhavoup, and G. Bertrand, *Inorg. Chem.*, 2008, **47**, 3949–3951.
86. R. S. Sternal and T. J. Marks, *Organometallics*, 1987, **6**, 2621–2623.
87. N. Wheatley and P. Kalck, *Chem. Rev.*, 1999, **99**, 3379–3420.
88. B. P. Greenwood, G. T. Rowe, C.-H. Chen, B. M. Foxman, and C. M. Thomas, *J. Am. Chem. Soc.*, 2010, **132**, 44–45.
89. G. C. Fortman, A. Poater, J. W. Levell, S. Gaillard, A. M. Z. Slawin, I. D. W. Samuel, L. Cavallo, and S. P. Nolan, *J. Chem. Soc. Dalton*, 2010, **39**, 10382.
90. S. Gaillard, J. Bosson, R. S. Ramón, P. Nun, A. M. Z. Slawin, and S. P. Nolan, *Chem.-Eur. J.*, 2010, **16**, 13729–13740.
91. P. Nun, S. Gaillard, A. M. Z. Slawin, and S. P. Nolan, *Chem. Commun.*, 2010, **46**, 9113.
92. P. B. Hitchcock, M. F. Lappert, R. G. Smith, R. A. Bartlett, and P. P. Power, *J. Chem. Soc. Chem. Commun.*, 1988, 1007.
93. H. A. Stecher, A. Sen, and A. L. Rheingold, *Inorg. Chem.*, 1988, **27**, 1130–1132.

94. H. J. Heeres, A. Meetsma, J. H. Teuben, and R. D. Rogers, *Organometallics*, 1989, **8**, 2637–2646.
95. H. J. Heeres, A. Meetsma, and J. H. Teuben, *J. Chem. Soc. Chem. Commun.*, 1988, 962.

Chapter 3 Attempted oxidation of Ce^{III} and Pr^{III} complexes and dinuclear complexes of Ce^{III} and Pr^{III}

3.1 Background

The lanthanides form mostly trivalent complexes. The +4 oxidation state is in some cases accessible but is harder to obtain because of the high ionisation energy. In the case of cerium and praseodymium the ionization energy for the +4 state is larger than the first three ionization energies combined. Despite this there are a few examples of Ce^{IV} molecular compounds, one of them being $[CeL_4]$ (L = $[C\{(N^iPr)\text{-}CHCHN\}CH_2CMe_2O]$) synthesised by our group.[1] The most commonly used and well known Ce^{IV} compound is CAN ($(NH_4)_2[Ce(NO_3)_6]$) which is widely used in organic synthesis and catalysis as a stoichiometric oxidant. There are methods in which CAN is added in catalytic amounts, where the Ce^{IV} is retrieved by another oxidant. Menéndez wrote an excellent review discussing the catalytic use of CAN in organic synthesis.[2] An example is the Belousov-Zhabotinsky reaction, where Ce^{III} is reduced by bromomalonic acid and then reoxidised by the bromated anion, Eq. (1).[3]

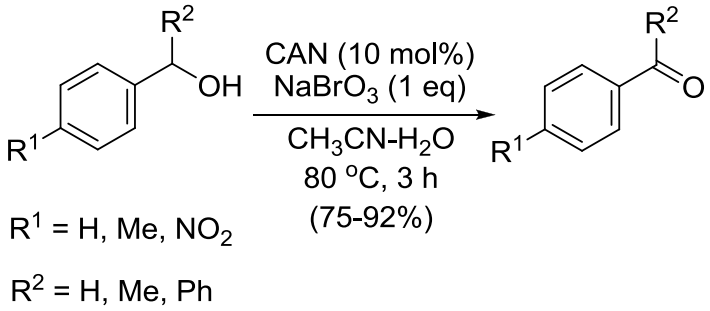

(1)

Examples of molecular tetravalent praseodymium compounds apart from PrF_4 are hitherto unknown. The only Pr^{IV} compounds known are metalloids such as $Rh(1\%)/Ce_{0.8}Pr_{0.2}O_{2-x}$ which are used as catalysts for three-way catalysts in catalytic convertors.[4]

3.2 Oxidation of $[Ce(L^M)_2N'']$

In this part the attempts to oxidise $[Ce(L^M)_2N'']$ **2** with oxidation agents is described.

3.2.1 Oxidation of $[Ce(L^M)_2N"]$ with Ph_3CCl

Recently, the facile oxidation of $[Ce(N")_3]$ and $[Ce(L^{Ar})(N")_2]$ with tritylchloride to $[Ce(Cl)(N")_3]$ and $[Ce(Cl)(L^{Ar})(N")_2]$ (Ar = diisopropylphenyl/mesityl) respectively, was shown by the Arnold group, Eq. (2).[5]

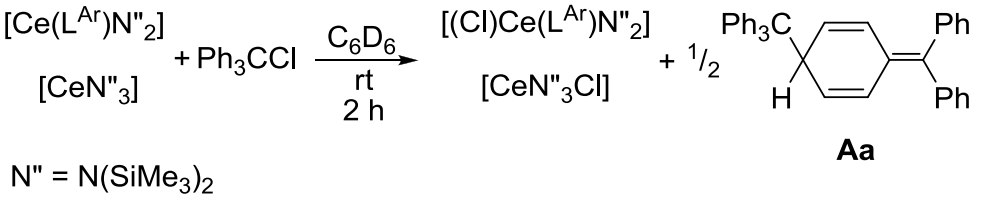

(2)

In this reaction the synthesis of the tetravalent cerium compounds is accompanied by the formation of Gomberg's dimer **Aa** (((4-(diphenylmethylene)cyclohexa-2,5-dienyl)methanetriyl)tribenzene), which shows characteristic resonances in the ^{1}H NMR spectrum in C_6D_6 at δ = 4.92 ppm, 5.92ppm, 6.44ppm and 7.07-7.30 ppm.

The oxidation reaction of $[Ce(L^M)(N")_2]$ **1** with one equivalent of Ph_3CCl to form $[(Cl)Ce(L^M)N"_2]$ **19** and **Aa** is shown in Eq. (3).

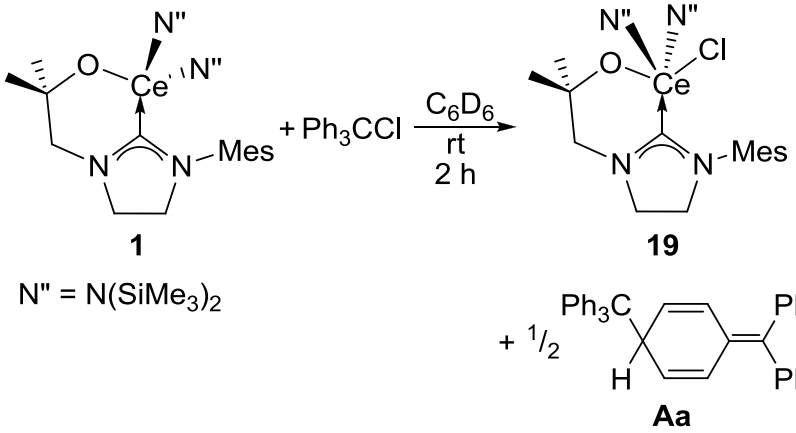

(3)

The ^{1}H NMR spectrum of the Ce^{IV} complex **18** and **Aa** is displayed in Figure 1.

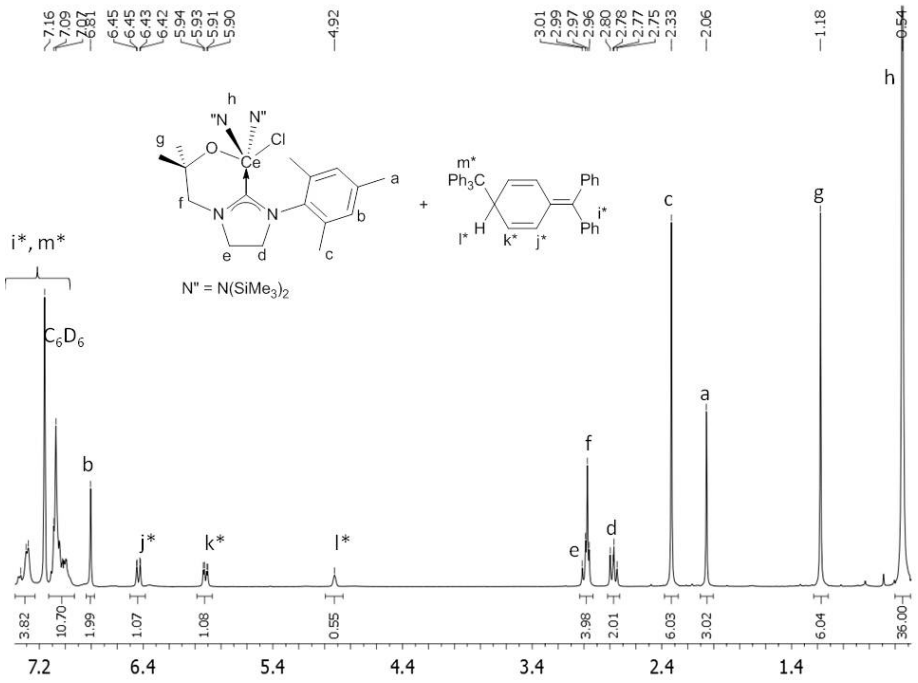

Figure 1 ^{1}H NMR spectrum of the products of the reaction of [Ce(L^{M})N"$_2$] with Ph_3CCl, the newly formed Ce^{IV} compound [Ce(L^{M})N"$_2$(Cl)] **19** and Gomberg's dimer **Aa**

The resonances of complex **19** are denoted by the letters a-h and the resonances of **Aa** are denoted by the letters j*-m*. The diamagnetic Ce^{IV} complex **19** displays resonances in the ^{1}H NMR spectrum between 0.54 and 6.81 ppm as opposed to the paramagnetic Ce^{III} starting material **1** that displays resonances between -6.54 and 14.04 ppm.

When **2** is treated with a slight excess of Ph_3CCl the expected oxidation reaction to the new Ce^{IV} complex [(Cl)Ce(L^{M})$_2$N"] and an equimolar formation of **Aa** does not occur, instead the cerium metal retains its oxidation state and forms the dinuclear complex **20**, Scheme 1. To a yellow suspension of **2** [Ce(L^{M})$_2$N"] in deuterated benzene a colourless solution of Ph_3CCl in deuterated benzene was added, this was warmed gently to ensure complete dissolution. The reaction solution changed colour to a dark red after 30 minutes. Orange single crystals suitable for X-ray crystallography were grown from this saturated benzene solution. These crystals confirmed the formation of **20** [ClCe(μ-L^{M})$_3$CeCl$_2$] a cerium dimer with three bridging oxygen atoms, Figure 3. The three bridging oxygen atoms O1, O2 and O3 are the oxogroups of the three ligands.

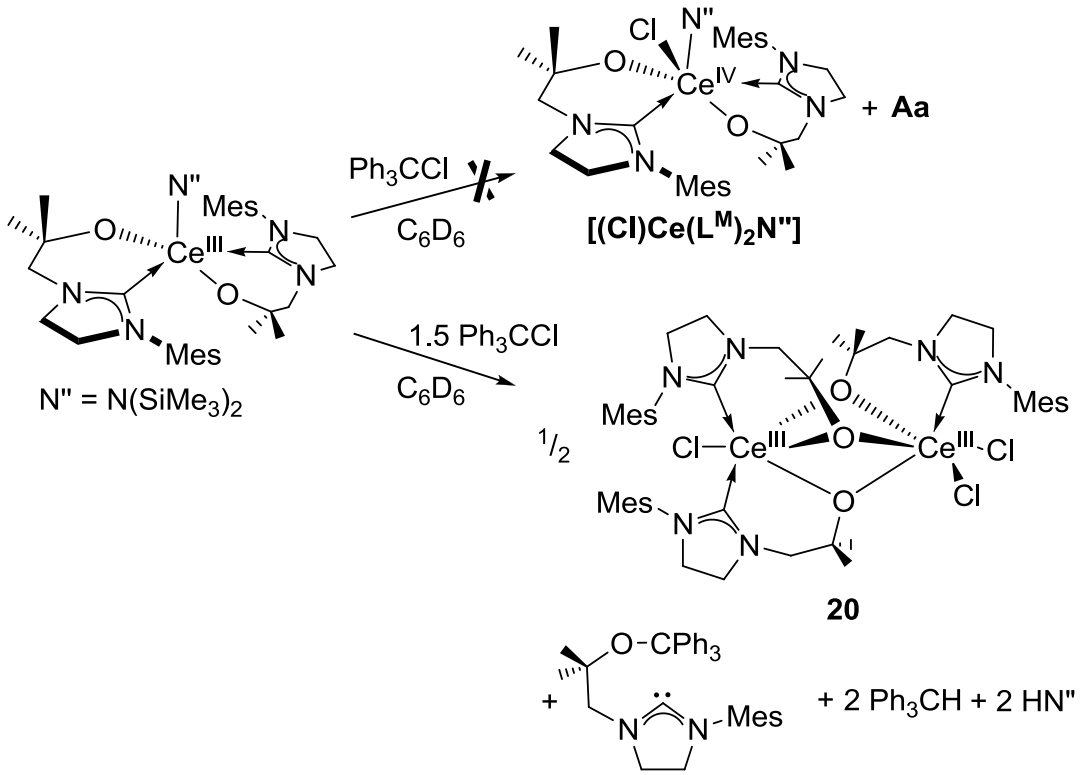

Scheme 1 Expected reaction of **2** with Ph_3CCl (shown above) and occurring reaction of **2** (below) with Ph_3CCl to form **20**

This reaction was initially considered to be an oxidation reaction to produce a Ce^{IV} complex because the ^1H NMR spectrum of an NMR scale reaction solely displays resonances in the diamagnetic region, between 0 and 8 ppm, Figure 2. However, an indication against oxidation is that no formation of Gomberg's dimer is observed in the ^1H NMR spectrum. Instead the formation of bis(trimethylsilyl)amine ($HN(SiMe_3)_2$) at 0.1 ppm ($HN(Si\mathit{Me}_3)_2$) and 1.18 ppm ($\mathit{H}N(SiMe_3)_2$) and the formation of triphenylmethane (Ph_3CH) at 5.38 ppm ($Ph_3C\mathit{H}$) and 6.98-7.35 ppm (Ph_3CH) are observed.

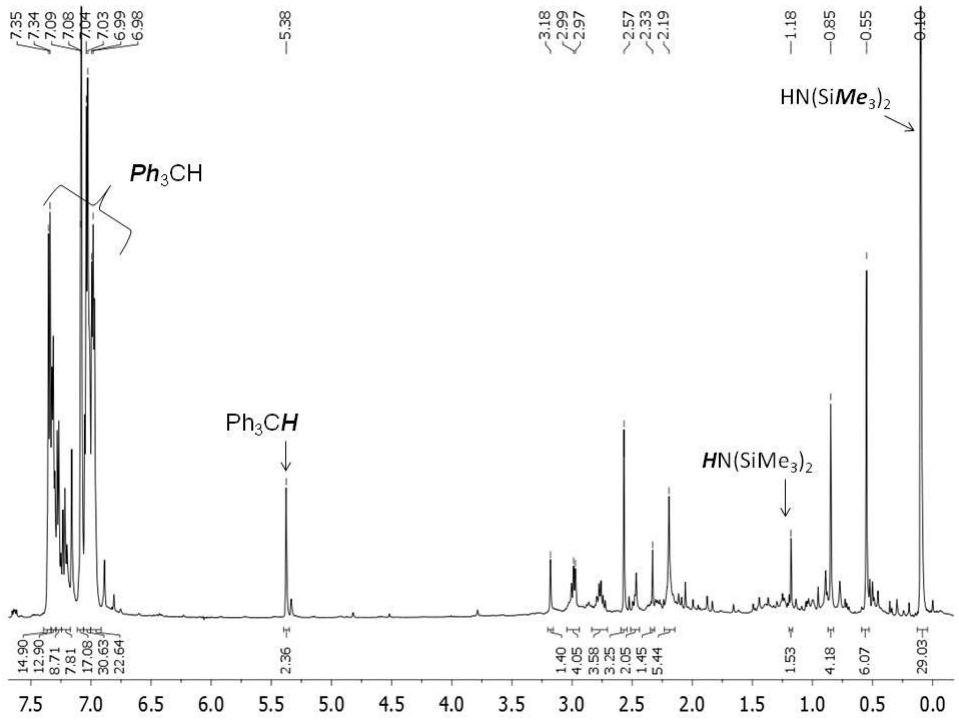

Figure 2 ^{1}H NMR spectrum of the products of the reaction of **2** with 3 equivalents of Ph_3CCl

The reaction was scaled up successfully by adding a yellow solution of **2** in toluene to a colourless solution of Ph_3CCl in toluene to give a dark red solution that was stirred for 12 h at room temperature, during which time a fine beige precipitate had formed. The supernatant was removed by filtration and the residual solid washed with hexanes. Removal of the volatiles under reduced pressure afforded **20** as a beige solid in a 31% yield.

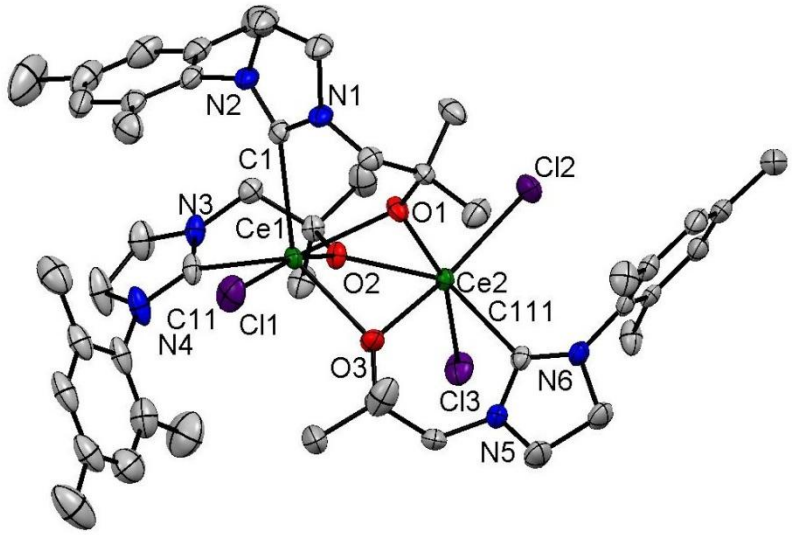

Figure 3 Displacement ellipsoid (50%) drawing of **20** [ClCe(μ-L^M)$_3$CeCl$_2$], H atoms omitted for clarity

The cerium centres are both six coordinate and surrounded in a distorted octahedral geometry. Selected bond distances (Å) and angles (˚) for **20** are displayed in Table 1.

Table 1 Selected bond distances (Å) and angles (˚) of **20** [(Cl)Ce(μ-L^M)$_3$CeCl$_2$]

Ce1-Ce2	3.5050(2)
Ce1-O_{av}	2.3752
Ce2-O_{av}	2.4143
Ce1-C_{av}	2.742
Ce2-C111	2.737(3)
Ce-Cl_{av}	2.7263
Ce1-O-Ce2$_{av}$	94.08

Ce1 is coordinated to two carbene carbons (C1 and C11) with an average bond distance of 2.742 Å which is comparable to the Ce-C bond of 2.786(4) Å in **2**. Ce2 is coordinated to one carbene carbon, C111 with a similar bond distance of 2.737(3) Å. The Ce-Cl bonds have an average bond distance of 2.7263 Å. The average bond distances of the three bridging oxygen atoms to the metal centres are 2.3752 Å to Ce1 and 2.4143 Å to Ce2.

Other cerium compounds with three bridging oxo groups have been reported, most compounds being tri- or tetrametallic cerium clusters.[6–15] One is the mixed oxidation state [{Ce(O^{t}Bu)$_2$}(μ-O^{t}Bu)$_2$(μ$_3$-O^{t}Bu)$_2$Ce(O^{t}Bu)(NO$_3$)}] trimer **A** containing one Ce^{III} and two Ce^{IV} centres.[16] Compounds **B**-**D** are bimetallic Ce^{IV} compounds.[17–19] Compounds **B**-**D** were synthesised by treating the respective cerium tetra(alkoxide) in a protonolysis reaction with 2 (**B**), 1.5 (**C**) or 0.5 (**D**) equivalents of an alkoxy ligand.

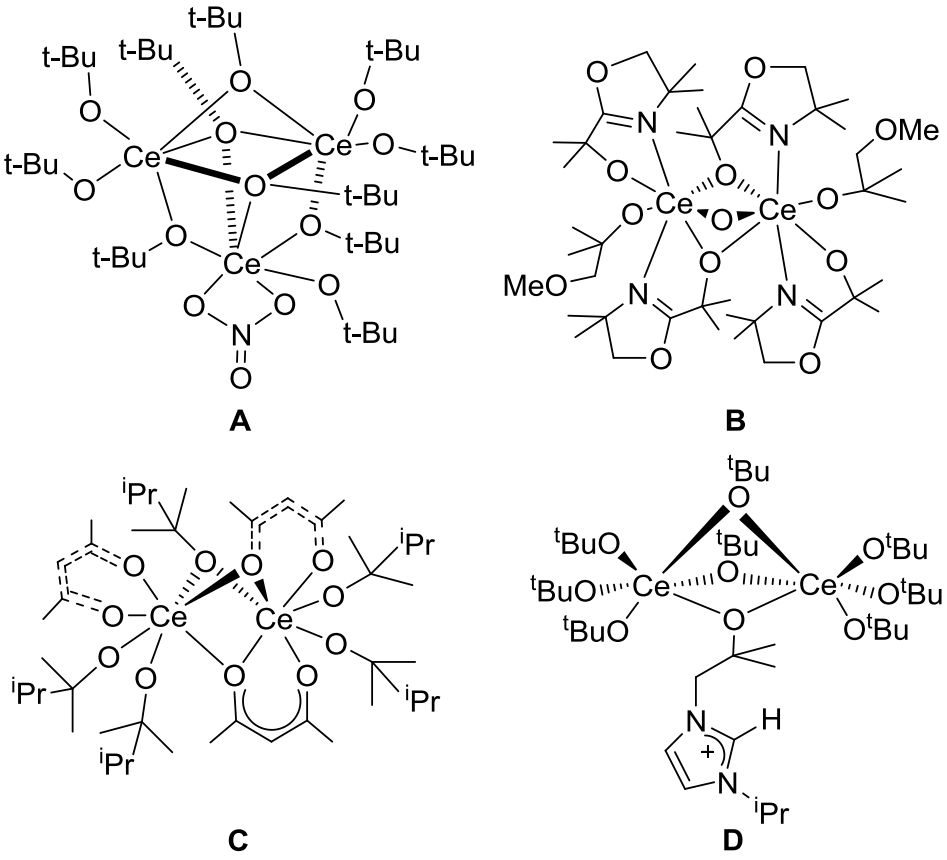

Figure 4 Tri and bimetallic cerium compounds **A**-**D**

Selected bond distances (Å) and angles (˚) are displayed in Table 2. For compound **D** only the connectivity of the structure was established.

Table 2 Selected distances (Å) and angles (˚) of the literature compounds **A**-**C**

	Ce1-O	Ce2-O, $(Ce3-O)_{av}$	Ce1-Ce2, $(Ce-Ce)_{av}$	Ce1-O-Ce2, $(Ce-O-Ce)_{av}$
A	2.5445_{av}	2.3955_{av}, (2.400_{av})	(3.7118_{av})	(97.5844_{av})
B	2.106(5), 2.395(5), 2.407(5)	2.106(4), 2.459(5), 2.379(5)	3.3800	94.94
C	2.508(4), 2.494(4), 2.367(4)	2.689(4), 2.475(4), 2.361(4)	3.7760	99.32

The Ce-Ce distance of 3.5050(2) Å of **20** is in between the reported bond distances of 3.380 Å (**B**) and 3.7 Å (A,C). The average Ce-O-Ce angle of 94.08˚ of **19** is slightly shorter than the smallest reported angle of 94.94˚ (**B**). The Ce-O bond distances of 2.3752 Å and 2.4143 Å are within the range of the Ce-O bond distances of 2.106(5) Å to 2.689(4) Å.

In order to balance this reaction, the stoichiometry of the reaction was modified to an analogous reaction where two equivalents of **2** were treated with 3 equivalents of tritylchloride as shown in Scheme 2.

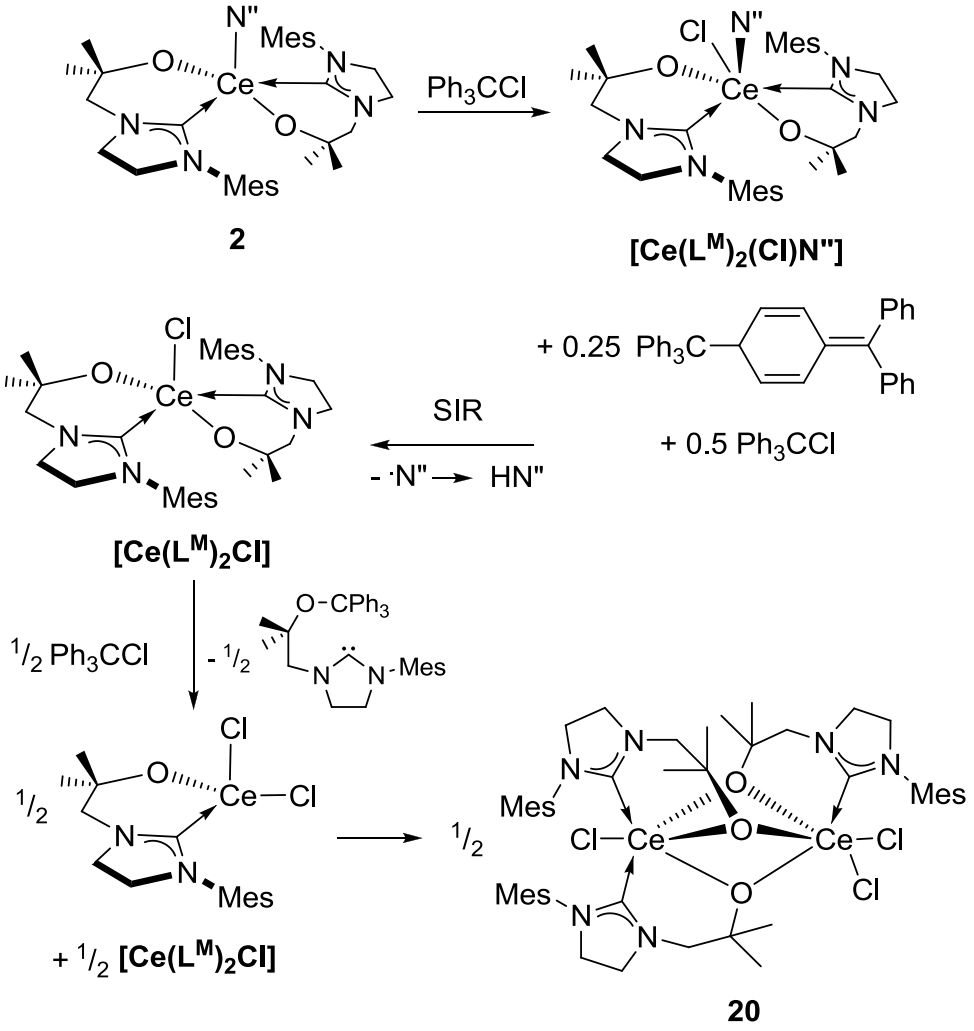

Scheme 2 Proposed mechanism for the formation of **20** [(Cl)Ce(μ-L^M)$_3$Ce(Cl)$_2$]

In this proposed mechanism one equivalent of **2** reacts with one equivalent of tritylchloride to form the formal addition product across the metal carbene carbon bond to form [Ce(L^M)(L^MCPh$_3$)(Cl)N"], which then loses one equivalent of triphenylmethane and bis-(trimethylsilyl)amine to form [Ce(L^M)$_2$Cl] in a sterically induced reduction (SIR). This then reacts with half an equivalent of tritylchloride to convert half of the [Ce(L^M)$_2$Cl] to [Ce(L^M)(L^MCPh$_3$)(Cl)$_2$], which undergoes ligand abstraction to form half an equivalent of the [(Cl)Ce(μ-L^M)$_3$CeCl$_2$] dimer. Presumably, this product is formed in preference to the zwitterionic [Ce(L^M)(L^MCPh$_3$)(Cl)$_2$] for steric reasons and the tendency of the bis-ligand cerium complex to easily undergo ligand abstraction.

Another route to synthesise the [(Cl)Ce(μ-L^M)$_3$CeCl$_2$] dinuclear complex **20** is by salt elimination. A mixture of [Li(L^M)]$_4$ and [CeCl$_3$(THF)$_{3.5}$] in THF was refluxed at

80 ˚C for 12 h. The solvent was removed under reduced pressure and the remaining solid extracted with toluene. Removal of solvent under reduced pressure yielded 32 % of **20** as an orange solid based on an assumed formula weight of $[(Cl)Ce(\mu\text{-}L^M)_3CeCl_2]$.

Further chemistry and characterisation of this compound proved to be difficult as it is insoluble in aromatic solvents and THF and only sparingly soluble in dichloromethane.

The diamagnetic ^1H NMR spectrum obtained from the NMR-scale reaction is most likely due to the byproducts of the reaction only being sufficiently soluble to show in the solution spectrum.

Attempts to synthesise the $[Ce(L^M)_2Cl]_2$ complex by treating **2** with one equivalent of Ph_3CCl were unsuccessful, Eq. (4).

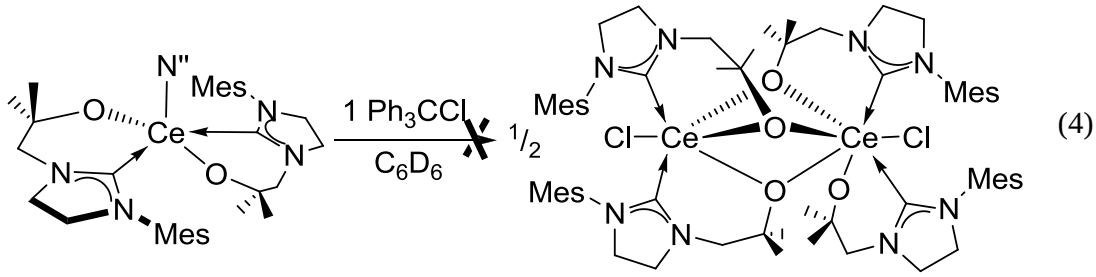

(4)

This is most likely due to steric crowding, which does not allow another ligand to coordinate to the cerium metal centre. No dinuclear cerium complexes with four bridging oxygen atoms are known apart from cerium peroxo complexes, which are not as sterically demanding as $[L^M]$.[20–22]

3.2.2 Attempted Oxidation of $[Ce(L^M)_2N"]$ with I_2

An attempt was made to oxidise **2** with elemental I_2. The reaction was carried out by adding iodine to a toluene suspension of **2** and continuous stirring at room temperature over 12 h.

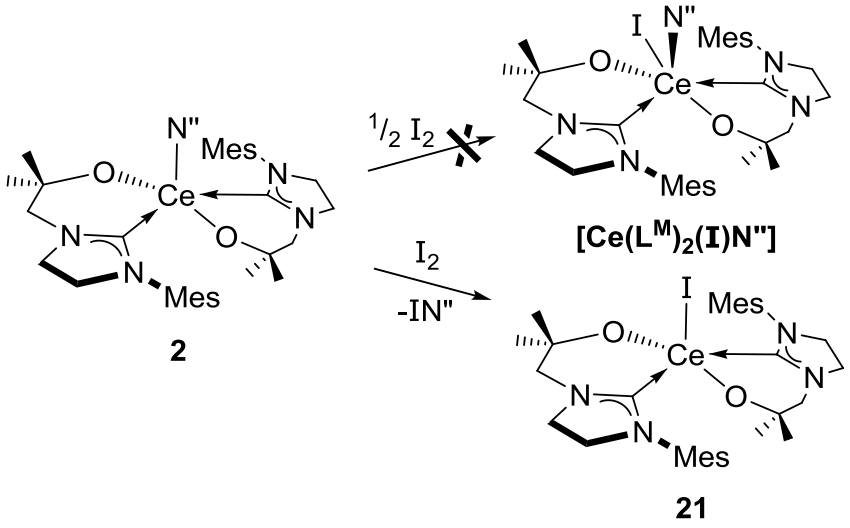

Scheme 3 Reaction of **2** with I_2. Shown above is the attempted oxidation reaction to form [Ce(L^M)$_2$(I)N"], below the observed reaction to form [Ce(L^M)$_2$I] **21**

When **2** was treated in an NMR scale experiment with half an equivalent of I_2 in an attempt to form [Ce(L^M)$_2$(I)N"] only conversion of half the amount of **2** was observed, forming the paramagnetic product **21**. Therefore a scale up reaction was performed adding one equivalent of I_2 to **2**. As soon as the iodine was added, the colour of the reaction changed from orange to a red-brown colour. Subsequent removal of the volatiles and washing with hexanes gave a yellow solid of **21** in a 48% yield. **21** is sparingly soluble in deuterated solvents, but elemental analysis results confirm its formation. The suggested byproduct N-iodohexamethyldisilazane has been reported in the literature and was formed by treating NaN($SiMe_3$)$_2$ with one equivalent of I_2 in heptanes at low temperatures.[23] It has a low melting point of 10 ˚C and decomposes slowly in light, which explains why only trace amounts of it could be found in the ^{1}H NMR spectrum of the NMR scale reaction. The formation of HN" is clearly visible and a product of the decomposition of IN".

3.2.3 Attempted Oxidation of [Ce(L^M)$_2$N"] with $PbCl_2$

When **2** is treated with one equivalent of $PbCl_2$ in toluene and stirred at room temperature a fine grey precipitate starts to form that indicates the formation of Pb^0, Eq. (5).

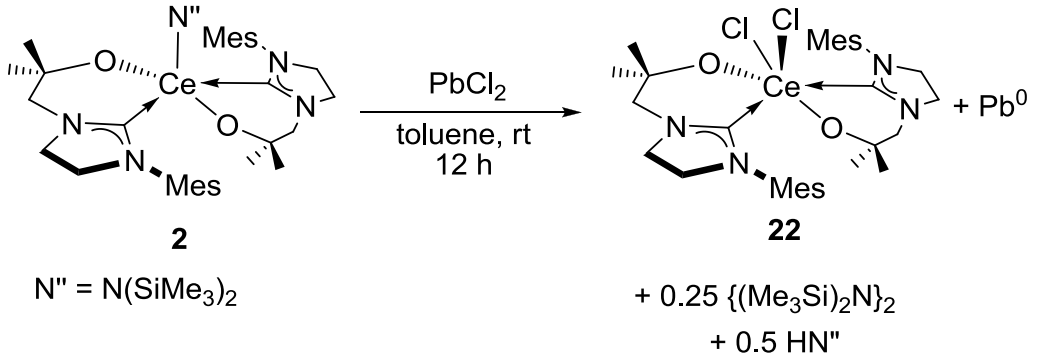

2

N" = $N(SiMe_3)_2$

22

+ 0.25 $\{(Me_3Si)_2N\}_2$

+ 0.5 HN"

(5)

Extraction of the solution from this precipitate and removal of the volatiles in vacuum yields a pale yellow solid. The formation of a new Ce^{IV} complex can be seen in the ^1H NMR spectrum which displays only diamagnetic resonances. The yield of 118% indicates that $[Ce(L^M)_2Cl_2]$ **22** cannot be the sole product. The ^1H NMR spectrum of an NMR scale reaction shows two broad resonances at 0.1 ppm and at 0.18 ppm each, which is consistent with the formation of $HN(SiMe_3)_2$ and $\{(SiMe_3)N\}_2$. Only a small amount of HN" can be seen in the ^1H NMR spectrum of the scale up, as it has a relatively low boiling point of 126 ˚C and is removed partially under vacuum. The tetrakis(trimethylsilyl)hydrazine on the other hand is reportedly a colourless solid with a melting point of 290-292 ˚C.[24] Attempts to remove this byproduct by sublimation or fractional crystallization were unsuccessful. **22** should be sparingly soluble in toluene and benzene, assuming it has similar properties to $[Ce(L^M)N"(Cl)]$ and $[CeN"(Cl)_2]$ complexes described in Chapter 2. The unusual solubility of this complex in C_6D_6 and even in hexanes during the work-up and the yield of over 100% led to the conclusion, that the $\{(SiMe_3)N\}_2$ byproduct is the cause of these findings. Another possibility is the incorporation of $[Pb(N")_2]$ into **22** to form $[(N")_2Pb\text{-}\mu_2\text{-}Cl_2Ce(L^M)_2]$. $[Pb(N")_2]$ shows a resonance shifted in the ^1H NMR spectrum in C_6D_6 of $\delta = 0.23$ ppm, which would also explain the resonance at 0.18 ppm in the ^1H NMR spectrum of the NMR scale reaction of **2** and $PbCl_2$.[25]

3.2.4 Other reagents used for the attempted oxidation of $[Ce(L^M)_2N"]$

Transition metal halides were investigated as suitable oxidising agents for **2**. For example the well known oxidants CuCl and $CuCl_2$ were used as well as HgI_2 and $NiCl_2$. None of these showed a reaction with **2**, even when heated for several days at 90 ˚C.

Other reagents that were investigated included N-bromosuccinimide and (dichloroiodo)benzene. Only decomposition could be observed in the reaction of **2** with N-bromosuccinimide. However, when **2** was treated with one equivalent of (dichloroiodo)benzene the ^{1}H NMR spectrum showed the formation of a new diamagnetic product but no carbene resonance could be found in the $^{13}C\{^{1}H\}$ NMR spectrum. This led to the conclusion that a Ce^{IV} compound had not been synthesised.

3.2.2 Reaction of [Ce(L^{M})N"$_2$] with phenols

The mono-ligand cerium complex **1** has been found to activate E-X bonds, in light of this the reaction of aryloxides with this compound were investigated to probe whether it was able to activate O-H bonds.

The reaction of **1** with an equimolar amount of $HOAr^{2,6\text{-}tBu}$ results in the formation of [Ce(L^{M})($OAr^{2,6\text{-}tBu}$)N"], Eq. (6). The reaction does not proceed at room temperature and must therefore be heated at 80 ˚C overnight to ensure complete conversion. No addition across the metal carbene carbon bond was observed by ^{1}H NMR spectroscopy.

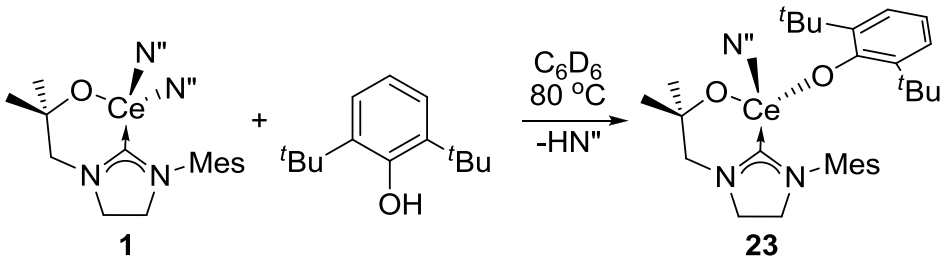

(6)

To a yellow solution of **1** in toluene a colourless solution of one equivalent of 3,5-di-*tert*-butylphenol in toluene was added and the mixture heated at 80 ˚C for 12 h. The volume of the toluene solution was reduced and hexanes added, upon which **24** crystallised out of solution upon storage at -30 ˚C overnight in a 68% yield, Eq. (7).

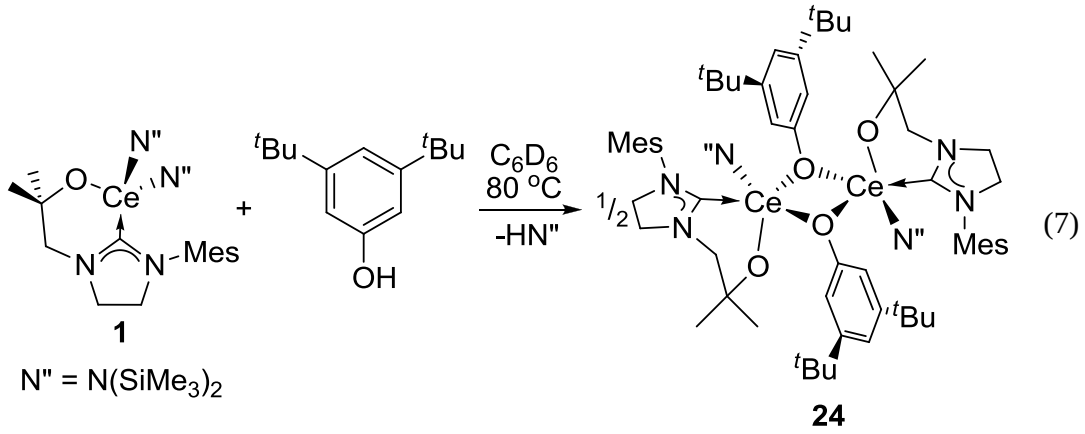

(7)

In contrast, the ^{1}H NMR spectrum of the crude reaction of **1** with HOAr$^{3,5\text{-tBu}}$ in deuterated benzene at 80 ˚C shows only small diamagnetic resonances that are due to impurities. Single crystals grown from this saturated benzene solution showed the [N"(L^{M})Ce(μ-OAr$^{3,5\text{-tBu}}$)$_2$Ce(L^{M})N"] dimer, bridged by the aryloxide oxygen atoms, Figure 5. The crystals are only sparingly soluble in toluene, THF or dichloromethane and the ^{1}H NMR spectrum shows very broad paramagnetic resonances.

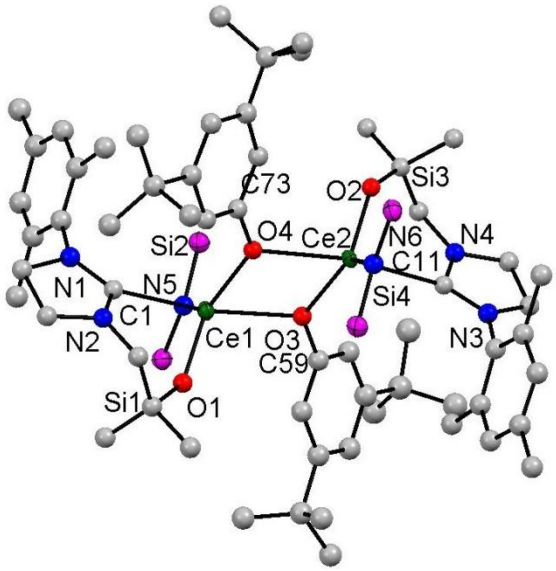

Figure 5 Connectivity of [N"(L^{M})Ce(μ-OAr$^{3,5\text{-tBu}}$)$_2$Ce(L^{M})N"] **24** displaying atom connectivity, H-atoms and the methyls of the bis(trimethylsilyl)amine groups omitted for clarity

The low quality of the X-ray crystallography data means that only the connectivity of **24** can be discussed.

Other examples of dimeric Ce^{III} complexes with bridging aryloxides are the $[Ce(OSiPh_3)_2(\mu\text{-}OSiPh_3)]_2$ **G** and analogous $[Ce(OCPh_3)_2(\mu\text{-}OCPh_3)]_2$ complex that were synthesized by Evans and coworkers, Eq. (8).[26]

$$2\ CeN"_3 + 6\ Ph_3SiOH \xrightarrow{\text{toluene}} [Ce(OSiPh_3)_2(\mu\text{-}OSiPh_3)]_2 + 6\ HN" \qquad (8)$$

$N" = N(SiMe_3)_2$ **G**

The dimeric triphenylmethoxide complex $[Ce(OCPh_3)_2(\mu\text{-}OCPh_3)]_2$ is only sparingly soluble in toluene, CH_2Cl_2 or THF and its dimeric structure is not broken up by coordinating solvents. But the dimeric triphenylsiloxide complex **G** readily dissolves to form the solvated $[Ce(OSiPh_3)_3(THF)_3]$ complex.

Another dimeric complex was synthesised by the facile reaction of dissolving $[Ce(TMP)_3(THF)]$ (TMP = 2,2,6,6-tetramethylpiperidine) in a Et_2O/hexanes (2/1), Eq. (9).[27] The likely byproducts Et(TMP) or H(TMP) were not isolated.

$$[Ce(TMP)_3(THF)] \xrightarrow{Et_2O,\ \text{hexanes}} {}^1/_2 \qquad (9)$$

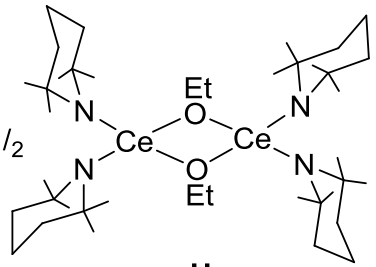

H

The $[Ce(OC^tBu_3)_2(O^tBu)]_2$ complex **I** was formed when using a slight deficiency of the $^tBuO\cdot$ radical, Scheme 4.[28] The dimer slowly crystallised out of solution at room temperature and it was found to be very difficult to redissolve. The paramagnetic broadening of the ^1H NMR spectrum precluded any meaningful analysis of it.

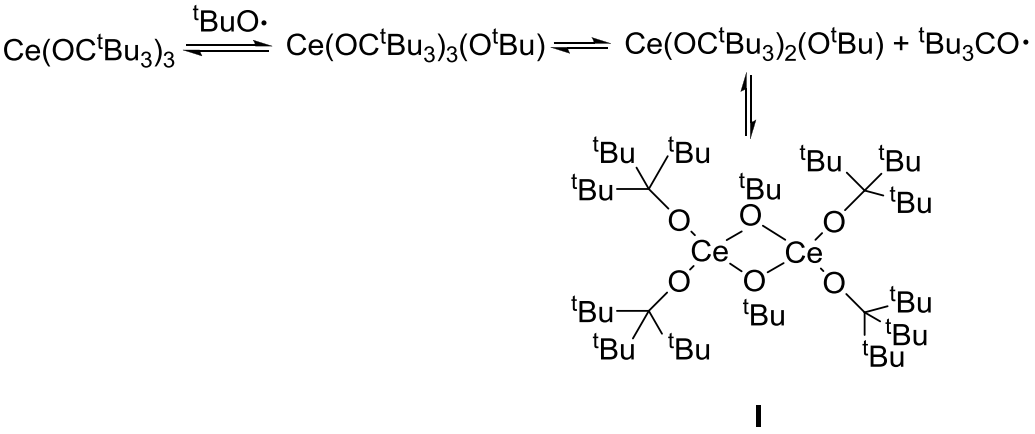

Scheme 4 Formation of $[Ce(OC^tBu_3)_2(O^tBu)]_2$

3.3 Attempted oxidation of Pr^{III} complexes

3.3.1 Synthesis of new Pr^{III}-NHC complexes [Pr(L^M)(N")$_2$] and [Pr(L^M)$_2$N"]

As previously mentioned the isolation of a tetravalent praseodymium compound is an interesting synthetic challenge. To achieve this $[Pr(N")_3]$ was synthesised according to literature procedures. This has lead to the isolation of the first molecular Pr^{III} N-heterocyclic carbene compounds which are analogous to the cerium compounds.

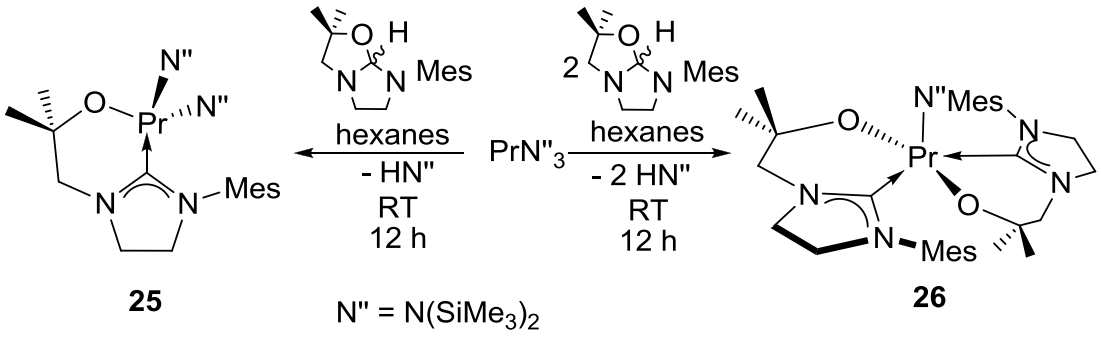

Scheme 5 Synthesis of $[Pr(L^M)N"_2]$ **25** and $[Pr(L^M)_2N"]$ **26** from $PrN"_3$

During the synthesis of the two praseodymium compounds **25** and **26** it became clear that the bis-ligand complex $[Pr(L^M)_2N"]$ **26** is the kinetically favoured product, to an even greater degree than the cerium compounds **1** and **2**. To form the mono-ligand

complex a solution of [HL^M] was slowly dropped into a solution of [$Pr(N'')_3$]. Immediately a small amount of bis-ligand product was observed to precipitate out of solution. This suspension was warmed to 80 ˚C with stirring for 4 hours and then the orange solution was extracted from the precipitated colourless solid. Removal of the volatiles under reduced pressure yielded the desired product **25** as an orange solid in a 59% yield. Consequently the yield of the mono-ligand [$Pr(L^M)N''_2$] complex **25** is not as high as the yield for the bis-ligand [$Pr(L^M)_2N''$] **26** synthesis.

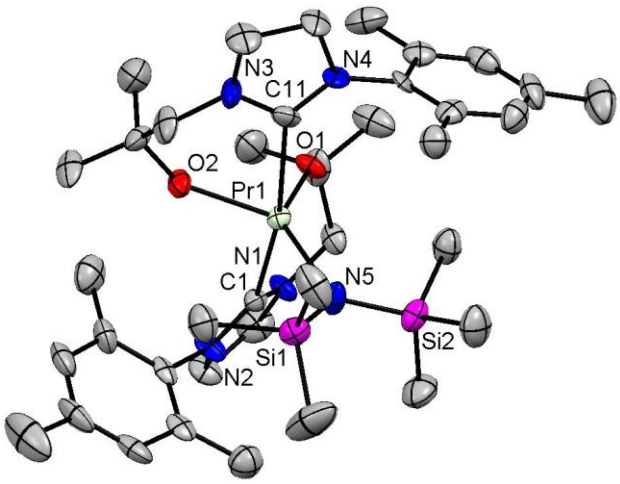

Figure 6 Displacement ellipsoid (50%) drawing of [$Pr(L^M)_2N''$] **26**, H atoms omitted for clarity

The praseodymium is surrounded in a distorted trigonal bipyramidal geometry. Selected bond distances (Å) and angles (˚) of **26** are displayed in Table 3.

Table 3 Selected bond distances (Å) and angles (˚) of **26**

Pr-C1	2.77(2)
Pr-C11	2.83(3)
Pr-N5	2.435(16)
N-C-N_{av}	106
C1-Pr-C11	167.5(3)
Pr-O1, Pr-O2	2.176(7), 2.154(6)

The vertical axis of the distorted trigonal bipyramid is the C1-Pr-C11 axis with an angle of 167.5(3)˚ and Pr-C1 and Pr-C11 bond distances of 2.77(2) Å and 2.83(3) Å. The metal is surrounded in the equatorial plane by O1, O2 and N5, with a Pr-O1 and Pr-

O2 distance of 2.176(7) Å and 2.154(6) Å respectively. The Pr-N5 is 2.435(16) Å. The average N-C-N angle of 106˚ is comparable with that of a metal bound imidazoline.

The structure of **26** is very similar to the cerium analogue **2**. The C1-Ce-C11 angle is almost identical at 167.55(10)˚. Similarly the Pr-C1 and Pr-C11 bond distances of 2.77(2) Å and 2.83(3) Å are very close to the Ce-C1 and Ce-C11 bond distances of 2.786(4) Å and 2.798(4) Å. The distance to the silylamide nitrogen N5 is 2.442(3) Å in **2** compared to 2.435(16) Å in **26**. The only difference between the two complexes is the M-O1, M-O2 bond distance of 2.172(3) Å and 2.184(3) Å in **2** compared to 2.176(7) Å and 2.154(6) Å in **26**.

No other praseodymium N-heterocyclic carbene complex could be found in the literature. The only comparable example of a praseodymium complex with a nucleophilic carbene ligand is $[Pr(C(PPh_2NSiMe_3)_2)(HC(PPh_2NSiMe_3)_2)]$ synthesised by the Liddle group, Eq. (10).[29]

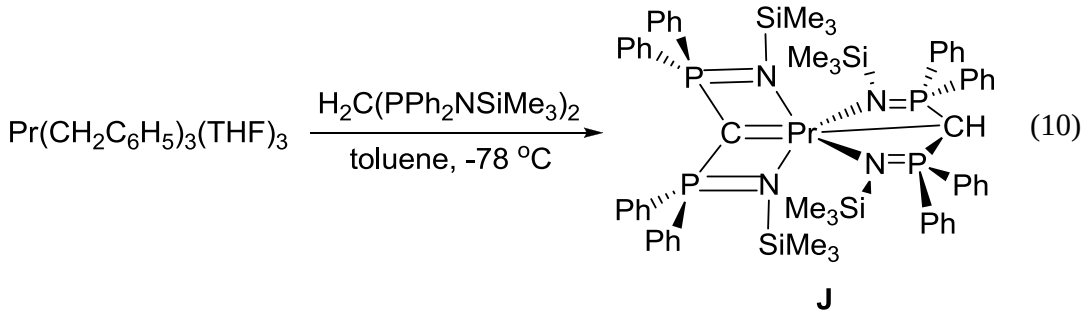

(10)

J

This compound **J** has a Pr-$C_{carbene}$ bond distance of 2.458(5) Å which is 0.3 Å shorter than the Pr-$C_{carbene}$ distance in **26**.

3.3.2 Attempted oxidation of Pr^{III}-NHC complexes

Many reagents were used in attempts to oxidise **25** and **26**, all resulted in the decomposition of the praseodymium compound. The reagents included AgX (X = CN, NO_3, BF_4, NO_2), Ag_2Y (Y = O, SO_4), $C_4H_4BrNO_2$ (N-bromosuccinimide), NO, Me_3SiCF_3, C_5H_5NO (pyridine-N-oxide), HgI_2, $PbCl_2$ and $CuCl_2$.

Cyclic voltammetry measurements were carried out to determine at what potential the electrochemical oxidation of the compound occurs. The electroanalysis carried out in THF showed no oxidation of the compound between a potential of -2 to 2 V at different scan rates. All experiments were conducted in dry THF with $[Bu_4N][BF_4]$

electrolyte (0.2 M) and complex (1.0 mmol L^{-1}) under an atmosphere of N_2 and referenced to ferrocene.

3.3.3 Synthesis of [Pr(OAr$^{2,6\text{-tBu}}$)$_3$]

Lanthanide aryloxides have been reported as valuable starting materials to synthesise neutral homoleptic carbyls, cyclopentadienyl and bis(trimethylsilyl)amine lanthanide complexes as described in chapter 2. [Pr(OAr$^{2,6\text{-tBu}}$)$_3$] was synthesised and its oxidation potential was measured. A solution of [Pr(N")$_3$] was treated with three equivalents of a solution of HOAr$^{2,6\text{-tBu}}$ in hexanes forming [Pr(OAr$^{2,6\text{-tBu}}$)$_3$] isolated as a yellow solid in a 66% yield, Eq. (11).

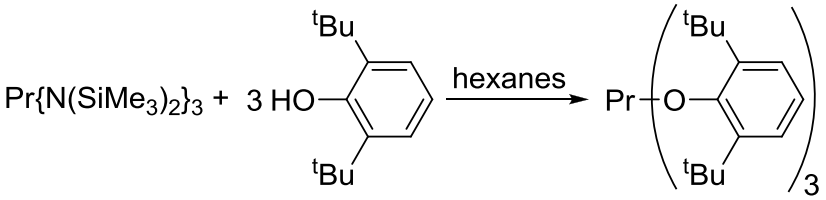

(11)

The [Pr(OAr$^{2,6\text{-tBu}}$)$_3$] complex was then treated with various oxidizing agents.

3.3.4 Attempted oxidation of [Pr(OAr$^{2,6\text{-tBu}}$)$_3$]

As with **25** and **26** numerous reagents were tried to oxidize [Pr(OAr$^{2,6\text{-tBu}}$)$_3$] and all resulted in the decomposition of the praseodymium compound, including AgX (X = BF_4, NO_2), Ag_2Y (Y = O, SO_4) and N-bromosuccinimide.

Cyclic voltammetry measurements were also carried out to determine at what potential the electrochemical oxidation of the compound occurs. The electroanalysis carried out in THF showed no oxidation of the compound between a potential of -2 to 2 V vs Fc^+/Fc at different scan rates. All experiments were conducted in dry THF with Bu_4NBF_4 electrolyte (0.2 M) and complex (1.0 mmol L^{-1}) under an atmosphere of N_2 and referenced to ferrocene.

3.4 Dinuclear/dimeric complexes of Ce and Pr and magnetic measurements

3.4.1 Synthesis of [Cl(N")Pr(μ-L^M)$_2$Pr(N")Cl]

As has been previously discussed [Ce(L^M)(N")$_2$] was found to be readily oxidised by tritylchloride. In light of this the analogous reaction with [Pr(L^M)(N")$_2$] was therefore attempted, Eq.(12).

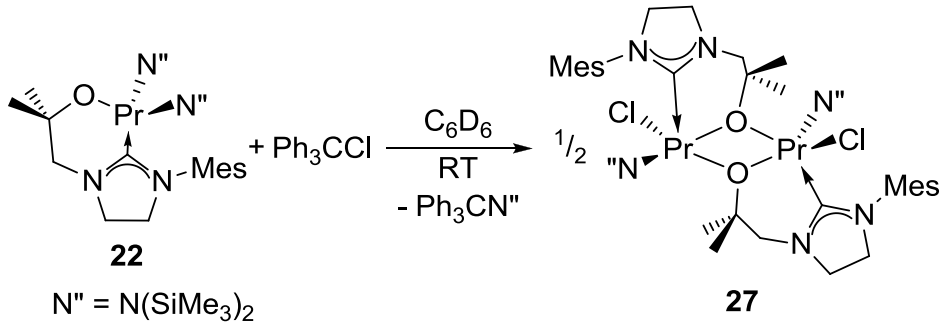

22

N" = N(SiMe$_3$)$_2$

27

(12)

Upon addition of one equivalent of tritylchloride in benzene to a solution of **25** in benzene the pale yellow solution immediately turned a dark, intensely violet colour. Despite the evident change in colour no evidence for the formation of Gomberg's dimer could be seen in the ^{1}H NMR spectrum. Purple crystals suitable for X-ray diffraction were grown from this saturated benzene solution. The product was not the expected [Pr(L^M)(Cl)N"$_2$] but the dimer [Cl(N")Pr(μ-L^M)$_2$Pr(N")Cl] **27.**

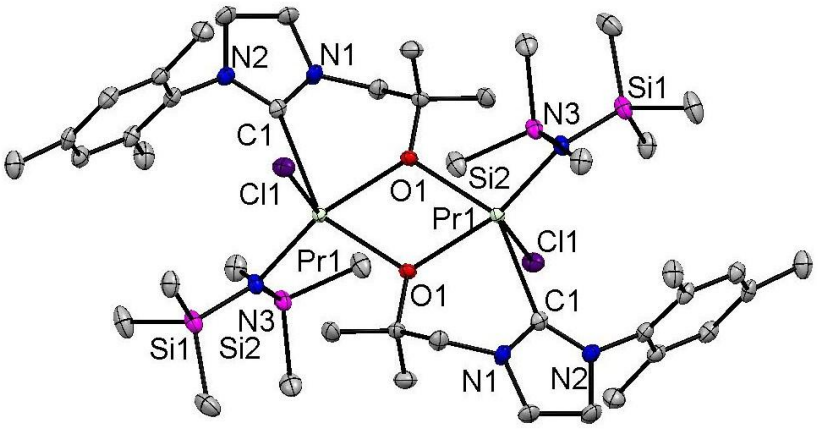

Figure 7 Displacement ellipsoid (50%) drawing of **27** [Cl(N")Pr(μ-L^M)$_2$Pr(N")Cl], H atoms omitted for clarity

The praseodymium cations in **27** are both five coordinate and in a distorted trigonal bipyramidal geometry. Selected bond distances (Å) and angles (˚) for **27** are displayed in Table 4.

Table 4 Selected distances (Å) and angles (˚) for **27** [Cl(N")Pr(μ-L^M)2Pr(N")Cl]

Pr-Pr	3.8886(2)
Pr-O	2.4065(14)
Pr-C	2.723(2)
Pr-Cl	2.6634(6)
Pr-O-Pr$_{av}$	109.94(5)

The praseodymium metal centres are each coordinated to one carbene carbon (C1) with a bond distance of 2.723(2) Å which is similar to the Ce-C bond of 2.792(4) in the bis-ligand complex **2**. The Pr-Cl bond distance is 2.6634 Å which is comparable to the average Ce-Cl bond distance of 2.737(3) Å in **20**. The Pr-O-Pr angle of 109.94(5)˚ is wider than the Ce-O-Ce angle of 94.08˚ in [(Cl)Ce(μ-L^M)$_3$Ce(Cl)$_2$] because only two oxygen atoms now need to be accommodated in between the metal centres.

Other Pr^{3+} compounds with bridging alkoxide groups are shown in Figure 8.[30–32] Compound **K** was synthesized by treating praseodymium nitrate with 2,6-diformyl-4-methylphenol in EtOH/MeCN and LiOH. Compound **L** was synthesized by treating a Schiff base ligand api^{3-} (H_3api = 2-(2-hydroxyphenyl)-1,3-bis[4-(2-hydroxyphenyl)-3-

azabut-3-enyl]-1,3-imidazolidine} with $Pr(NO_3)_3(H_2O)_6$. The other alkoxide bridged compound **M** was the only compound synthesised under anaerobic conditions. It was generated by combining [Pr(N")$_3$] with an excess of hexafluoro-2-methylisopropanol in benzene.

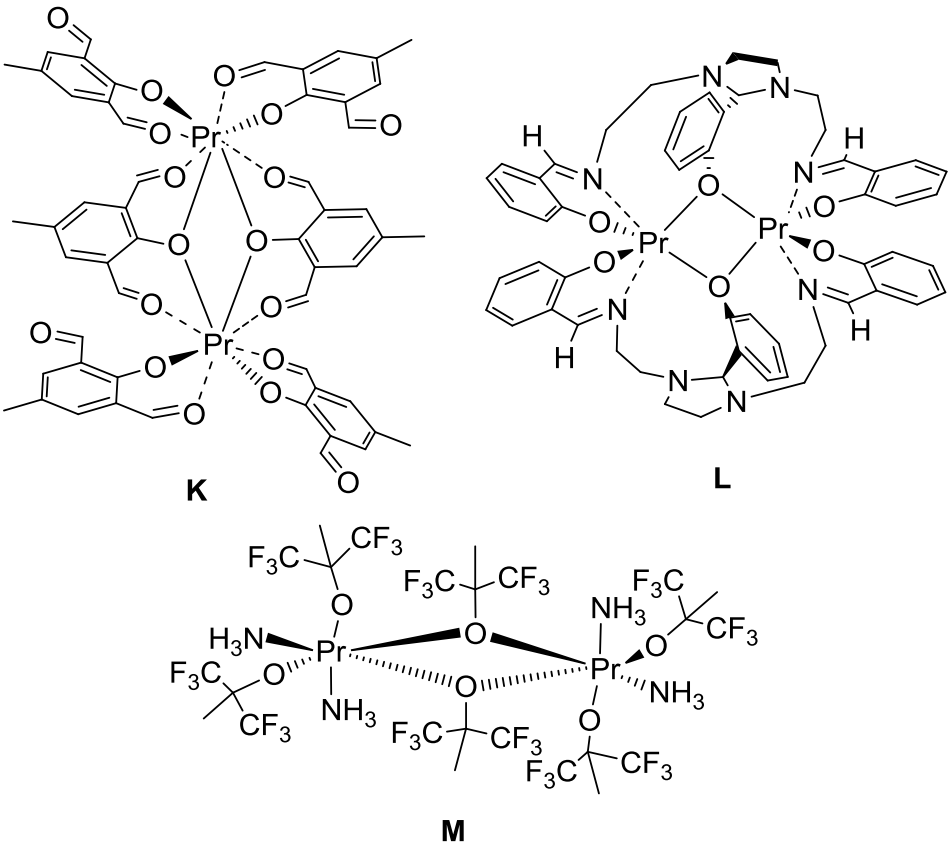

Figure 8 Pr^{3+} compounds with bridging alkoxides

Table 5 displays selected distances (Å) and angles (°) for alkoxide bridged Pr^{3+} compounds.

Table 5 Selected distances (Å) and angles (°) for alkoxide bridged Pr^{3+} compounds

	27	**K**	**L**	**M**
Pr-O	2.4065(14)	2.448(2), 2.481(2)	2.536(3), 2.418(4)	2.459, 2.505
Pr-Pr	3.8886(2)	4.071	3.96	4.001
Pr-O-Pr	109.94(5)	111.37(9)	109.35	107.4

It can be seen that **27** has the shortest Pr-O distance of 2.4065 Å and therefore the shortest Pr-Pr distance of 3.8886(2) Å.

3.4.2 Ln-Ln distances in literature (Ln = Ce, Pr)

A Table with the Ce-Ce distances (Å) found in literature complexes is shown below.

Table 6 Ce-Ce distances (Å) in literature compounds

Complex	Ce-Ce distance	Citation
$[\{Ce(N(SiMe_3)_2)_2(\mu\text{-}O)\}_2]$	3.320	[33]
$[Ce_2(O^iPr)_8(HO^iPr)_2]$	3.743	[34]
$Ce_2(OCMe_2{}^iPr)_5(acac)_3$	3.776	[18]
$[Ce(OCH^tBu_2)_3]_2$	3.815	[28]
$[\{C_5Me_5Ce(OCMe_3)_2\}_2]$	3.822	[35]
$[Ce(tpa)(\mu\text{-}OH)(MeCN)(H_2O)]_2{}^{4+}$	3.829(2)	[36]
$(Me_3C_5H_4)_4Ce_2(\mu\text{-}OCHMe_2)_2$	3.844	[37]
$[\{Ce(TMP)_2(\mu\text{-}OEt)\}_2]$	3.846	[27]
$[\{Ce(\eta\text{-}C_5H_3{}^tBu_2\text{-}1,3)_2(\mu\text{-}OMe)\}_2]$	3.887	[38]
$[Ce(OCMe_2{}^iPr)_4]_2$	3.895	[18]
$[Ce(OSi(C_6H_5)_3)_3]_2$	3.966	[26]
$Ce_2(O^iPr)_6(OC_2H_4NMeC_2H_4NMe_2)_2$	3.9837(7)	[39]
$[Ce(\mu\text{-}OCH{=}CH_2)(TMP)_2]_2$	4.034	[40]
$[Ce(\mu\text{-}DMP)(DMP)_2(THF)_2]_2$	4.078	[13]
20	3.5050(2)	this work

Comparing the Ce-Ce distance of 3.5050(2) Å of **19** with literature complexes, it is the second shortest reported Ce-Ce distance after $[\{Ce(N(SiMe_3)_2)_2(\mu\text{-}O)\}_2]$ that has a Ce-Ce distance of 3.320 Å. The other complexes range from 3.743 Å to 4.078 Å.

A table with the Pr-Pr distances (Å) found in literature complexes is shown below in Table 7.

Table 7 Pr-Pr distances (Å) in literature compounds

Complex	Pr-Pr distance	Citation
$[Pr_2\{OCMe(CF_3)_2\}_6(NH_3)_4]$	3.510	[30]
$[PrCp_2\{ON(C_2H_4\text{-}o\text{-}py)_2\}]$	3.804	[41]
$[\{Pr(en)_3\}_2(\mu\text{-}OH)_2][Sn_2Se_6]$	3.8927(6)	[42]
$[PrCp'_2(IBL)]_2$	3.925(1)	[43]
$[Pr(\mu\text{-}OPhC_4H_8N_2O)_2(NO_3)_4(H_2O)_4][NO_3]_2$	3.945	[44]
$[Pr(L^2)(NO_3)]_2\cdot HNO_3\cdot 3H_2O$	3.9485(4)	[45]
$[Pr(api)]_2$	3.949	[31]
$[Pr_2(hfacac)_4(bdmap)_2(H_2O)_2(THF)_2]$	3.951	[46]
$[LiPr(mmp)_3Cl]_2$	3.995	[47]
$[Pr(C_{13}H_8NO_2)_3]_2$	4.0024(4)	[48]
$[Pr_2(L1)_2(NO_3)(H_2O)]NO_3\cdot CH_3OH$	4.022	[49]
$[Pr(2,6\text{-diformyl-4-methylphenolato})_3]_2$	4.071	[32]
27	3.8886(2)	this work

Comparing the Pr-Pr distance of 3.8886(2) Å of **27** with literature complexes, it is the third shortest reported Pr-Pr distance after $[Pr_2\{OCMe(CF_3)_2\}_6(NH_3)_4]$ that has a Pr-Pr distance of 3.510 Å and $[PrCp_2\{ON(C_2H_4\text{-}o\text{-}py)_2\}]$ that has a Pr-Pr distance of 3.804 Å . The other complexes range from 3.892 Å to 4.071 Å.

Because of these short Ln-Ln distances the magnetic properties of **20**, **24**, and **27** were investigated.

3.4.3 Variable temperature magnetic measurements of complexes 20, 24 and 27

3.4.3.1 Background

The magnetic properties of the compounds described within this work will be discussed in units of the CGS-emu-system (**c**entimetre **g**ram **s**econd – **e**lectro**m**agnetic **u**nit). The machine used to measure the susceptibility of the compounds described is a magnetic flux detector, more specifically, a superconducting quantum interference device (SQUID).[50]

The magnetic behaviour of a compound can be deduced from the dependence of the molar magnetic susceptibility χ_M on temperature and the applied field.

Paramagnetism occurs if χ_M is dependent of the temperature and independent of the applied field (unless $\frac{B}{T}$ is extremely large, B = magnetic field, T = temperature). The permanent magnetic dipole in each atom or molecule orientate in an external magnetic field. Thermal randomisation of these permanent magnetic dipoles explains the temperature dependence of χ_M. The Curie law describes this relationship, with the Curie constant C, defined as

$$\chi_M = \frac{C}{T} \tag{13}$$

Antiferromagnetism occurs mainly at low temperatures and results in an antiparallel magnetic ordering of the dipoles. When the temperature rises this antiparallel alignment is increasingly interrupted and the susceptibility rises until the material specific Néel temperature T_N is reached, at which point the susceptibility decreases in a paramagnetic behaviour. Above T_N the susceptibility is described below, with Θ_N being the paramagnetic Néel temperature.

$$\chi_M = \frac{C}{T - \Theta_N} \tag{14}$$

Magnetic properties of the Ln^{3+} ions

The 4f electrons of free lanthanide ions are influenced by nuclear attraction, interelectronic repulsion and spin-orbit coupling. The Russell-Saunders term, also named LS coupling is described by $^{2S+1}L_J$ and determines the free ion ground multiplet. The electron configuration for Ce^{3+} is $[Xe]4f^1$ and the electron configuration for Pr^{3+} is $[Xe]4f^2$. Thus follows the free ion ground multiplet for Ce^{3+} is $^2F_{5/2}$ and that for Pr^{3+} is $^3H_4$. An example for an antiferromagnetic spin exchange of two Ce^{III} f^1 centres was shown with solid state magnetism measurements of the $[Ce_2(COT)_3]$ complex (COT = C_8H_8). The cerium centres are separated by about 4 Å and the $1/\chi$ vs T plot displays the expected uncorrelated spins at high temperatures of 300K, which changes at low

temperatures. At temperatures below 8K the value of χ increases with decreasing temperature until a maximum is reached and then declines with decreasing temperature which is indicative for antiferromagnetic spin coupling.[51]

3.4.3.2 Temperature dependent magnetic measurements of 20

Solid state magnetic studies were carried out on [(Cl)Ce(μ-L^M)$_3$CeCl$_2$] **20** (χ_{dia}= -2.42 × 10^{-4} emu mol^{-1}, m = 23 mg, M_W = 1164.69 g mol^{-1}) (χ_{dia} = diamagnetic contribution). The temperature dependence between 2 and 300K of the effective magnetic moment μ_{eff} and the inverse susceptibility 1/χ are shown in Figure 9. The magnetic susceptibility is independent of the strength of the applied magnetic field (1000 or 5000 Oe) and whether the sample was field or zero-field cooled.

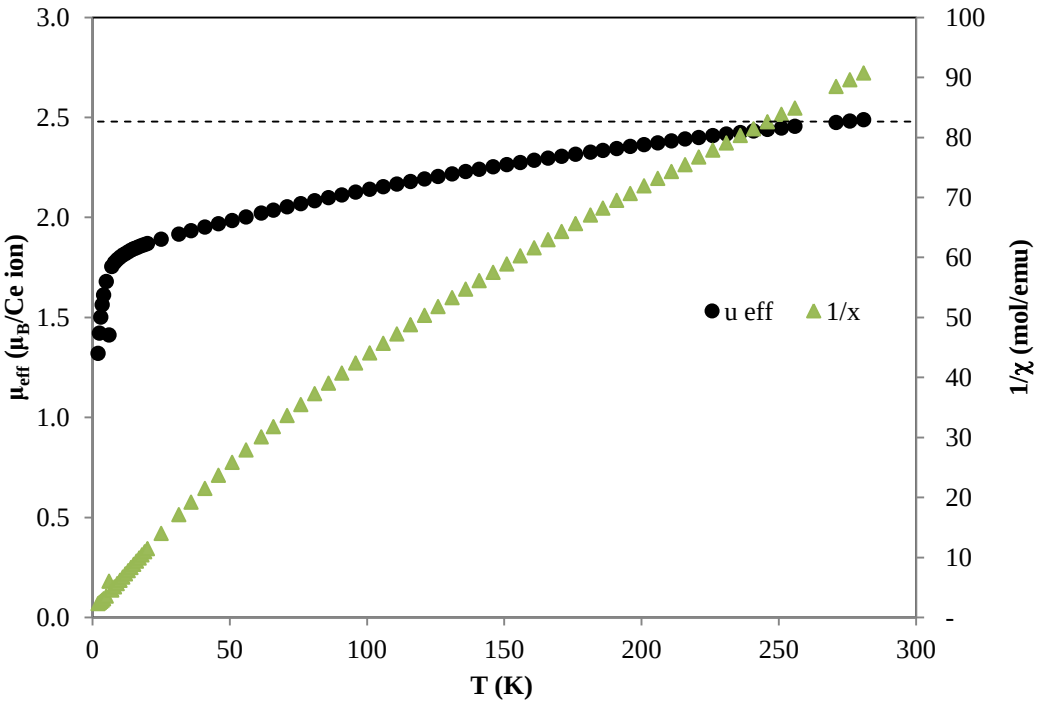

Figure 9 Temperature-dependent effective magnetic moment μeff of **20** in the range 2-300K measured at 5000 Oe with zero-field cooling and temperature-dependent inverse magnetic susceptibility 1/χ in the range of 2-300K measured at 5000 Oe with zero-field cooling

Approximate Curie-Weiss behaviour could only be observed in the high-temperature region from 300 to 150 K. Even at low temperatures of 2-10 K no antiferromagnetic interaction could be detected. These data show that the effective magnetic moment at room temperature is μ_{eff} = 2.48 μ_B/Ce ion and 1.32 μ_B/Ce ion at 5 K.

The temperature dependent magnetic susceptibility χ of **20** in the range 2-300K measured at 5000 Oe with zero-field cooling and χT vs T plot are shown in Figure 10. The χT vs T plot shows paramagnetic deviation and what is possibly an antiferromagnetic interaction below 10 K.

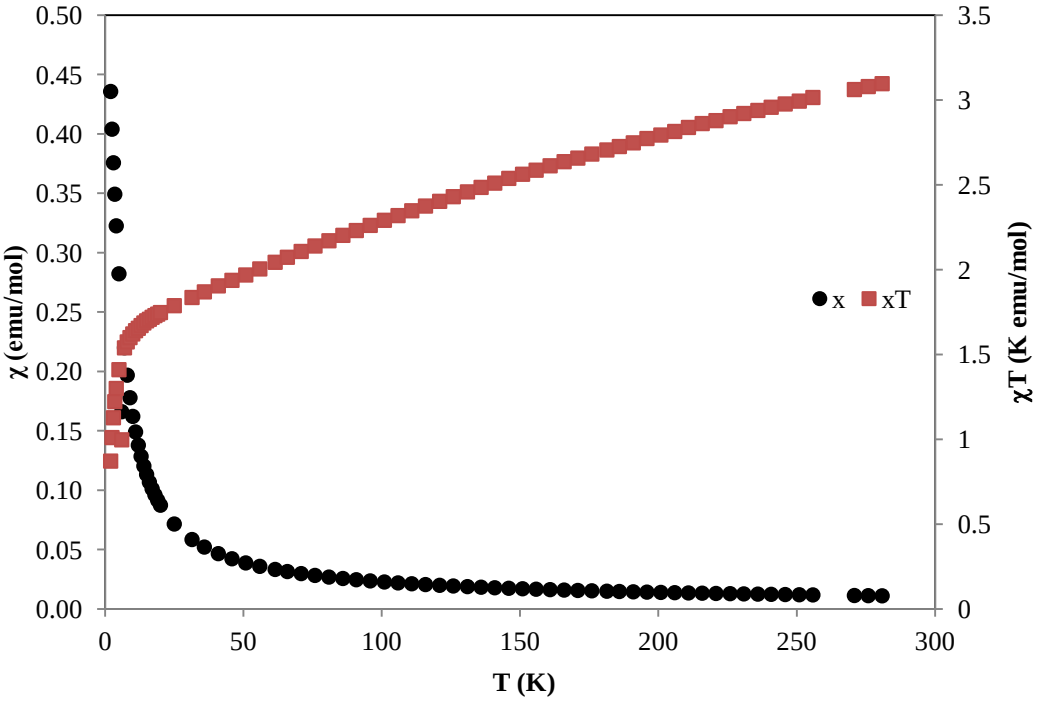

Figure 10 Temperature dependent magnetic susceptibility χ of **20** in the range 2-300K measured at 5000 Oe with zero-field cooling and χT vs T plot

3.4.3.2 Temperature dependent magnetic measurements of 24

Solid state magnetic studies were carried out on [N''(L^{M})Ce(μ-$OAr^{3,5\text{-}tBu}$)$_2$Ce(L^{M})N''] **24** (χ_{dia}= -4.08 × 10^{-4} emu mol^{-1}, m = 31.3 mg, M_W = 1192.22 g mol^{-1}). The temperature dependence between 2 and 300K of the effective magnetic moment μ_{eff} and the inverse susceptibility 1/χ are shown here in Figure 11. The magnetic behaviour is independent of the strength of the applied magnetic field (1000 or 5000 Oe).

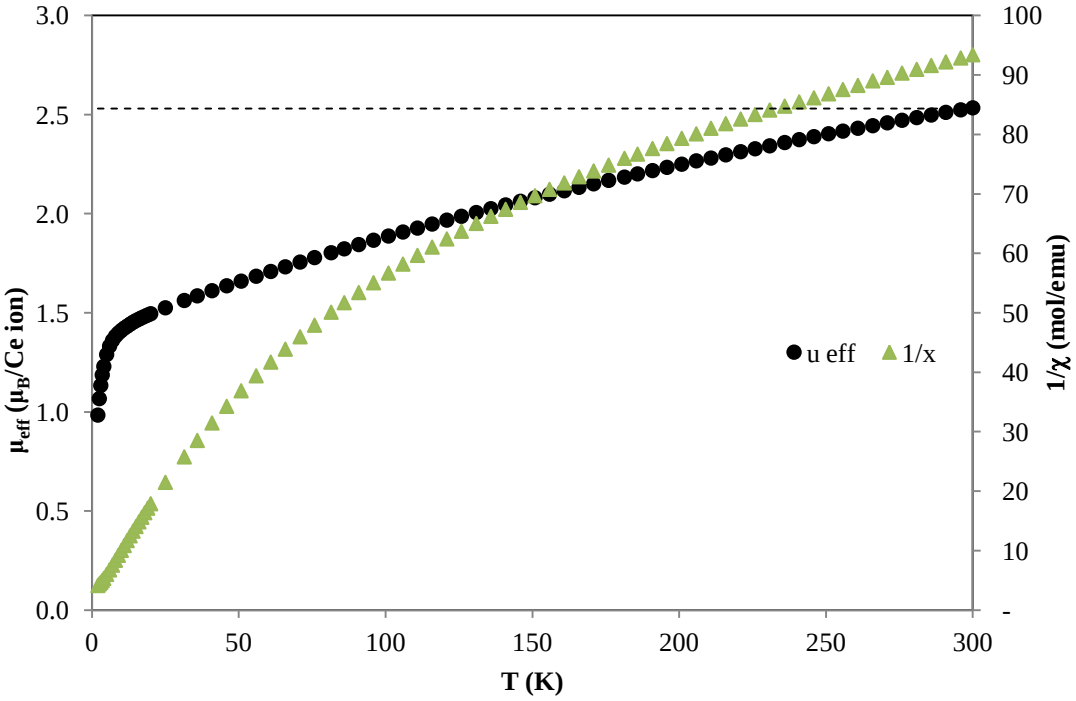

Figure 11 Temperature-dependent effective magnetic moment μeff of **24** in the range 2-300K measured at 5000 Oe with zero-field cooling and temperature-dependent inverse magnetic susceptibility 1/χ in the range of 2-300K measured at 5000 Oe with zero-field cooling

The inverse of the temperature-dependent magnetic susceptibility 1/χ in the range of 2-300 K measured at 5000 Oe with zero-field cooling is displayed in Figure 11. Approximate Curie-Weiss behaviour could only be observed in the high-temperature region from 300 to 150 K. Even at low temperatures of 2-10 K no antiferromagnetic interaction could be detected. These data show that the effective magnetic moment at room temperature is μ_{eff} = 2.53 μ_B/Ce ion and 0.98 μ_B/Ce ion at 5K.

The temperature dependent magnetic susceptibility χ of **24** in the range 2-300K measured at 5000 Oe with zero-field cooling and χT vs T plot are shown in Figure 12. The χT vs T plot shows typical paramagnetic deviation.

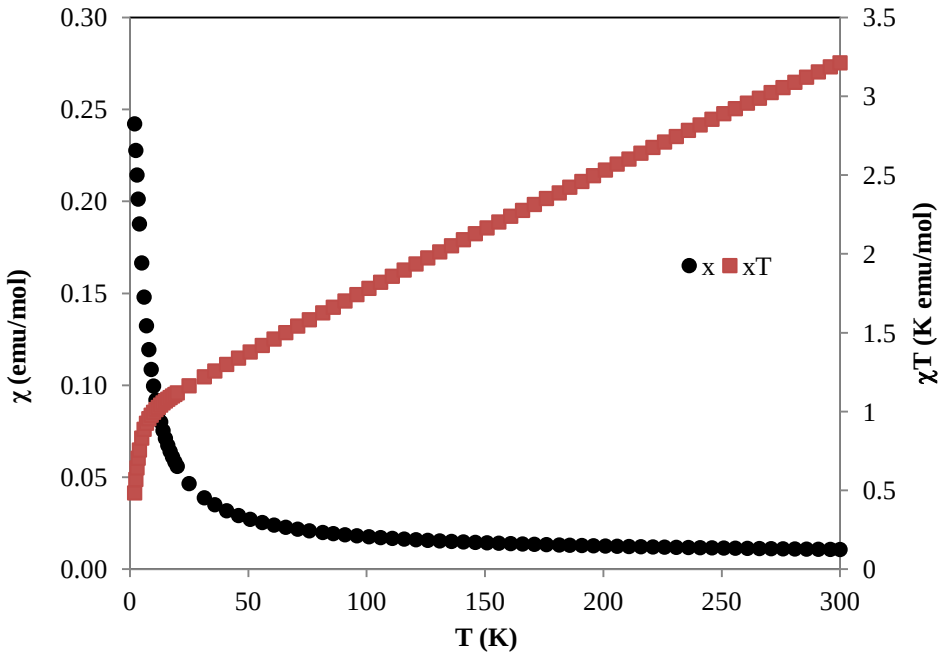

Figure 12 Temperature dependence of the magnetic susceptibility χ of **24** in the range 2-300K measured at 5000 Oe with zero-field cooling and χT vs T plot

3.4.3.3 Comparison to other paramagnetic cerium complexes

The paramagnetic behaviour of complex **20** and **24** can be compared to complex **N** reported in the literature.[35]

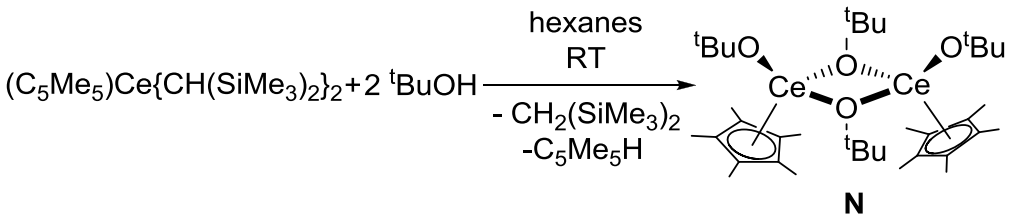

(15)

Compound **N** is readily soluble in aromatic solvents and ^{1}H NMR spectroscopy studies have been undertaken. Variable temperature studies (20 ˚C to 105 ˚C) showed a linear Curie-Weiss relation typical for a paramagnetic compound.

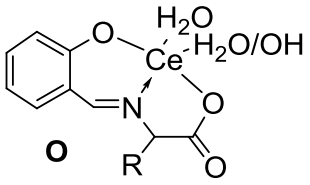

			μ_{eff} (BM)
O	**O¹** R = H	$[CeL'(H_2O)_2]NO_3$	1.87
	O² R = Me	$[CeL''(H_2O)_2]NO_3$	1.81
	O³ R = ^{i}Pr	$[CeL'''(OH)H_2O]$	1.66
	P¹	$Ce_2(IO_3)_6(O)$	0.26
	P²	$Ce_2(IO_3)_6(OH_{0.44})$	1.19
	Q	$[\{(H_6TrenSal)Ce\}_2\text{-}m^2\text{-}O_2]$	1.3

H_6TrenSal = tris-((2-hydroxybenzyl)-aminoethyl)amine

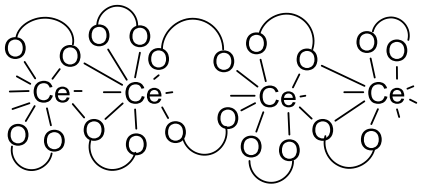

R¹ 2.33

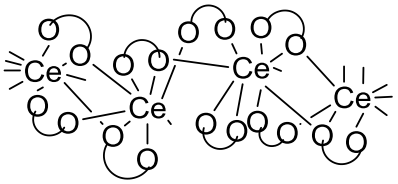

R² 2.35

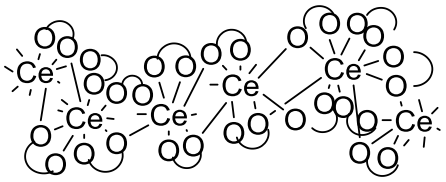

R³ 2.38

Figure 13 Effective magnetic moments of selected Ce^{III}, Ce^{IV} and mixed valence $Ce^{III/IV}$ compounds at room temperature

Effective magnetic moments of selected Ce^{III}, Ce^{IV} and mixed valence $Ce^{III/IV}$ compounds are displayed in Figure 13.[52–55] The magnetic moments for **20** and **24** have expected effective magnetic moments of 2.48 and 2.53 μ_B/Ce ion and are in good agreement with the reported Ce^{III} complexes **R¹**-**R³**.

3.4.3.4 Temperature dependent magnetic measurements of 27

Solid state magnetic studies were carried out on $[Cl(N'')Pr(\mu\text{-}L^M)_2Pr(N'')Cl]$ **27** (χ_{dia}= -4.08 × 10^{-4} emu mol^{-1}, m = 31.3 mg, M_W = 1192.22 g mol^{-1}). The temperature dependence between 2 and 300K of the effective magnetic moment μ_{eff} and the inverse susceptibility $1/\chi$ are shown in Figure 14. A plot of the magnetic susceptibility χ_M is also included. Magnetic behaviour is independent of the strength of the applied magnetic field (1000 or 5000 Oe) and whether the sample was field or zero-field cooled.

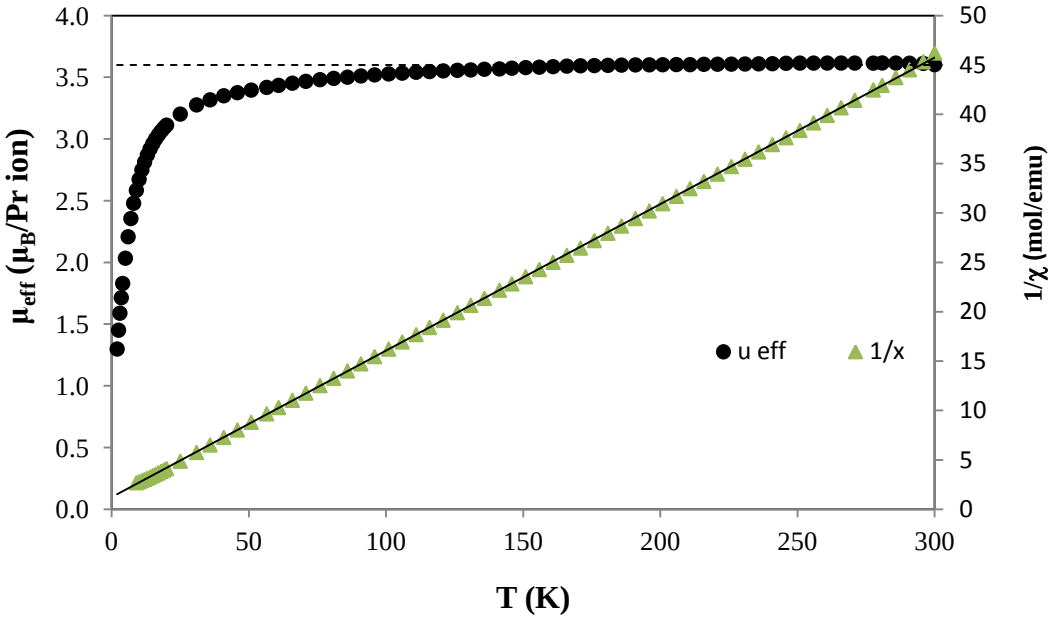

Figure 14 Temperature-dependent effective magnetic moment μ_{eff} of **27** in the range 2-300K measured at 5000 Oe with zero-field cooling and temperature-dependent inverse magnetic susceptibility $1/\chi$ in the range of 2-300K measured at 5000 Oe with zero-field cooling. The trendline in the plot is a fit of the high-temperature data to a Curie-Weiss function $1/\chi = (T-\Theta)/(8\mu_{eff}^2)$

The graph in Figure 14 shows the temperature dependence of the reciprocal magnetic susceptibility $1/\chi$ in the range of 2-300K measured at 5000 Oe with zero-field cooling. The linear fit of the high-temperature data to a Curie Weiss-function $1/\chi = (T-\Theta)/(8\mu_{eff}^2)$ gives us the Weiss constant Θ = -6.9K. The temperature-dependent effective magnetic moment μ_{eff} shows that the effective magnetic moment at room temperature is μ_{eff} = 3.6 μ_B/Pr ion and 1.3 μ_B/Pr ion at 5K.

The χT vs T plot shows typical paramagnetic deviation.

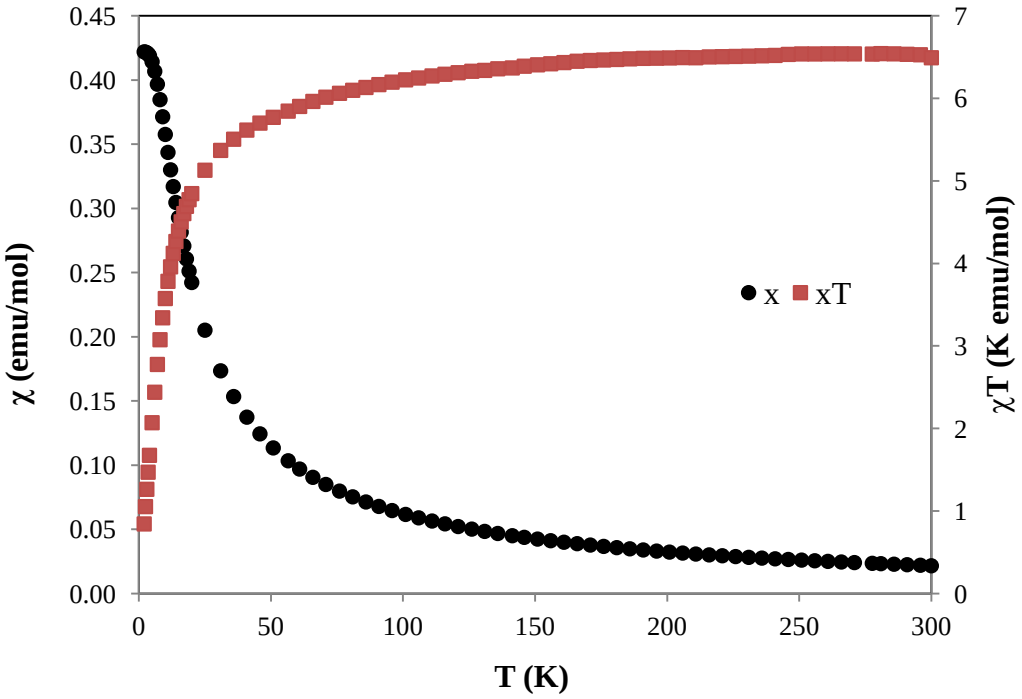

Figure 15 Temperature dependence of the magnetic susceptibility χ of **27** in the range 2-300K measured at 5000 Oe with zero-field cooling and χT vs T plot

3.5 Conclusions

The dinuclear cerium complex [ClCe(μ-L^M)$_3$CeCl$_2$] **20** was synthesised by treating [Ce(L^M)$_2$N''] **2** with Ph$_3$CCl.

Many attempts were made to oxidise [Ce(L^M)$_2$N''] **2**. Treatment with PbCl$_2$ and PhICl$_2$ suggested a reaction had occurred. However, not enough characterising data could be collected on the products, which are of more complex composition than anticipated, probably due to the incorporation of lead salts or amines.

If **1** is treated with HOAr$^{2,6\text{-tBu}}$ ligand exchange is observed whereas treatment of **1** with HOAr$^{3,5\text{-tBu}}$ yields the dimeric complex [N''(L^M)Ce(μ-OAr$^{3,5\text{-tBu}}$)$_2$Ce(L^M)N''] **24**.

The new praseodymium NHC complexes [Pr(L^M)(N'')$_2$] **25** and [Pr(L^M)$_2$N''] **26** and [Pr(OAr$^{2,6\text{-tBu}}$)$_3$] have been successfully synthesised. However, subsequent oxidation of these complexes was unsuccessful.

Treatment of [Pr(L^M)(N'')$_2$] **25** with Ph$_3$CCl gave the dimeric praseodymium complex [Cl(N'')Pr(μ-L^M)$_2$Pr(N'')Cl] **27**.

Solid-state temperature-dependent magnetic measurements of the complexes [ClCe(μ-L^M)$_3$CeCl$_2$] **20**, [N''(L^M)Ce(μ-OAr$^{3,5\text{-tBu}}$)$_2$Ce(L^M)N''] **24** and [Cl(N'')Pr(μ-

$L^M)_2Pr(N'')Cl]$ **27** showed no intermetallic antiferromagnetic interaction at temperatures as low as 2K.

3.6 References

1. I. J. Casely, S. T. Liddle, A. J. Blake, C. Wilson, and P. L. Arnold, *Chem. Commun.*, 2007, 5037.
2. V. Sridharan and J. C. Menéndez, *Chem. Rev.*, 2010, **110**, 3805–3849.
3. T.-L. Ho, *Synthesis*, 1978, **1978**, 936–936.
4. C. López-Cartes, S. Bernal, J. J. Calvino, M. A. Cauqui, G. Blanco, J. A. Pérez-Omil, J. M. Pintado, S. Helveg, and P. L. Hansen, *Chem. Commun.*, 2003, 644–645.
5. P. L. Arnold, Z. R. Turner, N. Kaltsoyannis, P. Pelekanaki, R. M. Bellabarba, and R. P. Tooze, *Chem.-Eur. J.*, 2010, **16**, 9623–9629.
6. H. C. Aspinall, J. Bacsa, A. C. Jones, J. S. Wrench, K. Black, P. R. Chalker, P. J. King, P. Marshall, M. Werner, H. O. Davies, and R. Odedra, *Inorg. Chem.*, 2011, **50**, 11644–11652.
7. C. Sirio, L. G. Hubert-Pfalzgraf, and C. Bois, *Polyhedron*, 1997, **16**, 1129–1136.
8. Y. K. Gun'ko, S. D. Elliott, P. B. Hitchcock, and M. F. Lappert, *J. Chem. Soc. Dalton*, 2002, 1852–1856.
9. V. Mereacre, A. Ako, M. Akhtar, A. Lindemann, C. E. Anson, and A. K. Powell, *Helv. Chim. Acta*, 2009, **92**, 2507–2524.
10. P. L. Arnold, I. J. Casely, S. Zlatogorsky, and C. Wilson, *Helv. Chim. Acta*, 2009, **92**, 2291–2303.
11. K. Yunlu, P. S. Gradeff, N. Edelstein, W. Kot, G. Shalimoff, W. E. Streib, B. A. Vaartstra, and K. G. Caulton, *Inorg. Chem.*, 1991, **30**, 2317–2321.
12. U. Baisch, *J. Mol. Catal. A-Chem.*, 2003, **204-205**, 259–265.
13. T. J. Boyle, L. J. Tribby, and S. D. Bunge, *Eur. J. Inorg. Chem.*, 2006, **2006**, 4553–4563.
14. M. Kritikos, M. Moustiakimov, and G. Westin, *Inorg. Chim. Acta*, 2012, **384**, 125–132.
15. A. Bilyk, J. W. Dunlop, R. O. Fuller, A. K. Hall, J. M. Harrowfield, M. W. Hosseini, G. A. Koutsantonis, I. W. Murray, B. W. Skelton, A. N. Sobolev, R. L. Stamps, and A. H. White, *Eur. J. Inorg. Chem.*, 2010, **2010**, 2127–2152.
16. Y. K. Gun'ko, S. D. Elliott, P. B. Hitchcock, and M. F. Lappert, *J. Chem. Soc. Dalton*, 2002, 1852–1856.
17. H. C. Aspinall, J. Bacsa, A. C. Jones, J. S. Wrench, K. Black, P. R. Chalker, P. J. King, P. Marshall, M. Werner, H. O. Davies, and R. Odedra, *Inorg. Chem.*, 2011, **50**, 11644–11652.
18. S. Suh, J. Guan, L. A. Mîinea, J.-S. M. Lehn, and D. M. Hoffman, *Chem. Mater.*, 2004, **16**, 1667–1673.
19. P. L. Arnold, I. J. Casely, S. Zlatogorsky, and C. Wilson, *Helv. Chim. Acta*, 2009, **92**, 2291–2303.
20. J. C. Barnes, C. S. Blyth, and D. Knowles, *Inorg. Chim. Acta*, 1987, **126**, L3–L6.
21. J. C. Barnes and C. S. Blyth, *Inorg. Chim. Acta*, 1985, **110**, 133–137.
22. G.-C. Wang, H. H. Y. Sung, I. D. Williams, and W.-H. Leung, *Inorg. Chem.*, 2012, **51**, 3640–3647.
23. R. E. Bailey and R. West, *J. Organomet. Chem.*, 1965, **4**, 430–439.
24. J. Ru Hwu and N. Wang, *Tetrahedron*, 1988, **44**, 4181–4196.
25. C. Erk, A. Berger, J. H. Wendorff, and S. Schlecht, *Dalton Trans.*, 2010, **39**, 11248.
26. W. J. Evans, R. E. Golden, and J. W. Ziller, *Inorg. Chem.*, 1991, **30**, 4963–4968.

27. P. B. Hitchcock, Q.-G. Huang, M. F. Lappert, and X.-H. Wei, *J. Mater. Chem.*, 2004, **14**, 3266.
28. H. A. Stecher, A. Sen, and A. L. Rheingold, *Inorg. Chem.*, 1989, **28**, 3280–3282.
29. A. J. Wooles, D. P. Mills, W. Lewis, A. J. Blake, and S. T. Liddle, *Dalton Trans.*, 2009, **39**, 500–510.
30. D. C. Bradley, H. Chudzynska, M. E. Hammond, M. B. Hursthouse, M. Motevalli, and W. Ruowen, *Polyhedron*, 1992, **11**, 375–379.
31. J. Chakraborty, S. Thakurta, G. Pilet, R. F. Ziessel, L. J. Charbonnière, and S. Mitra, *Eur. J. Inorg. Chem.*, 2009, **2009**, 3993–4000.
32. R. Gheorghe, V. Kravtsov, Y. A. Simonov, J.-P. Costes, Y. Journaux, and M. Andruh, *Inorg. Chim. Acta*, 2004, **357**, 1613–1618.
33. M. P. Coles, P. B. Hitchcock, A. V. Khvostov, M. F. Lappert, Z. Li, and A. V. Protchenko, *Dalton Trans.*, 2010, **39**, 6780.
34. P. Toledano, F. Ribot, and C. Sanchez, *Acta Crystallogr. C*, 1990, **46**, 1419–1422.
35. H. J. Heeres, J. H. Teuben, and R. D. Rogers, *J. Organomet. Chem.*, 1989, **364**, 87–96.
36. L. S. Natrajan, J. Pécaut, M. Mazzanti, and C. LeBrun, *Inorg. Chem.*, 2005, **44**, 4756–4765.
37. S. D. Stults, R. A. Andersen, and A. Zalkin, *Organometallics*, 1990, **9**, 1623–1629.
38. Y. K. Gun'ko, P. B. Hitchcock, and M. F. Lappert, *J. Organomet. Chem.*, 1995, **499**, 213–219.
39. L. G. Hubert-Pfalzgraf, N. El Khokh, and J.-C. Daran, *Polyhedron*, 1992, **11**, 59–63.
40. S. D. Daniel, J.-S. M. Lehn, J. D. Korp, and D. M. Hoffman, *Polyhedron*, 2006, **25**, 205–210.
41. B. J. Hellmann, A. Venugopal, A. Mix, B. Neumann, H.-G. Stammler, A. Willner, T. Pape, A. Hepp, and N. W. Mitzel, *Chem.-Eur. J.*, 2009, **15**, 11701–11709.
42. J. Liang, J. Chen, J. Zhao, Y. Pan, Y. Zhang, and D. Jia, *J. Chem. Soc. Dalton*, 2011, **40**, 2631.
43. A. Steudel, J. Stehr, E. Siebel, and R. D. Fischer, *J. Organomet. Chem.*, 1998, **570**, 89–96.
44. W. Po-Wan Lai, W.-T. Wong, B. King-Fai Li, and K.-W. Cheah, *New J. Chem.*, 2002, **26**, 576–581.
45. M. K. Thompson, A. J. Lough, A. J. P. White, D. J. Williams, and I. A. Kahwa, *Inorg. Chem.*, 2003, **42**, 4828–4841.
46. S. Wang, Z. Pang, K. D. L. Smith, Y. Hua, C. Deslippe, and M. J. Wagner, *Inorg. Chem.*, 1995, **34**, 908–917.
47. H. C. Aspinall, J. Gaskell, P. A. Williams, A. C. Jones, P. R. Chalker, P. A. Marshall, J. F. Bickley, L. M. Smith, and G. W. Critchlow, *Chem. Vapor. Depos.*, 2003, **9**, 235–238.
48. M. A. Katkova, A. P. Pushkarev, T. V. Balashova, A. N. Konev, G. K. Fukin, S. Y. Ketkov, and M. N. Bochkarev, *J. Mater. Chem.*, 2011, **21**, 16611.
49. I. A. Setyawati, S. Liu, S. J. Rettig, and C. Orvig, *Inorg. Chem.*, 2000, **39**, 496–507.
50. R. L. Fagaly, *Rev. Sci. Instrum.*, 2006, **77**, 101101.
51. M. D. Walter, C. H. Booth, W. W. Lukens, and R. A. Andersen, *Organometallics*, 2009, **28**, 698–707.
52. A. Mustapha, J. Reglinski, and A. R. Kennedy, *Inorg. Chim. Acta*, 2009, **362**, 1267–1274.
53. R. E. Sykora, L. Deakin, A. Mar, S. Skanthakumar, L. Soderholm, and T. E. Albrecht-Schmitt, *Chem. Mater.*, 2004, **16**, 1343–1349.
54. I. L. Malaestean, M. Kutluca-Alıcı, A. Ellern, J. van Leusen, H. Schilder, M. Speldrich, S. G. Baca, and P. Kögerler, *Cryst. Growth Des.*, 2012, **12**, 1593–1602.

55. P. Gürkan and N. Sari, *Syn. React. Inorg. Met.*, 1999, **29**, 753–765.

Chapter 4 Oxo-group functionalisation of the uranyl dication

4.1 Background

The highly soluble uranyl dication $[UO_2]^{2+}$ is a thermodynamically very stable species that is particularly inert to oxo-group functionalisation due to its strongly covalent U-O bonds and linear O≡U≡O geometry.[1,2] Other ligands that coordinate to the uranium metal centre are directed in the equatorial plane perpendicular to the linear O≡U≡O unit and are much more labile. Reduction of the uranyl cation UO_2^{2+} to U^{IV} in aqueous conditions is a strategy for the immobilisation of uranium in ground water as U^{IV} forms sparingly soluble minerals.[3–6] The reduction from $[U^{VI}O_2]^{2+}$ to $[U^{V}O_2]^{+}$ has been reported in literature and is a likely intermediate in this stepwise reduction.[7–13] $[UO_2]^{+}$ is difficult to isolate because of its aqueous instability and susceptibility to disproportionation, Eq. (1).

$$2\,[UO_2]^{+} + 4H^{+} \longrightarrow U^{4+} + [UO_2]^{2+} + 2\,H_2O \qquad (1)$$

Only a few examples of functionalised oxo-groups of the $[UO_2]^{2+}$ ion have been reported. Sarsfield and co-workers reported the synthesis of $[UO_2(NCN)_2(THF)]$ (NCN = $PhC(NSiMe_3)_2$) that can be treated with one equivalent of $B(C_6F_5)$ to form the $[UO_2(NCN)_2\{B(C_6F_5)_3\}]$ complex.[14] Hayton and co-workers also demonstrated that the reduction of a $[Cp^*_2Co]_2[U^{V}\{OB(C_6F_5)_3\}_2(^{Ar}acnac)_2]$ ($(^{Ar}acnac)$ = ArNC(Ph)CHC(Ph)O and Ar = 3,5-$^{t}Bu_2C_6H_3$) $[UO_2^{+}]$ complex with AgOTf to the U^{IV} species $[Cp^*_2Co][U^{IV}\{OB(C_6F_5)_3\}_2(^{Ar}acnac)_2]$ is possible without breaking the U-O bond.

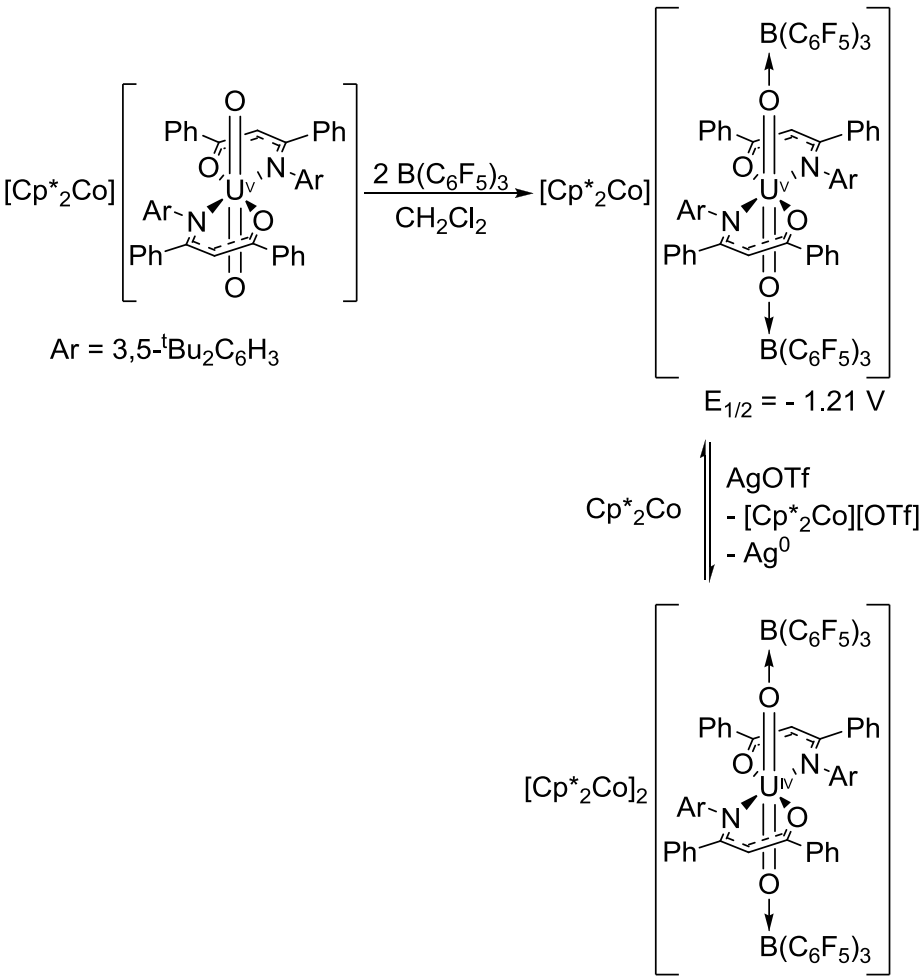

Scheme 1 Reduction of UO_2^+ to U^{IV} as shown by Hayton[15]

Further, Hayton and co-workers have shown that it is possible to functionalise the oxo-groups of the uranyl by oxo ligand silylation, reacting $[UO_2(^{Ar}acnac)_2]$ with an excess of Me_3SiI to form $[U(OSiMe_3)_2(^{Ar}acnac)I_2]$, Eq. (2).[16]

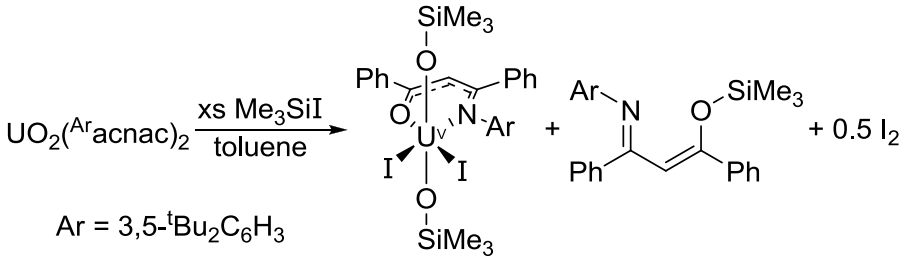

(2)

Uranyl oxo functionalisation with Lewis acids has only been observed in a few examples and only in the presence of an environment that amplifies the Lewis basicity of

the uranyl oxos. Examples of Lewis acid functionalised uranyl complexes include the uranyl benzaminato complex $[Na(THF)UO_2(NCN)_2]_2(\mu_2\text{-}O)$ (NCN = $PhC(NSiMe_3)_2$ **A** that shows coordination of a Na cation to the uranyl oxo group, Figure 1. Evidence of oxo-functionalisation is shown by the U=O bond stretch of ν = 757 cm^{-1}, which is elongated with respect to unfunctionalised uranyl (VI), ν = 912 cm^{-1}.[17]

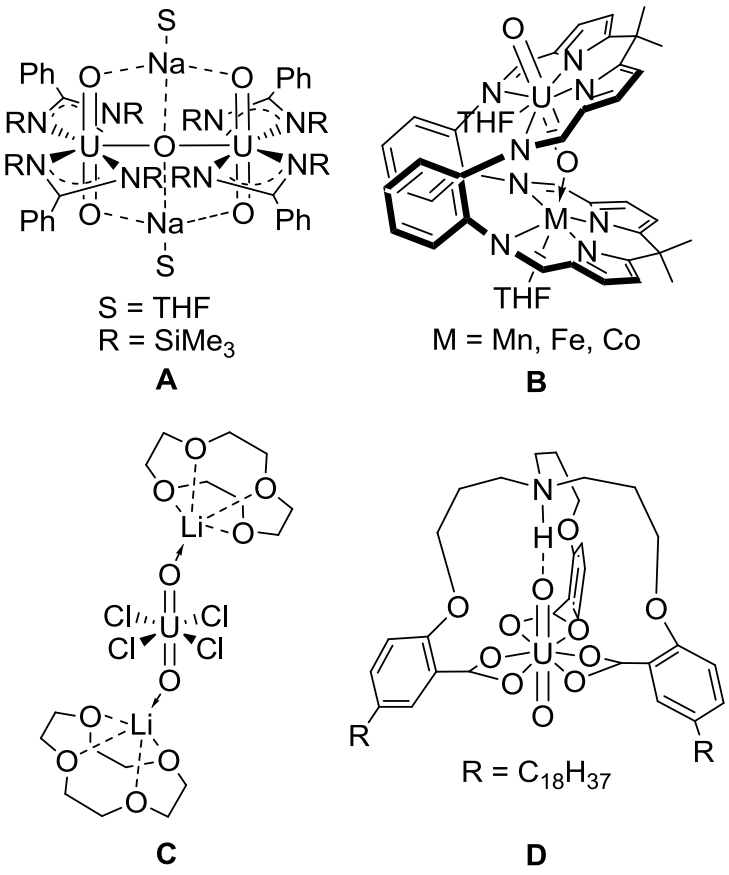

Figure 1 oxo functionalised uranyl complexes

The uranyl complex **B** contains a so called 'Pacman' ligand, which is a Schiff base macrocycle with a single uranyl dication in the upper pocket.[18] The lower pocket contains a 3d transition metal (Mn, Fe, Co) that shows interaction with the oxo group pointing towards the metal. Recently it was shown that addition of a lithium base to the unfunctionalised $[UO_2(H_2L)(THF)]$ complex, yields the oxo-lithiated hexavalent uranyl complex [UOU(THF){Li(THF)}(HL)] with lithium bound in the lower pocket to one imine-pyrrolide group.[11] The lithium 12-crown-4 ether uranyl chloride sandwich-type complex **C** $[Li(12\text{-crown-}4)]_2[UO_2Cl_4]$ was synthesised along with other alkali metal crown ether uranyl halide complexes from uranyl acetate dihydrate, the appropriate

alkali metal uranyl, the appropriate crown ether and halogenic acid.[19] Hydrogen bond donor interactions with oxo groups have been demonstrated by Raymond and co-workers in the $[UO_2(HNPOD)]$ complex **D** (NPOD = tris[3-(2-carboxy-4-octadecylphenoxy)propyl]amine).[20] Berthet and co-workers showed that it is possible to reduce $[UO_2I_2(THF)_3]$ or $[UO_2(OTf)_2]$ in acetonitrile by treating it with an excess of Me_3SiX (X = Cl, Br, I) to obtain the tetrahalide complexes $[UX_4(MeCN)_4]$.[21] Hayton and co-workers reported the functionalistation of $[UO_2]^{2+}$ to the U^V complex $[U(OSiMe_3)_2(I)_4][IPPh_3]$ **F** by treatment of the U^{VI} complex with Me_3SiI that will be discussed in section 4.2.2.[22]

Thus only a limited range of reagents has been used to date to either functionalise or completely abstract the uranyl oxo group, leading us to investigate the reactivity of $[UO_2(L^M)_2]$ towards small molecules such as Me_3SiX (X = I, N_3), H_2, CO, Ph_3CCl, 9-Iodo-9-borabicyclo[3.3.1]nonane (I-BBN), LiI and $LiSiPh_3$ in order to functionalise the U=O bond.

4.2 $[UO_2(L^M)_2]$ functionalisation

4.2.1 Synthesis of $[UO_2(L^M)_2]$

The uranyl NHC complex $[UO_2(L^M)_2]$ **28** was previously synthesised by the Arnold group on a small scale by layering a benzene solution of $[UO_2N"_2(THF)_2]$ onto a benzene solution of $[HL^M]$.[23] The scale up was successfully carried out by adding a colourless toluene solution of $[HL^M]$ dropwise to an orange solution of $[UO_2N"_2(py)_2]$ in toluene. Upon addition the solution turned dark brown and a bright yellow precipitate started to form immediately. The mixture was allowed to cool to room temperature with stirring over 12 hours. The resulting bright yellow solid was isolated by filtration and washed with hexanes. Removal of the volatiles under reduced pressure afforded **28** in a 75% yield.

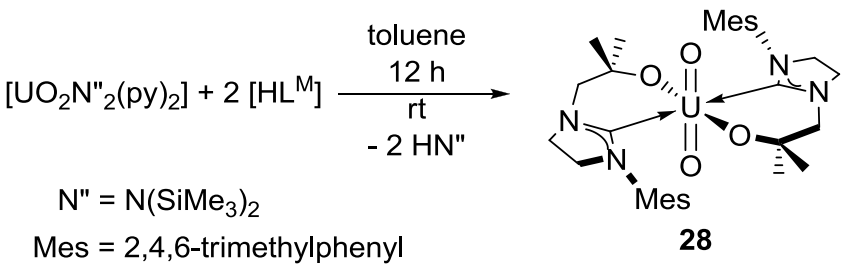

N" = $N(SiMe_3)_2$
Mes = 2,4,6-trimethylphenyl

28

(3)

An alternate route has now been devised to synthesise **28**. A suspension of $[UO_2Cl_2(THF)_2]$ in benzene is treated with half an equivalent of a solution of $[Li(L^M)]_4$ in benzene at room temperature to yield 60% of **28**, Eq.(4).

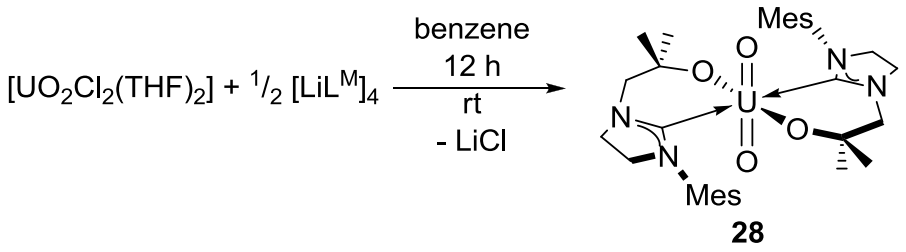

(4)

4.2.2 $[UI_4(L^MH)_2]$

When **25** was treated with I-BBN (9-Iodo-9-borabicyclo[3.3.1]nonane solution) in an NMR reaction in benzene, the formation of a new product was observed in the ^1H NMR spectrum. This product is poorly soluble and precipitates out of solution within minutes of formation.

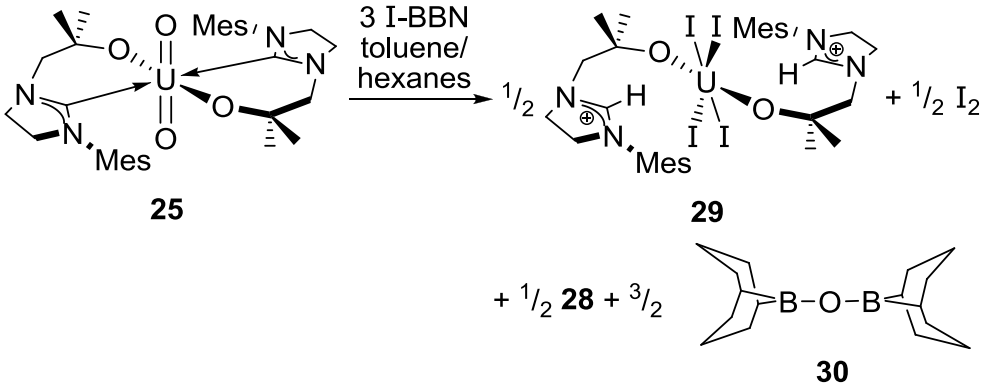

(5)

In an attempt to crystallize the product by slow diffusion, a yellow toluene solution of $[UO_2(L^M)_2]$ was carefully layered with three equivalents of a purple 1M hexanes solution of I-BBN in a YT-NMR tube, Eq. (5). After 12 h some of the starting material **28** had also precipitated out of the solution, and at the interface of the two phases a brown solid had formed. The mixture was sonicated for 20 minutes to afford a brown solid and an orange solution, the former of which was isolated by filtration and

recrystallised from a pyridine solution with hexane layering. This afforded crystals suitable for X-ray crystallography in a 15% yield, Figure 2.

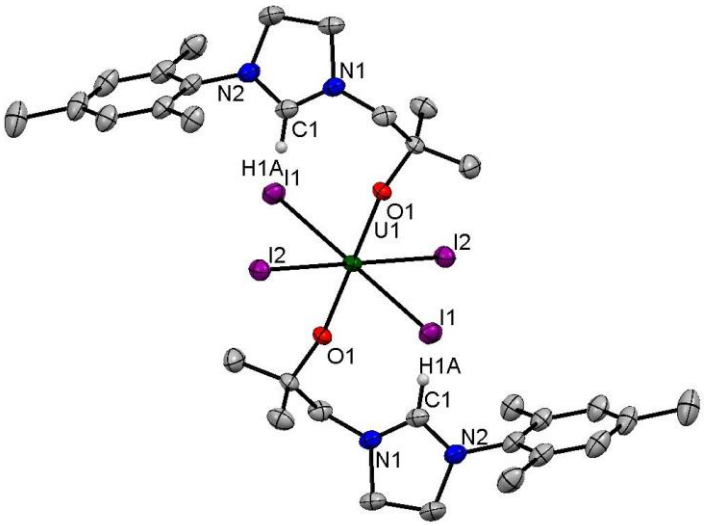

Figure 2 Displacement ellipsoid (50%) drawing of **29** $[UI_4(L^MH)_2]$, all H atoms except H1A and one pyridine solvent molecule are omitted for clarity

The solid state structure of **29** shows a six coordinate uranium centre in an octahedral geometry with four iodide atoms in the equatorial plane perpendicular to two axial oxygen atoms in a *trans*-(L^MH) geometry. Selected bond distances (Å) and angles (˚) for **29** are displayed in Table 1.

Table 1 Selected bond distances (Å) and angles (˚) for **29** $[UI_4(L^MH)_2]$

U1-O1	2.055(2)
U1-I1	3.1153(2)
U1-I2	3.1163(2)
C1-N1	1.299(4)
C1-N2	1.316(4)
N1-C1-N2	113.6(3)
O1-U1-I1	89.56(6)
O1-U1-I2	90.69(6)
I1-U1-I2	90.248(6)

The U1-O1 distance is 2.055(2) Å and the U1-I1 and U1-I2 distances are 3.1153(2) Å and 3.1163(2) Å respectively. The C1-N1 and C1-N2 bond distances of 1.299(4) Å and 1.316(4) Å and the N1-C1-N2 angle of 113.6(3)˚ are consistent with the formation of an imidazolinium and comparable to the imidazolinium complex **$[H_2L^D]Cl$**, Figure 3.[23]

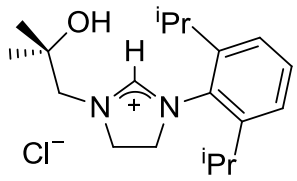

$[H_2L^D]Cl$

Figure 3 Imidazolinium complex $[H_2L^D]Cl$

The selected bond distances (Å) and angles (˚) for **29** and $[H_2L^D]Cl$ are displayed in Table 2.

Table 2 Selected bond distances (Å) and angles (˚) for **29** and $[H_2L^D]Cl$

	29	**$[H_2L^D]Cl$**
C1-N1	1.299(4)	1.305(3)
C1-N2	1.316(4)	1.317(3)
N1-C1-N2	113.6(3)	113.7(2)

The C1-N1 and C1-N2 bond distances of **$[H_2L^D]Cl$** are 1.305(3) Å and 1.317(3) Å respectively and the N1-C1-N2 angle is 113.7(2)˚, confirming that the NHCs in $[UI_4(L^MH)_2]$ are indeed imidazolinium ions. The O1-U1-I1, O1-U1-I2 and I1-U1-I2 angles are all very close to 90˚ giving the structure an almost perfect octahedral geometry.

Other $[UI_4L_2]$ complexes in the literature are the U^{VI} complex $[UI_4O_2][PPh_4]_2$ **E** by Crawford and Mayer and the U^V complex $[U(OSiMe_3)_2(I)_4][IPPh_3]$ **F** by Hayton that can be reduced to the U^{IV} complexes $[U(OSiMe_3)_2I(THF)_4][I_3]$ **G** and $[U(OSiMe_3)_2(bipy)_2I_2]$ **H**.[22,24] All four complexes **E**-**H** maintain the U=O oxygen atoms even when treated with an excess of substrate as in the synthesis of complex **F** from $[UO_2\{^tBuNC(Ph)CHC(Ph)O\}_2]$ and 10 equivalents of Me_3SiI. In contrast to complexes

E-**H** compound **29** has not retained the uranyl oxo atoms but the U=O bond has been cleaved completely.

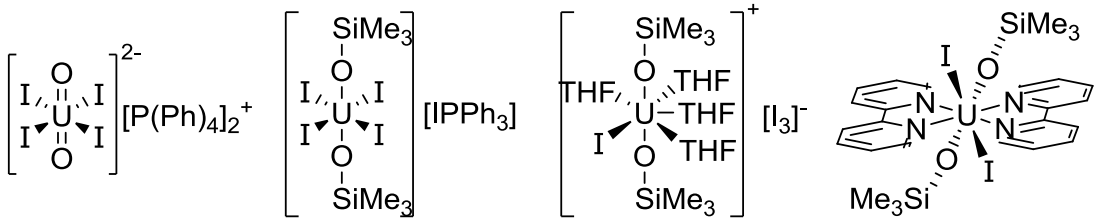

E **F** **G** **H**

Figure 4 Uranyl and uranium iodide complexes **E**-**H**

The trend of the U-O and U-I bond distances for complex **E**, **F**, **G** and **H** shows as expected that the U^{VI}-complex **E** has the shortest U-O bond distance and the U^{IV}-complexes **G** and **H** have the longest U-O bond distance, Table 3. The U-I bond distances show a slightly different behaviour with U^{V}-complex **F** and U^{VI}-complex **E** having shorter U-I bonds than the U^{IV}-complexes **G** and **H.**

Table 3 U-O and U-I bond distances (Å) for **26** and complexes **E**- **G**

	29	**E**	**F**	**G**	**H**
U-O	2.055(2)	1.772(5), 1.755(5)	1.990(6)	2.065(6), 2.080(6)	2.084(4)
U-I	3.1153(2), 3.1163(2)	3.0665(4), 3.0397(4)	2.984(19), 2.999(2)	3.1445(13)	3.2435(8)

The U-O distance in **29** is 2.055(2) Å and long compared to those in complex **E** that has bond distances of 1.771(5) Å and 1.755(5) Å. The U-O bond distances for **F**, **G** and **H** are 1.990(6) Å (**F**), 2.065(6) Å and 2.080(6) Å (**G**) and 2.084(4) Å (**H**). **G** and **H** have structural similarity to **29** as is reflected in the U-I bond lengths which are 3.1153(2) Å and 3.1163(2) Å for $[UI_4(L^MH)_2]$ and 3.1145(13) Å for **C** and 3.2435 Å for **H**. Complex **F** and **E** have shorter U-I bonds with 2.984(19) Å and 2.999(2) Å for **F** and 3.0665(4) Å and 3.0397(4) Å for **E**. This data is further evidence that $[UI_4(L^MH)_2]$ **29** is a U^{IV}-complex.

More common than $[UI_4L_2]^{2-}$ bis(monoanionic ligand) complexes are the U^{IV}-tetraiodide starting materials which contain two coordinating oxygen-donor solvents such as diethyl ether or dioxane along with four co-planar iodide atoms as complexes $[UI_4(dioxane)_2]$ **I** and $[UI_4(OEt_2)_2]$ **J**, Figure 5.[25,26]

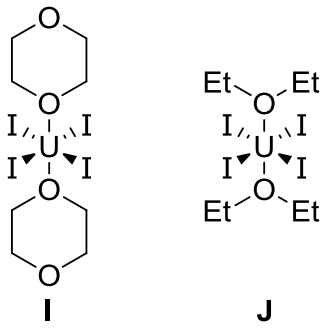

I **J**

Figure 5 $UI_4(solvent)_2$ complexes $[UI_4(dioxane)_2]$ **I** and $[UI_4(OEt_2)_2]$ **J** [25,26]

The U-O bonds in **I** and **J** are 2.333(6) Å and 2.366(8) Å respectively, 0.3 Å longer than those in **29**. The U-I bond distances in **I** and **J** are 2.9637(11) Å and 2.9588(10) Å and 2.9614(6) Å and are therefore about 0.15 Å shorter than the U-I bonds for **29** which are 3.1153(2) Å and 3.1163(2) Å.

The reduction from U^{VI} to a U^{IV} in complex **29** must have occurred at the same time as an oxidation of iodide to iodine. The expected formation of the U^{VI} complex $[UI_4(L^M)_2]$ was not observed but is proposed as a putative intermediate in the formation of complex **29**, Scheme 2.

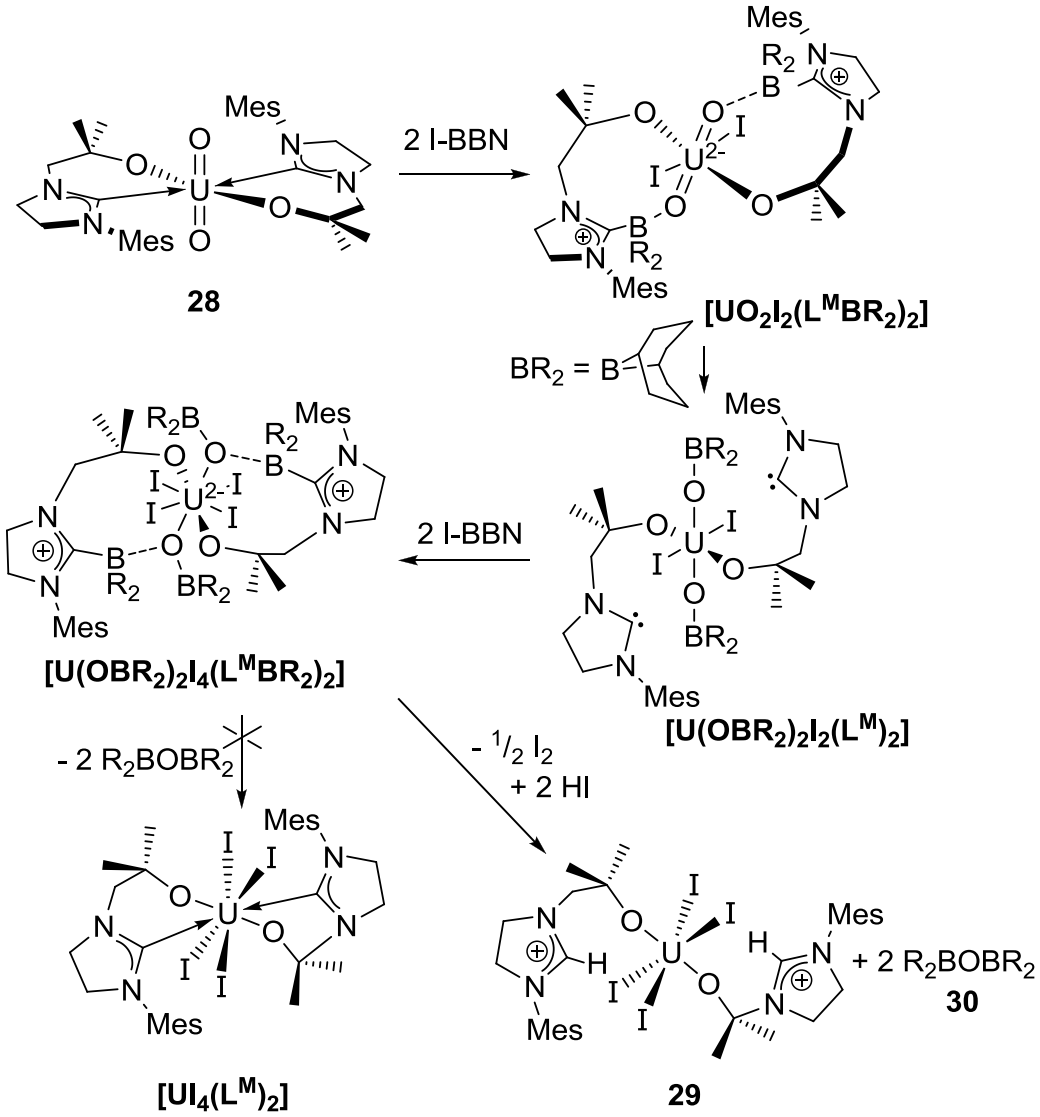

Scheme 2 Proposed mechanism for the formation of the putative intermediate $[UI_4(L^M)_2]$ from $[UO_2(L^M)_2]$

It is proposed that **28** reacts with two equivalents of I-BBN to form the product **$[UO_2I_2(L^MBR_2)_2]$** across the metal-carbene bond with the BR_2 adding to the carbene moiety and the iodide adding onto the uranium metal centre. This brings the BR_2 in close proximity to the uranyl oxo groups leading to the formation of **$[U(OBR_2)_2I_2(L^M)_2]$**. This complex can further be modified by treating it with two more equivalents of I-BBN forming the **$[U(OBR_2)_2I_4(L^MBR_2)_2]$** complex, resulting in the weakened U-OBR_2 bond being proximal to another BR_2 bond, enabling the formation of R_2BOBR_2 **27**. Elimination of **30** should yield the **$[UI_4(L^M)_2]$** complex instead of the observed

[$UI_4(L^MH)_2$] 29 complex. It is possible that the formation of **29** instead of **[$UI_4(L^M)_2$]** is due to an impurity of HI in the I-BBN starting material. An indication of the reduction of the U^{VI} to a U^{IV} centre would be the generation of I_2. Hayton reported the $^{31}P\{^1H\}$ NMR shift for $[Ph_3PI][I]$ in CD_2Cl_2 at δ = -20.29 ppm.[22] Godfrey and co-workers reported a shift in the $^{31}P\{^1H\}$ NMR spectrum at δ = 44.8 ppm for the same compound.[27] To test whether I_2 was generated in the formation of **29** one equivalent of PPh_3 was added to an NMR scale reaction of **28** with four equivalents of I-BBN. An orange solid that is believed to be $[Ph_3PI][I]$ precipitated out of solution within five minutes. The $^{31}P\{^1H\}$ NMR spectrum run in a mixture of a few drops of deuterated benzene and methylene chloride shows a resonance at 23.9 ppm.

It is difficult to obtain further characterisation for the proposed $[UI_4(L^M)_2]$ compound or **29** because of its poor solubility in deuterated solvents. Partial solubility was only observed in pyridine and methylene chloride. The poor solubility of **29** is no surprise as the U^{IV} complex $[UI_2(L^M)_2]$ (see Chapter 2) is also poorly soluble in any deuterated solvent. The starting material $[UO_2(L^M)_2]$ itself is sparely soluble in deuterated benzene or toluene.

Performing the reaction to form **29** in deuterated pyridine was not possible as boranes such as I-BBN react easily with one equivalent of pyridine to form a pyridine adduct **K**, Eq. (6).[28]

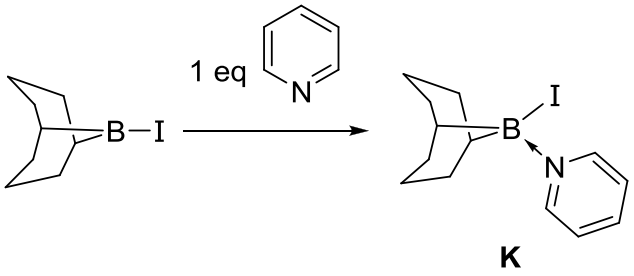

K (6)

The R_2BOBR_2 byproduct **30** (bis(1,5-cyclooctadienyl)diboroxane) was isolated and characterised by ^1H NMR spectroscopy, with its pyridine adduct also being synthesised and characterised by ^1H NMR spectroscopy by Yalpani.[29] In his studies, one equivalent of pyridine reacted with (bis(1,5-cyclooctadienyl)diboroxane) in $CDCl_3$ to give three resonances for the borabicyclononane moiety in the ^1H NMR spectrum at δ = 1.59 (m, 20H), 1.22 (m, 4H), 1.0 (br, 4H). When **28** was treated with four equivalents of

I-BBN in deuterated benzene or methylene chloride three resonances at δ (DCM) = 1.71 (20H), 1.21 (4H), 0.98 (4H) and δ (C_6D_6) = 1.88 (20H), 1.37 (4H), 1.31 (4H) were seen. To eliminate HI, which might be present in the I-BBN solution as the cause of the reaction of **28** with I-BBN to form **29**, the integrals of all protons were compared with those of deuterated benzene as internal standard. First, **28** was combined in a Young's tap NMR tube with one equivalent of I-BBN in deuterated benzene to give the aforementioned resonances. When a second equivalent of I-BBN was added to the reaction, the integrals assigned to the BBN resonances increased in size. Additional proof for these resonances being the bis(1,5-cyclooctadienyl)diboroxane are that the same resonances can be seen in the ^{1}H NMR spectrum of the reaction of [$UO_2N"_2(py)_2$] with I-BBN that is described in section 4.3.

4.2.3 $[UO_2I_4][(L^M)\text{-}B(cyoc)]_2$ (cyoc = cyclooctyl)

When the reaction of **28** with four equivalents of I-BBN is carried out at a low temperature of -78 ^{o}C, a new iodide complex **31** is synthesised in a 43% yield, Eq. (7).

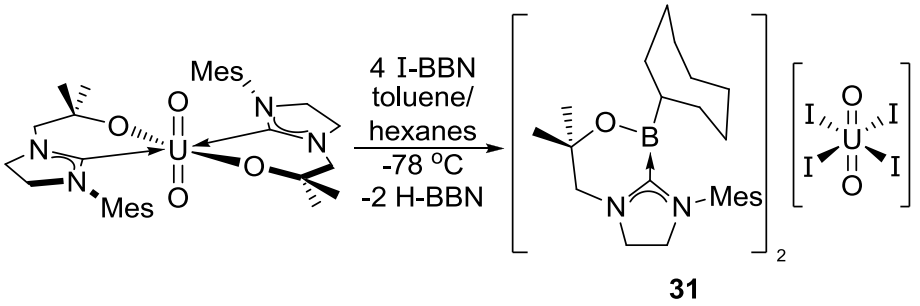

31 (7)

Instead of functionalising the oxo group of the uranyl dication as was seen in complex **29**, the low temperature reaction of **28** with I-BBN in toluene and hexanes yielded the yellow uranyl tetraiodide dianion complex [UO_2I_4][(L^M)-B(cyoc)]$_2$ (cyoc = cyclooctyl) **31** with two 1-(2-(cyclooctylboryloxy)-2-methylpropyl)-3-mesitylimidazolene counterions. Single crystals of **31** suitable for X-ray diffraction were grown from a saturated toluene/hexane solution, Figure 6.

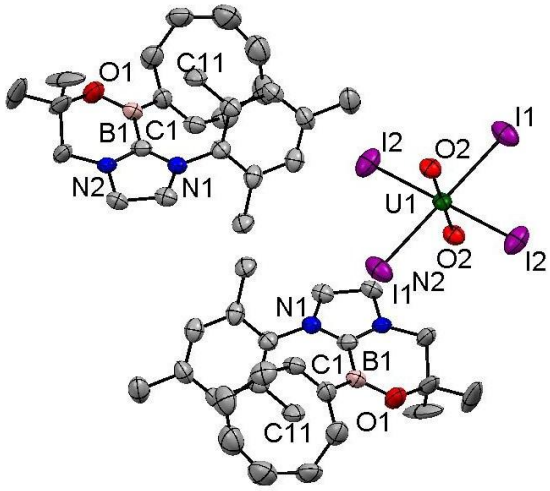

Figure 6 Displacement ellipsoid drawing (50%) of $[UO_2I_4][(L^M)\text{-}B(cyoc)]_2$ **31**, H atoms omitted for clarity

The uranium centre is six coordinate and surrounded in an octahedral geometry with four iodide atoms in the equatorial plane and two *trans* oxygen atoms, giving it a uranyl $[UO_2I_4]^{2-}$ structure. Selected bond distances (Å) and angles (˚) for **31** are displayed in Table 4.

Table 4 Selected bond distances (Å) and angles (˚) for **31**

U1-I1	3.0479(8)	N1-C1-N2	110.8(8)
U1-I2	3.0282(8)	I1-U1-I2	88.60(3)
U1-O2	1.756(7)	O2-U1-I1	89.6(2)
C1-B1	1.616(15)	O2-U1-I2	88.5(2)
B1-O1	1.345(14)	O2-U1-O2	180.0(2)

The U-I distances of **31** of 3.0479(8) Å and 3.0282(8) Å are similar to the U-I distances of 3.0195(3) Å and 3.0455(3) Å observed in **35**. Similar U1-O2 distances of 1.756(7) Å for **31** and 1.755(5) for **35** were also observed, which confirms a uranyl bond. The N-C-N angle of 110.8˚ in **31** is slightly wider than that in $[L^MBBN]$ **6** of 108.1(5)˚. The C1-B1 distance of 1.616(15) Å is slightly shorter than the 1.658(3) Å in **6**. The B1-O1 distance of 1.345(15) Å is shorter by 0.15 Å than the B1-O1 distance of 1.508(2) Å in $[L^MBBN]$ **8**.

The opening of the borabicyclo[3.3.1]nonane to form the cyclooctylboryl cation has not been described in this form in the literature, but an alternative opening of BBN to form new functionalised boryl complexes has been described.[30–33] Examples include the formation 9-methoxy-10-phenyl-9-borabicyclo[3.3.2]decane **L**, Eq. (8), that was synthesised by Canales *et al.*[30]

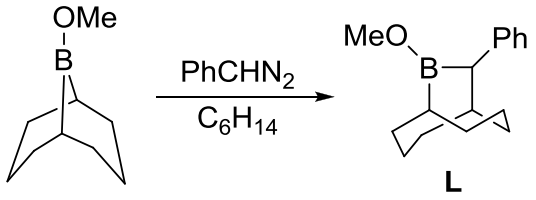

(8)

In this reaction the methoxy-BBN is treated with 1.1 equivalents of phenyldiazomethane in cyclohexane to give **L**. Another borenium ion has only recently been reported by the Curran group, the $[NHC\text{-}B(OH)_2]^+TfO^-$ complex (NHC = 1,3-bis(2,6-diisopropylphenyl)imidazol-2-ylidene), was obtained by treatment of $[NHC\text{-}BH_2Cl]$ with two equivalents of triflic acid.[34]

To further investigate the reaction to form **31**, **28** was treated with Br-BBN to seek the tetrabrominated bis-ligand complex, Eq. (9).

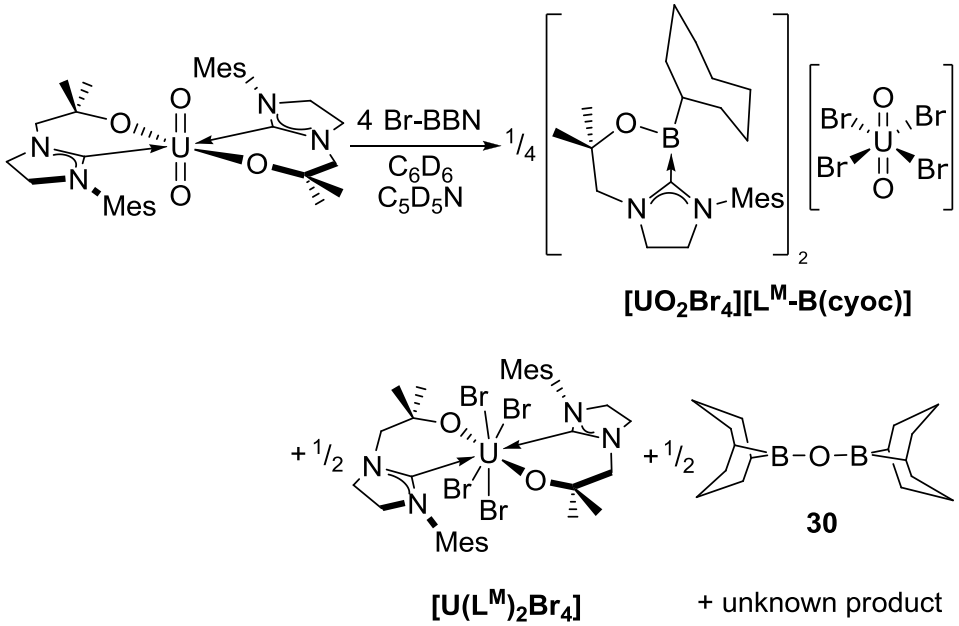

(9)

In a Young's tap NMR tube a colourless solution of Br-BBN in C_6D_6 was combined with a yellow suspension of **28** in C_6D_6, over 12 h a brown precipitate and a brown solution formed. The ^{1}H NMR spectrum of the solution shows the resonances attributed to the [L^M-B(cyoc)] cation in **31**. When the C_6D_6 was removed under reduced pressure and the brown solid partially dissolved in pyridine, the ^{1}H NMR now showed a second set of diamagnetic resonances corresponding to the major product. The integrals were assigned to a single set of coordinated ligand resonances bound to a metal and are therefore believed to be [U(L^M)$_2$Br$_4$]. The resonances for **30** are in the spectrum but are partially obscured by other resonances therefore precise integration is not possible. Other resonances belonging to an as yet unknown product could belong to the so far elusive [UO(L^M)$_2$X$_2$].

4.2.4 [UO_2{$O(BO_2C_6H_4)$-μ_2-O-(C_6H_4O)}$_2$] and [(L^M)(Bcat)]

To establish whether it is possible to isolate an intermediate of the form [UO(L^M)$_2$X$_2$] in the reaction of **25** with I-BBN to form **28**, it was treated with two equivalents of boron halide compounds such as 2-bromo-1,3,2-benzodioxaborole or I-BBN, Eq.
(10).

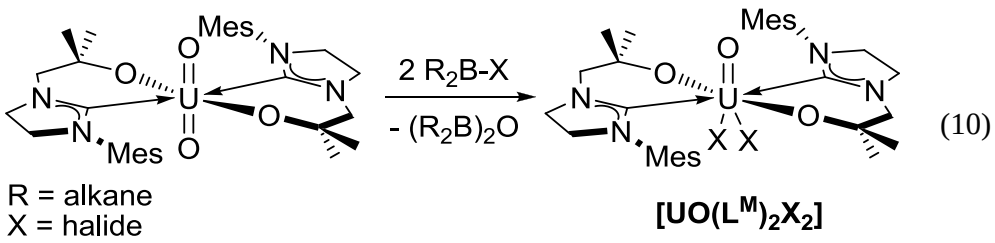

(10)

This reaction was carried out in a Young's tap NMR tube by treating an orange suspension of **28** in methylene chloride with 2 equivalents of a colourless solution of 2-bromo-1,3,2-benzodioxaborole in methylene chloride at room temperature. A green solution formed instantly with a small amount of brown-green precipitate; filtering and slow diffusion afforded single crystals suitable for X-ray crystallography, Figure 7. Instead of the expected product [UO(L^M)$_2$X$_2$], the new complexes **32** and **33** were formed in a combined yield of 12%, Eq. (11). The crystals must be a result of a reaction with the catechol and other impurities that are a byproduct of the synthesis.[35]

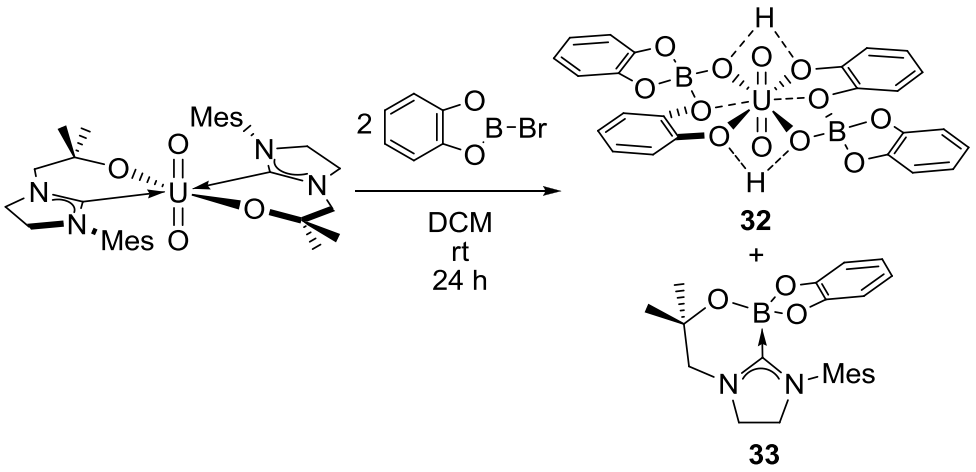

(11)

This reaction is similar to the aforementioned formation of **31** as the ligand [L^M] is abstracted by BR_2 instead of functionalising the uranyl oxo group. The cocrystal of **32** and **33** can be seen in Figure 7.

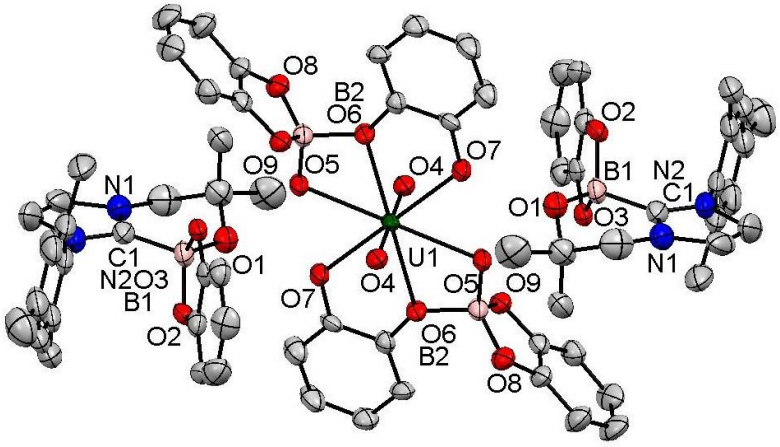

Figure 7 Displacement ellipsoid drawing (50%) of $[UO_2\{O(BO_2C_6H_4)\text{-}\mu_2\text{-}O\text{-}(C_6H_4O)\}_2]$ **32** and [(L^MBcat)] **33** cocrystals, H atoms and one methylene chloride omitted for clarity

The uranium metal centre is eight coordinate with a hexagonal bipyramidal geometry composed of eight oxygen atoms. Selected bond distances (Å) and angles (˚) are displayed in Table 5.

Table 5 Selected bond distances (Å) and angles (°) for $[UO_2I_4(L^M\text{-BBN})_2]$ **32** and $[L^M\text{-Bcat}]$ **33** cocrystal

U1-O4	1.766(6)	B1-C1	1.658(11)
U1-O5	2.417(5)	B1-O1	1.462(11)
U1-O6	2.457(5)	B1-O2	1.476(11)
U1-O7	2.538(5)	B1-O3	1.488(11)
B2-O5	1.471(10)	N1-C1-N2	112.3(8)
B2-O6	1.506(10)		

A hexagonal bipyramidal conformation with *trans* actinyl oxo groups occupying the axial positions are known in literature.[36] One example reported by Clark and co-workers is the neptunyl crown ether inclusion complex $[NpO_2([18]crown\text{-}6)]ClO_4$.[37] The uranyl oxo groups U1-O4 display the typical bond distance of 1.766(6) Å for a $[U^{VI}O_2]$. The metal centre in **32** is coplanar with its six equatorial bound oxygen atoms O5, O6 and O7 with bond distances of 2.417(5) Å, 2.457(5) Å and 2.538(5) Å respectively. The catechol fragments are also in the same plane, with the bridging oxo O6 slightly above the plane and the B2 slightly below the plane. The benzodioxoborole sits in a perpendicular manner to the plane. A hydrogen bond interaction can be seen between the O5 of **32** and the O3 of **33** and the O7 of **32** and the O1 of **33**, Figure 8.

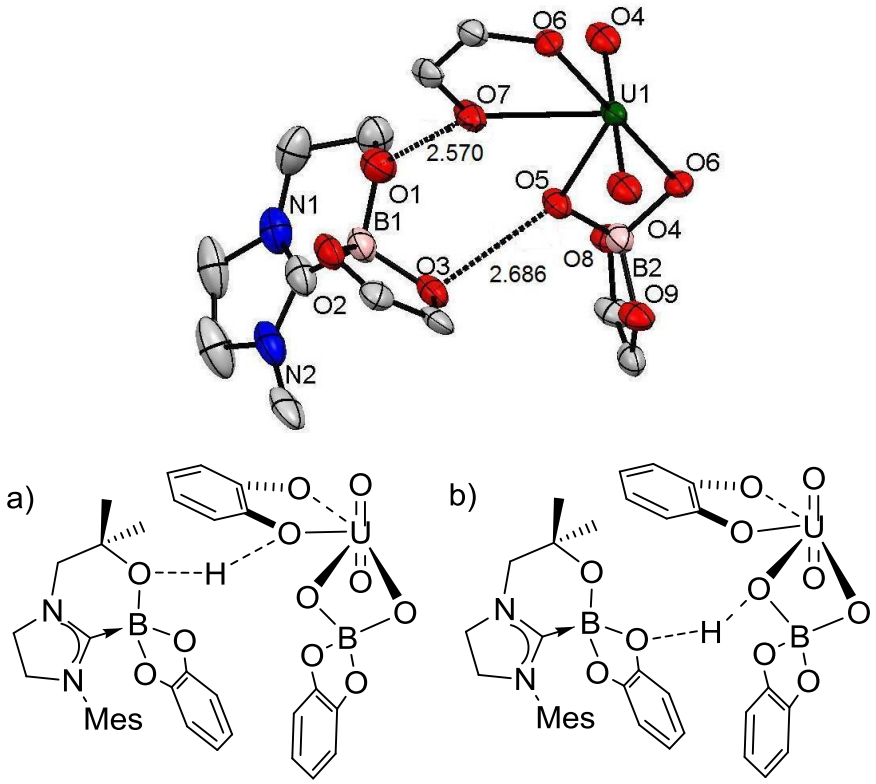

Figure 8 Potential H-bond bridges between O7-O1 and O5-O3 of **32** and **33** a) shows H-bond bridge between O7-O1 b) shows H-bon bridge between O5-)3

The O5-O3 and O7-O1 distances of 2.686(8) Å and 2.570(7) Å are comparable to OHO interactions.[38,39] The uranium centre is in a +VI oxidation state, therefore two cationic counterions or protons need to be added to the structure. It would make sense if the O7 was bound to a proton making it a hydroxyl group as the U1-O7 bond distance of 2.538(5) Å is slightly longer than the U1-O6 bond distance of 2.457(5) Å.

(This could be due to the poor quality of the crystal, which has a high R(int) value of 12.1.)

Catechols have been used before as ligands for actinides to form complexes of $Na_4[An(C_6H_4O_2)_4]\cdot 21H_2O$ (An = Th, U).[40] A similar reaction to the formation of **32** from **28** and 2-bromo-1,3,2-benzodioxaborole was observed by Barnea and co-workers when they treated a $[(Cp^*)_2An(Me)_2]$ (An = Th, U) complex with eight equivalents of catecholborane contaminated with 5% of dimethyl sulphide to form complex **M**, Eq.(12). In contrast to **32** the three catecholborates and three catechols form a macrocycle around the U^{IV} centre. The average U-O bond distance in **M** is 2.435 Å which is shorter than the

average U-O bond distance of the equatorial ligands of 2.471 Å of **32**. This agrees with the existence of an OH in **32**. As in **32** the catecholborate fragments in **M** are positioned perpendicularly to the catechol fragments.

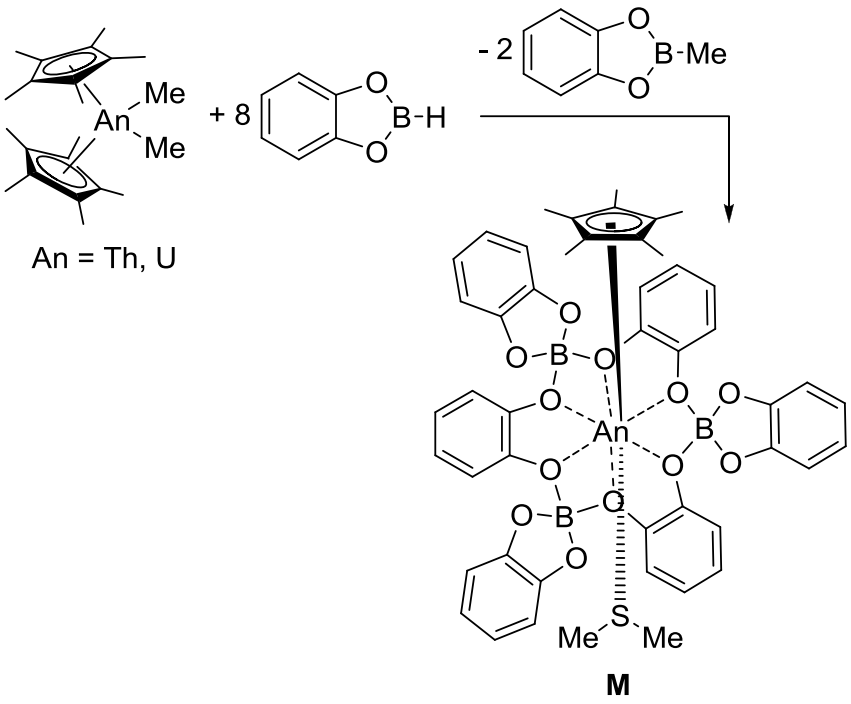

(12)

The boron centre of [L^M-Bcat] **33** is four coordinate and surrounded in a distorted tetrahedral geometry by C1 and O1 of the ligand and O2 and O3 of the oxaborazole. The phenyl ring of the borazole is aligned in a parallel fashion to the mesityl group of the ligand. The B1-C1 distance is 1.658(11) Å which is identical with the B1-C1 bond distance of 1.658(3) Å in [L^M-BBN] **8**. The N1-C1-N2 angle of 112.3˚ is unusually wide compared to the typical angle for a bound imidazoline and the angle of 108.49(15) of **8**. Instead the angle is closer to one in an imidazolinium complex as [H_2L^D]Cl with 113.7(2) Å or **29** with 113.6(3) Å. The B1-O1 distance of 1.462(11) Å is a bit shorter than the B1-O1 distance of 1.508(2) Å in **8**. The B1-O3 distance is similar to the B1-O2 distance, about 1.48 Å and slightly longer than the B1-O1 bond distance.

4.2.5 Treatment with BBr_3 and $Cl_2BN^iPr_2$

Other boron containing reagents were used to probe the reactivity of **28** towards uranyl oxo functionalisation. When **28** was treated with four equivalents of BBr_3 in

methylene chloride a brown solution formed immediately with addition of a few drops of deuterated benzene causing the precipitation of a small amount of brown solid.

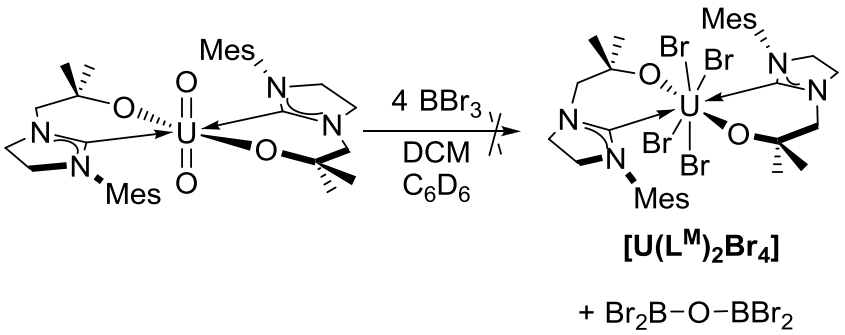

(13)

From the ^{1}H NMR spectrum it can be concluded that a multitude of diamagnetic products are formed. The resonances are too close together to identify the different products, which are perhaps oligomeric or polymeric structures.

The reaction of **28** with four equivalents of $Cl_2BN^iPr_2$ in pyridine yields a product with clean ^{1}H NMR spectrum that is believed to be $[UO_2Cl_4][(L^M)\text{-}BN^iPr_2]_2$, Eq. (14).

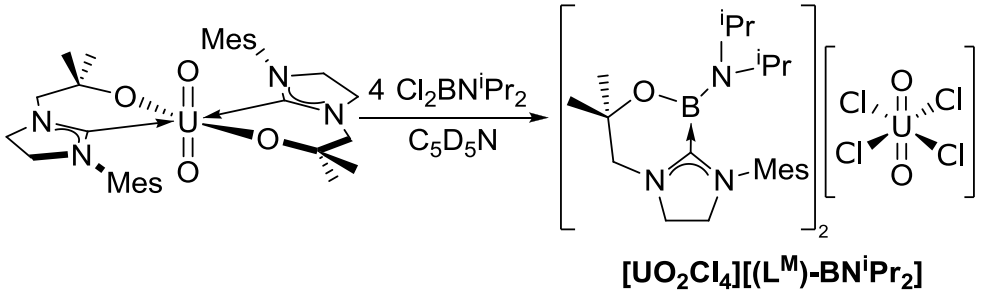

(14)

When **28** was treated with four equivalents of $Cl_2BN^iPr_2$ in toluene rather than pyridine, only 2.5 equivalents of the $Cl_2BN^iPr_2$ reacted to form 40% $[U(L^M)_2Cl_4]$, half an equivalent of $[\{^iPr_2N(Cl)B\}_2O]$ and half an equivalent of $[OBN^iPr_2]_3$ as identified by ^{1}H NMR spectroscopy, Eq. (15). A small amount of decomposition in the ^{1}H NMR spectrum was assigned to $[H_2L^M]Cl$, the chloride salt of the proligand.

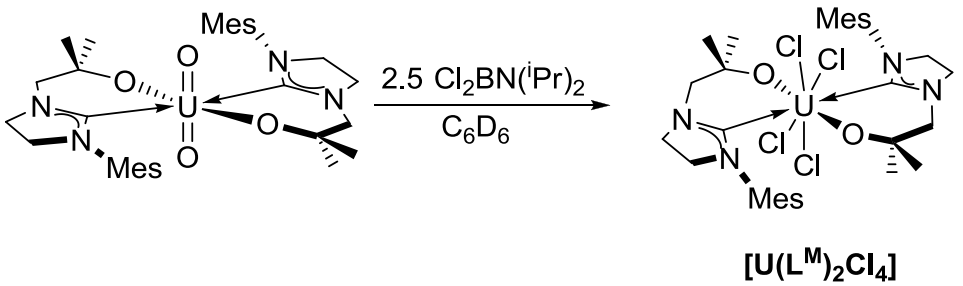

[U(L^{M})$_2$Cl$_4$] (15)

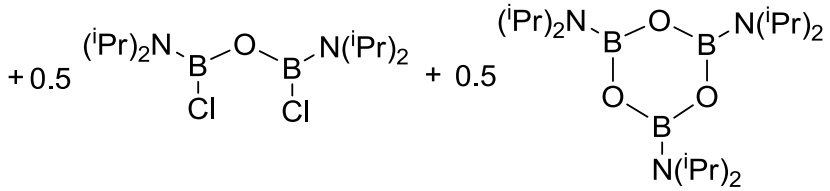

[{^{i}Pr$_2$N(Cl)B}$_2$O] **[OBN(^{i}Pr)$_2$]$_3$**

The tendency of $Cl_2BN^iPr_2$ to react to form the $[\{^iPr_2N(Cl)B\}_2O]$ and $[OBN^iPr_2]_3$ byproduct has been reported.[41] The crystallisation of what is believed to be $[U(L^M)_2Cl_4]$ was attempted several times with various scale ups of this reaction. Unfortunately, crystallisation of this compound has been unsuccessful to date. On account of the ^{1}H NMR resonances all being diamagnetic, it can be postulated that $[U(L^M)_2Cl_4]$ should be the main product as only one set of ligand resonances were observed.

4.2.6 Reaction with ClPPh$_2$

To test whether a similar oxo-abstraction reaction of **28** with boron containing reagents could be achieved with a phosphorus containing reagent, the complex was treated with four equivalents of $ClPPh_2$. The ^{1}H NMR spectrum of this reaction in C_6D_6 shows only broad resonances on account of the majority of the product precipitating out of solution. The resonances in the ^{1}H NMR spectrum are shifted like the ligand resonances of $[U(L^M)_2Cl_4]$ from the reaction of **28** with $Cl_2BN^iPr_2$. If the reaction is carried out in methylene chloride two clear doublets at 35.48 ppm and -22.73 ppm with a $^1J_{PP}$ coupling constant of 228 Hz in the ^{31}P NMR indicate the formation of $O=P(Ph_2)PPh_2$. This tetraphenyl diphosphine monoxide has been reported by Srinivasan with two doublets at 36.7 and -21.7 ppm in the ^{31}P NMR for with a $^1J_{PP}$ coupling of 228 Hz which is in good agreement with our observations. The proposed reaction is therefore Eq. (16). Other small resonances can be found in the ^{31}P NMR that cannot be assigned to a specific substance.

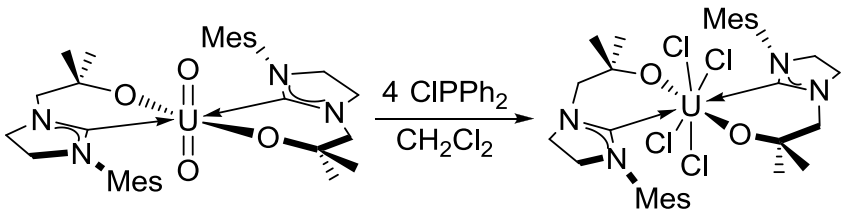

[U(L^{M})$_2$Cl$_4$]

(16)

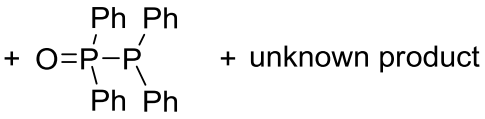

[OP(Ph$_2$)PPh$_2$]

If **28** was treated with $IPPh_2$ the ^{1}H NMR spectrum showed paramagnetic resonances that indicated the formation of $UI_2(L^M)_2$.

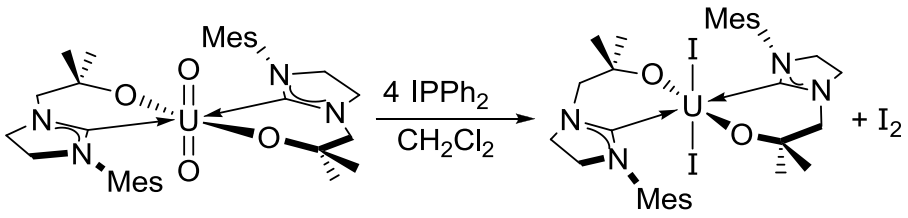

[U(L^{M})$_2$I$_2$]

(17)

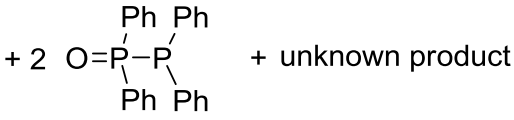

[OP(Ph$_2$)PPh$_2$]

4.2.7 Reactions with other reagents

Other reagents were reacted with **28** in order to probe the uranyl oxos towards functionalisation. **28** was treated with LiI in order to attempt formation of another uranium iodide, but no reaction was observed. The silicon containing reagents Me_3SiX (X = I, Cl), $LiSiPh_3$ and 2,6-*tert*butylphenyl *tris*chlorosilane were treated with **28** and showed a reaction but gave no clear results as multiple products could be observed in the ^{1}H NMR spectrum. Combining of **28** with $LiAlH_4$ also showed a reaction but again gave no clear results as multiple products could be observed in the ^{1}H NMR spectrum.

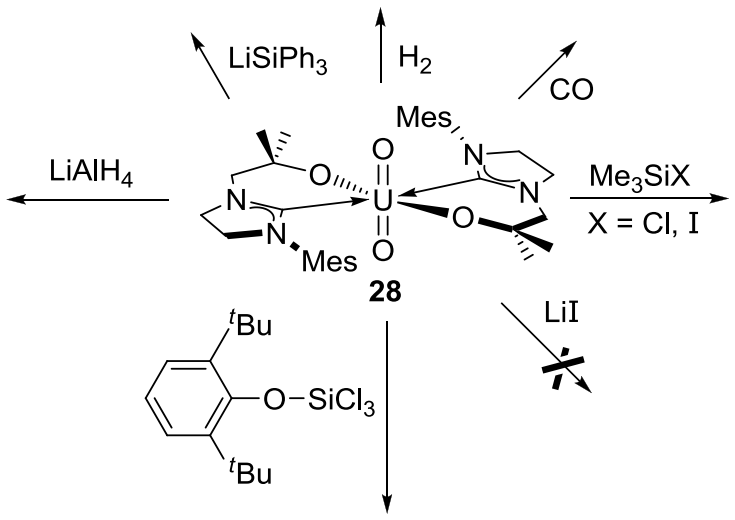

Scheme 3 Attempted functionalisations of the oxo uranyls of **28**

When **28** was treated with gases such as H_2 or CO only formation of [HL^M] could be detected in the ^{1}H NMR spectra. The IR spectrum showed no formation of a new CO complex.

4.3 [UO$_2${N(SiMe$_3$)$_2$}$_2$(py)$_2$] functionalisation

4.3.1 Rationale for using [UO$_2${N(SiMe$_3$)$_2$}$_2$(py)$_2$]

As the functionalisation of **28** with various reagents showed results the reactivity of [$UO_2(N'')_2(py)_2$] towards those reagents was explored as a control to establish the role of the NHC groups in the functionalisation of the uranyl oxos in spite of the coordinated pyridine, which was recognised as a potential problem.

4.3.2 [(UI$_5$)$_2$(py-BBN)$_2$]

A reaction of [$UO_2(N'')_2(py)_2$] was carried out with four equivalents of I-BBN to form the diamagnetic U^{VI} complex [$UI_4(N'')_2$]. The expected reaction is shown in Eq. (18).

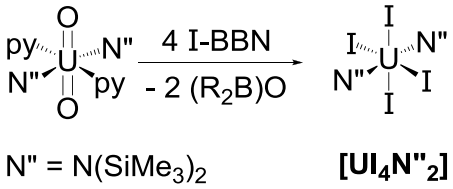

N" = N(SiMe$_3$)$_2$ **[UI$_4$N"$_2$]** (18)

Instead of the expected product $[UI_4(N'')_2]$, complex $[(UI_5)_2(py\text{-}BBN)_2]$ **34** was isolated in a 32% yield, Eq. (19).

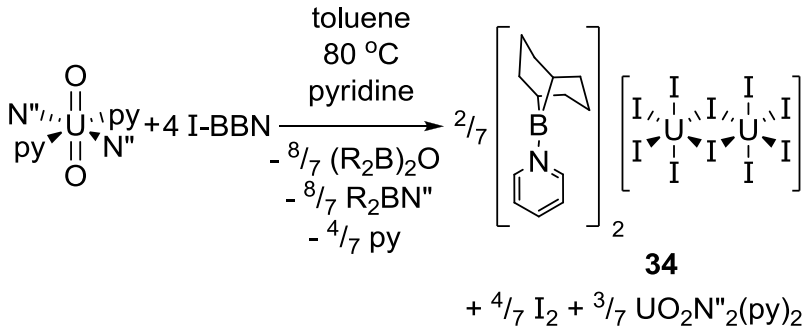

(19)

There are several precedents for f^2-f^2 coupled systems in the literature, one example is $[UCl_4(1,4\text{-dioxane})]_2$ reported by Kiplinger.[25]

In light of the formation of the U^{IV} complex $[(UI_5)_2(py\text{-}BBN)_2]$ the reaction was modified to treating one equivalent of $[(UO_2N''_2(py)_2]$ with 7 equivalents of I-BBN, Eq. (20).

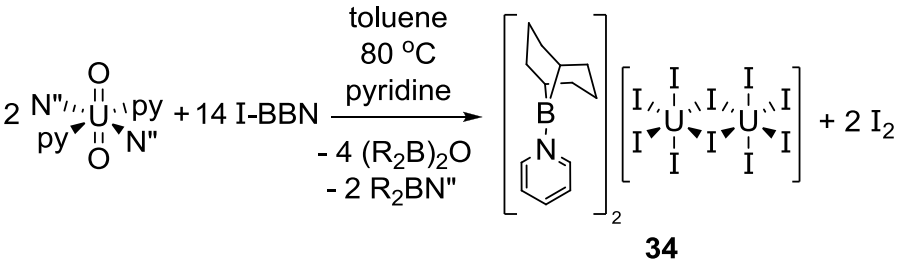

(20)

To a solution of $[UO_2(N'')_2(py)_2]$ in toluene was added a stoichiometric amount of a 1M solution of B-Iodo-9-BBN in hexanes and heated to 80 ˚C for 2 hours. It was then left to stir at room temperature for 12 hours. The volatiles were removed under reduced pressure and the brown solid washed with hexanes. The remaining volatiles were removed in vacuum, then pyridine was added and the solution stirred for 4 h. Removal of the volatiles gave 32 % of clean product. From a concentrated pyridine solution layered with hexanes it was possible to grow crystals suitable for X-ray diffraction.

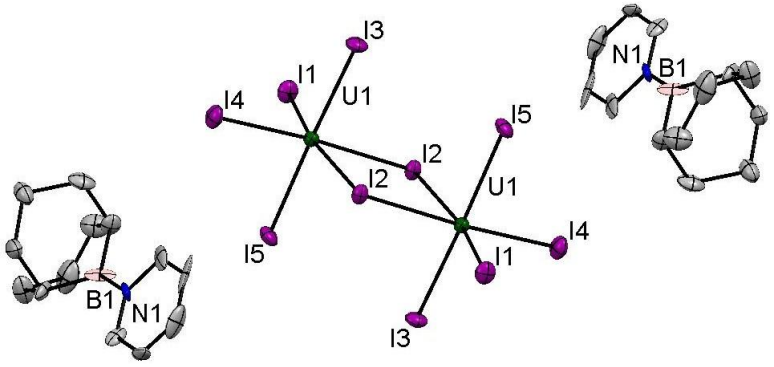

Figure 9 Displacement ellipsoid (50%) drawing of $[(UI_5)_2(py\text{-}BBN)_2]$ **34**, H atoms omitted for clarity

The $[U_2I_{10}]^{2-}$ anion consists of two edge-sharing UI_6 octahedra, with the I3-U1-I5 vertical axis having an angle of 174.90(8)˚. The horizontal axes of I1-U1-I2 and I2-U1-I4 have angles of 166.76(7)˚ and 176.19(8)˚ respectively. The U-I bond distances range from 2.919(3) Å to 3.096(2) Å, which is the normal range for a U^{IV} compound.

Table 6 Selected bond distances (Å) and angles (˚) for **34**

U1-I1	2.938(3)
U1-I2	3.096(2)
U1-I3	2.956(2)
U1-I4	2.975(3)
U1-I5	2.919(3)
N1-B1	1.41(5)
I5-U1-I3	174.90(8)
I1-U1-I2	166.76(7)
I4-U1-I2	176.19(8)

The $[UI_6]^{2-}$ species has been reported in literature[42,43] but there was only one other example found for a $[U_2I_{10}]^{2-}$ anion. The complex published by Ibers and Wells is $[Ta_7(Se_2)_{14}][U_2I_{10}]_2$ that was synthesised from the elements at 1173 K.[44] The U-I bond distances for this complex are between 2.9026(9) Å and 3.1270(5) Å and are comparable with the U-I bond distances for $[(UI_5)_2(py\text{-}BBN)_2]$. Complex **34** might be interesting to

spectroscopists because of its near perfect octahedral geometry allowing facile interpretation of uranium iodide vibrational spectra.

Two structurally similar uranium complexes **N** and **O** with bridging iodides are shown in Figure 10.[45,46]

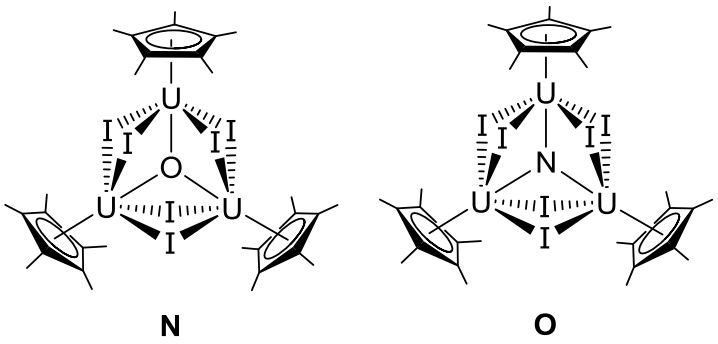

Figure 10 Uranium complexes with bridging iodides[45,46]

Complexes G and H are trimeric with a μ_3-oxo-group **N** or a nitrido **O**. The three uranium centres are each bridged by two μ-iodides. Complex **N** has two U^{IV} centres and one U^{III} centre whereas complex **O** consists solely of three U^{IV} centres. The U-I bond distances for **N** lie between 3.179(15) Å and 3.214(15) Å. The U-I bond distances for **O** lie between 3.1483(4) Å and 3.2109(4) Å. These bond distances are slightly longer than the U-I bond distances for $[(UI_5)_2(py\text{-}BBN)_2]$ but still within range.

4.3.3 $[UO_2I_4][(py)_2BBN]_2$

If the above reaction of $[UO_2(N'')_2(py)_2]$ with four equivalents of I-BBN is repeated at room temperature, a different reaction product is observed, Eq. (21).

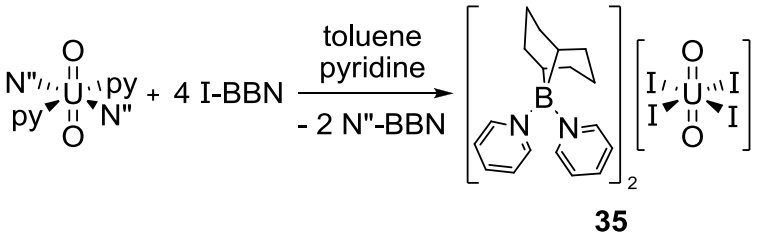

(21)

Instead of oxo functionalisation and reduction of the U^{VI} to a U^{IV}-centre, the U^{VI} remains in the same oxidation state and forms a $[UO_2I_4]^{2-}$ anion complex in a 32% yield.

It was possible to grow single crystals suitable for X-ray diffraction from a concentrated pyridine solution.

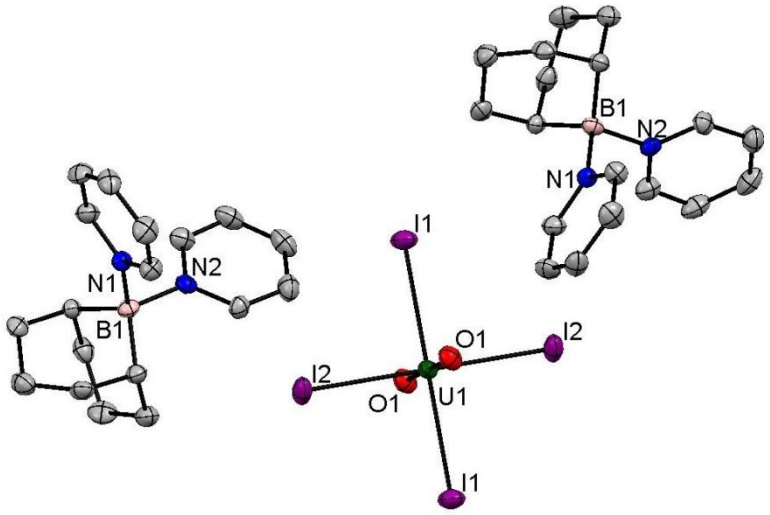

Figure 11 Displacement ellipsoid drawing (50%) of $[UO_2I_4(py\text{-}BBN)_2(py)]$ **35**, H atoms omitted for clarity

The six coordinate uranium centre is in an octahedral geometry with four iodide atoms in the equatorial axis and two oxygen atoms bound axially, giving it a *trans*$[UO_2I_4]^{2-}$ structure. Selected bond distances (Å) and angles (˚) for **35** are displayed in Table 7.

Table 7 Selected bond distances (Å) and angles (˚) for **35**

U1-O1	1.759(3)
U1-I1	3.0195(3)
U1-I2	3.0455(3)
B1-N1	1.619(6)
B1-N2	1.623(7)

The U1-O1 bond distance is 1.759(3) Å which is consistent with a uranyl bond distance.[47] The U1-I1 and U1-I2 bonds are all of similar distances to each other with 3.0195(3) Å and 3.0455(3) Å. This is close to the U-I bond distance in $[(UI_5)_2(py\text{-}BBN)_2]$ for the bridging iodide to the uranium centre of 3.096(2) Å.

The $[UO_2X_4]^{2-}$ anion (X = halogen) is known in the literature. The fluoride analogue is either a dimer or exists as an extended $[UO_2F_4]^{2-}$ framework.[48–50] The most

common uranyl tetrahalide anion is the $[UO_2Cl_4]^{2-}$ anion.[51–55] The bromide analogue $[UO_2Br_4]^{2-}$ is also known and has been applied in the synthesis of ionic liquids.[56–62] Only one $[UO_2I_4]^{2-}$ structure has been published; **E** in Figure 4, reported by Crawford and Mayer in 2005.[24] It was synthesised by slow addition of a dilute $Ph_4PI/CH_3CH_2CN/CH_3CN$ solution to a mixture of UO_2I_2 in CH_3CH_2CN, Eq.(22).

$$UO_2I_2 \cdot x\,H_2O + 2\,Ph_4PI \longrightarrow (Ph_4P)_2UO_2I_4 + x\,H_2O \qquad (22)$$

35 is similar to the U^{VI}-complex $[UO_2I_4][Ph_4P]_2 \cdot 2NCCH_3$ **E** described earlier. The compound was characterised by X-ray diffraction and computational investigations were undertaken. The U-O and U-I bond distances (Å) for $[UO_2I_4(py\text{-}BBN)_2(py)]$ **35** and **E** are shown in Table 8.

Table 8 U-O and U-I bond distances (Å) and angles (°) for **35** and **E**

	35	**E**
U1-O1	1.759(3)	1.772(5)
U1-O2	"	1.755(5)
U1-I1	3.0195(3)	3.0665(4)
U1-I2	3.0455(3)	3.0397(4)

Both compounds have similar U-O and U-I bond distances. The U-O bonds in each compound are almost identical with 1.759(3) Å for $[(UO_2I_4)(py\text{-}BBN)_2]$ and 1.772(5) Å and 1.755(5) Å for **E**. The same similarity is present in the U-I bonds with 3.0195(3) Å and 3.0455(3) Å for **35** and 3.0665(4) Å and 3.0397(4) Å for **E**. Schreckenbach and co-workers calculated the energy difference between the cis isomer with a bent uranyl group and the trans uranyl isomer with a linear uranyl group for $[UO_2F_4]^{2-}$, $[UO_2Cl_4]^{2-}$ and $[UO_2(OH)_4]^{2-}$, finding that the energy difference is relatively small.[63] In other calculations, Crawford and Mayer determined that the linear *trans*-OUO arrangement is favoured over the *cis*-OUO arrangement by 121.3 kJ mol^{-1}, using a B3LYP level of theory.[24]

4.4.4 Treatment of $[UO_2N"_2(py)_2]$ with $ClPPh_2$

When $[UO_2(N")_2(py)_2]$ was treated with $ClPPh_2$ no formation of the tetraphenyl diphospine monoxide described in section 4.2.6 was observed, indicating that the NHCs in $[UO_2(L^M)_2]$ promote the oxo functionalisation. The ^{31}P spectrum showed resonances at 10 and -16 ppm that are not coupled to other atoms. No compound could be assigned to these specific resonances.

4.4.5 Treatment of $[UO_2N"_2(py)_2]$ with bromocatechol borane

No reaction was observed in the ^1H NMR spectrum of the reaction of $[UO_2(N")_2(py)_2]$ and bromocatechol borane, giving further evidence for the involvement of the NHC groups for the functionalisation of the uranyl oxo groups.

4.4.6 Treatment of $[UO_2N"_2(py)_2]$ with $Cl_2BN^iPr_2$

As with the bromocatechol borane, no reaction was observed between $[UO_2(N")_2(py)_2]$ and $Cl_2BN^iPr_2$.

4.4 $[UO_2(OAr^{2,6\text{-}tBu})_2(py)_2]$ functionalisation

4.4.1 Synthesis of $[UO_2(OAr^{2,6\text{-}tBu})_2(py)_2]$

The synthesis of $[UO_2(OAr)_2(py)_2]$ was carried out *via* a modification of known literature procedures, Eq. (23).[64,65]

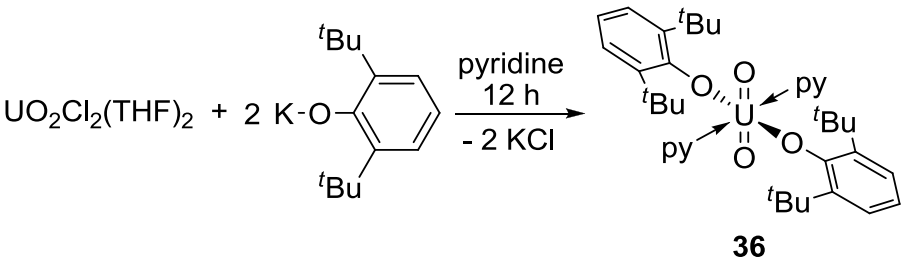

(23)

36

A pyridine solution of 2 equivalents of $KOAr^{2,6\text{-}tBu}$ was added slowly to a slurry of $[UO_2Cl_2(THF)_2]$ in pyridine in a salt elimination reaction. After a few hours KCl precipitated out of solution. Filtration and subsequent reduction of the solution in volume and washing with hexanes gave a dark red solid of $[UO_2(OAr)_2(py)_2]$ **36** in a 77% yield.

4.4.2 $[UO_2(py)_5][I]$

A toluene solution of **36** was treated with 4 equivalents of a hexane solution of I-BBN at -78 ˚C and then slowly warmed up to room temperature. A brown precipitate had formed which was isolated by filtration and dissolved in pyridine. Single crystals of the $[UO_2]^+$ complex $[UO_2(py)_5]I$ **37** were formed in a 36% yield after 48 h at -30 ˚C that were suitable for X-ray diffraction, Eq. (24).

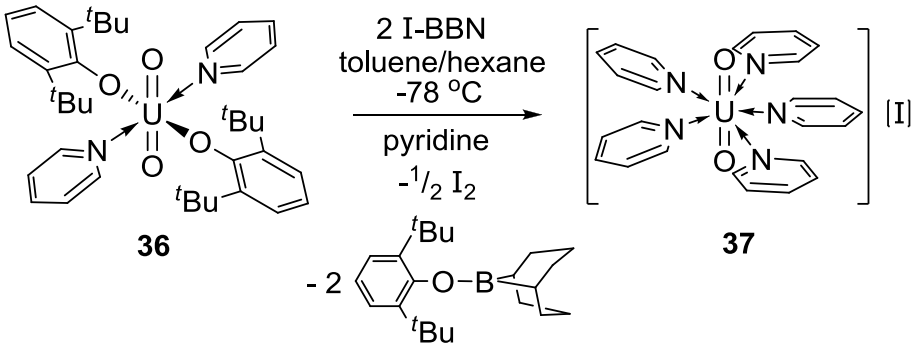

(24)

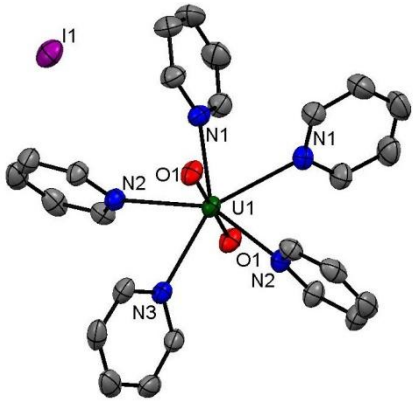

Figure 12 Displacement ellipsoid drawing (50%) of $[UO_2(py)_5]I$ **37**, H atoms and one pyridine solvent molecule omitted for clarity

The uranium metal centre is seven coordinate and in a pentagonal bipyramidal geometry. The uranium is surrounded by five nitrogen atoms in the equatorial plane and two oxygen atoms in the axial plane. Selected bond distances (Å) and angles (˚) are displayed in Table 9.

Table 9 Selected bond distances (Å) and angles (°) for **37**

U1-O1	1.8328(18)	N1-U1-N2	70.59(7)
U1-N1	2.624(2)	N2-U1-N3	73.91(5)
U1-N2	2.597(2)	O1-U1-O1	179.67(12)
U1-N3	2.633(3)	O1-U1-N1	87.83(8)

The uranium is in the +V oxidation state as is indicated by the U1-O1 bond distance of 1.8328(18) Å, which is typical for a $[UO_2]^+$ complex.[66] Complexes **P**, **Q**, **R** and **S** are all also pentavalent uranyl complexes, Figure 13.[67–70] **P** is the same as **37** and has been synthesised by Berthet *et al.*.[67]

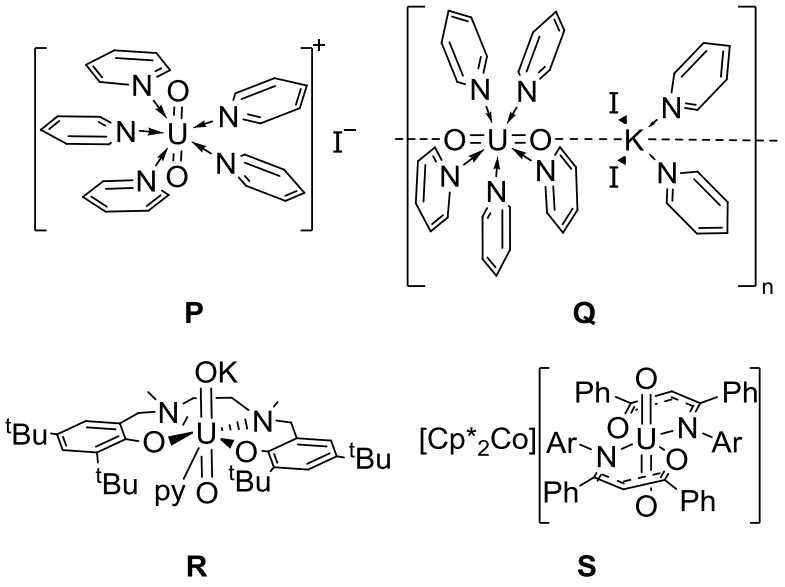

Figure 13 Pentavalent uranyl complexes **P** –**S**

The respective U-O bond distances (Å) and O-U-O angles (°) are displayed in Table 10.

Table 10 U-O bond distances (Å) and O-U-O angles (˚) for compounds **P**-**S** and **37**

	U-O	O-U-O
34	1.8328(18)	179.67(12)
P	1.839(4), 1.823(5)	179.5(2)
Q	1.834(2), 1.836(2)	178.88(7)
R	1.819(12), 1.830(12)	178.9(6)
S	1.838(5)	180

The U-O bond distances of the selected compounds range from 1.819(12) Å to 1.839(4) Å and the O-U-O angles from 179.5(2)˚ to 180˚. Compound **37** has a U-O bond distance of 1.8328(18) Å and an O-U-O angle of 179.67(12)˚. Unsurprisingly the closest resemblance of **37** is to the identical **P** that has an average U-O bond distance of 1.831 Å and an O-U-O angle of 179.5(2)˚. **P** was synthesised by treating one equivalent of $[UO_2I_2(THF)_3]$ with one equivalent of TlC_5H_5 in pyridine and then slowly diffusing pentane onto the mixture, Eq. (25).

$$[UO_2I_2(THF)_3] + TlC_5H_5 \xrightarrow[-TlI]{\text{pyridine}\atop\text{pentane}} \underset{\mathbf{P}}{[UO_2(py)_5][I]\cdot py} \qquad (25)$$

P can be desolvated under vacuum to form a powder of $[UO_2I(py)_{2.5}]$.

The similar polymer **Q** was synthesised in an oxidation reaction from a pyridine solution of $[UI_3(THF)_4]$ and a mixture of pyridine N-oxide and water before addition of KI, Scheme 4.

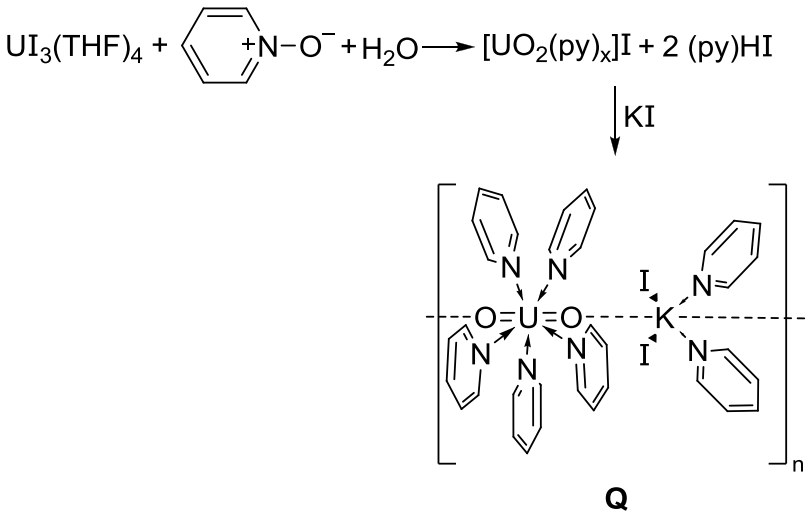

Q

Scheme 4 Synthesis of the polymeric $[\{UO_2(py)_5\}\{KI_2(py)_2\}]_n$ complex **Q**

The average U-N_{py} distances in all three complexes are very close. The average U-N bond distance for **37** is 2.618 Å, for **P** the average bond distance is 2.607 Å and for **Q** the average bond distance amounts to 2.606 Å. The average N-U-N angles are also in good agreement between **P** with 72.33˚ and **34** with 72.25˚.

4.5 Conclusions

The uranyl complex $[UO_2(L^M)_2]$ **28** was functionalised successfully with a variety of boron containing reagents. Depending on the reaction conditions the reaction with I-BBN at room temperature leads to formation of either the complex $[UI_4(L^MH)_2]$ **29** and with strong evidence for the U^{VI} complex $[UI_4(L^M)_2]$ forming. If the reaction is carried out under cold conditions formation of $[UO_2I_4][L^M\text{-BBN}]$ **31** is observed.

The reaction of $[UO_2(L^M)_2]$ **28** with bromocatechol borane leads to the formation of the uranyl complex $[UO_2\{O(BO_2C_6H_4)\text{-}\mu_2\text{-}O\text{-}(C_6H_4O)\}_2]$ **32** and $[(L^M\text{Bcat})]$ **33**, connected by hydrogen bridging.

Further reactivity is seen with $Cl_2BN^iPr_2$ and BBr_3 giving further evidence for the reaction path towards either a dianionic $[UO_2^{2+}]$ complex or the $[UX_4]$ (X = halide) route. It was shown that if the reaction is carried out in solvents such as pyridine the $[UO_2^{2+}]$ complex is favoured, whereas solvents such as methylene chloride and benzene favour the formation of the $[UX_4]$ complex.

Promising results were obtained when $[UO_2(L^M)_2]$ **28** was treated with $ClPPh_2$ that suggest the possibility of the formation of a $[UCl_4(L^M)_2]$ complex.

Probing the reactivity of $[UO_2N''_2(py)_2]$ towards boron containing reagents provided a route to new complexes. No formation of $[UI_4N''_2]$ is evident. If $[UO_2N''_2(py)_2]$ was treated with I-BBN at 80 ˚C, the formation of $[(UI_5)_2(py\text{-}BBN)_2]$ **34** was observed. If the reaction is carried out at room temperature the $[UO_2I_4][(py)_2\text{-}BBN]_2$ **35** complex is formed instead.

The lack of reactivity between $[UO_2N''_2(py)_2]$ and $ClPPh_2$, bromocatechol borane or $Cl_2BN^iPr_2$ is further evidence for the necessity of NHCs to functionalise the uranyl oxo group.

An easily accessible route to the known $[UO_2]^+$ complex $[UO_2(py)_5]I$ **37** was established by reacting $[UO_2(OAr)_2(py)_2]$ with I-BBN.

4.6 References

1. R. G. Denning, *J. Phys. Chem. A*, 2007, **111**, 4125–4143.
2. L. R. Morss, N. M. Edelstein, J. Fuger, and J. J. Katz, *The Chemistry of the Actinide and Transactinide Elements Volumes 1-6.*, Springer Verlag, 2010.
3. K. E. Fletcher, M. I. Boyanov, S. H. Thomas, Q. Wu, K. M. Kemner, and F. E. Löffler, *Environ. Sci. Technol.*, 2010, **44**, 4705–4709.
4. M. I. Boyanov, E. J. O'Loughlin, E. E. Roden, J. B. Fein, and K. M. Kemner, *Geochim. Cosmochim. Ac.*, 2007, **71**, 1898–1912.
5. W.-M. Wu, J. Carley, T. Gentry, M. A. Ginder-Vogel, M. Fienen, T. Mehlhorn, H. Yan, S. Caroll, M. N. Pace, J. Nyman, J. Luo, M. E. Gentile, M. W. Fields, R. F. Hickey, B. Gu, D. Watson, O. A. Cirpka, J. Zhou, S. Fendorf, P. K. Kitanidis, P. M. Jardine, and C. S. Criddle, *Environ. Sci. Technol.*, 2006, **40**, 3986–3995.
6. E. S. Ilton, A. Haiduc, C. L. Cahill, and A. R. Felmy, *Inorg. Chem.*, 2005, **44**, 2986–2988.
7. J. L. Brown, G. Wu, and T. W. Hayton, *Coordin. Chem. Rev.*, 2010, **132**, 7248–7249.
8. P. L. Arnold, D. Patel, C. Wilson, and J. B. Love, *Nature*, 2008, **451**, 315–317.
9. P. L. Arnold, D. Patel, A. J. Blake, C. Wilson, and J. B. Love, *J. Am. Chem. Soc.*, 2006, **128**, 9610–9611.
10. P. L. Arnold, E. Hollis, F. J. White, N. Magnani, R. Caciuffo, and J. B. Love, *Angew. Chem. Int. Edit.*, 2011, **50**, 887–890.
11. P. L. Arnold, A.-F. Pécharman, E. Hollis, A. Yahia, L. Maron, S. Parsons, and J. B. Love, *Nat. Chem.*, 2010, **2**, 1056–1061.
12. C. R. Graves and J. L. Kiplinger, *Chem. Commun.*, 2009, 3831–3853.
13. P. L. Arnold, J. B. Love, and D. Patel, *Coordin. Chem. Rev.*, 2009, **253**, 1973–1978.
14. M. J. Sarsfield and M. Helliwell, *J. Am. Chem. Soc.*, 2004, **126**, 1036–1037.
15. D. D. Schnaars, G. Wu, and T. W. Hayton, *J. Am. Chem. Soc.*, 2009, **131**, 17532–17533.
16. J. L. Brown, G. Wu, and T. W. Hayton, *J. Am. Chem. Soc.*, 2010, **132**, 7248–7249.
17. M. J. Sarsfield, M. Helliwell, and J. Raftery, *Inorg. Chem.*, 2004, **43**, 3170–3179.
18. P. L. Arnold, D. Patel, A. J. Blake, C. Wilson, and J. B. Love, *J. Am. Chem. Soc.*, 2006, **128**, 9610–9611.
19. J. A. Danis, M. R. Lin, B. L. Scott, B. W. Eichhorn, and W. H. Runde, *Inorg. Chem.*, 2001, **40**, 3389–3394.

20. T. S. Franczyk, K. R. Czerwinski, and K. N. Raymond, *J. Am. Chem. Soc.*, 1992, **114**, 8138–8146.
21. J.-C. Berthet, G. Siffredi, P. Thuéry, and M. Ephritikhine, *Eur. J. Inorg. Chem.*, 2007, **2007**, 4017–4020.
22. J. L. Brown, C. C. Mokhtarzadeh, J. M. Lever, G. Wu, and T. W. Hayton, *Inorg. Chem.*, 2011, **50**, 5105–5112.
23. P. L. Arnold, I. J. Casely, Z. R. Turner, and C. D. Carmichael, *Chem.-Eur. J.*, 2008, **14**, 10415–10422.
24. M.-J. Crawford and P. Mayer, *Inorg. Chem.*, 2005, **44**, 5547–5549.
25. M. J. Monreal, R. K. Thomson, T. Cantat, N. E. Travia, B. L. Scott, and J. L. Kiplinger, *Organometallics*, 2011, **30**, 2031–2038.
26. C. D. Carmichael, N. A. Jones, and P. L. Arnold, *Inorg. Chem.*, 2008, **47**, 8577–8579.
27. S. M. Godfrey, D. G. Kelly, C. A. McAuliffe, A. G. Mackie, R. G. Pritchard, and S. M. Watson, *Chem. Commun.*, 1991, 1163.
28. C. K. Narula and H. Noeth, *Inorg. Chem.*, 1985, **24**, 2532–2539.
29. M. Yalpani, J. Serwatowski, and R. Köster, *Chem. Ber.*, 1989, **122**, 3–7.
30. E. Canales, K. G. Prasad, and J. A. Soderquist, *J. Am. Chem. Soc.*, 2005, **127**, 11572–11573.
31. W. Fraenk, T. Habereder, T. M. Klapötke, H. Nöth, and K. Polborn, *J. Chem. Soc. Dalton*, 1999, 4283–4286.
32. E. Khan, S. Bayer, R. Kempe, and B. Wrackmeyer, *Eur. J. Inorg. Chem.*, 2009, **2009**, 4416–4424.
33. E. Khan, R. Kempe, and B. Wrackmeyer, *Appl. Organomet. Chem.*, 2009, **23**, 204–211.
34. A. Solovyev, S. J. Geib, E. Lacôte, and D. P. Curran, *Organometallics*, 2012, **31**, 54–56.
35. W. Gerrard, M. F. Lappert, and B. A. Mountfield, *J. Chem. Soc.*, 1959, 1529.
36. Y. Li and P. C. Burns, *J. Solid State Chem.*, 2002, **166**, 219–228.
37. D. L. Clark, D. W. Keogh, P. D. Palmer, B. L. Scott, and C. D. Tait, *Angew. Chem. Int. Edit.*, 1998, **37**, 164–166.
38. M. Ichikawa, *J. Cryst. Mol. Struct.*, 1981, **11**, 167–172.
39. M. Ichikawa, *Acta Crystallogr. B*, 1978, **34**, 2074–2080.
40. S. R. Sofen, K. Abu-Dari, D. P. Freyberg, and K. N. Raymond, *J. Am. Chem. Soc.*, 1978, **100**, 7882–7887.
41. W. Maringgele, M. Noltemeyer, and A. Meller, *Organometallics*, 1997, **16**, 2276–2284.
42. J.-C. Berthet, P. Thuéry, and M. Ephritikhine, *Inorg. Chem.*, 2005, **44**, 1142–1146.
43. A. E. Enriquez, B. L. Scott, and M. P. Neu, *Inorg. Chem.*, 2005, **44**, 7403–7413.
44. D. M. Wells and J. A. Ibers, *Z. Anorg. Allg. Chem.*, 2010, **636**, 440–442.
45. C. P. Larch, F. G. N. Cloke, and P. B. Hitchcock, *Chem. Commun.*, 2007, 82–84.
46. W. J. Evans, K. A. Miller, J. W. Ziller, and J. Greaves, *Inorg. Chem.*, 2007, **46**, 8008–8018.
47. John Wiley & Sons. and S. Cotton, *Lanthanide and actinide chemistry*, Wiley,, Chichester, England ;;Hoboken, NJ :, 2006.
48. C. L. Cahill and P. C. Burns, *Inorg. Chem.*, 2001, **40**, 1347–1351.
49. C. E. Talley, A. C. Bean, and T. E. Albrecht-Schmitt, *Inorg. Chem.*, 2000, **39**, 5174–5175.
50. K. M. Ok, M. B. Doran, and D. O'Hare, *J. Mater. Chem.*, 2006, **16**, 3366–3368.
51. O. Pons y Moll, T. Le Borgne, P. Thuéry, and M. Ephritikhine, *Acta Crystallogr. C*, 2001, **57**, 392–393.
52. A. Zalkin, D. Perry, L. Tsao, and D. Zhang, *Acta Crystallogr. C*, 1983, **39**, 1186–1188.
53. C. Bois, N. Q. Dao, and N. Rodier, *J. Inorg. Nucl. Chem.*, 1976, **38**, 755–757.

54. D. L. Kepert, J. M. Patrick, and A. H. White, *J. Chem. Soc. Dalton*, 1983, 381–384.
55. R. J. Baker, E. Hashem, M. Motevalli, H. V. Ogilvie, and A. Walshe, *Z. Anorg. Allg. Chem.*, 2010, **636**, 443–445.
56. D. A. Clemente and A. Marzotto, *Acta Crystallogr. B*, 2003, **59**, 43–50.
57. L. H. Jensen, D. Dickerson, and Q. Johnson, *Acta Crystallogr. B*, 1974, **30**, 840–841.
58. N. P. Deifel and C. L. Cahill, *C. R. Chim.*, 2010, **13**, 747–754.
59. P. Nockemann, K. Servaes, R. Van Deun, K. Van Hecke, L. Van Meervelt, K. Binnemans, and C. Görller-Walrand, *Inorg. Chem.*, 2007, **46**, 11335–11344.
60. R. Bohrer, E. Conradi, and U. Müller, *Z. Anorg. Allg. Chem.*, 1988, **558**, 119–127.
61. K. Goossens, K. Lava, P. Nockemann, K. Van Hecke, L. Van Meervelt, K. Driesen, C. Görller-Walrand, K. Binnemans, and T. Cardinaels, *Chem.-Eur. J.*, 2009, **15**, 656–674.
62. M.-O. Sornein, M. Mendes, C. Cannes, C. Le Naour, P. Nockemann, K. Van Hecke, L. Van Meervelt, J.-C. Berthet, and C. Hennig, *Polyhedron*, 2009, **28**, 1281–1286.
63. G. Schreckenbach, P. J. Hay, and R. L. Martin, *J. Comput. Chem.*, 1999, **20**, 70–90.
64. J. A. Bertke and S. D. Bunge, *J. Chem. Soc. Dalton*, 2007, 4647–4649.
65. M. P. Wilkerson, C. J. Burns, D. E. Morris, R. T. Paine, and B. L. Scott, *Inorg. Chem.*, 2002, **41**, 3110–3120.
66. P. L. Arnold, D. Patel, C. Wilson, and J. B. Love, *Nature*, 2008, **451**, 315–317.
67. J.-C. Berthet, G. Siffredi, P. Thuéry, and M. Ephritikhine, *Dalton Trans.*, 2009, 3478.
68. T. W. Hayton and G. Wu, *Inorg. Chem.*, 2009, **48**, 3065–3072.
69. P. Horeglad, G. Nocton, Y. Filinchuk, J. Pécaut, and M. Mazzanti, *Chem. Commun.*, 2009, 1843.
70. L. Natrajan, F. Burdet, J. Pécaut, and M. Mazzanti, *J. Am. Chem. Soc.*, 2006, **128**, 7152–7153.

Chapter 5 Conclusion

A number of cerium, praseodymium and uranyl N-heterocyclic carbene complexes has been synthesised and studied. Differences in reactivity, steric and electronic properties of these complexes were identified in order to give a better insight into the chemistry of the electropositive metal N-heterocyclic carbene compounds.

The structural and electronic characterisation of the cerium mono- and bis-ligand cerium silylamide NHC complexes $[Ce(L^M)(N'')_2]$ **1** and $[Ce(L^M)_2N'']$ **2** were carried out and their reactivity towards small molecules such as Me_3SiCl or I-BBN described. Both complexes show no reaction chemistry of the saturated backbone CH bonds, which had been a problem with the relatively acidic backbone protons of the unsaturated versions of the ligand. An important reactivity of **1** is the ability to add reagents such as EX (E = BBN, $SiMe_3$, X = I,Cl) across the dative metal-carbon bond and to subsequently afford EN'' and $[Ce(L^M)XN'']$ **3**. This was not possible for the unsaturated analogues.

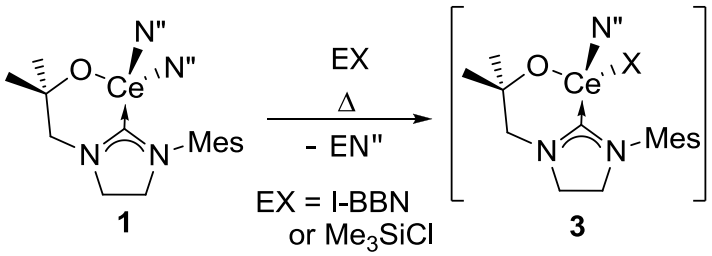

It was found that the reactivity of **1** towards such small molecules is superior to **2** in terms of functionalisation as the latter undergoes ligand abstraction instead of facilitating the desired formation of EN''. When **2** was treated with one equivalent of I-BBN the cerium halide complex $[Ce(L^M)IN'']$ **4** and the boron-NHC compound $[L^MBBN]$ **5** were afforded. Similarly, if **2** was treated with one equivalent of Me_3SiX (X = I, Cl), $[Ce(L^M)(N'')Cl]$ **6** and the enetetramine $[Me_3SiOL^M]_2$ **7** were formed. This difference in reactivity between $[Ce(L^M)(N'')_2]$ **1** and $[Ce(L^M)_2N'']$ **2** is proposed to be due to the steric demand of the NHC $[L^M]$ that prevents the formation of EN'' as opposed to $[L^M]$ abstraction.

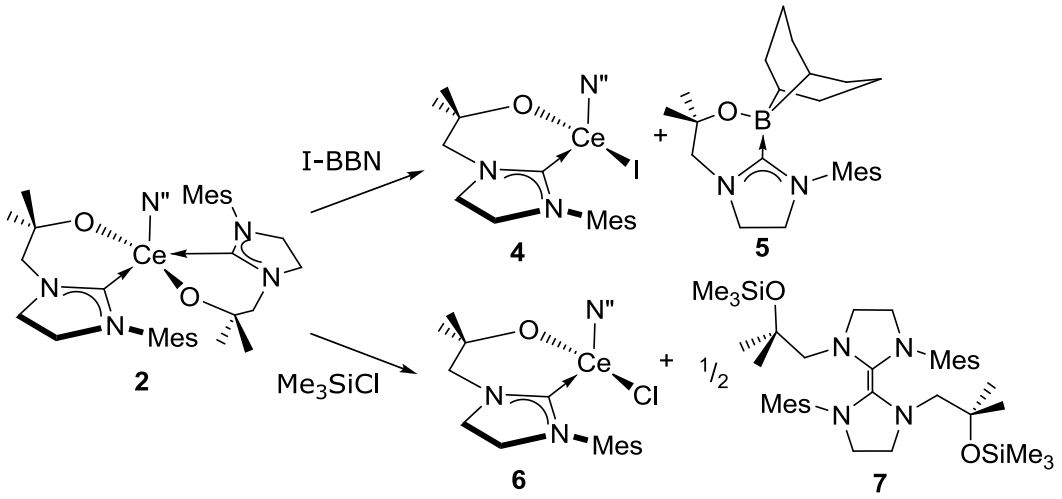

In an attempt to form acyl NHC adducts, the cerium hexachloride anion $[(Ph_2CO)_2H]_3[CeCl_6]$ was formed instead, in a Friedel-Crafts acylation-type reaction with benzoyl chloride, in the stoichiometry of $[Ce(L^M)_2N"]$ and six equivalents of PhC(O)Cl. This indicates that C-Cl bond activation with cerium compounds is a viable goal and that cerium complexes are potential catalysts for acyl transfer reactions but the ligand sets will need to be optimised.

Deprotonation of the bicyclic $[HL^M]$ to form the new $[Li(L^M)]_4$ was achieved by treating $[HL^M]$ either with a mixture of TMEDA/*n*BuLi or with LiN" and a catalytic amount of $[La(N")_3]$. The latter was discovered after attempts to synthesise $[La(L^M)(N")_2]$ and $[La(L^M)_2N"]$ both yielded $[Li(L^M)]_4$ which would crystallise out of solution as the main product. The synthesis of $[Li(L^M)]_4$ opened new salt elimination routes for the synthesis of $[UI_2(L^M)_2]$ and the new $[U^{IV}(L^M)(\eta^5\text{-Cp})_3]$ complex. Preliminary testing of $[U^{IV}(L^M)(\eta^5\text{-Cp})_3]$ towards small molecule activation ($ClPPh_2$, Me_3SiI, H-BNN, I-BBN, BBr_3, Br-catecholborane) showed promising results. The formation of Me_3SiCp was observed by ^1H NMR spectroscopy when $[U^{IV}(L^M)(\eta^5\text{-Cp})_3]$ was treated with Me_3SiI indicating that U^{IV} NHC complexes and $[U^{IV}(L^M)(\eta^5\text{-Cp})_3]$ in particular should be further explored in their ability to activate E-X bonds (E = Me_3Si, BBN, catecholborane; X = I, H, Br).

$[Li(L^M)]_4$ was also employed to synthesise the new $[Ce(L^M)(OAr^{2,6\text{-}tBu})_2]$ complex that could not be synthesised by protonolysis. $[Ce(L^M)(OAr^{2,6\text{-}tBu})_2]$ can be explored in the future towards E-X (E = BBN, $SiMe_3$, X = I, Cl) activation and

comparisons drawn to the cerium silylamide complexes **1** and **2**. Further, investigation into the oxidation chemistry to obtain a Ce^{IV} complex would give valuable insights.

The first praseodymium N-heterocyclic carbene complexes $[Pr(L^M)(N'')_2]$ and $[Pr(L^M)_2N'']$ were synthesised. Oxidation of these complexes was unsuccessful, demonstrating the stability of the +3 oxidation state in molecular praseodymium compounds.

Treatment of $[Pr(L^M)(N'')_2]$ and $[Ce(L^M)_2N'']$ with the oxidant Ph_3CCl afforded the Ln^{III} complexes $[ClCe(\mu\text{-}L^M)_3CeCl_2]$ **8** and $[Cl(N'')Pr(\mu\text{-}L^M)_2Pr(N'')Cl]$ **10**. The dimeric $[N''(L^M)Ce(\mu\text{-}OAr^{3,5\text{-}tBu})_2Ce(L^M)N'']$ **9** was also structurally characterised and solid state variable temperature magnetic measurements were carried out on all Ln^{III} complexes which confirmed their paramagnetic nature. Though suspected to be present no antiferromagnetic interaction between the close f^1 metal cations was found in the three compounds.

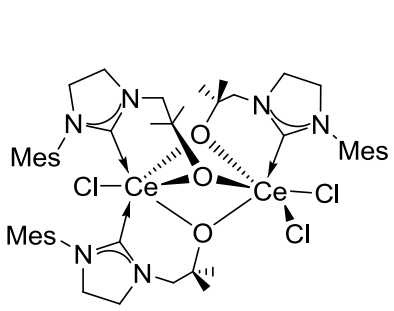

8

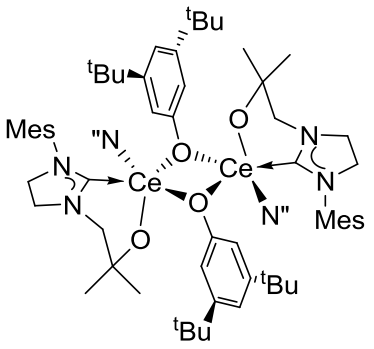

9

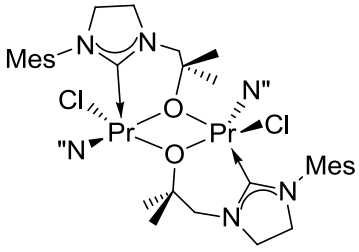

10

The uranyl complexes $[UO_2(L^M)_2]$, $[UO_2N''_2(py)_2]$ and $[UO_2(OAr)_2(py)_2]$ were treated with I-BBN to form the functionalised and deoxygenated uranyl products $[UI_4(L^MH)_2]$ **11**, $[(UI_5)_2(py\text{-}BBN)_2]$ **12** and $[UO_2(py)_5]I$ **13** respectively. The formation of $[UO_2(py)_5]I$ was especially intriguing as it represents an unusual example of $[UO_2]^+$ complex formed through a new route.

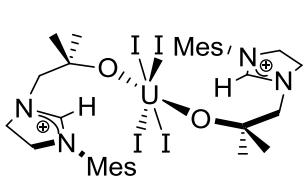

11

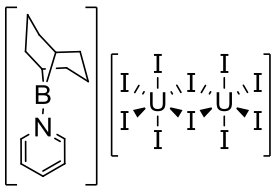

12

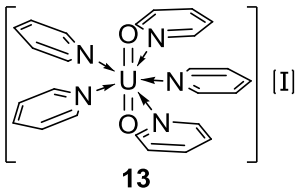

13

When the reaction of $[UO_2(L^M)_2]$ with I-BBN was carried out at low temperature of -70 ˚C formation of the uranyl iodide anion $[UO_2I_4]^{2-}$ was observed. The uranyl halide anion $[UO_2X_4]^{2-}$ (X = Br, Cl) was also afforded when $[UO_2(L^M)_2]$ was treated with other boron reagents such as $C_6H_4BBrO_2$ or $Cl_2BN^iPr_2$. No observable reaction of $[UO_2N''_2(py)_2]$ or $[UO_2(OAr)_2(py)_2]$ with $C_6H_4BBrO_2$ or $Cl_2BN^iPr_2$ emphasised the importance of the NHCs for the functionalisation of the uranyl moiety.

Chapter 6 Experimental Details

6.1 General methods and instrumentation

All manipulations were carried out under a dry, oxygen free dinitrogen atmosphere using standard Schlenk techniques or in a drybox unless otherwise stated. The solvents used were sparged with dinitrogen, dried by passage through activated alumina towers and stored over a potassium mirror (diethyl ether, hexanes, toluene) or activated 4 Å molecular sieves (THF). Deuterated solvents were refluxed over potassium, vacuum transferred and freeze-pump-thaw degassed three times prior to use.

^{1}H NMR spectra were recorded at 298 K unless otherwise stated on a Bruker ARX250, DPX360, AVA400, DMX500 or AVA600 spectrometer at 250.13, 360.13, 500.00 and 599.92 MHz respectively. ^{13}C-{^{1}H}NMR spectra were recorded at 298 K on a Bruker ARX250, DPX360, AVA400 and DMX500 spectrometer at 62.90, 90.55, 100.58 and 125.00 MHz respectively. ^{7}Li-{H} NMR spectra were recorded on a Bruker DMX 500 externally referenced to LiCl at 0 ppm at 194.32 MHz. ^{11}B NMR spectra were recorded at 298 K on a Bruker DMX 500 operating at 160.46 MHz. ^{1}H and ^{13}C-{^{1}H} spectra were referenced internally to residual protio-solvent (^{1}H) or solvent (^{13}C) resonances and are reported to tetramethylsilane (δ = 0 ppm). Chemical shifts are quoted in δ (ppm) and coupling constants in Hertz.

Elemental analyses were carried out by Mr. Stephen Boyer at the London Metropolitan University.

IR spectra were recorded on a JASCO 410 spectrometer and a JASCO 460 plus.

Mass spectra were recorded by the mass spectrometry service at the Department of Chemistry at the University of Edinburgh.

Crystallographic X-ray data were collected at 150 K on a Bruker SMART APEX CCD diffractometer using Mo-Kα radiation (λ = 0.71073 Å) or at 170 K on an Oxford Diffraction Excalibur diffractometer using Cu-Kα radiation (λ = 1.5418 Å). SHELX was used to solve the structures using direct methods and refined using SHELXL-97. All non-hydrogen atoms were refined with anisotropic displacement parameters unless otherwise stated and hydrogen atoms were refined using a riding model.

CeN''_3, LaN''_3,[1] $UI_4(Et_2O)_2$, $UI_3(THF)_4$, UCp_3I,[2] UN''_3,[3] $UO_2Cl_2(THF)_2$, $UO_2N''_2py_2$,[4] KN'',[5] KBz[6] and [HL^{M}][7] were prepared with reference to published

methods. Me_3SiI, Me_3SiCl, Me_3SiN_3, Ph_2PCl and *N,N,N',N'*-tetramethylethylendiamine were distilled under reduced pressure and stored under N_2 prior to use. KO^{t}Bu was sublimed prior to use. Ph_3CCl was recrystallised from toluene and washed with hexanes, LiN" was purchased from Sigma-Aldrich, recrystallised from hexanes and sublimed prior to use. The COS cylinder specifications were 200 ppm of COS in N_2 equipped with a fixed flow regulator (0.5 L/min).

All other reagents were used as purchased.

Microcrystalline samples of **19**, **22** and **24** were prepared under an atmosphere of nitrogen in a glove-box for magnetic measurements. The pulverized mass of the sample was weighed into a gelatin capsule. This capsule was inserted into a sample straw and fixed in place. To avoid exposure to air this sample was transported in a Schlenk tube.

6.2 Synthetic procedures described in Chapter 2

6.2.1 [Ce(L^M)N"$_2$]

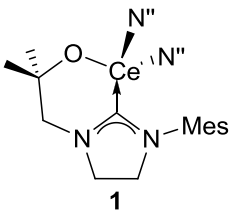

1

A colourless solution of [HL^M] (83.8 mg, 0.32 mmol) in hexanes (5 mL) was added slowly to a yellow solution of [Ce(N")$_3$] (200.0 mg, 0.32 mmol) in hexanes (10 mL) and the solution was stirred at room temperature for 12 hours. Filtration of the clear yellow solution to remove a small quantity of insoluble materials and removal of the volatiles from the filtrate under reduced pressure at 80 °C afforded an orange solid characterised as [Ce(L^M)N"$_2$] (332 mg, 0.46 mmol, 72%). Single crystals suitable for X-ray crystallography were grown from a saturated pyridine solution at 2 °C. **^{1}H (C_6D_6) δ:** -6.29 (6H, *o*-C*H*$_3$), -4.99 (36H, N(Si{C*H*$_3$}$_3$)$_2$), 0.43 (2H, *Ar-H*), 0.77 (3H, *p*-C*H*$_3$), 2.11 (2H, NC*H*$_2$CH$_2$N), 2.31 (2H, NC*H*$_2$C), 11.11 (2H, NCH$_2$C*H*$_2$N), 13.73 (6H, C(C*H*$_3$)$_2$); **Analysis (%)** calc. for $C_{38}H_{64}CeN_5OSi_4$: C, 46.69; H, 8.26; N, 7.78; found: C, 46.74; H, 8.16; N 7.69.

6.2.2 [Ce(L^M)$_2$N"]

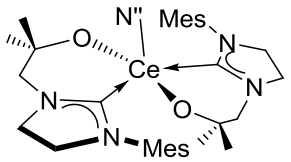

2

A colourless solution of [HL^M] (0.417 g, 1.6 mmol) in toluene (5 mL) was added to a yellow solution of [Ce(N")$_3$] (0.5 g, 0.8 mmol) in toluene (10 mL) from which crystalline yellow blocks formed within 10 minutes. During storage at room temperature for 12 hours a yellow microcrystalline product precipitated from the solution, which was isolated by filtration, washed with hexanes (2 x 5 mL) and dried under reduced pressure affording crystalline yellow [Ce(L^M)$_2$N"] (0.44 g, 67%). **^{1}H (C_6D_6) δ:** 22.4, 15.8, 9.6, 5.5, -9.9 (very broad), 6.45 (bs, 6H, *p*-CH_3), 0.81 (12 H, C(CH_3)$_2$), -0.97 (18H, N(Si{CH_3}$_2$); **Analysis (%)** calc. for $C_{38}H_{64}CeN_5O_2Si_2$: C, 55.70; H, 7.89; N, 8.55; found: C, 55.60; H, 7.80; N 8.63.

6.2.3 Reaction of 2 with Me_3SiN_3

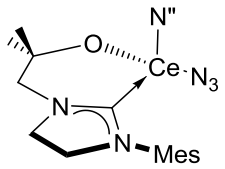

3

a. In an NMR scale experiment one equivalent of colourless Me_3SiN_3 (3.5 μL, 0.02 mmol) was added to an orange solution of **2** (20 mg, 0.02 mmol) in C_6D_6 (0.7 mL) the formation of the paramagnetic [Ce(L^M)(N_3)N"] **3** could be observed by ^{1}H NMR spectroscopy. **^{1}H (C_6D_6) δ:** -6.38 (6H, *o*-CH_3), -5.05 (16H, N(Si{CH_3}$_3$)$_2$, 11.22 (2H, NCH$_2$CH_2N), 13.88 (6H, C(CH_3)$_2$).

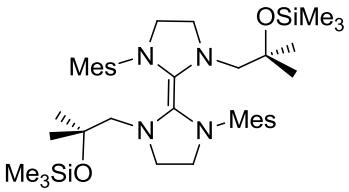

4

b. An orange suspension of **2** (939 mg, 1.1 mmol) in toluene (20 mL) was heated to 60 ˚C for 15 minutes while stirring it vigorously to obtain a clear orange solution. To this solution were added 2 equivalents of Me_3SiN_3 (0.23 mL, 1.7 mmol) with a syringe. Upon addition the colour of the solution turned from dark orange to red. This solution was stored at 3 ˚C for 16 h during which time colourless crystals suitable for X-ray crystallography of [L^MOSiMe_3]$_2$ **4** formed in a 62% yield (453 mg, 0.68 mmol). **^{1}H (C_6D_6) δ:** 0.15 (9H, Si(CH_3)$_3$), 1.27 (6H, C(CH_3)$_2$), 2.15 (6H, *o*-CH_3), 2.28 (3H, *p*-CH_3), 3.28-3.32 (2H, NCH_2CH$_2$N, ^{2}J = 10 Hz), 3.54-3.58 (2H, NCH$_2$CH_2N, ^{2}J = 10 Hz), 3.60 (2H, NCH_2C), 6.81 (2H, *Ar-H*); **^{13}C{^{1}H} (C_6D_6) δ:** 2.75(Si(*C*H$_3$)$_3$), 17.37 ((*C*H$_3$)$_2$N), 18.40 ((*C*H$_3$)$_2$N), 21.04 (*p*-*C*H$_3$), 28.16 (*o*-*C*H$_3$), 50.96 (N*C*H$_2$CH$_2$N), 51.49 (NCH$_2$*C*H$_2$N), 62.81 (N*C*H$_2$C), 76.05 ((*C*H$_3$)$_2$C), 129.39 (*Ar*-C), 130.42 (*Ar*-C), 136.08 (*Ar*-C), 139.70 (*Ar*-C),243.93 (N*C*N).

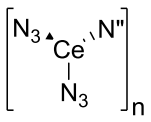

5

Spectroscopic analysis of the proposed byproduct **5** shows a band at 2090 cm^{-1} assigned as an azide stretch.

6.2.4 Reaction of 2 with Me_3SiCl

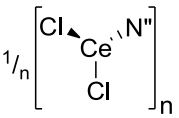

6

An orange suspension of **2** (500 mg, 0.6 mmol) in toluene (10 mL) was heated to 60 ˚C for 15 minutes with vigorous stirring to obtain a clear orange solution. To this solution were slowly added 2 equivalents of Me_3SiCl (0.15 mL, 1.2 mmol) *via* syringe. Upon addition the colour of the solution turned from orange to yellow and $^1/_n[Ce(Cl)_2N"]_n$ **6** precipitates as a yellow solid. The ^{1}H NMR spectrum shows the resonances of the ligand redistribution product $[L^MOSiMe_3]_2$ **4** and some very broad resonances of the proposed compound $^1/_n[Ce(Cl)_2N"]_n$ **6**. **^{1}H (C_6D_6) δ:** -6.60 (6H, *o*-CH_3), -5.16 (16H, N(Si{CH_3}$_3$)$_2$, 11.68 (2H, NCH_2CH_2N), 14.19 (6H, C(CH_3)$_2$).

6.2.5 Reaction of 2 with I-BBN

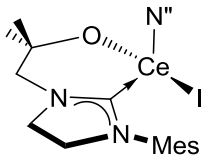

7

a. One equivalent of an orange toluene (10 mL) suspension of **2** (130 mg, 0.16 mmol) was treated with one equivalent of a purple solution of 9-iodo-9-boracyclo[3.3.3]nonane (0.16 mL, 0.16 mmol) in hexanes. Upon addition the reaction mixture turned brown and a brown solid precipitated. The mixture was stirred for 12 hours at room temperature. Then the solution was extracted and the remaining brown filtrand was analysed by solution ^{1}H NMR spectroscopy. The ^{1}H NMR spectrum of the crude mixture shows resonances of [Ce(L^M)(N")I] **7** at **^{1}H (C_6D_6) δ:** -6.31 (6H, *o*-CH_3), -5.01 (16H, N(Si{CH_3}$_3$)$_2$, 11.18 (2H, NCH_2CH_2N), 13.75 (6H, C(CH_3)$_2$). The brown filtrate was reduced under vacuum (4 mL). From this saturated solution colourless single crystals of $[L^MBBN]$ **8** suitable for X-ray crystallography were grown at 3 ˚C in a 66% yield (40 mg, 0.11 mmol). **^{1}H (C_6D_6) δ:** 0.93, 1.18-1.22 (4H, BBN), 1.31 (6H, C(CH_3)$_2$), 1.55-1.58, 1.892-2.04 (5H, BBN), 2.02 (3H, *p*-CH_3), 2.19 (6H, *o*-CH_3), 2.17-2.23 (3H,BBN), 2.68-2.79 (2H, NCH_2CH_2N), 2.80-2.90 (2H, BBN), 2.88-2.91 (2H, NCH_2CH_2N), 2.97 (2H, NCH_2C), 6.65 (2H, *Ar-H*); **Analysis (%)** calc. for $C_{24}H_{37}BN_2O$: C, 75.78; H, 9.80; N, 7.36; found: C, 75.83; H, 9.70; N 7.28.

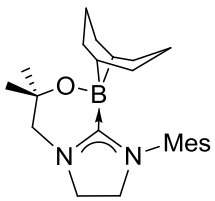

8

b. In an NMR-scale experiment one equivalent of an orange suspension of **2** (20 mg, 0.03 mmol) in deuterated benzene (0.7 mL) was treated with two equivalents of a purple solution of 9-iodo-9-boracyclo[3.3.3]nonane (60 μL, 0.06 mmol) in hexanes. Upon addition, the reaction mixture turned brown and a brown solid precipitated. In the crude mixture of the ^{1}H NMR spectrum in C_6D_6 a broad resonance at δ = -2.84 ppm is assigned to the proposed compound $^{1}/_{n}$[Ce(I)$_2$N''] **9**.

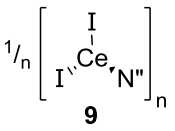

9

6.2.6 [(Ph$_2$CO)$_2$H]$_3$[CeCl$_6$]

An orange suspension of **2** (30 mg, 0.037 mmol) in benzene (0.7 mL) was layered with a hexanes solution of an excess of C_6H_5COCl and left at room temperature for 48 hours, yellow crystals of complex [(Ph$_2$CO)$_2$H]$_3$[CeCl$_6$] **10** formed which could be isolated in a 20% yield (10 mg, 0.007 mmol). **^{1}H (C_6D_6) δ:** -7.33 (br, 10H, Ph-*H*).

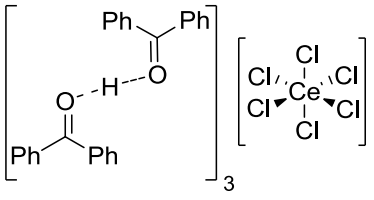

10

6.2.7 [Ce(L^{M})$_2$(OSiMe$_3$)]

a. An orange solution of **2** (40 mg, 0.049 mmol) in toluene (10mL) was treated with one equivalent of COS (5.5 L). The products precipitated immediately as fine beige solid. The products were insoluble in aromatic NMR solvents, infrared spectroscopy was therefore used to characterise the afforded compounds. The N=C=S stretch of the isothionate by-product [Me$_3$SiNCS] of this reaction is clearly assignable in the IR spectrum at 2278 cm^{-1}.

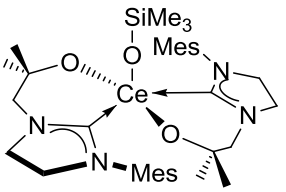

11

b. An orange solution of **2** (7 mg, 0.008 mmol) in THF (0.7 mL) was treated with an excess of CO_2. The products precipitated immediately as a colourless solid. The products were insoluble in aromatic NMR solvents, infrared spectroscopy was therefore used to characterise the afforded compounds. The N=C=O stretch of the isocyanate by-product [Me$_3$SiNCO] of this reaction is clearly assignable in the IR spectrum at 2128 cm^{-1}.

6.2.8 Attempted synthesis of [Ce(L^M)(N")(N^{t}Bu)]

In an NMR scale experiment a yellow solution of [Ce(L^M)(N")$_2$] **1** (20 mg, 0.027 mmol) in deuterated benzene (0.3 mL) was treated with one equivalent of a colourless solution of Ph_3CCl (8 mg, 0.027 mmol) in deuterated benzene (0.3 mL) to form a red solution of [Ce(L^M)(N")$_2$Cl] in situ. This was treated with one equivalent of LiNH^{t}Bu. Analysis by ^{1}H NMR spectroscopy showed that upon addition of the LiNH^{t}Bu the starting material [Ce(L^M)(N")$_2$] **1** had reformed.

6.2.9 [LiL^M]$_4$

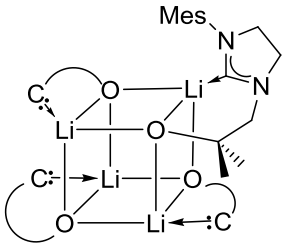

12

a. To a colourless solution of [HL^M] (0.3 g, 1.15 mmol) in THF (10 mL) were quickly added 0.28 mL (1.84 mmol) of TMEDA *via* syringe. Then 0.92 mL (1.47 mmol) of *n*-buthyllithium were added dropwise. The red solution was stirred for 12 hours. After removing the solvent under reduced pressure the beige precipitate was washed with 3 x 10 mL of hexane and the volatiles removed under vacuum to yield yellow [LiL^M]$_4$ **12** in a 52% yield (0.23 g, 0.6 mmol).

b. A colourless solution of [La(N")$_3$][LiN"] (250 mg, 0.32 mmol) in hexanes (5 mL) was combined with a colourless solution of one equivalent of [HL^M] (83 mg, 0.32 mmol) in hexanes (5 mL) and stirred at room temperature for 12 h. The colourless hexanes solution was concentrated under reduced pressure and stored at -30 ˚C for 10 h. At that time colourless single crystals of [LiL^M]$_4$ **12** had formed in a 56% yield (200 mg, 0.18 mmol).

^{1}H (C_6D_6) δ: 1.17 (3H, (C*H*$_3$)$_2$C), 0.95 (3H, (C*H*$_3$)$_2$C), 2.09 (3H, (C*H*$_3$)$_2$N), 2.13 (6H, *o*-C*H*$_3$), 2.26 (3H, (C*H*$_3$)$_2$N), 2.37 (3H, *p*-C*H*$_3$), 2.41 (3H, (C*H*$_3$)$_2$N), 2.46 (3H, (C*H*$_3$)$_2$N), 2.85 – 3.24 (m, 8H, NC*H*$_2$C*H*$_2$N), 6.85 (2H, Ar-*H*); **^{13}C (C_6D_6) δ:** 19.21 (*p*-*C*H$_3$), 21.35 (*o*-*C*H$_3$), 46.37 ((*C*H$_3$)$_2$N), 49.57 ((*C*H$_3$)$_2$C), 54.73 ((*C*H$_3$)$_2$NCH$_2$CH$_2$N(*C*H$_3$)$_2$), 58.59 (NCH$_2$C(*C*H$_3$)$_2$), 65.34 (N*C*H$_2$CH$_2$N), 70.36 (NCH$_2$*C*H$_2$N), 129.57 (*m*-*C*H), 136.27 (*p*-*C*), 136.37 (*o*-*C*), 136.47 (*i*-*C*), 191. 65 (N*C*N); **^{7}Li (C_6D_6) δ:** 0.23; **Analysis (%)** calc.: C, 69.08; H, 10.28; N, 14.65, found: C, 69.00; H, 10.18; N 14.59.

6.2.10 NMR scale synthesis of [$L^M BH_2$]

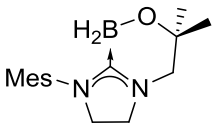

13

[HL^M] (20 mg, 0.8 mmol) was given in a Young-tap NMR tube with $Me_3N{\cdot}BH_3$ (9 mg, 0.12 mmol) and dissolved in deuterated benzene (0.7 mL). The colourless solution was heated at 80 °C for 5 days. Removal of the volatiles and washing with hexane afforded 14.6 mg of **13** (0.54 mmol, 67 %) as a colourless solid. **^{1}H-NMR (C_6D_6) δ**: 1.48 (6H, C(CH_3)$_2$), 2.17 (3H, *p*-Me), 2.40 (6H, *o*-Me), 2.98 (t, 2H, N$CH_2$$CH_2$N), 3.17 (t, 2H, N$CH_2$$CH_2$N), 3.99 (2H, N$CH_2$C), 6.84 (2H, *Ar-H*); **^{13}C (C_6D_6) δ:** 18.97 (*o-C*H_3), 27.69 (C-(*C*H_3)$_2$), 48.10 (*p-C*H_3), 51.17 (N*C*$H_2$$CH_2$N), 57.11 (N$CH_2$*C*$H_2$N), 76.30 (*C*($CH_3$)$_2$), 76.79 (N*C*$H_2$C($CH_3$)$_2$), 130.25 (*Ar-m-C*), 135.19 (*Ar-i-C*), 138.37 (*Ar-o-C*), 136.37 (*o-C*), 143.35 (*Ar-p-C*); **IR (hexane); $\bar{\nu}$ (cm^{-1}):** 2279 (s).

6.2.11 [$U(L^M)_2I_2$]

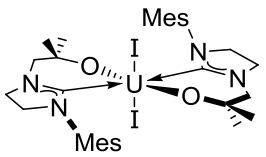

14

a. To a -78 ˚C cooled red solution of [$UI_4(OEt_2)_2$] (117 mg, 0.13 mmol) in diethyl ether (10 mL) was given a -78 ˚C cold yellow solution of [LiL^M·TMEDA] (100 mg, 0.26 mmol) in diethyl ether (10 mL) and stirred while slowly warming up to room temperature. After 30 minutes the solution had turned pink and a pink precipitate formed as the main product. It was isolated by filtration and washed with diethyl ether (3 × 5 mL). The volatiles were removed under reduced pressure to yield [$U(L^M)_2I_2$] **14** as a pink solid (190 mg, 0.10 mmol, 77%). The product is insoluble in aromatic NMR solvents.

b. $UI_3(thf)_4$ (20 mg, 0.03 mmol) and LiL^M·TMEDA (12 mg, 0.03 mmol) were given together in a Young's tap NMR-tube and dissolved in thf (0.7 mL). The solution turned pink and [$U(L^M)_2I_2$] **14** formed as a pink precipitate. The product is insoluble in aromatic NMR solvents.

6.2.12 Attempted crystallisation of [$Cp_3UFe(Cp)(CO)_2$] and [$Cp_3UFe(Cp^*)(CO)_2$]

[$Cp_3UFe(Cp)(CO)_2$] and [$Cp_3UFe(Cp^*)(CO)_2$] were synthesised after the method described by Marks and Sternal and the formation of the respective product confirmed by ^{1}H NMR spectroscopy.[8] The recrystallisation of the products [$Cp_3UFe(Cp(CO)_2$] or [$Cp_3UFe(Cp^*)(CO)_2$] in solution was attempted by storing a concentrated solution

(solvents used were toluene, THF, diethyl ether, hexanes, dimethoxyethane and pyridine) of the complex in one of the solvents listed above at different temperatures of -4 ˚C, -30 ˚C or -70 ˚C. Layering of toluene and hexanes solution and slow solvent evaporation techniques were used as well. A low yield of crystalline solid was afforded. Unfortunately, all single crystals that were suitable for X-ray crystallography were of a byproduct of the reaction the dimer $[Fe(CO)_2Cp]_2$.

6.2.13 Attempted synthesis of $[U(L^MSiPh_3)(N")_2(AuR)]$

a. A colourless solution of $[(Ph_3P)AuSiPh_3]$ (5 mg, 0.007 mmol) in deuterated benzene (0.3 mL) and a blue solution of $[U(L^M)N"_2]$ (5 mg, 0.007 mmol) in deuterated benzene (0.3 mL) were combined in an ambered Young's Tap NMR tube. No reaction was observed at room temperature by ^{1}H NMR spectroscopy. The solution was heated to 80 ˚C for 12 hours. After that time the colour of solution changed to green. Single crystals of a $[Au(L^M)_2]$ complex suitable for X-ray crystallography were grown by slow evaporation of benzene.

b. A colourless solution of $[(IPr)AuSiPh_3]$ (10 mg, 0.015 mmol) in dimethoxyethane (0.3 mL) and a blue solution of $[U(L^M)N"_2]$ (5 mg, 0.007 mmol) in dimethoxyethane (0.3 mL) were combined in an ambered Young's Tap NMR tube. No reaction was observed at room temperature by ^{1}H NMR spectroscopy. The solution was heated to 80 ˚C for 48 hours but no reaction was observed.

6.2.14 Attempted synthesis of $[U(L^MSiPh_3)(Cp)_3(AuR)]$

A colourless solution of $[(IPr)AuSiPh_3]$ (9 mg, 0.01 mmol) in deuterated benzene (0.3 mL) and a brown solution of $[U(L^M)(\mu^5\text{-}Cp)_3]$ (9 mg, 0.01 mmol) in benzene (0.3 mL) were combined in an ambered Young's Tap NMR tube. No reaction was observed at room temperature. The solution was heated to 80 ˚C for 48 hours but no reaction was observed.

6.2.15 [U(L^{M})(μ^5-Cp)$_3$]

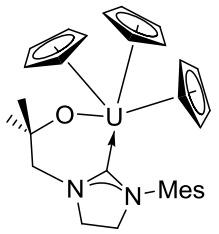

16

A yellow solution of [LiL^{M}]$_4$ (130 mg, 0.34 mmol) in THF (5 mL) was added to a brown suspension of [Cp$_3$UI] (190 mg, 0.34 mmol) in THF (5 mL) and the mixture was refluxed at 80 ˚C for 12 h. Then the volatiles were removed under reduced pressure to yield a brown solid that was dried under reduced pressure for 10 h at 40 ˚C. Extraction with toluene (15 mL) and subsequent washing with hexanes (10 mL) yielded 71 % (170 mg, 0.24 mmol) of [U(L^{M})(μ^5-Cp)$_3$] **15** as a brown solid. **^{1}H-NMR (C$_6$D$_6$)** δ: -18.65 (3H, C(C*H*$_3$)$_2$), -18.32 (3H, C(C*H*$_3$)$_2$),, -0.75 (5H, Cp-*H*), -0.27 (5H, Cp-*H*), 0.98 (5H, Cp-*H*), 1.66 (3H, *p*-Me), 3.13 (m, 2H, NC*H*$_2$CH$_2$N), 3.14 (m, 4H, NC*H*$_2$CH$_2$N and NC*H*$_2$C) , 4.86 (1H, *Ar-H*), 5.00 (1H, *Ar-H*), 18.05 (3H, *o*-Me), 18.675 (3H, *o*-Me); **Analysis (%)** calc.: C, 53.75; H, 5.53; N, 4.04, found: C, 43.88; H, 5.37; N 4.72 the difference between the calculated and measured elemental analysis for carbon is due to the formation of uranium carbide

6.2.16 Reactions of [U(L^{M})(μ^5-Cp$_3$] with EX

NMR experiments were carried out in Young's Tap NMR tubes where a benzene solution (0.3 mL) of **13** was treated with one equivalent of a benzene solution (0.3 mL) of one equivalent of EX (EX = Me$_3$SiI, I-BBN, Br-catecholborane and H-BBN). The solutions were then heated to 80 ˚C for 12 h. Upon cooling to room temperature a solid precipitated out of solution. Analyses by ^{1}H NMR spectroscopy indicated a reaction.

6.2.17 Attempted synthesis of [Ce(OAr$^{3,5\text{-}tBu}$)$_3$]

A yellow solution of [Ce(N")$_3$] (20 mg, 0.032 mmol) in THF (0.4 mL) was treated with 3 equivalents of a colourless solution of HOAr$^{3,5\text{-}tBu}$ (20 mg, (0.97 mmol) in THF (0.3 mL) and as no reaction was observed at room temperature, refluxed at 80 ˚C for 48 h. The ^{1}H-NMR spectrum indicated that a multitude of products had been formed. Performing the reaction at a different temperature (40 ˚C, 60 ˚C) or in a different solvent (coordinating or non) did not yield a result from which the desired product could be isolated.

6.2.18 [Ce(OAr$^{2,6\text{-tBu}}$)$_3$]

[Ce(OAr$^{2,6\text{-tBu}}$)$_3$] was synthesised in a variation of the experimental synthesis published by Lappert and co-workers (Inorganic Synthesis 1990, 27, 164-168). To a yellow solution of [Ce(N")$_3$] (1274 mg, 2.05 mmol) in toluene (10 mL) was given a yellow solution of HOAr$^{2,6\text{-tBu}}$ (1269 mg, 6.15 mmol) in toluene (5 mL) and stirred for 2 days at room temperature. After removal of the volatiles under reduced pressure the residue was washed with hexanes (3 × 5 mL) and dried under reduced pressure to yield [Ce(OAr$^{2,6\text{-tBu}}$)$_3$] as a green solid (740 mg, 0.8 mmol,). **^{1}H (C_6D_6) δ:** -3.04 (54H, *tBu*), 9.58 (3H, *p*-Ar), 10.88 (6H, *m*-Ar).

6.2.19 [Ce(OAr$^{2,6\text{-tBu}}$)$_3$(HL^M)]

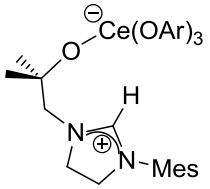

17

To a solution of [Ce(OAr$^{2,6\text{-tBu}}$)$_3$] (349 mg, 0.46 mmol) in toluene (10 mL) was added a solution of [HL^M] (120 mg, 0.46 mmol) in toluene (5 mL) and stirred at room temperature for 12 hours. The volatiles were reduced in vacuum to yield a colourless solid that was washed with hexanes (3 × 5 mL) to yield [Ce(OAr$^{2,6\text{-tBu}}$)$_3$(HL^M)] as a white solid (361 mg, 0.35 mmol, 77%). Single crystals suitable for X-ray crystallography were grown from a saturated toluene solution at -30 ˚C. **^{1}H (C_6D_6) δ:** -3.92 (6H, *o*-C*H*$_3$), -1.17 (36H, *tBu*), 1.42-1.63 (8H, C(C*H*$_3$)$_2$, NC*H*$_2$CH$_2$N), 1.65-1.81 (2H, NCH$_2$C*H*$_2$N), 2.44 (2H, NC*H*$_2$C), 3.19 (3H, *p*-C*H*$_3$), 7.34 (2H, *Ar-H*), 9.04 (2H, Ar$^{2,6\text{-tBu}}$ p-*H*), 10.12 (4H, Ar$^{2,6\text{-tBu}}$ m-*H*); **Analysis (%)** calc. for $C_{58}H_{87}CeN_2O_4$: C, 68.54; H, 8.63; N, 2.76; found: C, 68.65; H, 8.72; N 2.63.

6.2.20 [Ce(OAr$^{2,6\text{-tBu}}$)$_2$(L^M)]

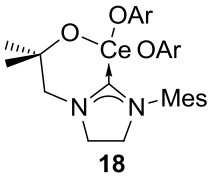

18

A yellow solution of [LiL^M] (39 mg, 0.15 mmol) in toluene (4 mL) was added to a green solution of [Ce(OAr$^{2,6\text{-tBu}}$)$_3$] (110 g, 0.15 mmol) in toluene (4 mL) to give a yellow solution that was stirred for 12 h at room temperature. [LiOAr$^{2,6\text{-tBu}}$] **17** started to precipitate out of solution as a brown solid after 10 minutes. The solid was isolated by filtration and washed with hexanes (3 x 2 mL). Removal of the volatiles under reduced pressure afforded [Ce(OAr$^{2,6\text{-tBu}}$)$_2$(L^M)] **17** as a yellow solid in a 50% yield (56 mg, 0.07 mmol). **^{1}H (C_6D_6) δ:** -3.92 (6H, *o*-C*H*$_3$), -1.17 (36H, *tBu*), 1.42-1.63 (8H, C(C*H*$_3$)$_2$, NC*H*$_2$CH$_2$N), 1.65-1.81 (2H, NCH$_2$C*H*$_2$N), 2.44 (2H, NC*H*$_2$C), 3.19 (3H, *p*-C*H*$_3$), 7.34

(2H, *Ar-H*), 9.04 (2H, $Ar^{2,6\text{-}tBu}$ p-*H*), 10.12 (4H, $Ar^{2,6\text{-}tBu}$ m-*H*); **Analysis (%)** calc. for $C_{44}H_{65}CeN_2O_3$: C, 65.23; H, 8.09; N, 3.46; found: C, 65.18; H, 8.17; N 3.37.

6.3 Synthetic procedures described in Chapter 3

6.3.1 [Ce(L^M)(N")$_2$Cl]

A colourless solution of [HL^M] (79 mg, 0.3 mmol) in toluene (3 mL) was added to a dark red slurry of [Ce(N")$_3$Cl] (200 mg, 0.3 mmol) in toluene (5 mL). The mixture turned dark purple immediately and was stirred for 5 h at room temperature. Recrystallisation from toluene at -30 ˚C afforded [Ce(L^M)(N")$_2$Cl] as a red solid in a 17% yield (40 mg, 0.05 mmol). **^{1}H (C_6D_6) δ:** 0.54 (36H, N(Si{C*H*$_3$}$_3$)$_2$), 1.17 (6H, C(C*H*$_3$)$_2$), 2.05 (3H, *p*-C*H*$_3$), 2.32 (6H, *o*-C*H*$_3$), 2.74-2.79 (m, 2H, NC*H*$_2$CH$_2$N), 2.96-3.01 (m, 2H, NCH$_2$C*H*$_2$N), 2.97 (2H, NC*H*$_2$C), 6.80 (2H, *Ar-H*).

6.3.2 [ClCe(μ-L^M)$_3$CeCl$_2$]

a. To a yellow solution of **2** (50 mg, 0.061 mmol) in toluene (3 mL) was added a colourless solution of Ph_3CCl (26 mg, 0.092mmol) in toluene (2 mL) to give a dark red solution that was stirred for 12 h at room temperature by which time a beige precipitate has formed. The solution was removed by filtration and the solid washed with hexanes (3 × 3 mL). Removal of the volatiles under reduced pressure afforded [ClCe(μ-L^M)$_3$CeCl$_2$] **19** in a 31% yield as a beige solid (23 mg, 0.019 mmol). Single crystals suitable for X-ray crystallography were grown from a saturated benzene solution at room temperature.

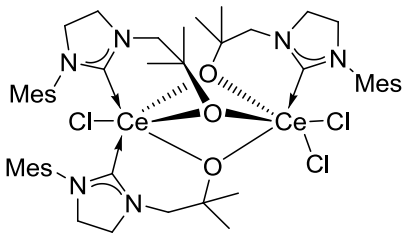

20

b. A mixture of [LiL^M] (118 mg, 0.48 mmol) and [CeCl$_3$(THF)$_{3.5}$] (122 mg, 0.32 mmol) in THF (10 mL) was refluxed at 80 ˚C for 12 h. The solvent was removed under reduced pressure and the remaining solid extracted with toluene (3 × 5 mL). Removal of solvent from the filtrate under reduced pressure yielded an orange solid (120 mg, 0.10 mmol, 32 %).

^{1}H (C_6D_6) δ: 0.55 (3H, *p*-C*H*$_3$), 0.62 (6H, *o*-C*H*$_3$), 0.82 (6H, *o*-C*H*$_3$), 0.84 (3H, *p*-C*H*$_3$), 1.16 (6H, C(C*H*$_3$)$_2$), 2.17 (3H, *p*-C*H*$_3$), 2.19 (6H, *o*-C*H*$_3$), 2.42 (12H, C(C*H*$_3$)$_2$), 2.56 (2H, NC*H*$_2$C), 2.73 (2H, NC*H*$_2$CH$_2$N), 2.85 (4H, NC*H*$_2$C*H*$_2$N), 2.97 (4H,

NCH_2CH_2N), 3.15 (4H, NCH_2C, 2H, NCH_2CH$_2$N), 3.34 (2H, NCH_2C), 6.85 (2H, *Ar-H*), 6.86 (2H, *Ar-H*), 6.88 (2H, *Ar-H*); **Analysis (%)** calc. for $C_{48}H_{69}Ce_2Cl_3N_6O_3$: C, 49.50; H, 5.97; N, 7.22; found: C, 49.39; H, 5.90; N 7.12.

6.3.3 [Ce(L^M)$_2$I]

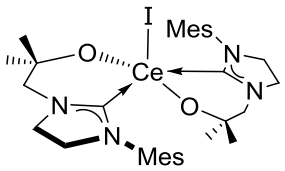

21

A purple solution of I_2 (31 mg, 0.12 mmol) in toluene (2 mL) was added to an orange slurry of **2** (99 mg, 0.12 mmol) in toluene (5 mL). The brown solution was stirred for 12 h at room temperature at which point [Ce(L^M)$_2$I] **20** had precipitated as a brown solid with a brown solution. The solution was removed by filtration and the brown solid washed with hexanes (3 × 1 mL). The solid was dried under reduced pressure to afford [Ce(L^M)$_2$I] **20** in a 49% yield (46 mg, 0.06 mmol). **^{1}H (C_6D_6) δ:** -3.68 (3H, *p*-CH_3), -3.33 (6H, *o*-CH_3), 0.31 (6H, C(CH_3)$_2$), 2.11 (2H, NCH$_2$CH_2N), 2.98 (2H, NCH_2CH$_2$N), 8.63 (2H, NCH_2C), 12.55 (2H, *Ar-H*); **Analysis (%)** calc. for $C_{32}H_{46}CeIN_4O_2$: C, 48.91; H, 5.90; N, 7.13; found: C, 48.83; H, 5.99; N 7.05.

6.3.4 Attempted synthesis of [Ce(L^M)$_2$(N")Cl] by treatment of 2 with $PbCl_2$

Toluene (10 mL) was added to a mixture of $PbCl_2$ (100 mg, 0.36 mmol) and **2** (200 mg, 0.24 mmol) to give an orange solution and white solid at room temperature while stirring. The orange solution turned brown within 10 minutes and the white insoluble $PbCl_2$ had turned dark gray. After 3 hours a brown solution was extracted from a gray solid that was believed to be elemental lead. The volatiles of the filtrate were removed under reduced pressure to yield 207 mg of an orange solid. **^{1}H (C_6D_6) δ:** 1.25 (6H, *o*-CH_3), 1.57 (6H, *o*-CH_3), 2.01 (6H, C(CH_3)$_2$), 2.02 (6H, C(CH_3)$_2$), 2.16 (6H, *p*-CH_3), 2.59 (d, 2H, NCH_2C), 2.66-2.75 (m, 2H, NCH_2CH$_2$N), 2.91-3.01 (m, 2H, NCH$_2$CH_2N), 4.08 (d, 2H, NCH_2C), 6.59 (2H, *Ar-H*), 6.72 (2H, *Ar-H*).

6.3.5 Attempted oxidation of 2

a.Treatment of **2** with CuCl, $CuCl_2$, HgI_2 and $NiCl_2$

A slurry of **2** (20 mg, 0.02 mmol) in deuterated benzene (0.7 mL) was added to one equivalent of the respective metal halide. When no reaction could be observed at

room temperature the mixture was heated to 80 ˚C for 7 days and checked by ^{1}H NMR spectroscopy at regular intervals. No reaction was observed.

b. Treatment of **2** with N-bromosuccinimide

A colourless slurry of N-bromosuccinimide (4 mg, 0.024 mmol) in deuterated benzene (0.3 mL) was added to an orange slurry of **2** (20 mg, 0.024 mmol) in deuterated benzene (0.3 mL) to give a brown solution. A brown solid precipitated immediately. THF (0.5 mL) was added to solubilise the mixture. ^{1}H NMR spectroscopy showed decomposition and resonances of [HL^{M}].

c. Treatment of **2** with (dichloroiodo)benzene

A colourless slurry of (dichloroiodo)benzene (7 mg, 0.024 mmol) in deuterated benzene (0.3 mL) was added to an orange slurry of **2** (20 mg, 0.024 mmol) in deuterated benzene (0.3 mL) to give a brown solution. ^{1}H NMR spectroscopy showed only diamagnetic resonances but no carbene resonance could be found in the ^{13}C NMR spectrum.

6.3.6 [Ce(L^{M})(OAr$^{2,4,6\text{-}tBu}$)N"]

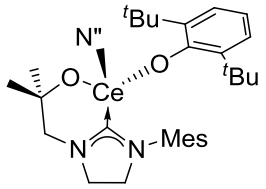

23

To a yellow solution of **1** (20 mg, 0.027 mmol) in deuterated benzene (0.3 mL) was added a colourless solution of 2, 6-di-*tert*-butylphenol (7 mg, 0.027 mmol) in deuterated benzene (0.3 mL) and heated to 80 ˚C h, for 72 h. **^{1}H (C$_6$D$_6$) δ:** -3.83 (3H, *p*-C*H*$_3$), -2.13 (18H, N(Si{C*H*$_3$}$_3$)$_2$), -1.18 (18H, *o*-^{t}Bu), -0.78 (2H, NC*H*$_2$CH$_2$N), -0.67 (6H, C(C*H*$_3$)$_2$), 0.67 (6H, *o*-C*H*$_3$), 2.29 (1H, Ar-*H*), 3.28 (2H, Ar-*H*), 9.07 (2H, NCH$_2$C*H*$_2$N), 10.18 (2H, NC*H*$_2$C), 10.77 (2H, Ar-*H*).

6.3.7 [N"(L^{M})Ce(μ-OAr$^{3,5\text{-}tBu}$)$_2$Ce(L^{M})N"]

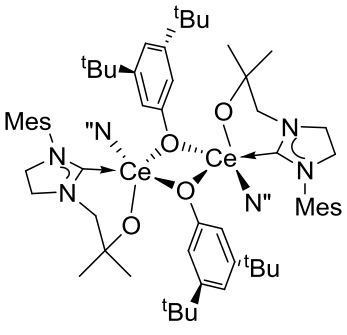

24

To a yellow solution of [Ce(L^{M})N"$_2$] (366 mg, 0.51 mmol) in toluene (10 mL) was added a colourless solution of 3,5-di-*tert*-butylphenol (105 mg, 0.51 mmol) in toluene (5 mL) and heated to 80 ˚C for 12 h. The volume of the toluene solution was reduced, hexanes added (3 mL) and [N"(L^{M})Ce(μ-OAr$^{3,5\text{-}tBu}$)$_2$Ce(L^{M})N"] **21** recrystallised in a 68% yield (530 mg, 0.35 mmol) after storage at -30 ˚C for 12 h. **^{1}H (C$_6$D$_6$) δ:** -9.84 (9H), -7.67

(18H), -2.85 (18H), 6.43 (6H), 8.30 (6H), 10.24 (3H); **Analysis (%)** calc. for $C_{71}H_{123}Ce_2N_6O_5Si_4$: C, 56.51; H, 8.09; N, 5.48; found: C, 56.43; H, 8.08; N 5.47.

6.3.8 [Pr(L^M)N"$_2$]

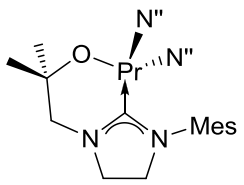

25

To a pale green solution of [PrN"$_3$] (200 mg, 0.38 mmol) in toluene (10 mL) was added a colourless solution of [HL^M] (99 mg, 0.38 mmol) in toluene (5 mL) to give a light pink solution that was stirred for 12 h at room temperature. Removal of the volatiles under reduced pressure, washing with hexanes (2 × 5 mL) and subsequent removal of solvent under reduced pressure afforded [Pr(L^M)N"$_2$] **22** in a 59% yield as a light pink solid (161 mg, 0.22 mmol). **^{1}H (C_6D_6) δ:** -17.77 (6H, C(C*H*$_3$)$_2$), -12.09 (2H, NC*H*$_2$C), -8.59 (36H, Si(C*H*$_3$)$_3$), -0.66 (2H, NC*H*$_2$CH$_2$N), 1.07 (3H, *p*- C*H*$_3$), 5.53 (2H, NCH$_2$C*H*$_2$N), 35.46 (6H, ***o***- C*H*$_3$), 62.19 (2H, *Ar*); **Analysis (%)** calc. for $C_{28}H_{59}N_4OPrSi_4$: C, 46.69; H, 8.96; N, 7.78; found: C, 46.52; H, 8.93; N 7.75.

6.3.9 [Pr(L^M)$_2$N'']

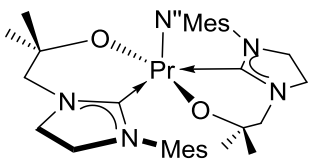

26

To a pale green solution of [PrN"$_3$] (200 mg, 0.38 mmol) in toluene (10 mL) was added a colourless solution of [HL^M] (198 mg, 0.76mmol) in toluene (5 mL) to give a pale pink solution that was stirred for 12 h at room temperature. Removal of the volatiles under reduced pressure, washing with hexanes (2 × 5 mL) and subsequent removal of solvent under reduced pressure afforded [Pr(L^M)$_2$N''] **23** in a 62% yield as a colourless solid (192 mg, 0.23 mmol). Crystals suitable for X-ray crystallography were grown from a saturated toluene solution. **^{1}H (C_6D_6) δ:** -17.58 (12H, ***o***-C*H*$_3$), -1.77 (6H, *p*- C*H*$_3$), -0.69 (4H, *Ar-H*), 3.69 (4H, NC*H*$_2$C), 8.63 (18H, Si(C*H*$_3$)$_3$), 20.69 (br, 4H, NC*H*$_2$CH$_2$N), 22.49 (br, 12H, C(C*H*$_3$)$_2$), 31.80 (br, 4H, NCH$_2$C*H*$_2$N); **Analysis (%)** calc. for $C_{38}H_{64}N_5O_2PrSi_2$: C, 55.66; H, 7.87; N, 8.54; found: C, 55.59; H, 7.96; N 8.44.

6.3.10 Attempted oxidation of [Pr(L^M)N"$_2$] and [Pr(L^M)$_2$N'']

Attempted oxidation experiments of [Pr(L^M)N"$_2$] and [Pr(L^M)$_2$N''] were carried out in NMR scale experiments in a Young's Tap NMR tube. Typically a deuterated benzene solution (0.3 mL) of the respective praseodymium complex (20 mg, (0.028 mmol for **22** and 0.024 mmol for **23**) was combined with one equivalent of an oxidising

agent in deuterated benzene (0.3 mL). The oxidants used were: pyridine-N-oxide, AgO, $AgNO_2$, Ag_2SO_4, *N*-bromosuccinimide, Ph_3CCl, $AgNO_3$, AgCN, $AgBF_4$, HgI_2, $PbCl_2$ and $CuCl_2$.

6.3.11 [Pr(OAr$^{2,6\text{-}tBu}$)$_3$]

[Pr(OAr$^{2,6\text{-}tBu}$)$_3$] was synthesised in a variation of the experimental synthesis published by Lappert and co-workers (Inorganic Synthesis 1990, 27, 164-168). To a green solution of [Pr(N")$_3$] (730 mg, 1.4 mmol) in toluene (10 mL) was given a yellow solution of HOAr$^{2,6\text{-}tBu}$ (862 mg, 4.2 mmol) in toluene (5 mL) and stirred for 2 days at room temperature. After removal of the volatiles under reduced pressure the residue was washed with hexanes (3 × 5 mL) and dried under reduced pressure to yield [Pr(OAr$^{2,6\text{-}tBu}$)$_3$] as a green solid (636 mg, 0.8 mmol, 57%). **^{1}H (C_6D_6) δ:** -3.03 (54H, *tBu*), 9.59 (t, 3H, *p*-Ar), 10.88 (d, 6H, *m*-Ar).

6.3.12 Attempted oxidation of [Pr(OAr$^{2,6\text{-}tBu}$)$_3$]

Attempted oxidation experiments of [Pr(OAr$^{2,6\text{-}tBu}$)$_3$] were carried out in NMR scale experiments in a Young's Tap NMR tube. Typically a solution of [Pr(OAr$^{2,6\text{-}tBu}$)$_3$] (20 mg, 0.026 mmol) in deuterated benzene (0.3 mL) was combined with one equivalent of an oxidating agent in deuterated benzene (0.3 mL). The oxidants used were: $AgBF_4$ and Ph_3CCl. Cyclic voltammetry measurements were carried out to determine at what potential the electrochemical oxidation of the compound occurs. The voltammetry study in THF showed no oxidation of the compound between a potential of -2 to 2 V at different scan rates.

6.3.13 [Cl(N")Pr(μ-L^M)$_2$Pr(N")Cl]

To a colourless solution of [Pr(L^M)N"$_2$] (23 mg, 0.03 mmol) in deuterated benzene (0.3 mL) was added a colourless solution of Ph_3CCl (9 mg, 0.03 mmol) in deuterated benzene (0.3 mL). Upon addition the solution turned purple. Single crystals of [Cl(N")Pr(μ-L^M)$_2$Pr(N")Cl] **24** suitable for X-ray crystallography were grown by slow evaporation of the volatiles in a 38% yield (92 mg, 0.08 mmol). **^{1}H (C_6D_6) δ:** -19.64 (6H, *p*- C*H*$_3$), -5.09 (36H, Si(C*H*$_3$)$_3$), -0.67 (12H, ***o***- C*H*$_3$), 5.47 (4H,

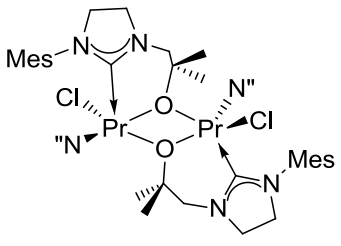

27

NCH_2C), 12.94 (12H, C(CH_3)$_2$), 14.61 (4H, NCH_2CH_2N), 19.42 (4H, NCH$_2$CH_2N), 22.43 (4H, Ar-*H*); **Analysis (%)** calc. for $C_{44}H_{82}Cl_2N_6O_2Pr_2Si_4$: C, 44.33; H, 6.93; N, 7.05; found: C, 44.43; H, 6.82; N 6.98.

6.4 Synthetic procedures described in Chapter 4

6.4.1 [$UO_2(L^M)_2$]

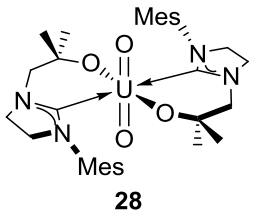

28

a. To a red solution of [UO_2(N")$_2$(py)$_2$] (2.14 g, 2.9 mmol) in toluene (20 mL) was added a colourless solution of [HL^M] (1.48 g, 5.7 mmol) in toluene (5 mL) and stirred at room temperature for 12 hours. Yellow [$UO_2(L^M)_2$] **25** had precipitated out of solution, was isolated by filtration and then the solid was washed with hexanes (3 × 5 mL). The volatiles were removed under reduced pressure to yield [$UO_2(L^M)_2$] **25** as a yellow solid (1.70 g, 2.2 mmol, 74%).

b. To a slurry of [$UO_2Cl_2(THF)_2$] (100 mg, 0.2 mmol) in toluene (5 mL) was added a solution of [LiL^M]$_4$ (110 mg, 0.1 mmol) in toluene (3 mL) and stirred at room temperature for 12 hours. Extraction with toluene (3 × 5 mL) and subsequent removal of the volatiles under reduced pressure afforded [$UO_2(L^M)_2$] **25** in a 60% yield (47 mg, 0.06 mmol) as a yellow solid.

^{1}H (C_6D_6) δ: 1.48 (6H, C(CH_3)$_2$), 2.23 (3H, *p*-CH_3), 2.29 (6H, *o*-CH_3), 3.13 (4H, NCH_2CH_2N), 3.68 (2H, NCH_2C), 6.82 (2H, *Ar-H*).

6.4.2 [$UI_4(HL^M)_2$]

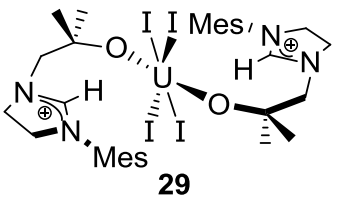

29

A yellow suspension of [$UO_2(L^M)_2$] (20 mg, 0.025 mmol) in toluene (0.5 mL) was layered with 2 equivalents of a purple 1M hexanes solution of I-BBN (51μL, 0.051 mmol) in a YT-NMR tube. After 12 h some of the starting material [$UO_2(L^M)_2$] had also precipitated out of the solution, and at the interface of the two phases a brown solid had formed. The mixture was sonicated for 20 minutes to afford a brown solid and an orange solution. The brown solid was isolated by filtration and recrystallised from a pyridine solution by hexane layering. This afforded single crystals of [$UI_4(HL^M)_2$] **27** suitable for X-ray crystallography in a 15% yield (7 mg,

0.005 mmol). **^{1}H (C_6D_6) δ:** -30.18 (12H), -27.04 (4H), -6.71 (4H), -1.75 (2H), 9.35 (6H), 11.59 (4H), 57.84 (4H), 83.85 (12H).

6.4.3 $[UO_2I_4][(L^M)\text{-}B(cyoc)]_2$

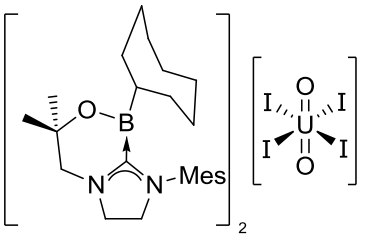

31

A yellow suspension of **25** (230 mg, 0.29 mmol) in toluene (5 mL) was treated with four equivalents of a purple 1M hexanes solution of I-BBN (1.17 mL, 1.17 mmol) at -78 ^{o}C and slowly warmed up over night. After 12 h a brown solid had precipitated out of solution. It was isolated by filtration and washed with hexanes (3 × 1 mL). Residual solvents were removed by solvent to yield $[UO_2I_4][(L^M)\text{-}B(cyoc)]_2$ **28** in a 43% yield (192 mg, 0.13 mmol). Single crystals suitable for X-ray crystallography were grown from a saturated toluene solution layered with hexanes at -30 ^{o}C. **^{1}H (C_6D_6) δ:** 0.95-0.97 (m, 2H, cyoc), 1.00-1.06 (m, 2H, cyoc), 1.08-1.13 (m, 2H, cyoc), 1.30 (6H, C(C*H*$_3$)$_2$), 1.35-1.40 (m, 2H, cyoc), 1.65-1.73 (m, 2H, cyoc), 1.76-1.81 (m, 3H, cyoc), 1.95-2.00 (m, 2H, cyoc), 2.02 (3H, *p*-C*H*$_3$), 2.19 (6H, *o*-C*H*$_3$), 2.69-2.74 (m, 2H, NC*H*$_2$CH$_2$N), 2.90-2.95 (m, 2H, NCH$_2$C*H*$_2$N), 2.98 (2H, NC*H*$_2$C), 6.65 (2H, *Ar-H*).

6.4.4 Treatment of 25 with Br-BBN

A yellow suspension of $[UO_2(L^M)_2]$ **25** (20 mg, 0.03 mmol) in deuterated benzene (0.3 mL) was treated with two of a colourless solution of Br-BBN (10 mg, 0.05 mmol) in deuterated benzene (0.3 mL). The ^{1}H NMR spectrum shows the same resonances as for $[UO_2I_4][(L^M)\text{-}B(cyoc)]_2$ **28** and is therefore believed to be $[UO_2Br_4][(L^M)\text{-}B(cyoc)]_2$ **^{1}H (C_6D_6) δ:** . **^{1}H (C_6D_6) δ:** 0.95-0.97 (m, 2H, cyoc), 1.00-1.06 (m, 2H, cyoc), 1.08-1.13 (m, 2H, cyoc), 1.30 (6H, C(C*H*$_3$)$_2$), 1.35-1.40 (m, 2H, cyoc), 1.65-1.73 (m, 2H, cyoc), 1.76-1.81 (m, 3H, cyoc), 1.95-2.00 (m, 2H, cyoc), 2.02 (3H, *p*-C*H*$_3$), 2.19 (6H, *o*-C*H*$_3$), 2.69-2.74 (m, 2H, NC*H*$_2$CH$_2$N), 2.90-2.95 (m, 2H, NCH$_2$C*H*$_2$N), 2.98 (2H, NC*H*$_2$C), 6.65 (2H, *Ar-H*) and paramagnetic resonances that integrate to $[UBr_4(HL^M)_2]$ **^{1}H (C_6D_6) δ:** -34.09 (12H), -27.65 (4H), -5.53 (4H), -2.36 (2H), 9.23 (6H), 11.33 (4H), 54.81 (4H), 83.93 (12H).

6.4.5 $[UO_2\{O(BO_2C_6H_4)\text{-}\mu_2\text{-}O\text{-}(C_6H_4O)\}_2]$ and $[(L^M)(Bcat)]$

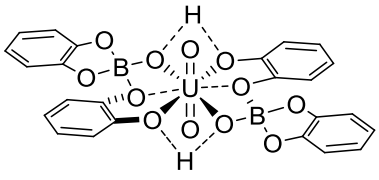

32

+

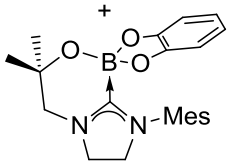

33

An orange suspension of $[UO_2(L^M)_2]$ **25** (100 mg, 0.13 mmol) in toluene (5 mL) was treated with 2 equivalents of a colourless solution of 2-bromo-1,3,2-benzodioxaborole (50 mg, 0.26 mmol) in toluene (5 mL) at room temperature. A green solution formed instantly with a small amount of brown-green precipitate; filtering and slow diffusion of the eluate afforded single crystals of $[UO_2\{O(BO_2C_6H_4)\text{-}\mu_2\text{-}O\text{-}(C_6H_4O)\}_2]$ and $[(L^M)(Bcat)]$ **30** in a 22% yield (34 mg, 0.03 mmol) suitable for X-ray crystallography. **^{1}H (C_6D_6) δ:** 1.33 (6H, C(C*H*$_3$)$_2$), 2.11 (6H, *o*-C*H*$_3$), 2.19 (3H, *p*-C*H*$_3$), 2.52 (2H, NC*H*$_2$C), 2.65-2.71 (2H, NC*H*$_2$CH$_2$N), 2.87-2.93 (2H, NCH$_2$C*H*$_2$N), 6.42 (2H, *Ar*-*H*), 6.45-7.15 (20H, Ph-*H*).

6.4.6 Treatment of $[UO_2(L^M)_2]$ with BBR_3

An orange suspension of **25** (20 mg, 0.03 mmol) in CH_2Cl_2 (0.3 mL) was treated with 4 equivalents of a colourless solution of BBr_3 (25 mg, 0.10 mmol) in CH_2Cl_2 (0.3 mL) at room temperature. A brown solution formed instantly. Although the addition of a few drops of deuterated benzene (lock solvent) precipitated a small amount of brown solid, the ^{1}H NMR spectrum of the bulk material in solution showed multiple diamagnetic products that could not be identified.

6.4.7 Treatment of $[UO_2(L^M)_2]$ with $Cl_2BN^iPr_2$

a. An orange suspension of $[UO_2(L^M)_2]$ **25** (15 mg, 0.02 mmol) in deuterated pyridine (0.3 mL) was treated with 4 equivalents of a colourless solution of $Cl_2BN^iPr_2$ (14 mg, 0.08 mmol) in deuterated pyridine (0.3 mL) at room temperature. A yellow solution formed instantly. The ^{1}H NMR spectrum shows resonances for what is proposed to be $[UO_2Cl_4][(L^M)\text{-}BN^iPr_2]_2$ **^{1}H (C_5D_5N) δ:** 0.46 (d, 6H, ^{i}Pr), 1.19 (d, 6H, ^{i}Pr), 1.36 (6H, C(C*H*$_3$)$_2$), 2.19 (3H, *p*-C*H*$_3$), 2.27 (6H, *o*-C*H*$_3$), 2.91 (m, 1H, ^{i}Pr), 2.99 (m, 1H, ^{i}Pr), 3.81 (2H, NC*H*$_2$C), 4.24-4.30 (2H, NC*H*$_2$CH$_2$N), 4.66-4.71 (2H, NCH$_2$C*H*$_2$N), 6.85 (2H, *Ar*-*H*).

b. An orange suspension of **25** (148 mg, 0.13 mmol) in toluene (8 mL) was treated with 4 equivalents of a colourless solution of $Cl_2BN^iPr_2$ (137 mg, 0.75 mmol) in

toluene (5 mL) and was stirred at room temperature for 12 h. A yellow solution formed instantly. Removal of solvents under reduced pressure yielded 87 mg of a yellow solid, that is believed to be a mixture of $[U(L^M)_2Cl_4]$, $[\{^iPr_2N(Cl)B\}_2O]$ and $[OBN^iPr_2]_3$. **^{1}H (C_6D_6) δ:** 0.55 (d, 6H, ^{i}Pr), 1.19 (d, 9H, ^{i}Pr), 1.37 (6H, C(C*H*$_3$)$_2$), 1.95 (3H, *p*-C*H*$_3$), 2.28 (6H, *o*-C*H*$_3$), 2.33 (m, 1H, ^{i}Pr), 2.63 (2H, NC*H*$_2$C), 2.76 (m, 1.5H, ^{i}Pr), 2.99-3.04 (m, 2H, NC*H*$_2$CH$_2$N), 3.05-3.10 (m, 2H, NCH$_2$C*H*$_2$N), 6.55 (2H, *Ar-H*).

6.4.8 Treatment of $[UO_2(L^M)_2]$ with $ClPPh_2$

An orange suspension of **25** (20 mg, 0.03 mmol) in CH_2Cl_2 (0.3 mL) was treated with 4 equivalents of a colourless solution of $ClPPh_2$ (22 mg, 0.10 mmol) in CH_2Cl_2 (0.3 mL) at room temperature. The solution turned red upon addition and a red solid precipitated immediately. A few drops of deuterated benzene were added. The ^{1}H NMR spectrum showed diamagnetic resonances that are proposed to be $[U(L^M)_2Cl_4]$ and an unidentified compound. **^{1}H (C_6D_6/DCM) δ:** 1.10 (3H), 1.64 (3H, *p*-C*H*$_3$), 1.88 (3H), 1.99 (6H), 1.93 (6H, *o*-C*H*$_3$), 2.00 (6H, C(C*H*$_3$)$_2$), 3.38 (1H), 3.72 (2H, NC*H*$_2$C), 3.78-3.89 (m, 2H), 3.96-4.07 (m, 2H, NC*H*$_2$CH$_2$N), 4.10-4.19 (m, 2H, NCH$_2$C*H*$_2$N), 6.34 (2H), 6.35 (2H, *Ar-H*); **^{31}P (DCM) δ:** 35.48 (d), -22.73 (d), $^1J_{PP}$ = 228 Hz ($O=PPh_2PPh_2$).

6.4.9 Treatment of $[UO_2(L^M)_2]$ with $IPPh_2$

An orange suspension of **25** (20 mg, 0.03 mmol) in CH_2Cl_2 (0.3 mL) was treated with 4 equivalents of a colourless solution of $IPPh_2$ (32 mg, 0.10 mmol) in CH_2Cl_2 (0.3 mL) at room temperature. The solution turned red upon addition and a red solid precipitated immediately. A few drops of deuterated benzene were added. The ^{1}H NMR spectrum showed paramagnetic resonances between -18.88 and 22.76 ppm that are believed to be $[U(L^M)_2I_2]$. **^{31}P (DCM) δ:** 35.48 (d), -22.73 (d), $^1J_{PP}$ = 228 Hz ($O=PPh_2PPh_2$), 16.32, 17.26.

6.4.10 Attempted functionalisation of 25 with various reagents

a. Attempted functionalisation of **25** with LiI

An orange suspension of **25** (15 mg, 0.02 mmol) in deuterated benzene (0.3 mL) was treated with an excess of a colourless solution of LiI (25 mg, 0.19 mmol) in deuterated benzene (0.3 mL) at room temperature. When no reaction was observed the

mixure was heated to 80 ˚C for 1 week and checked at regular intervals by ^{1}H NMR spectroscopy. No reaction was observed.

b. Attempted functionalisation of **25** with Me_3SiX (X = I, Cl), $LiSiPh_3$, $LiAlH_4$ and 2,6-*tert*butylphenyl *tris*chlorosilane

An orange suspension of **25** (15 mg, 0.02 mmol) in deuterated benzene (0.3 mL) was treated with two equivalents of a solution of the respective compound (0.03 mmol) in deuterated benzene (0.3 mL) at room temperature. A reaction was observed and multiple products could be detected in the ^{1}H NMR spectrum.

c. Attempted functionalisation of **25** with H_2 or CO

In a typical reaction a suspension of **25** (20 mg, 0.02 mmol) in deuterated benzene (0.7 mL) was freeze-thaw-degassed three times in a Young's tap NMR tube prior to treatment with H_2 or CO respectively. ^{1}NMR spectroscopy showed formation of [HL^{M}]. The FTIR spectrum showed no formation of a new H_2 or CO complex.

6.4.11 $[(UI_5)_2(py\text{-}BBN)_2]$

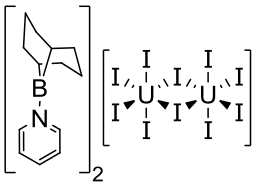

34

To a solution of $[UO_2(N'')_2(py)_2]$ (230 mg, 0.37 mmol) in toluene (10 mL) was added a 1M solution of B-Iodo-9-BBN in hexanes (0.92 mL, 0.92 mmol) and stirred at room temperature for 12 hours. The volatiles were removed under reduced pressure and the brown solid washed with hexanes (3 x 5 mL). The remaining volatiles were removed under reduced pressure before pyridine was added and the solution stirred for 4 h. Removal of the volatiles gave 219 mg (0.1 mmol, 32 %) of clean product. Crystals suitable for X-ray crystallography could be grown from a saturated pyridine solution layered with hexanes. **^{1}H (C_5D_5N) δ:** 1.28, 1.55, 1.87, 2.30 (14H, BBN), 7.59 (4H, py), 7.97 (4H, py), 9.52 (2H, py).

6.4.12 $[UO_2I_4][(py)_2BBN]_2$

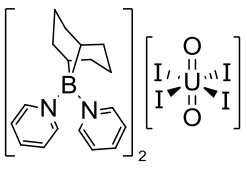

35

To a red solution of $[UO_2N''_2(py)_2]$ (240 mg, 0.32 mmol) in toluene (5 mL) was added a 1M solution of B-Iodo-9-BBN (1.6 mL, 1.6 mmol) in hexanes and the brown solution was stirred at room temperature for 12 hours. The volatiles were removed in vacuum and the brown filtrant washed with hexanes (3 x 2 mL). The remaining volatiles were removed under reduced pressure, then pyridine was added and the solution stirred

for 4 h. Removal of the volatiles gave $[UO_2I_4][(py)_2BBN]_2$ **32** in a 32 % yield (135 mg, 0.1 mmol). Single crystals suitable for X-ray diffraction were grown from a concentrated pyridine solution. **^{1}H (C_5D_5N) δ:** 1.31, 1.57, 1.89, 2.29 (14H, BBN), 7.93 (4H, py), 8.19 (2H, py), 9.49 (4H, py); **Analysis (%)** calc. for $C_{36}H_{48}B_2I_4N_4O_2U{\cdot}2C_5H_5N$: C, 36.97; H, 3.91; N, 5.62; found: C, 36.79; H, 4.44; N 5.25.

6.4.13 Treatment of $[UO_2N''_2(py)_2]$ with $ClPPh_2$

A red solution of $[UO_2(N'')_2(py)_2]$ (20 mg, 0.03 mmol) in methylene chloride (0.3 mL) was treated with 4 equivalents of a colourless solution of $ClPPh_2$ (24 mg, 0.11 mmol) in methylene chloride (0.3 mL) at room temperature. A red solution formed instantly. No formation of the tetraphenyl diphospine monoxide is observed in the ^{31}P NMR spectrum. **^{31}P (DCM) δ:** -16, 10.

6.4.14 Treatment of $[UO_2N''_2(py)_2]$ with bromocatechol borane

A red solution of $[UO_2N''_2(py)_2]$ (20 mg, 0.03 mmol) in methylene chloride (0.3 mL) was treated with 4 equivalents of a colourless solution of bromocatechol borane (22 mg, 0.11 mmol) in methylene chloride (0.3 mL) at room temperature. No reaction could be observed by ^{1}H NMR spectroscopy even after heating the solution at 80 ˚C for a week.

6.4.15 Treatment of $[UO_2N''_2(py)_2]$ with $Cl_2BN^iPr_2$

A red solution of $[UO_2N''_2(py)_2]$ (20 mg, 0.03 mmol) in methylene chloride (0.3 mL) was treated with 4 equivalents of a colourless solution of $Cl_2BN^iPr_2$ (19 mg, 0.11 mmol) in methylene chloride (0.3 mL) at room temperature. No reaction could be observed by ^{1}H NMR spectroscopy even after heating the solution at 80 ˚C for a week.

6.4.16 $[UO_2(OAr^{2,6\text{-}tBu})_2(py)_2]$

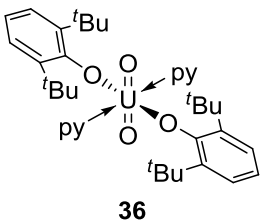

36

A red solution of $[UO_2N''_2(py)_2]$ (1.61 g, 2.2 mmol) in pyridine (10 mL) was treated with 2 equivalents of a yellow solution of 2,6-di-*tert*-butylphenol (0.89 g, 4.3 mmol) in pyridine (5 mL) at room temperature. The brown solution was stirred for 48 h before the volatiles were removed under reduced pressure and the resulting brown solid washed with hexanes (3 × 3 mL). Removal of the solvents under reduced pressure afforded $[UO_2(OAr^{2,6\text{-}tBu})_2(py)_2]$ **33** in a 77% yield (1.4 g, 1.7

mmol). **^{1}H (C_6D_6) δ:** 1.79 (36H, ^{t}Bu), 6.57 (4H, py), 6.80 (4H, py), 7.70 (2H, py), 7.72 (2H, Ar-*H*), 9.21 (4H, Ar-*H*).

6.4.17 $[UO_2(py)_5][I]$

A brown solution of $[UO_2(OAr^{2,6\text{-}tBu})_2(py)_2]$ **33** (200 mg, 0.25 mmol) in toluene (5 mL) was treated with 4 equivalents of a hexane solution of I-BBN (0.99 mL, 0.99 mmol) at -78 ˚C and then slowly warmed to room temperature. A brown precipitate had formed which was isolated by filtration and dissolved in pyridine and the solution concentrated. Single crystals of $[UO_2(py)_5][I]$ **34** were formed in a 36% yield (73 mg, 0.09 mmol) after 48 h at -30 ˚C.

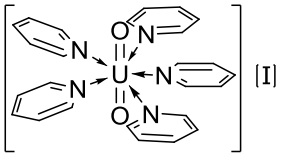

37

6.5 References

1. D. C. Bradley, J. S. Ghotra, and F. A. Hart, *J. Chem. Soc. Dalton Trans.*, 1973, 1021.
2. C. D. Carmichael, N. A. Jones, and P. L. Arnold, *Inorg. Chem.*, 2008, **47**, 8577–8579.
3. L. R. Avens, S. G. Bott, D. L. Clark, A. P. Sattelberger, J. G. Watkin, and B. D. Zwick, *Inorg. Chem.*, 1994, **33**, 2248–2256.
4. P. L. Arnold, D. Patel, C. Wilson, and J. B. Love, *Nature*, 2008, **451**, 315–317.
5. W. J. Evans, D. B. Rego, and J. W. Ziller, *Inorg. Chem.*, 2006, **45**, 3437–3443.
6. P. J. Bailey, R. A. Coxall, C. M. Dick, S. Fabre, L. C. Henderson, C. Herber, S. T. Liddle, D. Loroño-González, A. Parkin, and S. Parsons, *Chem.-Eur. J.*, 2003, **9**, 4820–4828.
7. P. L. Arnold, I. J. Casely, Z. R. Turner, and C. D. Carmichael, *Chem.-Eur. J.*, 2008, **14**, 10415–10422.
8. R. S. Sternal and T. J. Marks, *Organometallics*, 1987, **6**, 2621–2623.

Appendix

Table 1 CIF data for compounds **1_{py}** - **12**

Compound reference	**1_{py}**	**4**	**8**	**10**	**12**
Chemical formula	$C_{33}H_{64}CeN_5OSi_4C_5H_5N$	$C_{38}H_{64}N_4O_2Si_2$	$C_{48}H_{74}B_2N_4O_2C_{14}H_{16}$	$C_{64}H_{52}Ce_2Cl_{22}O_4C_{12}H_{12}$	$C_{64}H_{92}Li_4N_8O_4C_3H_7$
Formula Mass	878.47	665.11	945.00	2101.41	1108.3
Crystal system	Monoclinic	Monoclinic	Monoclinic	Monoclinic	Monoclinic
a/Å	16.1984 (6)	15.1806 (4)	9.0381 (5)	34.9833 (12)	52.5527 (14)
b/Å	13.4476 (5)	9.0006 (2)	12.1174 (6)	14.3789 (5)	11.3887 (3)
c/Å	22.0515 (9)	15.1228 (5)	12.6341 (7)	15.0412 (4)	23.0623 (7)
α/°	90.00	90.00	90.00	90.00	90.00
β/°	98.384 (2)	104.994 (3)	100.939 (6)	96.293 (3)	97.659 (2)
γ/°	90.00	90.00	90.00	90.00	90.00
Unit cell volume/Å^3	4752.1 (3)	1995.94 (10)	1358.52 (13)	7520.5 (4)	13679.8 (7)
Temperature/K	150	150	150	150	170
Space group	$P2_1/c$	$P2_1/c$	$P2_1$	$C2/c$	$C2/c$
Z	4	2	1	4	8
Radiation type	Mo *K*α	Mo *K*α	Mo *K*α	Mo *K*α	Mo *K*α
Absorption coefficient, μ/mm^{-1}	1.09	0.12	0.07	2.03	0.07
No. of reflections measured	30810	28859	10607	20855	75814
No. of independent reflections	9754	4574	58774	9034	15027
R_{int}	0.064	0.03	0.022	0.031	0.051
R [$F^2 > 2\sigma(F^2)$]	0.055	0.042	0.047	0.043	0.060
$wR(F^2)$	0.132	0.112	0.103	0.106	0.168
Goodness of fit on F^2	1.05	1.04	1.02	1.05	1.04

Table 2 CIF data for compounds **17** - **27**

Compound reference	**17**	**20**	**24**	**26**	**27**
Chemical formula	$C_{65}H_{95}CeN_2O_4C_7H_8$	$C_{48}H_{69}Ce_2Cl_3N_6O_3C_{12}H_{12}$	$C_{84}H_{129}Ce_2N_6O_4Si_4$	$C_{38}H_{64}N_5O_2PrSi_2$	$C_{44}H_{82}Cl_2N_6O_2Pr_2Si_4$
Formula Mass	1200.68	1320.9	1679.57	820.03	1192.24
Crystal system	Triclinic	Triclinic	Monoclinic	Triclinic	Monoclinic
a/Å	10.9396 (4)	13.0403 (3)	12.4347 (5)	11.122 (5)	8.7365 (3)
b/Å	14.0616 (5)	15.5745 (5)	27.7308 (11)	11.500 (5)	14.7905 (4)
c/Å	24.2373 (7)	17.8164 (6)	26.4042 (11)	18.063 (5)	21.9419 (7)
α/°	96.171 (3)	65.148 (3)	90.00	90.222 (5)	90.00
β/°	97.783 (3)	89.606 (2)	96.435 (4)	91.063 (5)	101.389 (3)
γ/°	90.755 (3)	77.958 (2)	90.00	112.927 (5)	90.00
Unit cell volume/Å^3	3671.2 (2)	3197.77 (17)	9046.5 (6)	2127.3 (15)	2779.44 (15)
Temperature/K	150	150	150	150	150
Space group	$P\bar{1}$	$P\bar{1}$	*Cc*	$P\bar{1}$	$P2_1/n$
Z	2	2	4	2	2
Radiation type	Mo *K*α	Mo *K*α	Mo *K*α	Mo *K*α	Mo *K*α
Absorption coefficient, μ/mm^{-1}	0.66	1.58	8.54	1.24	1.95
No. of reflections measured	68029	26919	10710	17971	24816
No. of independent reflections	15453	14553	9244	7058	6852
R_{int}	0.068	0.029	0.157	0.174	0.036
R [$F^2 > 2s(F^2)$]	0.073	0.028	0.113	0.081	0.027
$wR(F^2)$	0.226	0.061	0.277	0.181	0.055
Goodness of fit on F^2	1.11	0.92	0.97	0.96	1.06

Table 3 CIF data for compounds **29** -**35**

Compound reference	**29**	**31**	**32**	**34**	**35**
Chemical formula	$C_{28}H_{46}I_4N_4O_2UC_{10}H_{10}N_2$	$C_{48}H_{76}B_2I_4N_4O_4U$	$C_{68}H_{70}B_4N_4O_{18}UC_2H_4Cl_4$	$C_{26}H_{38}B_2I_{10}N_2U_2$	$C_{36}H_{48}B_2I_4N_4O_2U$
Formula Mass	1422.56	1540.38	1682.4	2145.26	1336.03
Crystal system	Monoclinic	Triclinic	Monoclinic	Monoclinic	Monoclinic
a/Å	14.3215 (4)	8.4845 (6)	13.3808 (5)	10.0047 (4)	15.7046 (7)
b/Å	8.7771 (2)	12.5173 (9)	18.3594 (6)	8.1323 (4)	13.9267 (5)
c/Å	20.0710 (6)	14.5355 (12)	14.6373 (5)	30.6712 (14)	19.6298 (7)
α/°	90.00	96.138 (7)	90.00	90.00	90.00
β/°	106.604 (3)	96.705 (6)	94.979 (3)	95.417 (4)	103.608
γ/°	90.00	101.817 (6)	90.00	90.00	90.00
Unit cell volume/Å^3	2417.75 (11)	1487.01 (19)	3582.3 (2)	2484.30 (19)	4172.8 (3)
Temperature/K	150	150	150	150	150
Space group	*C*2/*c*	$P\bar{1}$	$P2_1/n$	$P2_1/n$	*C*2/*c*
Z	2	1	2	2	4
Radiation type	Mo *K*α	Mo *K*α	Mo *K*α	Mo *K*α	Mo *K*α
Absorption coefficient, μ/mm^{-1}	5.95	4.85	8.35	12.74	6.89
No. of reflections measured	67023	17391	26746	16275	19686
No. of independent reflections	6406	14151	7148	5255	4264
R_{int}	0.033	0.225	0.121	0.065	0.051
R [$F^2 > 2s(F^2)$]	0.023	0.171	0.071	0.119	0.031
$wR(F^2)$	0.061	0.421	0.192	0.266	0.061
Goodness of fit on F^2	1.04	1.86	1.01	1.21	1.03

Table 4 CIF data for compound **37**

Compound reference	**37**
Chemical formula	$C_{35}H_{35}I_2N_7O_2U$
Formula Mass	1077.53
Crystal system	Monoclinic
a/Å	21.8598 (10)
b/Å	12.2599 (2)
c/Å	19.3962 (10)
α/°	90.00
β/°	130.540 (8)
γ/°	90.00
Unit cell volume/Å^3	3950.4 (3)
Temperature/K	150
Space group	*C*2/*c*
Z	4
Radiation type	Mo *K*α
Absorption coefficient, μ/mm^{-1}	5.71
No. of reflections measured	23401
No. of independent reflections	4529
R_{int}	0.03
R [$F^2 > 2s(F^2)$]	0.021
$wR(F^2)$	0.046
Goodness of fit on F^2	1.04